

TESIS DE LA UNIVERSIDAD
DE ZARAGOZA

2019

123

Unai Mutilba Larrea

Traceable onboard metrology for machine tools and large-scale systems

Departamento
Ingeniería de Diseño y Fabricación

Director/es
Yagüe Fabra, José Antonio
Gómez-Acedo Bilbao, Eneko

<http://zaguan.unizar.es/collection/Tesis>

ISSN 2254-7606



Prensas de la Universidad
Universidad Zaragoza



Reconocimiento – NoComercial – SinObraDerivada (by-nc-nd): No se permite un uso comercial de la obra original ni la generación de obras derivadas.

© Universidad de Zaragoza
Servicio de Publicaciones

ISSN 2254-7606



Universidad
Zaragoza

Tesis Doctoral

TRACEABLE ONBOARD METROLOGY FOR
MACHINE TOOLS AND LARGE-SCALE SYSTEMS

Autor

Unai Mutilba Larrea

Director/es

Yagüe Fabra, José Antonio
Gómez-Acedo Bilbao, Eneko

UNIVERSIDAD DE ZARAGOZA
Ingeniería de Diseño y Fabricación

2019



Universidad
Zaragoza

TESIS DOCTORAL

**Traceable onboard metrology for machine tools and
large-scale systems**

Unai Mutilba Larrea

Zaragoza, 2019



Universidad
Zaragoza

**Traceable onboard metrology for machine tools and
large-scale systems**

Unai Mutilba Larrea

Dirigida por

Dr. José Antonio Yagüe Fabra

Dr. Eneko Gomez-Acedo

Para la obtención del Título de Doctor

por la Universidad de Zaragoza

Zaragoza, abril de 2019

Esta tesis se presenta como un compendio de las siguientes publicaciones:

- Mutilba U, Gomez-Acedo E, Kortaberria G, Olarra A, Yagüe-Fabra JA. Traceability of On-Machine Tool Measurement: A Review. MDPI Sensors 2017;17:40. doi:10.3390/s17071605. The journal JCR index in 2017 was 2.475.
- Mutilba U, Sandá A, Vega I, Gomez-Acedo E, Bengoetxea I, Yagüe-Fabra JA. Traceability of on-machine tool measurement : Uncertainty budget assessment on shop floor conditions. Measurement 2019;135:180–8. doi:10.1016/j.measurement.2018.11.042. The journal JCR index in 2017 was 2.218.
- Mutilba U, Gomez-Acedo E, Sandá A, Vega I, Yagüe-Fabra JA. Uncertainty assessment for on-machine tool measurement: an alternative approach to the ISO 15530-3 technical specification. Precision Engineering 2019;57:45–53. doi: 10.1016/j.precisioneng.2019.03.005. The journal JCR index in 2017 2.582.
- Mutilba U, Yagüe-Fabra JA, Gomez-Acedo E, Kortaberria G, Olarra A. Integrated multilateration for machine tool automatic verification. CIRP Annals 2018;67:555–8. doi:10.1016/j.cirp.2018.04.008. The journal JCR index in 2017 3.333.
- Mutilba U, Egaña F, Kortaberria G, Gomez-Acedo E, Olarra A, Yagüe-Fabra JA. Integrated volumetric error mapping for large machine tools : An opportunity for more accurate and geometry connected machines. Procedia Manufacturing 2019:1–8.
- Mutilba U, Kortaberria G, Egaña F, Yagüe-Fabra JA. 3D Measurement Simulation and Relative Pointing Error Verification of the Telescope Mount Assembly Subsystem for the Large Synoptic Survey Telescope. Sensors 2018;18:20–2. doi:10.3390/s18093023. The journal JCR index in 2017 was 2.475.
- Mutilba U, Kortaberria G, Egaña F, Yagüe-Fabra JA. Telescope mount assembly pointing accuracy assessment for the Large Synoptic Survey Telescope : A large-scale metrology challenge. EUSPEN 19th International Conference & Exhibition 2019;1:9–12.

Parte del trabajo realizado en esta tesis forma parte de los proyectos:

- Programa de apoyo a la I+D empresarial HAZITEK 2016 financiando el Gobierno Vasco. El proyecto “Máquinas herramienta de precisión volumétrica con capacidad de medición trazable - (MH2020)” con número de expediente ZE-2016/00023.
- Proyecto Europeo “Twin-model based virtual manufacturing for machine tool-process simulation and control” financiado por: Public Private Partnership (PPP) for Factories Of the Future (FOF) within the European Framework Programme for Research and Innovation, Horizon 2020 (grant agreement nº 680725).

D. José Antonio Yagüe Fabra, Doctor por la Universidad de Zaragoza y Profesor Titular del departamento de Ingeniería de Diseño y Fabricación de la Universidad de Zaragoza.

INFORMA:

Que la tesis titulada “Traceable onboard metrology for machine tools and large-scale systems”, elaborada por D. Unai Mutilba Larrea, ha sido realizada bajo mi dirección, se ajusta al proyecto de tesis inicialmente presentado y cumple los requisitos exigidos por la legislación vigente para optar al grado de Doctor por la Universidad de Zaragoza. Una vez finalizada, autorizo su presentación en la modalidad de compendio de publicaciones para ser evaluada por el tribunal correspondiente.

Zaragoza, a 12 de abril de 2019,

Fdo. D. José Antonio Yagüe Fabra

D. Eneko Gomez-Acedo Bilbao, Doctor por la Universidad del País Vasco e investigador de la unidad de ingeniería mecánica del centro tecnológico IK4-TEKNIKER.

INFORMA:

Que la tesis titulada “Traceable onboard metrology for machine tools and large-scale systems”, elaborada por D. Unai Mutilba Larrea, ha sido realizada bajo mi codirección, se ajusta al proyecto de tesis inicialmente presentado y cumple los requisitos exigidos por la legislación vigente para optar al grado de Doctor por la Universidad de Zaragoza. Una vez finalizada, autorizo su presentación en la modalidad de compendio de publicaciones para ser evaluada por el tribunal correspondiente.

Eibar, a 25 de abril de 2019,

Fdo. D. Eneko Gomez-Acedo Bilbao

Aita eta ama, eskerrikasko

Manex, Paul eta Bera, zuengatik

Nere, zuretako

Lagun eta familia beharrez bizi naizelako

Statement of originality

The work contained in this thesis has not been previously submitted for a degree or diploma at any other higher education institution. To the best of my knowledge and belief, the thesis contains no material previously published or written by another person except where due references are made.

Unai Mutilba Larrea

April of 2019

ACKNOWLEDGEMENT

Firstly, I would like to express my sincere gratitude to my advisor Prof. José Antonio Yagüe-Fabra for the continuous support of my PhD study and related research, for his advice, motivation and immense knowledge about industrial metrology. His guidance helped me in all the time of research and writing of this thesis. I could not have imagined having a better advisor and mentor for my PhD study.

Besides my advisor, I would like to thank Eneko Gomez-Acedo, my mentor at IK4-TEKNIKER, for his insightful comments and encouragement. I am thankful to him for being there for me whenever I needed guidance, advice and support.

My sincere thanks also go to Aitor Olarra, Gorka Kortaberria, Mikel Zubieta, Alex Sanda, Fernando Egaña, Jon Etxarri, Jon Bengoetxea, Ibon Vega, Sergio Gomez, Antonio Gutierrez, José Ángel Solas, Josune Narbaiza, Iban del Rio, Mikel Armendia, Ion Iturbe, Itziar Cenoz, Javier Arzamendi, Aitor Alzaga, Ana Aranzabe and Luis Gerardo Uriarte at IK4-TEKNIKER and Emilio Prieto at the Spanish Metrology Institute, who helped me with their assistance and their knowledge throughout my PhD study. They also gave me the opportunity to undertake this thesis at IK4-TEKNIKER.

I am especially thankful to my parents, Belen and Manu. Without their love, support and help I would not have come far in my life. They have provided me through moral and emotional support in my life. They have always believed in me and none of this would have been possible without their assistance. Thank you from the bottom of my heart.

I am extremely grateful to my wonderful wife Nerea. I thank her for the support she extended in a myriad of ways to see this thesis to completion. My two beautiful children, Manex and Paul, and Bera who is on the way deserve a special thanks. Their love and energy kept me going. They are the key to my success and they give meaning to my life.

A very special thank you to my other family members and friends who have supported me along the way. They all kept me going, and this work would not have been possible without them. Their support and encouragement showed the way to me.

TABLE OF CONTENTS

ACKNOWLEDGEMENT.....	x
LIST OF FIGURES.....	xii
LIST OF TABLES.....	xiv
LIST OF ABBREVIATIONS	xv
ABSTRACT	xvii
1. INTRODUCTION.....	2
1.1 Motivation	2
1.2 A literature review of on-MT measurement	3
2. PRESENTATION OF THE PUBLISHED WORK	32
2.1 Research framework	32
2.2 List of published works.....	34
2.3 Presentation of published works.....	35
3. RESEARCH ARTICLES.....	69
4. SUMMARY.....	168
4.1 Objectives	168
4.2 Scientific contribution	169
4.3 Methodology.....	170
4.4 Conclusions	180
4.5 Future work.....	181
5. RESUMEN.....	184
5.1 Objetivos	184
5.2 Contribución científica	185
5.3 Metodología.....	186
5.4 Conclusiones	197
5.5 Trabajo futuro	199
APPENDIX.....	202
A.1 The impact factor of the published work.....	202
A.2 Author’s contribution to the published work	202
A.3 Acceptance letters for the pending publishing work	204
BIBLIOGRAPHY	208

LIST OF FIGURES

Figure 1-1 On-MT measurement scenario.	4
Figure 1-2 Monitoring of the MT performance.	4
Figure 1-3 Tactile on-MT probing.	5
Figure 1-4 WZL RWTH Aachen approach to convert an MT into a CMM, a) previous volumetric calibration approach and b) external and real-time metrology framework.	6
Figure 1-5 Total error sources of MTs.	9
Figure 1-6 Direct measurements of positioning error through a laser interferometer.	11
Figure 1-7 Bending of a straightness reference beam due to local and global gradients.	12
Figure 1-8 Multidimensional equipment for five dof.	13
Figure 1-9 3D artefact for VCMM characterisation. (Zeiss UPMC Carat 850 CMM at IK4-TEKNIKER premises).	14
Figure 1-10 Artefact measurement-based MT characterisation.	14
Figure 1-11 Tracking interferometer on a sequential multilateration combination approach.	15
Figure 1-12 Space diagonal measurement before and after the volumetric compensation.	19
Figure 1-13 Multiline technology, a) example on a large MT and b) a unique line measurement technology.	21
Figure 1-14 Thermal distortions on large MTs based on an automatic multilateration, a) the YZ plane measurement and b) thermal drift assessment on the YZ plane.	22
Figure 1-15 Contact touch probes: a) Hard; b) touch-trigger; and c) measuring probe.	23
Figure 1-16 Kinematic resistive probe principle.	23
Figure 1-17 Aspects of probing systems.	25
Figure 1-18 TTP kinematics: a) serial; and (b) parallel.	25
Figure 1-19 Typical values of tolerances vs. dimensions for most common free form shaped parts.	27
Figure 2-1 On-MT measurement experimental exercise: a) Workpiece manufacturing scenario; and b) on-MT measurement with RENISHAW OMP 400 tactile probe.	38
Figure 2-2 The workpiece replica standard with the measured geometry.	38
Figure 2-3 Laser tracer NG multilateration exercise on the KONDIS MAXIM MT	38
Figure 2-4 Temperature variation during the experimental test.	39
Figure 2-5 On-MT experimental uncertainty budget.	39
Figure 2-6 The proposed systematic error assessment methodology.	43
Figure 2-7 On-MT measurement contact points, a) General overview of the measurement strategy (contact points in green), and b) the measurement scenario where the workpiece and the calibrated ring are shown.	43
Figure 2-8 Volumetric error mapping of MT and measured point grid. (in black)	44
Figure 2-9 MT volumetric error mapping results. (vector mode)	44
Figure 2-10 Systematic error (ub) assessment according to ISO 15530-3 technical specification and VDI 2617-11 guideline.	45
Figure 2-11 Uncertainty budget according to VDI 2617-11 guideline.	46
Figure 2-12 Integrated multilateration distribution on an MT.	47
Figure 2-13 Uncertainty values obtained by simulation of four 3D measurement approaches	49
Figure 2-14 Integrated multilateration concept demonstration on a KUKA KR60 industrial robot: a) real setup at IK4-TEKNIKER premises; b) the virtual model and c) the AT960 laser tracker integration upside-down.	50

Figure 2-15 a) Uncertainty result for point grid in X, Y and Z directions; and b) Uncertainty result for fiducial point measurements in X, Y and Z directions. (U_x , U_y and U_z respectively)	50
Figure 2-16 Length residuals results for the concept demonstration measurement a) Numerical format; and b) histogram format	51
Figure 2-17 Sequential multilateration scheme: a) ZAYER MEMPHIS large MT employing a laser tracer NG; and b) virtual representation of the measurement sequence scheme. (Measurement performed by IK4-TEKNIKER in collaboration with ZAYER)	53
Figure 2-18 Simultaneous multilateration scheme: a) ZAYER KAIROS large MT employing three laser trackers and one laser tracer NG; and b) virtual representation of the measurement scheme. (Measurement performed by IK4-TEKNIKER in collaboration with ZAYER)	53
Figure 2-19 Integrated multilateration validation approach on a ZAYER MEMPHIS large MT employing a LEICA AT960 laser tracker. (Measurement performed by IK4-TEKNIKER in collaboration with ZAYER)	54
Figure 2-20 Uncertainty results of the fiducial points after the multilateration exercise: a) typical approach and b) integrated approach.	55
Figure 2-21 Uncertainty results for the point grid after the multilateration exercise: a) typical approach and b) integrated approach.	55
Figure 2-22 3D comparison at the point cloud level between both measurement approaches.	56
Figure 2-23 Typical multilateration-based kinematic output results.....	56
Figure 2-24 Integrated multilateration-based kinematic output results.	57
Figure 2-25 Measurement scenario for RPE assessment. (a) M1M3 measurement plane (measurement targets in red); and (b) Complete LSST measurement scenario.	59
Figure 2-26 Mapping matrix for the RPE test.	59
Figure 2-27 Visibility study overview from inside placed laser tracker, from the zenith to the horizon pointing direction.	60
Figure 2-28 Measurement uncertainty for metrology network characterisation.	61
Figure 2-29 RPE measurement uncertainty results. (in arcseconds)	62
Figure 2-30 RPE measurement uncertainty results with floor movement consideration. (in arcseconds)	62
Figure 2-31 The fully automatic RPE verification procedure flow chart.	63
Figure 2-32 The real measurement scenario at ASTURFEITO premises.	63
Figure 2-33 Laser tracker visibility a) TMA horizon pointing position; and b) TMA zenith pointing position.	64
Figure 2-34 a) Fiducial point definition; and b) laser tracker arrangement in M1M3.	64
Figure 2-35 Real point distribution for the TMA pointing accuracy test.	65
Figure 2-36 Uncertainty assessment for the real measurement scenario.	65
Figure 2-37 Measurement uncertainty for the metrology network characterisation. (real measurement scenario-based simulation)	65
Figure 2-38 Direct measurement methods for pointing the repeatability test.	67
Figure 2-39 Reflectors attached to M2 secondary plane (3 out of 4 reflectors are shown).	68
Figure 2-40 Reflectors attached to M1M3 primary plane.....	68

LIST OF TABLES

Table 1-1 Comparison table between kinematic and strain gauge probing technology.	24
Table 2-1 Error budget for small and medium-size MTs.	36
Table 2-2 Error budget for large size MTs.	36
Table 2-3 Expanded measurement uncertainties (U_{MP} and U_{MS} , with $k=2$) of the experimental test. (in μm)	40
Table 2-4 MT volumetric error mapping results. (numerical mode)	45
Table 2-5 Uncertainty budget according to VDI 2617-11 guideline and comparison with ISO 15530-3 technical specification. (results in μm)	46
Table 2-6 RPE test results for the TMA subsystem. (Real results obtained on the in-situ survey)	66
Table 2-7 TMA repeatability results obtained with laser tracker technology.	67

LIST OF ABBREVIATIONS

ADM	Absolute distance measurement
AFM	Basque cluster for advanced and digital manufacturing
AIFM	Absolute interferometer measurement
CAD	Computer aided design
CAM	Computer aided manufacturing
CAS	Continuous analog scanning
CERN	European organization for nuclear research
CECIMO	European association of the machine tool industries
CMM	Coordinate measurement machine
CNC	Computer numerical control
Dof	Degree of freedom
Doi	Digital object identifier
DMIS	Dimensional measurement interface standard
EC	European commission
€	Euro
etc	Etcetera
e.g	For example
EU	European Union
i.e.	That is
FEM	Finite element model
FSI	Frequency scanning interferometer
GD&T	Geometric dimensioning and tolerancing
GDP	Gross domestic product
GUM	Expression of uncertainty in measurement
IFM	Interferometer
ISO	International organization for standardization
JCR	Journal citation reports
JCGM	Joint committee for guides in metrology
KET	Key enabling technology
KPI	Key performance indicator
LAN	Local area network
LBT	Large binocular telescope
LSM	Large scale metrology
LSST	Large synoptic survey telescope
LUMINAR	Large volume unified metrology for industry
MH	Máquina herramienta
MMC	Máquina de medir por coordenadas
MT	Machine tool
MPE	Maximum permissible error

NAS	National aerospace standard
NC	Numerical control
NMI	National metrology institute
NPL	National physical laboratory
OEE	Overall equipment effectiveness
OEM	Original equipment manufacturer
ORKESTRA	Basque Institute of competitiveness
PSD	Position sensitive detector
PhD	Doctor of philosophy
PTB	The national metrology institute of Germany
PTV	Pre-travel variation
R&D	Research and development
RPE	Relative pointing error
ROI	Return of investment
SA	Spatial analyzer
SI	International system of units
SJR	Scimago journal rank
SME	Small and medium-size enterprises
TCP/IP	Transmission control protocol/internet protocol
TIM	Traceable in-process metrology
TMA	Telescope mount assembly
TTP	Touch trigger probe
TRL	Technology readiness level
UES	Uncertainty evaluation software
USMN	Unified spatial metrology network
VCMM	Virtual coordinate measurement machine
VDI	The association of German engineers
VLT	Virtual laser tracker
VMP	Virtual measurement process

ABSTRACT

The machine tool (MT) industry is characterised by its family-owned small and medium-size enterprises (SME) dominated landscape, strong concentration on flexible and small-batch production of custom-built and high-precision machines, and the export orientation of companies. Product features such as precision and accuracy are far more important than unit labour costs in a technology-intensive sector such as MTs, as a source of competitive advantage. High-tech MT builders seek for differentiation and sources of uniqueness by creating value for their customers through the development of new processes, functionalities and services which help achieve high productivity levels, meet the precision needs of their customers and help lower their costs, looking for a positive impact on the overall equipment effectiveness (OEE) indicator of their customers, the MT users.

In this context, this PhD study aims to improve the accuracy of MTs and also to develop knowledge for traceable coordinate measurement machine (CMM) measurements on MTs. The technology to run a dimensional measurement on an MT already exists but the knowledge to do traceable measurements is under research, as it is reported in this thesis. There are several factors that affect the measurement accuracy in shop-floor conditions, so the traceability of the measurement process on an MT is not ensured yet and therefore the measurement is not sufficiently reliable for self-adapting manufacturing processes.

The starting point of this PhD study is to fully present a qualitative approach of the error sources that contribute to the uncertainty budget for on-MT measurement. An error budget-type classification is proposed to predict the accuracy and repeatability of an MT working as a CMM. Thus, the error budget for traceable on-MT measurement is comprised of the measurement system (the MT with the touch trigger probe and the measuring software), the component under measurement and the interaction between both of them.

The next milestone presents a quantitative approach to the proposed uncertainty budget. Here, a medium-size on-MT measurement experimental test is performed in shop floor conditions according to the ISO 15530-3 technical specification. The obtained results demonstrate that traceable CMM measurements are realisable in MTs. Test results highlight the significance and the error source of each uncertainty contributor. In this way, the measurement procedure uncertainty is the main contributor to the uncertainty budget and the geometric error of the MT is the main error source for the systematic error contributor. However, the ISO 15530-3 technical specification presents a strong limitation, it depends on a calibrated workpiece to understand how the systematic error contributor performs. Therefore, the scalability of the solution is limited to a medium-size MT. To deal with this limitation, an alternative on-MT measurement methodology is presented here based on a volumetric error mapping of the MT prior to the measurement process execution, which allows understanding how the systematic error contributor performs and it is a gateway to large on-MT traceable measurements.

Next, an integrated MT volumetric error mapping procedure that enables the scalability of traceable on-MT measurements to large MTs is developed. The integration of a tracking interferometer measurement device on the MT spindle breaks with the typical multilateration approach, based on sequential measurement scheme, and permits to measure the geometric error of an MT automatically within the complete working volume.

This PhD study focuses on making a special effort towards large scale manufacturing scenarios, where high-value components require fast and reliable feedback on the manufacturing scenario. Thus, either the measurement

procedure for on-MT measurement without a calibrated workpiece or the integrated measurement procedure for automatic MT geometric verification are focused on large MTs and therefore both measurement procedures are developed within the large scale metrology (LSM) field. It means that when it comes to large-scale manufacturing scenarios, the traceability of on-MT measurement faces similar challenges to what the LSM does and therefore the measurement procedures developed within this PhD study consider the current state of the art to select the suitable technologies and measurement sequences.

Finally, a new LSM survey procedure is developed for the pointing accuracy assessment of the cutting-edge large synoptic survey telescope (LSST) project. From the methodology design and previous simulation to the in-situ measurement execution, the automatic measurement procedure shows how the LSM can help to execute major scientific projects.

1. INTRODUCTION



1. INTRODUCTION

Touch probes are commonly employed in new MTs, and enable machining and measuring processes to occur on the same MT. It offers the possibility of measuring components during or after the machining process, providing the traceability of the quality inspection in the original setup on the MT. Nevertheless, there are several factors that affect measurement accuracy in shop-floor conditions, such as MT geometric error, temperature variation, probing system, vibrations and dirt. Thus, the traceability of a measurement process on an MT is not guaranteed and measurement results are therefore not sufficiently reliable for self-adapting manufacturing processes.

On-MT measurement functionality is particularly required by large parts with critical tolerances, such as shipbuilding, nuclear power, aerospace, large science facilities, large optics or wind power that need complex and accurate components that demand close measurements and fast feedback into their manufacturing processes. Mainly, for large-scale manufacturing scenarios where manufactured parts have to be measured in-situ or in-process, the integration of the measurement process into the MT can improve the process efficiency by preventing the workpiece from being carried to a temperature-controlled measuring room.

The aim of this PhD study is to generate new knowledge for traceable CMM measurements on MTs, but there are some key differences between a CMM and an MT, mainly because CMMs are designed for measurement purposes and MTs are focused on manufacturing production. The main problem when executing a measurement on an MT is that the machining and measuring processes are performed using the same machine, and some error sources, therefore, cannot be distinguished if a calibration process is not realised before the measurement execution. This is currently the main limitation to close the calibration chain for on-MT measurement.

In parallel, this PhD study has been performed within the LSST project. It is a new kind of telescope, currently under construction in Chile that aims to be built to rapidly survey the night-time sky. From its mountaintop site in the foothills of the Andes, the LSST will take more than 800 panoramic images each night with its 3.2 billion-pixel camera, recording the entire visible sky twice each week. Making a parallel with a large CMM, the LSST is a high accuracy sky measurement machine and therefore it is also affected by a measurement error. Thus, the uncertainty budget characterisation of the telescope is within the scope of this PhD study.

1.1 Motivation

The main motivation to undertake the research presented within this PhD study is the knowledge gap concerning the use of MTs for traceable CMM measurements and the great opportunity that exists nowadays to improve the current state of the art with the latest developments within the metrology field. In fact, the technology to run an MT working as a CMM already exists, such as TTPs and measurement software for MTs, but there are several factors that affect the on-MT measurement which leads to a lack of a metrological traceability chain, which in turn means a lack of reliability of the manufacturing process. Thus, the closed calibration chain of on-MT measurement is the main scientific objective within this thesis that shall be accompanied by the development of rules and standards to guide MT traceable measurements to industrial adoption. This PhD study proposes that the guidelines for the traceability of CMMs are adapted to the challenges of an MT, such as the ISO 15530-3 technical specification and the VDI 2617-11 guideline.

Personally, 10 years of professional experience within the industrial metrology field, mainly in LSM applications, provides an overview of the current limitations that the technology faces on several applications. Global megatrends such as the efficient use of natural resources and the continued globalization do not only influence daily life but also affect any industrial sector. Some of the rapidly growing industries of the last two decades can be found in the fields of energy and mobility. Applications in wind energy, aerospace, the industry of science and automotive require an increasing number of sophisticated and individualized large components with critical tolerances. Thus, the quality inspection of these components often faces the limits of manufacturing and production metrology. The trade-off between increasing workpiece dimensions and constant or even decreasing tolerances and the necessity of making measurements in uncontrolled environments greatly complicate accurate and traceable LSM. Having worked with some of the most important local industry players performing the dimensional quality control of their components, such as: wind energy and aeronautic components, telescope assemblies or large-scale high-accuracy machined parts; this PhD study provides the author with the opportunity to update and enhance his knowledge; and also, to continue adding value to the manufacturing industry. Finally, the LSST project has also been a great opportunity for the author to participate in a unique scientific challenge and contribute to the state of art of LSM.

1.2 A literature review of on-MT measurement

The MT industry is characterized by its family-owned SME dominated landscape, strong concentration on flexible and small-batch production of custom-built and high precision machines, and the export orientation of companies. Product features such as precision and accuracy are far more important than unit labour costs in a technology-intensive sector such as MTs, as a source of competitive advantage [1]. High-tech MT builders seek for differentiation and sources of uniqueness by creating value for their customers through the development of new processes, functionalities and services which help achieve high productivity levels, meet the precision needs of their customers and help lower their costs, looking for a positive impact on the OEE indicator of their customers, the MT users.

Flexible manufacturing processes for high-quality products at low costs are one of the main research objectives in the field of production technology in industrialized countries [2–4]. Nowadays, the quality inspection of high-value components usually takes place on a CMM, either beside the production line or in an isolated measurement room, so the manufacturing processes are interrupted and transportation, handling and the loss of the original manufacturing setup influence the workpiece quality. The high invest for a CMM and the mentioned influences show the need for an MT integrated traceable measuring process for product's quality assurance. Thus, the MT industry major players, either manufacturers or users, are looking for traceable on-MT measurement functionalities to improve the impact on the MT OEE and improve their KPI across the manufacturing plant.

1.2.1 Benefits and Limits of on-MT Measurement

Dimensional measurements can be employed at different stages of the manufacturing cycle [5]: a) monitoring of the MT geometry performance by employing a calibrated standard; b) workpiece setup on the MT coordinate system; c) in-process measurements to provide correction values for the manufacturing process; and d) the performance of a final metrology validation of the finished product for final quality inspection as well as statistical trend analysis of the manufacturing process. Figure 1-1 shows the general concept of on-MT measurement.

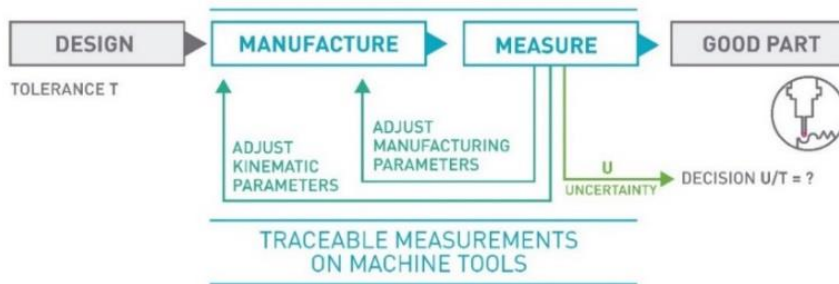


Figure 1-1 On-MT measurement scenario. [6]

In this way, the top four reasons and benefits of on-MT measurement could be listed as follows [4]:

- a) Monitoring MT performance: MT geometry may change during machining operation due to many reasons. By applying an appropriate in-process measurement method with the TTP integrated within the MT, geometry changes can be measured. These changes can be monitored to avoid making bad parts and to optimally schedule machine maintenance [5]. Figure 1-2 shows the monitoring of MT performance based on a 3D ball-standard.



Figure 1-2 Monitoring of the MT performance. [6]

- b) Part setup: Part cutting programs are created based on an assumed workpiece holding coordinate system. Especially for large parts such as the case for aerospace or automotive applications, this process could take a long time. For small part manufacturing and multi-operation processing, precise part locations could be detected automatically. This would reduce both the setup time and the processing time as parts could be cut from optimally size blocks [5].
- c) In-process measurement: One of the main reasons for performing a metrological measurement [2] of a manufactured part is to provide correction values to manufacturing parameters based on any deviations from the target dimensions found. Having this capability directly on the MT allows to feedback these metrological data to the MT controller allowing an automatic flexible manufacturing process. This could

be done several times during the manufacturing process, and not just at the end, in order to optimize the part cutting process [5]. Figure 1-3 depicts a tactile on-MT probing example.

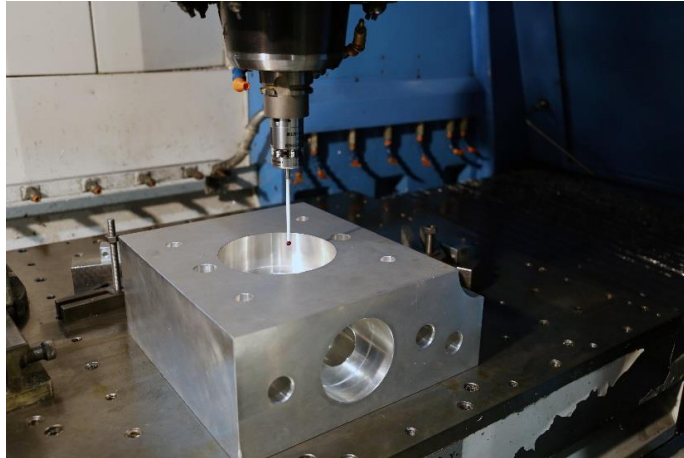


Figure 1-3 Tactile on-MT probing. [6]

- d) Post-process control: Programming and running a manufacturing machine as if it were a CMM for in-process measurement generates complete inspection reports without additional effort. For large part manufacturing, moving the part to an external CMM may not even be an option. For mass production, just measuring a few control features would not only generate inspection reports for all the parts but also provide a statistical view of the manufacturing process. In addition, it would help to create historical data monitoring for intelligent process control which is aimed within the Industry 4.0 initiative [7].

Although on-MT measurement can supply advantages for more flexible and intelligent manufacturing processes, limitations should also be known to make optimal use of it[8,9]:

- e) MT time: The natural limit of on-MT measurement is given by the time spent on the MT doing measurements. It is known that MT time is more expensive than CMM time, so the measurements done on an MT should clearly add value to the manufacturing process.
- f) Lack of MT accuracy: MT accuracy is affected by many error sources that change the geometry of the machine's structural loop. As explained in the ISO TR 16907 technical specification [10], there are different compensation possibilities to enhance MT geometric accuracy.
- g) Lack of MT traceability: Another limitation is given by the lack of traceability of the MT as a CMM. Both machining and measurement operations are performed at the same machine, so if the MT's geometric error is repeatable, both processes may observe the same geometric error on the measurand.
- h) Metrology software insufficiencies (real-time performance): Currently software employed in the MT is insufficient for metrology purposes. To perform the complex mathematical calculations required for metrology-based real-time decision making, a powerful metrology software needs to be integrated within the manufacturing system.
- i) Changing environmental conditions: Industrial environments normally suffer from unstable conditions, so it becomes a challenge to reduce measurement uncertainties with unfavourable measuring conditions.

1.2.2 Converting an MT into a Traceable CMM

Some research works focus on the idea of using an MT for traceable CMM measurements: In 2010 Schmitt et al. proposed that a large MT could be employed as a comparator to measure the geometry of large-scale components during the manufacturing process [11]. In 2013, Schmitt et al. also presented a research work where a specific workpiece was manufactured and calibrated on a CMM for several on-MT measurement experimental tests [3]. In 2015, Schmitt et al. went a step further presenting an approach on the uncertainty assessment for on-MT measurement according to the VDI 2617-11 guideline, they define an MPE [2] for MTs to assess the systematic error of the on-MT measurement error budget. Recently, Holub et al. and Uekita et al. presented a capability assessment for on-MT measurement assisted by an external laser interferometer [12,13].

The main problem of CMM measurements performed on an MT is that the machining and measuring operations are performed at the same machine. Therefore, both processes may observe the same geometric error on the measurand, which leads to the disadvantage that geometric error of the measurand may not be observed if a previous geometric error characterisation of the MT is not performed. In addition, repeatability can also be a big challenge for a traceable on-MT measurement where the non-controlled shop floor environment becomes a major uncertainty source. Researchers have recognized that environmental temperature has a significant impact on the thermal error of the MT and therefore, on any metrology activity performed on it [14–19]. Hence, time and space-dependent thermal effects become the dominant uncertainty source for the measurement of large-scale measurement scenarios [4,20].

Schmitt et al. [2] propose two main alternatives to convert an MT into a traceable CMM, the scheme of which is shown in Figure 1-4. The first approach increases the process capability by a volumetric calibration and compensation. It means that a calibration process is done prior to the manufacturing and measuring processes. However, this approach does not ensure that thermal effects do not affect the compensated MT. Achievable accuracy can be compared to large CMMs. The second approach applies an external high-precision metrological frame to TCP position monitoring in real time. This option requires a line of sight between the measuring tracking interferometers and the TCP, which cannot be ensured when the workpiece is on the MT. Moreover, this option is very sensitive to dirt and dust. The current cost of the solution is very high since four tracking interferometers are needed at the same time. However, it offers the possibility of being a self-calibrating system and represents a scalable measuring solution.

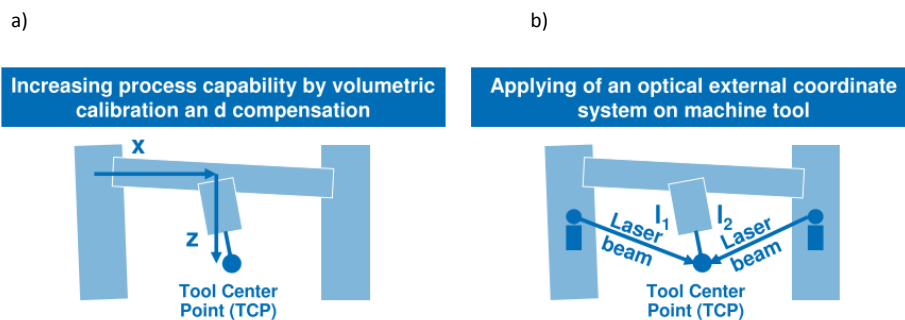


Figure 1-4 WZL RWTH Aachen approach to convert an MT into a CMM, a) previous volumetric calibration approach and b) external and real-time metrology framework. [11]

Currently, the first approach is under research, where the MT geometric error reduction is of particular importance. Although the first approach is being researched in detail, Wendt et al. presented a high accuracy large CMM called M3D3 based on the second approach [21]. In this case, four accurate tracking interferometers are employed for large part calibration directly on-site in production. Schwenke et al. also presented an independent traceable metrology solution for MT measurement, based on integrated length monitoring lines on an MT [9].

Measurement in a shop floor rarely takes place in a temperature-controlled environment which means that it is not enough to just measure and compensate geometric errors of the MT, but it must be accompanied by an understanding of how the MT changes. Time and space-dependent dimensional and gravitational drifts on both MT and the measurand shall be either compensated dynamically or be considered on the uncertainty budget for traceability assessment of on-MT measurements.

1.2.3 Approaches to determining the measurement uncertainty on an MT

Due to the similarity between a CMM and MT, some of the methods for a correct assessment of uncertainty in a CMM are adopted for MTs. The general guide for a suitable evaluation of measurement data is given in the ISO Guide 98-3: 2008, on the GUM [22]. Three different approaches are considered for the uncertainty assessment of the CMM measurements performed on an MT:

1.2.3.1 ISO 15530-3 technical specification

The first approach as described in the ISO 15530-3 technical specification is a method of substitution that simplifies the uncertainty evaluation by means of similarity between the dimension and shape of the workpiece and one calibrated reference part. Furthermore, the measurement procedure and environmental conditions shall be similar during the evaluation of the measurement uncertainty and the actual measurement [23]. Due to the similarity requirement between the machined workpiece and the calibrated part, this approach is very tedious and expensive for large components. However, it is a suitable approach for small and medium-size uncertainty assessment exercises where it is affordable to manufacture and calibrate a reference part for uncertainty assessment purposes.

Across the EURAMET research project TIM [24], high precision and robust material standards were developed, not just for mapping the geometric errors of MTs in the harsh environment of the production floor but for determining the uncertainties associated with task-specific measurements, such as size, form and position measurements for different geometrical shapes such as sphere, cone, cylinder and plane [25–31] by a procedure adopted from ISO 15530-3 technical specification [23].

1.2.3.2 ISO 15530-4 technical specification

The second approach is based on the ISO 15530-4 technical specification, a method that is consistent with GUM to determine the task-specific uncertainty of coordinate measurements. It is based on a numerical simulation of the measuring process allowed for uncertainty influences, where important influence quantities are considered [32]. For that purpose, CMM suppliers, research companies and NMIs as PTB and NPL created a UES which is based on Monte-Carlo simulation of the error behaviour of a real CMM [33,34]. In recent years, VCMM-Gear and VLT have been developed but they have not been integrated into a manufacturer software yet [35]. Nowadays, some research activities are focused on transferring the VCMM concept to VMP [4,36].

1.2.3.3 VDI 2617-11 guideline

The third approach is as stated in the GUM and the VDI 2617-11 guideline. In this case, uncertainty evaluation is done based on an uncertainty budget where the budget should comprise the uncertainty sources that affect the measurement processes and the correlation between them [37]. Thus, a correct assessment of the measurement uncertainty requires contributions from the measurement system, from the component under measurement and from the interaction between them [4,37]. Currently, this approach is being considered for large-scale uncertainty assessment. Schmitt et al. are developing a software-based solution for uncertainty evaluation for large on-MT measurement [2].

In conclusion, for small batch production, mainly in large scale manufacture, the substitution method is not an affordable solution because a calibrated workpiece similar to the manufactured part is needed. This requirement makes the solution expensive. Therefore, the uncertainty budget-based solution is being adopted for the on-MT measurement of large workpieces. For serial production, usually, for small and medium-size components, the substitution method simplifies uncertainty evaluation. Thus, task-specific uncertainty can be assessed.

1.2.4 Uncertainty error sources affecting the on-MT measurement

The uncertainty budget for on-MT metrology should comprise contributions from the measurement system—i.e. the MT itself (Section 1.2.5) with the TTP (Section 1.2.6) and the measuring software (Section 1.2.7), from the component under measurement (Section 1.2.8) and the interaction between both of them [2,38].

The ISO 10360-1 international standard [39] defines a CMM as a measuring system with the means to move a probing system and the capability to determine spatial coordinates on a workpiece surface [40]. Due to the similarity between a CMM and an MT, some of the methods for a correct assessment of uncertainty in CMMs are adopted for MTs. However, there are some key differences between a CMM and an MT, mainly because a CMM is designed for measurement purpose and an MT is focused on manufacturing production. For that reason, here an error budget approach will be proposed for on-MT measurement uncertainty assessment.

As stated by Slocum, MT errors can be divided into systematic errors and random errors [41]. While the former can be measured and compensated, the latter is difficult to predict. Therefore, an MT should have three main properties: accuracy, repeatability and resolution [42]. Figure 1-5 represents the errors sources of an MT according to the described criteria.

In addition, an error budget is a fast and low-cost tool to predict the accuracy and repeatability of an MT [42]. Hence, drawing a comparison between design and measurement purposes, an error budget will be established, where each component will be comprised of:

- Accuracy: Systematic geometric errors of the MT (induced by kinematic errors, static loads and control software), TTP errors and measuring software errors are considered. The accuracy will mean the systematic error of the MT as a CMM, so it could be characterised and compensated to a high extent.
- Repeatability: Random error sources that affect the repeatability of the MT. Dynamic loads that affect the MT (such as backlash, forces and thermo-mechanical loads) and environmental influences that affect either the MT or the TTP are considered. Repeatability will mean the random error of the MT as a CMM, so it is difficult to measure and compensate.

- Resolution: Quality of sensors and quality of control system are considered.

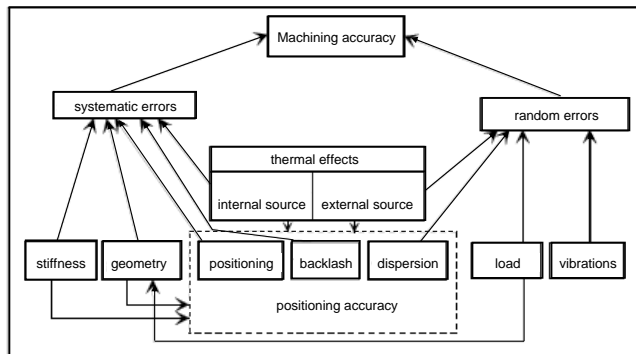


Figure 1-5 Total error sources of MTs. [6]

1.2.5 Error sources on the MT side

1.2.5.1 Geometric errors

Either for a CMM or an MT, geometric errors to be considered are relative motion errors between the end effector and the object under measurement. Geometric errors can be measured and compensated when both the MT and the measurement procedure have high repeatability so that the systematic errors can be reduced and not be considered into the uncertainty budget of on-MT measurement [8].

There are several error sources that affect systematically to the accuracy of the relative end-effector position and orientation [8,43–46]:

- Kinematic errors: Kinematic errors are errors due to imperfect geometry and dimensions of the machine components as well as their configuration in the machine's structural loop, axis misalignment and errors of the machine's measuring systems [8,47–52].
- Static loads: In the case of static errors, non-rigid body behaviour shall be considered. Location errors and component errors change due to internal or external forces. The weight of the workpiece and the moving carriages can have a significant influence on the machine's accuracy due to the finite stiffness of the structural loop [8,53].
- Control software: The effect of the control software on the geometric error of the MT could be considerable. Hence, different speed and accelerations can be applied for a known motion path to make control software errors distinguishable. Anyway, the measurement process is usually executed at small feed speeds, so dynamic forces are usually not considered as an error source on the on-MT measurement uncertainty budget [8].

In practice, the interaction between these effects plays an important role in the overall system behaviour. Here the research is focused on the overall system behaviour, which means the systematic geometric error of the MT [8].

1.2.5.1.1 Description of geometric errors

Under the assumption of the rigid body behaviour, each movement of a machine axis can be described by six components of error, three translations and three rotations. As stated in ISO 230-1 standard [54], the six component

errors of a linear axis are the positioning error, straightness errors, roll error motion and two tilt error motions. For a rotary axis, the six component errors are one axial error motion, two radial error motions and the angular positioning error. Moreover, location errors are defined as an error from the nominal position and orientation of an axis in the machine coordinate system. In general, for a linear axis, three location errors are considered, while for a rotary axis five location errors are considered [8,54].

1.2.5.1.2 Mapping of geometric errors

Currently, there are different technologies and measurement methods to characterize all the geometrical errors of a serial kinematic configuration machine. As stated by Schwenke et al. [8,54] “direct” and “indirect” methods can be distinguished. While direct methods allow the measurement of mechanical errors for a single machine axis without the involvement of other axes, indirect measurements require from the movement of multi-axes of the machine under characterisation.

1.2.5.1.2.1 Direct Measurement Methods

As stated by Uriarte et al. [55], direct measurement methods allow measuring the component of errors separately regardless of the kinematic model of the machine and the motion of the other axes. Direct measurement can be classified into three different groups according to their measurement principle:

- Standard-based methods, such as straight-edges, linear scales, step gauges or orthogonal standards [27,54,56–59]. Such artefacts contribute also to the uncertainty of the measuring results. This is why their own calibration uncertainty should be as low as possible. However, this is not always reachable, mainly when considering the longest ones and the newest highly accurate MTs. Nonetheless, as concluded by Viprey et al., most of the existing material standards are developed for CMM calibration, except ball plates, 1D-ball array and telescopic magnetic ball bar [27], which are suitable for MTs.
- Laser-based methods or multidimensional devices, such as interferometers or telescope bars [60–63]. They are usually applied in order to measure principally the machine positioning properties, because of the suitability of the laser wavelength for long length measurements, due to its long coherence length. The most used is the laser interferometer which, with different optics configurations, allows detecting position, geometrical and form errors.
- Gravity-based methods that use the direction of the gravity vector as a metrological reference, such as levels [54,64].

While direct measurement methods are frequently employed in small and medium-size MT, they are rarely employed for large MT where they are very time-consuming and have strong limitations for a volumetric performance characterisation [55]. However, there are some measuring scenarios where direct methods offer advantages compared with indirect methods, such as:

- In small and medium-size working volumes direct measurement of an error can approximate the geometric behaviour of an MT.
- Specific error motion shall be checked in a very specific line or position. This is depicted in Figure 1-6.
- Specific verification protocol shall be applied for a machine’s acceptance.

- Iterative “measure and adjust” type of work, which can be needed for the component assembly operation.
- Results required in real time.
- High accuracy requirement for a specific application.

For the direct measurement of the positioning errors, calibrated artefacts (step gauges, gauge blocks, line scales and calibrated encoder system) or laser interferometers are applied as a metrological reference aligned to the axis of interest [8,54,65]. The most accurate/time-consuming approach for either short or long machine axis is the use of laser interferometers. Nevertheless, some error sources shall be considered for a correct length measurement:

- Errors in laser wavelength (environmental factors, such as temperature, pressure, humidity and density influence the wavelength compensation).
- Beam deflection shall occur due to temperature changes and gradients.
- Misalignment between interferometer and axis of motion can cause Abbe errors.
- Any movement of the equipment during the measuring process.

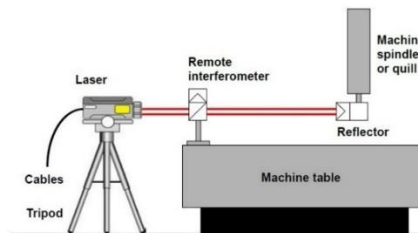


Figure 1-6 Direct measurements of positioning error through a laser interferometer. [6]

Straightness errors of the machine axis can be measured by any of the three measuring principles previously mentioned. For large MTs, the most practical way to evaluate straightness is to utilize the direction of gravity as a reference. Thus, an electronic level is placed on the head of the MT and a reference level is fixed to a non-moving part to distinguish movements of the machine [8]. Measured angle over the stepwise displacement is integrated to get the straightness as a result. However, the linear propagation of a laser interferometer is the industry-leading method for large-size MT straightness measurement. In this case, a Wollaston prism acts as a beam splitter and the lateral displacement is calculated from two separate beams that exit the prism at an angle [65,66]. For small and medium-size MT, a standard-based method is commonly applied. Hence, a displacement indicator (capacitance gauges, electronic gauges or material dial gauges) is fixed to the machine head and it detects lateral displacements along the direction of the axis travel [54].

For large MTs and large volume applications, where straightness reference should be long and flat for a long range, a taut wire technique can be used as a straight reference to overcoming the limitations of previously mentioned methods [8,67,68]. Even though it has been an extended applied method for very large MTs and applications such as CERN components and assemblies [69], the main reasons why this method is not widely used at accurate large MTs are its low accuracy and inefficient data gathering methods. Another approach under investigation for straightness measurements on large volume applications is the use of a laser beam as a straight reference and a PSD as a pointing sensor unit. Generally, the use of a laser beam as a straightness reference is highly critical in normal shop floor environment, because local and global temperature gradients, as well as air turbulence, may have a high

influence on the straightness of the beam. Therefore, this method is mostly used for axes length below 1.5 metres, where the influence in most cases is sufficiently small. The pointing stability (thermal drift) of optical straightness setups can also be a major source of uncertainty [6,70]. Figure 1-7 shows beam deflection according to measuring conditions.

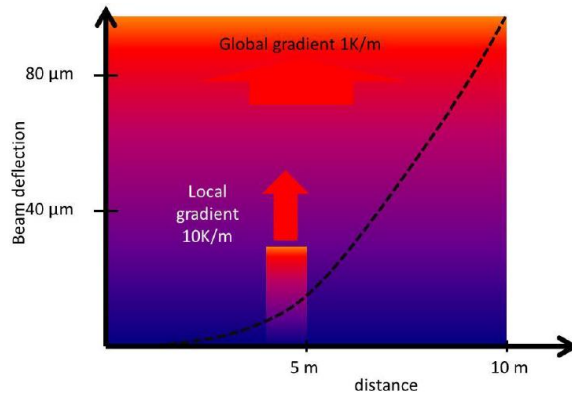


Figure 1-7 Bending of a straightness reference beam due to local and global gradients. [6]

The main approach for squareness measurement in small and medium-size MT is to employ a granite or ceramic standards with a displacement indicator fixed on the MT head according to the measuring procedure stated in ISO 230-1 standard [54]. Nevertheless, the main disadvantage of this approach for large MTs is that large and heavy standards are required to verify squareness in large machines. In addition, laser interferometry can also be employed for this purpose but the setup of the laser source and the prism are also very challenging for the squareness error measurement [8].

To measure angular errors in any translation movement either the use of electronic levels or laser interferometer-based-techniques are performed. When applying interferometry, two laser beams are generated with a beam splitter so the angular deviation results in a path length difference of the two beams, but the setup of the measuring system can be very challenging for a correct error assessment in a large axis. In the case of electronic levels, they do not depend on an optical path, so they are suitable for the measurement of long strokes in unstable temperature environments. A limitation of electronic levels is that they cannot measure rotations around the gravity vector. For this purpose, in small and medium-size axes, an autocollimator is usually employed. A collimated light beam is aligned to the machine axis where a mirror is fixed. The reflected beam travels back to the autocollimator where rotations are measured either visually or through a PSD sensor. However, the unique direct technique to measure the rotation around the axis of motion is based on the use of electronic levels, since an autocollimator or laser interferometer cannot measure this rotation directly [8].

The ISO 230-1 standard describes an affordable method for the calibration of rotary axes [54]. Displacement indicators are fixed to the centre hole of the rotation axis to measure the radial and axial run-out deviations. For the radial and axial error motions, three or more sensors are needed to be placed on such a way that errors are measured with a linear indicator. If multiple linear indicators are applied, a single measurement combination can be enough for the measurement of the five degrees of freedom [71–73]. For the positioning error of the rotation axis, the most practical approach is to use laser interferometry combined with a self-centring device and the proper optical optics

for angle measurement. This approach is commonly employed in large MTs with a rotary table, the measuring range is around $\pm 10^\circ$ and the resolution is better than 0.01 arcseconds [72].

Recently, multidimensional laser interferometers have been introduced to measure more than one dof simultaneously. Thus, several error components of an MT axis are determined with a unique measurement system setup through direct measurement methods. This measuring solution offers two main possibilities in the near future. On the one hand, measuring time is reduced to a far extent because different setups and measuring systems are not required anymore. On the other hand, the possibility to be embedded into an MT, where TCP position could be monitored in real time by monitoring six dof of each machine movement at the same time, with several measuring systems performing all at once.

In fact, there are two main multidimensional solutions [74–76] and the main difference between them is based on the straightness measurement principle. The first solution is a multi-interferometer-based solution, where a unique interferometer source is divided into three beams to get a five dof measurement laser interferometer. The second solution employs the laser beam as a straight reference and a PSD as a pointing sensor unit to measure straightness. Therefore, the second option is suitable for small and medium-size MT, but not for large MTs [70]. The principle used by the first solution is explained in Figure 1-8.

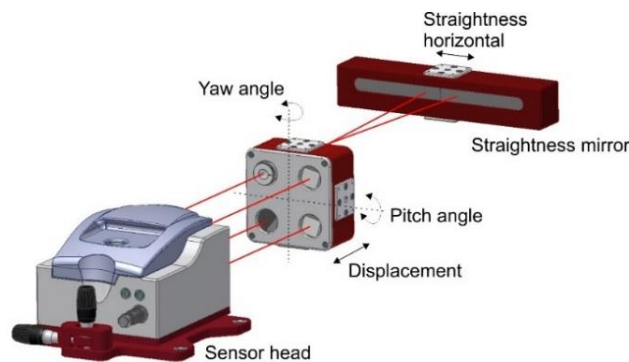


Figure 1-8 Multidimensional equipment for five dof. [6]

As above-mentioned, direct methods are very time-consuming and have strong limitations for large MTs volumetric performance assessment. As explained by Ibaraki et al. [77], for volumetric error compensation, the efficiency of the direct measurement can be a critical issue. In that sense, indirect methods have the advantage of offering fast and reliable volumetric error mapping and compensation possibilities and take less time than direct measurement.

1.2.5.1.2.2 Indirect Measurement Methods

Indirect methods produce a global correction of errors and require less time than direct measurement. They are based on the multi-axis movement of the MT under test and can be broken down into two main possibilities [77]:

- Indirect measurement for orthogonal linear axes.
- Indirect measurement for five-axis kinematics with a rotary axis.

As stated by Ibaraki et al. [77] there are different procedures and technologies for linear axis indirect characterisation:

- Circular tests: The circular test, described in the ISO 230-4: 2005 standard [78] describes a procedure for the characterisation of indirect measurement of the geometric accuracy of two orthogonal linear axes. It is usually performed by a ball-bar, but it can also be performed by a laser tracer or two-dimensional digital scale [8].
- Diagonal and step-diagonal test: As described in ISO 230-6: 2002 standard [79], it allows the estimation of the volumetric performance of an MT, but it is not possible to identify the 21 components of geometric error from four body diagonal measurements only. Hence, this test is usually employed for linear scale and squareness error calculation [80]. It is suitable for fast verification of MTs.
- Measurement of artefacts: The use of calibrated artefacts is widely employed either for MT calibration or CMM calibration. As described by Cauchick-Miguel et al. [57], artefact-based calibration is employed with one dimensional, two-dimensional and three-dimensional artefacts. The three-dimensional artefact is widely employed mainly in a CMM calibration for 21 component of geometric error measurement [81] where a pre-calibrated position of spheres are measured by the machine for error characterisation. Figure 1-9 shows a CMM characterisation process for VCMM error assessment on a ZEISS UPMC CARAT 850 CMM at IK4-TEKNIKER research centre premises. Since almost every MT integrates a touch probe nowadays, MT builders are looking for fast calibration procedures based on the measurement of artefacts, as it is shown in Figure 1-10.

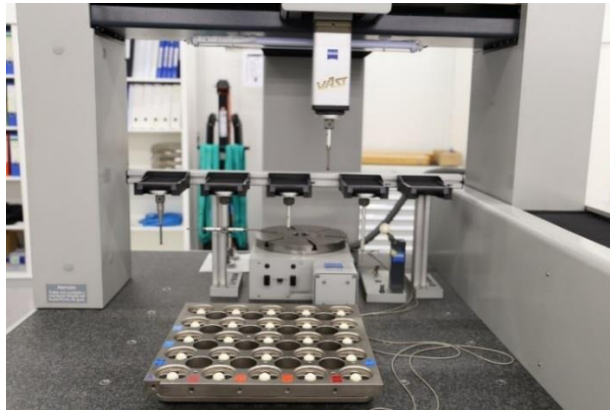


Figure 1-9 3D artefact for VCMM characterisation. (Zeiss UPMC Carat 850 CMM at IK4-TEKNIKER premises). [6]



Figure 1-10 Artefact measurement-based MT characterisation.

- Passive links: Calibrated kinematics of the link mechanism attached to and passively driven by the machine to be measured can be used as a reference [77]. Different link configurations are employed nowadays, either serial links with three orthogonal linear axes or parallel links configurations.
- Tracking interferometer: Tracking interferometers, such as laser trackers or laser tracers can be employed for indirect error measurement. Laser trackers can directly measure three-dimensional position by measuring the distance and direction of a laser beam [82], but angular measurement uncertainty affects to the measuring uncertainty of the target position and it is rarely employed for MT error measurement. This is the main reason why multilateration-based measurement is applied for MT error mapping. In this case, the MT position is measured by the distance from at least four tracking interferometers to the target [83,84]. Either laser tracers or laser trackers are usually employed for that purpose. Figure 1-11 shows a sequential multilateration based scheme, where a tracking interferometer is fixed to the table and the MT or the CMM describes a volumetric path through a volumetric point cloud.

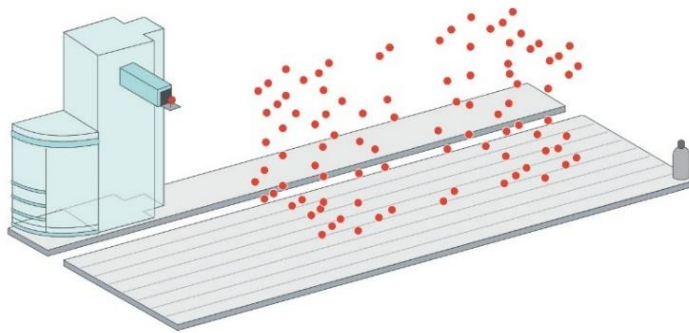


Figure 1-11 Tracking interferometer on a sequential multilateration combination approach.

For indirect measurement for five-axis kinematics with a rotary axis, there are also different measuring possibilities:

- Ball bar measurement: As described by Ibaraki et al [77], there are some standards such as the ISO 10791-1:2015 [85] and the ISO 10791-6:1998 [86] that define measuring procedures for indirect rotary axis calibration. The calibration of the rotary axis location with a ball bar is not solved yet and it remains a challenge.
- R-test: Another approach is to employ the so-called R-test to measure the relative movements between the machine and the workpiece side. A sphere is fixed to the machine table and a measuring sensor, based on three or more length displacement sensors, is coupled to the machine head [87–89]. The measurement consists of a sequence of discrete angles of the rotary table. When moving to the next measurement point the linear axes follow the rotation of the rotary table. At each position the probe head measures the relative displacement of the sphere in X, Y and Z direction simultaneously [87]. Compared to the traditional method that employs the “Siemens 996” static cycle to locate a rotary axis in the working volume of an MT, the R-test offers the possibility to do static and dynamic measurements [88].
- Measurement of artefacts: As explained for the linear axes indirect measurement, any MT has already on-MT measurement capability. This is the basis to the MT probing for the calibration of offset errors of

rotary axis [77] mainly within an approach based on a contact probe combined with several positions of a calibrated sphere on the MT table, i.e. the SIEMENS kinematics measuring cycle 996 [90].

- Machining tests: As explained by Ibaraki et al. [77], MT users are concerned with workpiece's final accuracy rather than MT accuracy. The NAS 979 [91] defines the procedure for a five-axis machining test of a cone frustum, which is widely accepted as a final performance test by MT builders.

However, multilateration-based approaches are by far the most used techniques to characterise large-size MTs nowadays [8,11,83,84,92–97]. The approach relies on interferometric displacement measurements between reference points that are fixed to the machine base and offset points fixed to the machine spindle, near to the TCP [98]. At least four measuring systems are needed for a complete volumetric verification but usually, only one measuring device is available, so in practice, multilateration measurements are usually done in a sequential scheme. Thus, machine movements are repeated several times and measurements are taken from different positions. If four measuring devices are available at the same time, simultaneous multilateration avoids some of the limitations of the sequential multilateration, such as total time consumption, MT repeatability requirement and MT drift due to thermal variation during the measuring process.

Several uncertainty sources shall be considered for a complete uncertainty assessment in a sequential multilateration process [94]:

- The measurable volume of the MT.
- Spatial displacement measurement uncertainty of the employed tracking interferometer.
- As stated by Aguado et al. [94], the number of measuring systems to be used and the arrangement of them.
- Repeatability of the measured points does not just depend on the repeatability of the machine itself. As far as the measuring time is extended, environmental influences (e.g. shop-floor temperature) generally lead to slow changes in MT temperatures affecting the whole volumetric performance. Therefore, time consumption is a crucial factor.

Currently, three tracking interferometers are being employed on the LSM field when applying multilateration with different displacement measurement uncertainty:

- Tracking interferometers based on optimized laser trackers. They rely on a high accuracy sphere as an optical reference for interferometric measurement. This measurement equipment, called laser tracer [84], was developed by NPL and PTB and commercialised by Etalon AG. It has a spatial displacement measurement uncertainty of $U(k=2) = 0.2 \mu\text{m} + 0.3 \mu\text{m}/\text{m}$ [99]. While laser tracer is a suitable solution for medium and large size MTs, there is a similar solution to the laser tracer, called "laser tracer MT", with a telescopic scheme and employed for maximum measuring volumes of 1 m^3 [100].
- An ADM-based laser tracker has a spatial displacement measurement uncertainty of $U(k=2) = 10 \mu\text{m} + 0.4 \mu\text{m}/\text{m}$ in its whole working range [101].
- An AIFM-based laser tracker has a spatial displacement measurement uncertainty of $U(k=2) = 0.4 \mu\text{m} + 0.3 \mu\text{m}/\text{m}$ [102].

The tracking interferometer employed for multilateration shall fit inside the measuring volume in order to execute the measurement procedure. Such a requirement restricts the tracking interferometer to be employed for any size

MT. For small size MTs, the equipment that suitably fits into the measuring volume is the so-called laser tracer MT, it makes use of a metrological beam guiding method of the laser interferometer [100]. For medium and large size MTs, either laser tracers or laser trackers are suitable for the error mapping. However, it should be stated that new laser trackers are portable devices that offer the possibility to be embedded into large manufacturing or measuring systems and they transfer data through an integrated wireless LAN communication [102] which allows to wireless employment of the acquisition technology.

In this context, different solutions have been developed based on a tracking interferometer and multilateration combination mainly for large MT geometric characterisation, where the volumetric performance of the MT is of special interest: Olarra et al. [97] showed an intermediate approach where linear components of error are measured with a laser tracker based on sequential multilateration. Hence, by combining the data coming from the different measurement systems, multilateration is applied to measure 3D positions with enough accuracy. Once that measured coordinates are calculated, they are compared with nominal positions and geometric errors of the MT are deduced from an analytical solution. Additionally, electronic levels are employed for the measurement of the two rotational errors along the two horizontal axes. A self-developed software makes it easier to synchronise data acquisition for both measurement systems and it allows to run the calculation to achieve the aimed volumetric performance of the MT [97]. This approach is similar to the approach described in the ISO 10360-2 standard where a calibrated artefact is employed for volumetric error determination [103,104].

Aguado et al. developed an approach where several commercial laser trackers are employed for sequential multilateration measurement [94]. The adopted technical solution is similar to the solution developed by Olarra et al, where laser trackers are applied to acquire information and multilateration is employed to sort out the mathematical issue. The biggest difference is that Aguado et al. do not use electronic levels for the measurement of the rotational errors of the MT.

Schwenke et al. presented a self-developed hardware and software solution for small to large size MT and CMM volumetric characterisation. The commercial laser tracer [99] is employed for point cloud acquisition and from the error of those points and the kinematic model of the machine it is possible to iterate to minimize the global volumetric error of the machine at considered points. For the measurement of angular errors, different orientation offsets on the spindle side are needed, which makes the verification more time-consuming. Nowadays, new configurations and ways of utilisation are appearing for tracking interferometers for MT and CMM geometric error characterisation. Etalon AG presented a solution called "Linecal" where several permanently installed measuring lines replace a motorized tracking and device conversion [105].

To sum up, it seems that interferometer-based non-contact measuring technology will guide the LSM into traceable MT metrology in the near future, mainly because the absolute distance measurements allow an easy handling in industry where purely interferometric length measurements depending on fringe counting are quite demanding due to the need of an unbroken line-of-sight between the measuring instrument and the reflector [4]. However, it shall be remarked that technology has some key limitations nowadays, such as:

- Thermal and refractive index distortions: The uncertainty of interferometry technique is proportional to the stability of the refractive index of air. Hence, the correct determination of this parameter is of utmost importance for achieving small measurement uncertainties on interferometer-based measurements.

However, industrial environments normally suffer from unstable conditions, so it becomes a challenge to reduce measurement uncertainties with unfavourable measuring conditions.

- Real-time: Real-time coordinate metrology is a requirement for a factory of the future where metrology and manufacture are integrated into a single engineering process that enables 'zero defects'.
- Dimensional traceability to the SI metre: It shall be ensured for any metrology-based solution in a factory environment.
- Automation: For a successful integration of the technology into machine and manufacturing processes, wireless and automation capacity shall be improved.

1.2.5.1.3 Compensation of geometric errors

Traditionally, the majority of MTs have been compensated along lines parallel to the moving axis and centred in the working volume, which is called positioning error compensation. The ISO230-2 standard and VDI 3441 guideline have been widely employed for that purpose and the most common measuring system for the positioning error mapping is the laser interferometer [106,107]. Going further, cross-error compensation considers the positioning error in addition to the straightness error in both directions and squareness error for a specific line within the MT volume. However, this approach is also considered a local approach because it does not consider the entire MT volume.

Volumetric error compensation allows the 6 dof errors compensation on the entire MT volume either for linear axes or for rotary axes [8] and it is the main reason why volumetric compensation was broadly introduced for CMMs compensation between 1995 ÷ 2000 years. Nowadays, it is being introduced by main MT controller manufacturers on three or even five-axis for MT volumetric compensation [55]. In general, methodologies based on the rigid body kinematics have been proposed [48,108] because the kinematic structure of an MT can be modelled with a kinematic chain and therefore, calculate the position and orientation of the tool in the workpiece coordinate system as the superposition of error motions of each axis [77]. The MT rigid body assumption simplifies the error mapping and compensation because it allows the motion to be implemented by a transformation matrix [109]. Nevertheless, in the case of large MTs, owing to their size, they suffer from remarkable thermal and mechanical deformations. In order to minimize this effect either on error mapping or compensation, special strategies shall be employed. In compensation, extra compensation factors for the deformation of some parts of the machine, such as column bending and tilt for moving column MTs and CMMs or table torsion factor for moving table CMMs, are considered [55,70].

Successful volumetric compensation requires quantified knowledge of MT geometry and long term repeatability but MT geometry changes due to temperature variation, either internal or external. This is the main reason why volumetric compensation faces some limitations [10,70]:

- Repeatability of the MT: Backlash errors and temperature variation (internal and external) lead to a lack of repeatability. Therefore, long term stability will not be improved.
- Use of long tools: The compensation of orientation requires from three orthogonal rotational axes, which only very few MTs offer. Compensation of angular errors remains a challenge.
- Model conformity: The majority of controllers assume a rigid body model behaviour of the MT in their compensation models. However, deformations such as column bending and tilt for moving column MTs or table torsion for moving tables CMMs does not fit to a 21-component error model. In these cases,

additional parameters shall be included in the compensation model. Therefore, if a model-based compensation is employed, it should be consistent with the MT real behaviour.

The ISO/TR 16907 technical specification [10] provides the information associated with the numerical compensation of geometric errors of MTs. It describes traditional compensation methods such as positioning and cross-error compensations and all the compensation possibilities within volumetric compensation. Figure 1-12 shows the potential improvement of the volumetric compensation for a large MT, it shows a space diagonal measurement before and after the volumetric compensation.

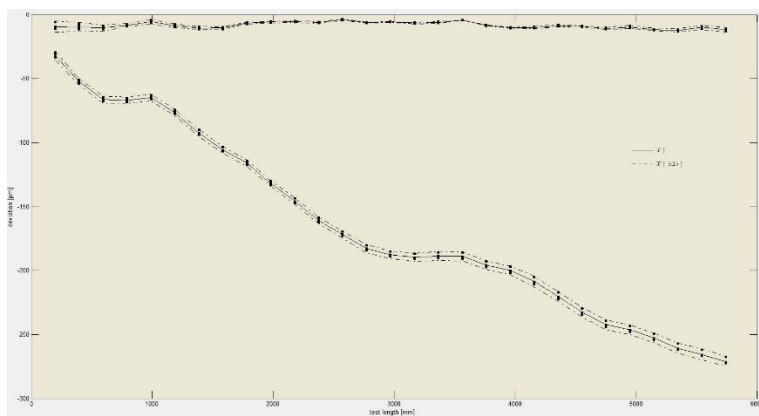


Figure 1-12 Space diagonal measurement before and after the volumetric compensation.

1.2.5.2 Dynamic errors

The repeatability of the MT, usually expressed as a standard deviation, is a part of any uncertainty budget and it is mainly affected by dynamic errors. As stated by Slocum, repeatability is difficult to predict and it is often more important to obtain mechanical repeatability because accuracy can often be obtained by the sensor and control system [42].

There are different error sources that affect to the repeatability of the MT working as a CMM: Dynamic loads that affect the MT (such as backlash, dynamic forces and thermo-mechanical loads) and environmental influences that affect either the MT or the touch probe are considered [8,42,44,46,49,110]. Between the dynamic loads that affect the MT backlash, dynamic forces and thermo-mechanical loads can be highlighted:

- **Backlash:** Backlash error is a position-dependent error affecting the contouring accuracy. When the axis changes direction from one side to the other, there is a lag before the table starts moving again, that would cause position error - backlash error [111]. Modelling it is challenging, because the multiple sources and complex behaviour. In general, the backlash vector depends on the motion history of all axes. It can result from mechanical play in drives and guideways, cable track forces, and stick/slip effects [8].
- **Dynamic forces:** Dynamic behaviour of the MT affects the aimed working path. Any varying behaviour, such as accelerations, varying forces, vibrations or machining forces are hard to measure and compensate [112–114].
- **Thermo-mechanical errors:** Internal and external heat sources combined with different expansion coefficients of machine part materials generate a thermal distortion of the machine's structural loop

which can affect to the accuracy of the measuring process [115–117]. Expansion coefficient differences may lead to thermal stresses if rules of exact constraint design have not been met carefully.

Apart from the dynamic loads affecting the MT, dynamics error sources coming from the touch probe should be also considered. Deviations from the reference temperature of 20°C lead to thermal expansion or shrinkage of the measuring probe. In addition, temperature variations either inside the workpiece or the stylus can cause effects like bending. Vibrations may affect the measurement result because it causes a deformation in the metrology loop between the probe tip and workpiece. As explained in the previous point, any varying behaviour is hard to measure and compensate, so they contribute directly to the uncertainty of on-MT metrology [118].

In this scenario, the overall system behaviour is of interest. Some error sources, such as dynamic forces or internal heat sources, lead to a fast change of the structural loop that is very hard to measure and compensate. However, there are other error sources such as environmental temperature or simple backlash errors that induce a quasi-static geometric error of the MT that can be monitored and assessed. In fact, quasi-static errors are one of the most important error sources for large scale precision manufacturing [4].

1.2.5.3 Quasi-static Error Assessment and Monitoring

The aim of some international research projects, such as the “Light-controlled factory” or LUMINAR and TIM, is to tackle several fundamental issues affecting users of LSM equipment and techniques in industrial environments [119,120] where non-controlled conditions affects. A strong evolution of the interferometry-based technology seems to trace the roadmap for the future research of LSM in the industrial environment.

Peggs et al. [82] rely on ADM technology as distance measurement principle for future error mapping and monitoring technology. Achievable uncertainty with an ADM (typically 10 mm + 0.4 mm/m) is already being reduced so it is becoming similar to the conventional IFM embedded into laser trackers (typically $\pm 0.4 \mu\text{m} + 0.3 \mu\text{m}/\text{m}$) [102]. Consequently, for the built-in displacement device, increasingly ADM is used beside the IFM in commercial laser trackers [4]. While IFM can determine relative distances with accuracies on the nanometre level almost instantaneously, which makes IFM suitable for dynamic measurements, ADM measures absolute distances. However, ADM technology cannot perform dynamic measurements because it must deal with integration times, the time required to perform the operations that determine the target’s position [121].

Hughes et al. [92] mentioned the extension of the application of interferometry-based technology, which is not only used as a dependent measuring unit but also in the multilateration applications, for CMM and MT calibration. An external metrological frame is implemented as a virtual reference based on lengths measured with tracking interferometers. The target positions are calculated using the length measurements with the multilateration principle [21].

Based on ADM technology, multiline technology developed by the University of Oxford is a dynamic FSI system scaled up to make many hundreds of measurements for only a small fractional increase in cost compared to laser tracer technology, simply by using multiple interferometers whose components are cheap [122]. Despite not having a real-time capability (functionality that is under research), this technology allows monitoring large components and structures within an accuracy of 0.5 $\mu\text{m}/\text{m}$. Measurement range is up to 20 m. It is currently being used in the LSM field for monitoring of long-time stability, deformation by temperature; workpiece weight and foundation drift in many applications [122,123]. An example application can be seen in Figure 1-13.

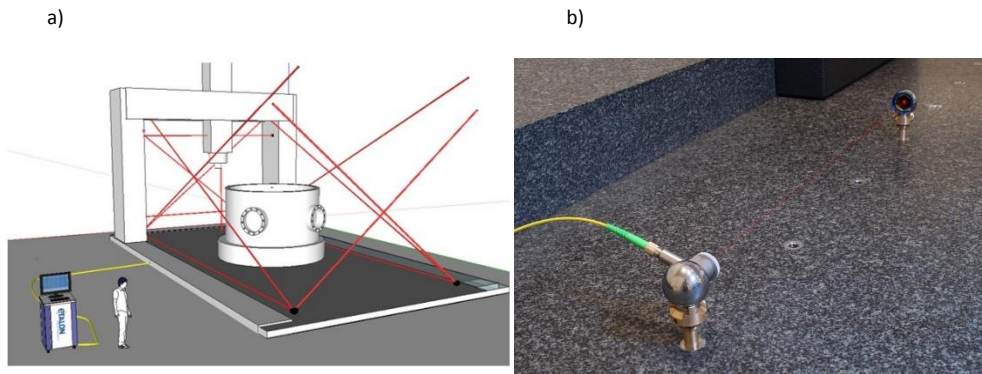


Figure 1-13 Multiline technology, a) example on a large MT and b) a unique line measurement technology. [6]

As an evolution of the multiline system, a system based on divergent FSI is under development at NPL for real-time coordinate metrology for a factory environment [124]. The measuring system comprises several sensor heads that are placed within the MT volume. Measuring targets, either on the MT or the component under measurement, are defined by spherical retroreflectors. Each sensor head is able to measure absolute distance to multiple targets simultaneously using the mentioned FSI principle. The traceability is ensured through a gas absorption cell embedded into the system and it is used to determine the scale factor for the FSI based distance measurement.

To overcome thermal and refractive index distortions in large volumes, a tracking refractive index compensated interferometer for absolute length measurements, the ‘3D-lasermeter’, has been developed by PTB within LUMINAR project [119]. It combines the absolute distance measurement by multi-wavelength interferometry, the compensation of the refractive index of air by using the dispersion between two wavelengths, and the tracking capabilities of laser tracers.

More practical approaches are presented nowadays. Schwenke et al. present a multilateration-based continuous data acquisition solution (on the fly) where calibration is speeded up significantly by a continuous measurement at a constant speed. This option permits to increase the number of sampling points and reduce drastically the measurement time, allowing the measurement of quasi-static errors of MTs [99]. However, the measurement process cannot be automated entirely because multilateration is executed in sequence and the device is located by hand. Gomez-Acedo et al. propose an automatic approach for fast measurement of thermal distortion on large MTs based on an automatic multilateration measuring procedure [125]. A multilateration scheme is conducted using a single laser tracking device positioned on top of the machine table which moves automatically. As depicted in Figure 1-14, the YZ plane is measured with a sampling period of 20 min during a thermal cycle of 5 h. Nowadays, Oliver Martin et al. present a similar solution called “Baseline” where a LEICA AT960 laser tracker is fixed to a rotary plate to verify the volumetric error map of a large MTs [126]. In addition, Ibaraki et al. [127] present a similar approach where the identification of 2D geometric errors of linear axes by single-setup tests is aimed.

A mobile climate simulation chamber was developed within the mentioned TIM project in order to simulate the variety of influencing factors related to harsh environmental conditions in shop floors [128]. Thus, it is possible to imitate a variety of environments and research the behaviour of an MT and on-MT measurement functionality under these influences.

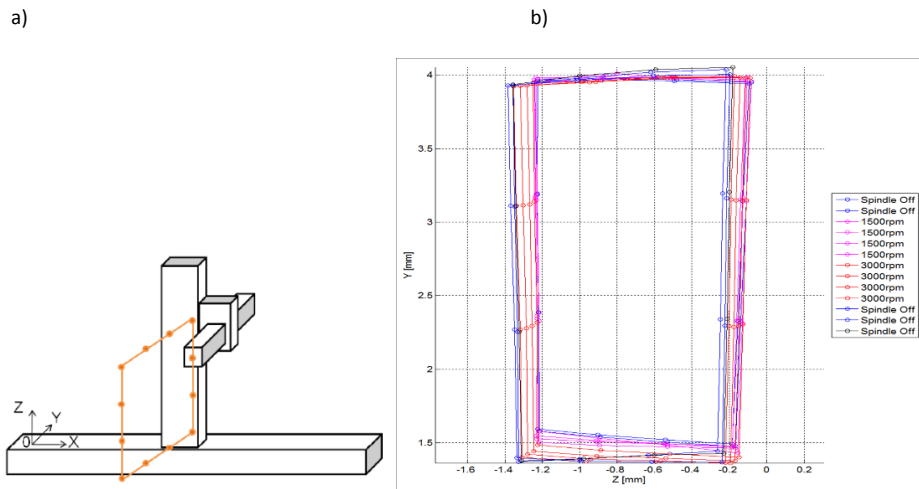


Figure 1-14 Thermal distortions on large MTs based on an automatic multilateration, a) the YZ plane measurement and b) thermal drift assessment on the YZ plane. [6]

1.2.6 Error sources on the touch probe side

Probing has become a vital component of automated production processes on-MTs. The probing system should ensure reproducibility during the sensing process even when any adverse influence appears during the process [118,129]. It is necessary to probe the desired point on the real workpiece surface by touching it with a sensing element or by sensing it in a non-contact way [129–131].

There are two main options when choosing a probing solution: contact or non-contact. There are major differences between both options. The first is that the accuracy of the individual points in contact measurements is higher to that of non-contact measurements. The second is the amount of collected data: non-contact technology can collect millions of sampled points at high speed without touching the workpiece. The third difference is that some surfaces, due to glossiness or transparency, are not suitable for optical measurement and cause special errors [132].

This PhD study is focused on developing traceable on-MT measurement capability based on already available contact TTPs. Therefore, contact touch probes and their error sources are described in detail next.

1.2.6.1 Contact touch probe

Contact probes can be divided into two general groups, scanning and discrete, based on the type of data being taken, differences are shown in Figure 1-15. Discrete probes, or TTP, are the most prevalent technology available [133,134]. They have the advantage of being less expensive than some of the other options and are good when fewer data points are needed, such as measurements for position or size [135]. Scanning probes, or analogue probes, are continuous contact probes that sense the part as the probe is moved along the expected contour, they are useful in the gathering of high-speed data on a part's form characteristics [136].

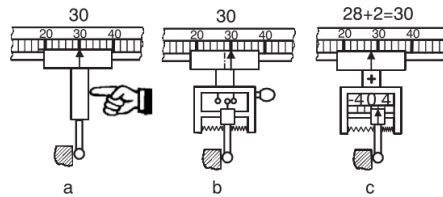


Figure 1-15 Contact touch probes: a) Hard; b) touch-trigger; and c) measuring probe. [6]

1.2.6.1.1 Touch trigger probe

The two main TTP technologies available for MTs are kinematic resistive/reactive probes and strain-gage probes [137,138]. As for kinematic resistive probes, most touch trigger probes utilize a kinematic seating arrangement for the stylus. Three equally spaced rods rest on six tungsten carbide balls providing six points of contact in a kinematic location. An electrical circuit is formed through these contacts. The mechanism is spring loaded which allows deflection when the probe stylus contacts the part and also allows the probe to reseat in the same position within $1\ \mu\text{m}$ when in free space (not in contact). Under the load of the spring, contact patches are created through which the current can flow. Reactive forces in the probe mechanism cause some contact patches to reduce, which increases the resistance of those elements. On contacting the workpiece (touch), the variable force on the contact patch is measured as a change in electrical resistance. When a defined threshold is reached, a probe output is triggered. The probing sequence is explained in Figure 1-16.

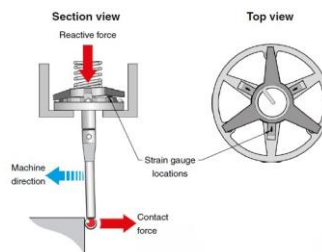


Figure 1-16 Kinematic resistive probe principle. [6]

A number of factors affect the kinematic touch probe measuring performance. From the point at which the stylus ball contacts the workpiece there is bending of the stylus prior to electrical triggering of the probe. This is known as PTV. PTV will vary dependent on the length and stiffness of the stylus and the contact force. PTV otherwise is commonly known as lobbing, probe measuring error or roundness measuring error and it can affect measurement performance. Lobbing occurs because the pivot distance varies depending on the direction in which the contact force acts in relation to the probe mechanism [139].

On the other hand, strain gauge probe technology has improved the performance limitations of the kinematic resistive probe technology, mainly because modern compact electronics and solid-state sensing have been embedded. Thus, the kinematic mechanism retains the stylus and strain gauge technology senses the trigger to acquire the measuring point. As a result, a lower trigger force is needed, and uniform pre-travel variation is achieved in all directions [139]. Main differences between both probing technologies are explained in Table 1-1.

Table 1-1 Comparison table between kinematic and strain gauge probing technology. [6]

	Kinematic Resistive Probe	Strain gauge probe
Pros	<ul style="list-style-type: none"> - Simple mechanism - Low mass (so low inertia at the triggering instant) - Cost-effective - Easy to retrofit to all types of CMM 	<ul style="list-style-type: none"> - Improved repeatability - Low and almost uniform pre-travel variations in all directions - More accurate measurements - Low bending deflection (leading low hysteresis) - Low trigger force - Support much longer styli
Cons	<ul style="list-style-type: none"> - Directional dependent pre-travel variation - Micro-degradation of contact surfaces - Exhibit re-seat failures over time - Limiting the length of stylus - Resistance through the contact elements as the means to sense trigger 	<ul style="list-style-type: none"> - Extra mass - (filtering circuitry) - Expensive

1.2.6.1.2 Analog scanning probes

Analogue scanning probe ensures a permanent and continuous contact between the probe and the component under measurement, so it is particularly suitable for free-form and contoured shaped components as well as for the measurement of large sheet metal assemblies, such as automobile components. CAS is a relatively new technology. Its main advantage is the high acquisition speed, which reduces dramatically the measuring time while offers a high density of data acquisition for a full definition of the part's size, position and shape, enabling completely new opportunities for on-MT metrology [118]. Nowadays, there are several CAS systems commercially available for MTs [140,141].

1.2.6.1.3 Factors affecting the probing performance

The weight of the TTP uncertainty on the on-MT uncertainty budget depends upon the scale of the measurement scenario. On a small on-MT measurement the TTP uncertainty contribution shall be of major importance in applications such as micro and nano manufacturing. However, the TTP uncertainty contribution on a large-size on-MT measurement could become negligible if a previous calibration of the TTP is performed and the measurement scenario is free of swarf. Thus, there are different factors that affect the probing performance of TTP and therefore, their uncertainty must be considered for traceable CMM measurements on MTs. They are depicted in Figure 1-17 [118].

- Operation principle: As commented before, TTP can be broken into two general groups, scanning and discrete, based on the type of data being taken. Based on uncertainty sources, such as pre-travel variation and repeatability, the uncertainty varies between TTP configuration.
- Measurement strategy: A disadvantage of discrete-point probing is that it may take a long time to measure a free-form shaped part. If CAS technology is employed a continuous data acquisition is ensured so the acquisition time can be reduced considerably.
- Movement during probing: Static probing is executed while the component under measurement is motionless. However, dynamic measurement involves a component movement during data acquisition. With TTP there is no possibility for static measurements as the trigger signal can only be generated during movement [118].
- Movement: The suspension can work either passively, with no actuation, or actively with a spring or electro-mechanical actuator. The active acquisition system offers the possibility to ensure a direction-

independent probing force. However, the passive system provides better dynamic properties while probing the component and it is also cheaper [118].



Figure 1-17 Aspects of probing systems. [6]

- Kinematics: TTP can be mechanically fitted in either a parallel or serial configuration. The configuration influences the static and the dynamic behaviour of the probe system because the size and the weight of the probe change considerably. Serial kinematics comprises several self-independent axes, which are frequently mutually orthogonal. Instead, parallel kinematics configuration involves two axis movement with a coordinate, similar to a hexapod structure [142,143]. Serial and parallel kinematics probes are shown in Figure 1-18.

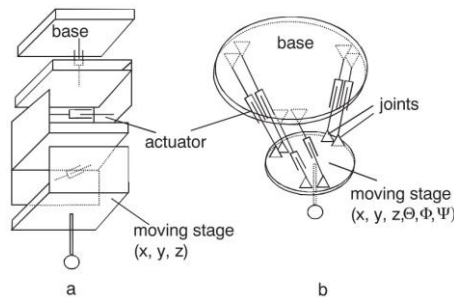


Figure 1-18 TTP kinematics:a) serial; and (b) parallel. [6]

- Directional response pattern: TTP can show varying directional sensitivity response [144,145]; mainly affected by the asymmetric arrangement of sensors, an asymmetric moment of inertia of stylus, tip ball form error or direction-dependent sensitivity of sensors [40]. The effect of direction-dependent sensitivity has the result that the same displacement of the tip ball leads to different output signals dependent on the direction of the displacement [146]. However, a correct behaviour characterisation offers the possibility to compensate this anisotropic effect through the control software [147–150].
- Environmental influences: The variation of environmental influences affects every metrology measurement. Consequently, it shall be considered as a part of the uncertainty associated with the measurement procedure of on-MT measurement.
- Cleanliness of the surface: The cleanliness of the surface and the tip ball directly affect the measurement result. Therefore, a clean environment helps to uncertainty reduction in the probing process. In addition, if the measurement is executed during the machining process, the swarf could seriously influence the

probing result. In fact, every effect is related to the probing force. If the probing force is near zero and soft surface contaminations (e.g., oil film) are probed, the signal to noise ratio of the probing system will decrease because of attenuation, which can make a reliable surface detection impossible [118].

- **Tip ball:** It is the contacting element between the MT and the component under measurement, so it is of utmost importance to characterize its position with the lowest uncertainty. The corrected measured point is achieved by correcting the tip ball centre point by adding a tip correction vector of the length of tip ball radius in the direction from the centre point to the probed point [151]. The radius value of the tip ball is measured during a specific measuring process, called qualification procedure of the TTP. If the probing direction is needed for the coordinate correction process, it can be calculated from the probing system, by interpolation (from at least three probed points in the neighbourhood of the surface point) or by estimation (e.g., CAD model). Usually, real surfaces show, in addition to long-wave form deviations, random short-wave deviations known as roughness [152]. For such a surface the measured geometric properties represent a superposition of measurand and touching element [153] leading to a non-linear mechanical filtering effect. This filtering effect has a characteristic similar to a low pass depending on the tip ball diameter because a smaller tip ball can penetrate smaller roughness valleys than a bigger ball. Because of this effect, one gets for measured features different parameter values (size, position, form deviation) dependent on the diameter of the tip ball. As the measurement result is a superposition of tip ball and surface geometry, also form deviations of the ball directly lead to measurement errors. Thus, it is necessary to use a tip ball of negligible form deviation compared to the required measurement uncertainty [118].
- **Probing force:** The probing force not just causes a bending of the stylus, but also has an effect on the elastic deformation of surface and tip ball due to Hertzian stress. Hertzian stress is the elastic deformation of two bodies touching each other [154]. The extent of deformation is dependent on the materials, micro and macro geometrical forms and the force. The effect of elastic deformations can be compensated to a certain extent by the probing system qualification process.
- **Wear of tip ball, plastic deformation and wear of the workpiece surface:** Wear and plastic deformation may happen during the probing process. This happens because there are some parameters such as probing force or hardness of contact surfaces that affect to the measurement process. Hence, there are three main effects that cause bad probing results: a) plastic deformation: Roughness peaks of the workpiece at the probed points may be considered as wear of the workpiece surface [155]. The compressive strength of the workpiece material can be exceeded even by the small probing force because of the very small contact area between tip ball and roughness peak leading to high pressure. It affects the appearance of the probed surface; b) wear of tip ball can occur during the scanning measuring process on a hard-rough surface; and c) materials of tip ball and workpiece interact. It may occur that microscopic small particles break out of the surface due to local welding effects. Under normal circumstances, very little pick-up occurs [118].
- **Probing system qualification:** The position of the tip ball centre point related to the reference point of the probing system, the radius of the tip ball and the lobbing error must be characterised to perform low uncertainty measurements [156,157]. These parameters are determined by a measuring procedure called probing system qualification.

The ISO 230-10 standard [158] specifies test procedures to evaluate the measuring performance of contact probing systems considering many of the factors affecting probing performance presented here. Its scope is limited to probing systems used in a discrete-point probing mode, integrated with a numerically controlled MT. It does not include other types of probing systems, such as those used in a scanning mode or non-contacting probing systems. As this standard explicitly indicates, it does not address the evaluation of the performance of the MT, used as a CMM, since such performance evaluation involves traceability issues and is strongly influenced by MT geometric accuracy.

1.2.6.2 Non-contact touch probe

The availability of non-contact 3D data capture systems capable of acquiring dense geometric data from complex surfaces has increased considerably over the past ten years [159]. Optical non-contact inspection techniques have revolutionized CMM inspection applications in the last decade, due to the cost and coverage of the technology. Nevertheless, a very small percentage of applications with non-contact measurement is already established, especially in robot and machine tool industry [160].

In this scenario, where a few approaches of non-contact technology integration are known, Karadayi presented a blue light laser sensor integration within a five-axis MT, explaining sensor integration and calibration [161]. The laboratory for machine tools and production engineering of the RWTH Aachen University is also exploring the possibility to integrate non-contact sensors into MTs. Hence, de Moraes et al. integrated a 2D laser into a machine tool for an in-process 3D measurement [162].

In the manufacturing industry, there is an increasing need to measure accurately 3D shapes. Freeform shaped parts are of great interest in many applications, either for functional or aesthetic reasons. Their relevance for the industry is well-known in the design and manufacturing of products having complex functional surfaces [163–167]. These parts are important components in industries such as automotive, aerospace, household appliances and others. Figure 1-19 shows measuring requirements for most common free form shaped parts.

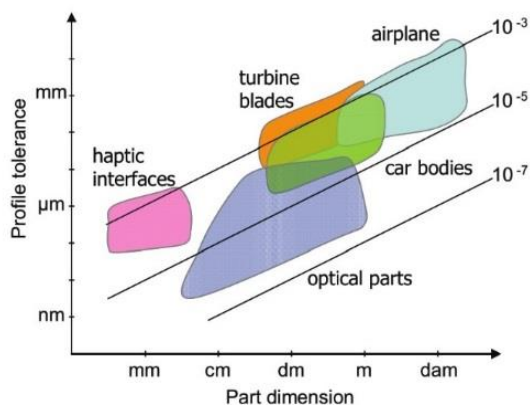


Figure 1-19 Typical values of tolerances vs. dimensions for most common free form shaped parts. [165]

Considering the usage of CMM-based inspection by tactile probes and the non-contact optical triangulation systems, it seems that MT sensing roadmap will follow the CMM current scenario. Hence, triangulation-based technology is prone to be integrated into MT in the near future complementing the usage of tactile probes in MTs.

1.2.7 Error sources on the measuring software side

To perform the complex mathematical calculations required for metrology-based real-time decision making, powerful metrology software needs to be integrated within the manufacturing system. Because the system is expected to function by itself without human interaction, it also needs to work autonomously within the manufacturing process. The following characteristics are required from a software program to truly make an MT function similar to a CMM [5]:

- **Offline programming:** A CAM-style programming environment with good MT virtual modelling, simulation capabilities, automatic path generation with collision avoidance, and complete geometrical fitting and tolerancing functionality is required. Programming languages such as DMIS also allow interfacing and collaborating with CMMs for efficient programming.
- **Bi-directional interface:** A direct and bi-directional interface is a must to analyse data in real time as soon as the measurement of a feature is completed. The calculated metrology characteristics are used as a part of the on-the-fly decision making and written back to the MT controller as a part of the adaptive cycle.
- **Ability to handle high-density point cloud data:** When interfacing with a laser to measure large parts, very large amounts of data will be gathered. The software, in addition to offering a live interface with the MT, must also be able to handle the display and interaction with such data.
- **Geometric feature extractions:** For on-machine geometrical feature measurements and GD&T applications, automatic feature extraction is necessary. Most point cloud systems today are offline and need operator interaction to calculate the required features. An on-machine measurement software that will interface with a laser system should also have a robust automatic feature extraction capability.
- **Ease of operation:** The measurement program must be integrated into the machining centre similar to any other machining program. This allows the measuring to be integrated as a part of manufacturing cycles and can be automatically started by itself. G-Code NC program is created by post-processing the DMIS measurement routine and resides in the controller.

1.2.8 Error Sources on the measured object side

Measurement processes are strongly influenced by the measurement systems and especially for large-size components, by the object under measurement. Temperature fluctuations, either in the environment or during the machining process brings to temperature gradients that sensibly influence the geometry of the part, making a significant contribution to the measurement uncertainty. In addition, gravity affects the geometry of the component under measurement. These influences are evident during the manufacturing process of the component and also when performing on-MT measurement [4].

Component temperature variations comprise a significant uncertainty source for traceable on-MT measurement. The uncertainty increases proportionally with temperature differences and component size. Therefore, for large-size components measured in a thermally unstable production environment, thermal effects can represent a high percentage of the total measurement uncertainty on the uncertainty budget [4,14,15,18,19,168,169].

Another heat source is the machining process, which creates a transient and non-homogeneous temperature distribution inside the component. Complex or asymmetric workpieces with different wall thicknesses or materials enhance this thermal inhomogeneity. The heat inside the component affects its characteristics (shape, position and size) when compared to their thermal reference state at 20 °C [4].

Additionally, all the geometric measurements done on earth suffer from gravitational deformations. These elastic deformations depend on the positioning and orientation, the material characteristics and the geometry of the component. Moreover, due to variability on the clamping operation during the machining process, the object suffers from varying gravity deformations that affect to the on-MT measurement during the machining process.

When it comes to the object under measurement, quasi-static errors are not as important as they are for large measuring systems, but it is crucial to determine the behaviour of the component according to a specific temperature and gravitational influences when the measurement is executed [4].

To undertake the necessary modelling to understand and predict how large measurand behaves under specific thermal and gravitational conditions, FEM software is widely used. It should be noted that any computational method that can accept temperatures and gravitational forces as a load condition to calculate localized displacements could be applied for such an application [170].

The first step is to define with high accuracy the boundary and initial conditions of the simulation. In addition, temperature related information should be characterized, such as the environment temperature information and the initial temperature distribution. If the workpiece temperature is homogeneous and it is being measured during the manufacturing process, numerical compensation may be employed. However, inhomogeneous temperature distributions are difficult to compensate and it should be assigned to the measurement uncertainty [120]. On the other hand, gravity related influences shall be added to the simulation. Information about: a) fixtures that locate and clamp the component on the MT table; b) clamping orientation related to the gravity vector; and c) detailed information about the component (mass and geometry) are achieved generally from the CAD.

The second step is to run the simulation. The simulation results represent the compensation values to be applied as an input to the measurement software for compensating thermal geometry and gravitational effects to a certain homogeneous reference temperature and position.

Finally, post-processing is done to achieve results that can be viewed and analysed depending upon the requirements of the on-MT measurement to be performed.

2. PRESENTATION OF THE PUBLISHED WORK



2. PRESENTATION OF THE PUBLISHED WORK

2.1 Research framework

This PhD study that has been undertaken by published works is comprised of seven research articles, five of them published in JCR international journals:

Traceability of On-Machine Tool Measurement: A Review

As a starting point of the research, the state of the art of traceable on-MT measurement is carefully presented within the first article. There are advantages and disadvantages to performing a measurement on an MT. The advantages include the reduction of the so-called quality losses for the manufacturing operation, because dimensional measurements can be employed at different stages of the manufacturing cycle: a) monitoring of the MT geometry performance by employing a calibrated standard; b) workpiece setup on the MT coordinate system; c) in-process measurements to provide correction values for the manufacturing process; and d) the performance of a final metrology validation of the finished product for final quality inspection as well as statistical trend analysis of the manufacturing process. Among the disadvantages, two main barriers limit traceable CMM measurements on MTs: a) Lack of volumetric MT accuracy; and b) a closed calibration chain for those measurements performed on an MT. This article also proposes a qualitative approach to the error sources that contribute to the uncertainty budget of on-MT measurement: the measurement system, the MT itself with the TTP and the measuring software, the component under measurement and the interaction between both of them.

Traceability of on-machine tool measurement: Uncertainty budget assessment on shop floor conditions

The second article presents a quantitative approach to the uncertainty budget of on-MT measurement. Thus, a medium-size on-MT measurement uncertainty assessment is performed in shop floor conditions. A complete experimental test was performed according to the ISO 15530-3 technical specification on a medium-size MT. Five workpiece replica standards were manufactured and subsequently measured on an MT. To understand the systematic error of the on-MT measurement, these workpieces were calibrated on a CMM with the VCMM tool which permitted to realise a task-specific uncertainty assessment. Experimental results show that traceable CMM measurements can be performed on an MT. Furthermore, every expanded measurement result is within 20 μm and results also highlight the significance of each uncertainty contributor where the measurement procedure uncertainty is the main contributor to the uncertainty budget. It also demonstrates that the geometric error of the MT is the main error source within the systematic error contributor.

Uncertainty assessment for on-machine tool measurement: an alternative approach to the ISO 15530-3 technical specification

The third article proposes a new methodology for traceable on-MT uncertainty assessment without using a calibrated workpiece, assuming that previous research article concludes that geometric error of the MT is the main error source for the systematic error contributor. The ISO 15530-3 technical specification presented in the second article faces a strong limitation, it depends on a calibrated workpiece to understand how the systematic error contributor performs on the on-MT measurement uncertainty budget. For small batch production, mainly in large scale manufacture, the approach is not affordable because a calibrated workpiece similar to the manufactured part

is needed, which makes the solution tedious and expensive. Therefore, the scalability of the solution is limited to a medium-size MT. In this scenario, this article proposes a volumetric error mapping of the MT immediately before the measurement process execution to avoid the use of a calibrated component on the systematic error contributor assessment. An experimental exercise shows that traceable on-MT measurements can be realised without the use of a calibrated workpiece. Obtained results are similar to those results obtained with the ISO 15530-3 technical specification.

Integrated multilateration for machine tool automatic verification

The fourth article presents an integrated MT volumetric error mapping solution that enables the scaling of traceable on-MT measurement to large MTs. The integration of a tracking interferometer measurement device on the MT spindle breaks with the typical multilateration approach, based on sequential measurement scheme, and allows to measure the geometric error of an MT automatically in the complete volume. It reduces (depending on the MT volume) the volumetric error mapping process time consumption and the measurement uncertainty. This article shows a complete simulation scheme of the proposed integrated solution and presents an initial validation exercise mounting a LEICA AT402 laser tracker on a KUKA KR60 industrial robot.

This integrated measurement procedure for automatic MT geometric verification is focused mainly on large MTs and therefore the measurement procedure is developed within the large scale metrology (LSM) field. It means that when it comes to large-scale manufacturing scenarios, the MTs face similar challenges to what the LSM does and therefore this measurement procedure considers the current LSM state of the art to select the suitable technologies and measurement sequences.

Integrated volumetric error mapping for large machine tools: An opportunity for more accurate and geometry connected machines

The fifth article demonstrates the integration exercise of the multilateration-based measurement solution on a large MT, conceptually presented in the previous article. The integration work was performed on a ZAYER MEMPHIS large MT and it was realised with a LEICA AT960 laser tracker. Obtained results were compared to the typical multilateration approach, realised with a laser tracer NG measurement device on the same MT and immediately after the integrated measurement approach. In this way, results show that the integrated measurement approach improves the typical volumetric error mapping measurement procedure.

3D Measurement Simulation and Relative Pointing Error Verification of the Telescope Mount Assembly Subsystem for the Large Synoptic Survey Telescope

The sixth research article proposes a new verification method for the RPE assessment of the TMA for the LSST project. At this point, this challenge benefits from the generated new knowledge within the LSM field for MTs and looks for a suitable measurement solution for the accuracy assessment of the LSST. The telescope size matches the size of extremely large MTs, and therefore some of the technologies and measurement techniques researched before are adapted for the LSST project.

The presented new measurement procedure, based on laser tracker technology and several fiducial points fixed to the floor, was designed and simulated within SA software thanks to the knowledge developed in the fourth and the fifth articles above-mentioned. The measurement scenario is up to 40 m in diameter and 10 m in height, so the

measurement challenge is within the LSM field. Monte-Carlo-based simulation results show that the presented methodology is fit for purpose on the simulation stage, even if a floor movement occurs owing to a temperature variation during the measurement acquisition process.

Telescope mount assembly pointing accuracy assessment for the Large Synoptic Survey Telescope: A large-scale metrology challenge

Finally, the seventh article presents the TMA pointing accuracy survey performed in-situ for the LSST project. Following the custom engineered measurement procedure presented in the previous article, the RPE assessment measurements were performed at Asturfeito company premises, in the north of Spain during September of 2018. These measurements were realised on an engineering validation framework, where it is aimed to execute major performing tests at the subsystem level to verify the overall engineering performance of the observatory. Results demonstrate that the RPE assessment is similar to what previously obtained within the simulation model, so the survey uncertainty requirements were successfully fulfilled.

2.2 List of published works

2.2.1 JCR international journals

A list of the published works in JCR international journals is presented below:

- Traceability of On-Machine Tool Measurement: A Review. MDPI Sensors 2017;17:40. (doi:10.3390/s17071605).
- Traceability of on-machine tool measurement : Uncertainty budget assessment on shop floor conditions. Measurement 2019;135:180–8. (doi:10.1016/j.measurement.2018.11.042).
- Uncertainty assessment for on-machine tool measurement: an alternative approach to the ISO 15530-3 technical specification. Precision Engineering 2019;57:45–53. doi: 10.1016/j.precisioneng.2019.03.005.
- Integrated multilateration for machine tool automatic verification. CIRP Annals 2018;67:555–8. (doi:10.1016/j.cirp.2018.04.008).
- 3D Measurement Simulation and Relative Pointing Error Verification of the Telescope Mount Assembly Subsystem for the Large Synoptic Survey Telescope. Sensors 2018;18:20–2. (doi:10.3390/s18093023).

2.2.2 Non-JCR published research documents

A list of the published works in a non-JCR international journal is presented next:

- Telescope mount assembly pointing accuracy assessment for the Large Synoptic Survey Telescope : A large-scale metrology challenge. EUSPEN 19th International Conference & Exhibition 2019;1:9–12.
- A new methodology for the assessment of relative pointing accuracy and active alignment requirements of the Large Synoptic Survey Telescope. Journal of CMSC 2018.
- Relative pointing error verification of the Telescope Mount Assembly subsystem for the Large Synoptic Survey Telescope. Proc. Of: 5th IEEE International Workshop on Metrology for AeroSpace (MetroAeroSpace), Rome, Italy: 2018. (doi:10.1109/MetroAeroSpace.2018.8453570).
- Integrated volumetric error mapping for large machine tools : An opportunity for more accurate and geometry connected machines. Procedia Manufacturing 2019:1–8.

2.2.3 Additional research documents

A list of additional research documents of the author related to this PhD content but not developed within the undertaken research work is presented below:

- Retos y tendencias de la metrología como herramienta de la calidad en el nuevo paradigma de la industria 4.0. Proc. Of: XXI Congreso de Calidad en la Automoción, 2016. Bilbao
- Las medidas en un mundo dinámico: El papel de la metrología en la industria 4.0. Proc. Of: Seminario Intercongreso Nacional de Metrología, Madrid: 2016.
- Multilateración simultánea para MH. Proc. Of: Machine-Tool and Manufacturing Technologies Congress, 2017.
- Requerimientos sobre la metrología dimensional para la mejora de los procesos de fabricación en el contexto industria 4.0. Proc. Of: Congreso nacional de metrología, 2017.
- A new methodology for the assessment of relative pointing accuracy and active alignment requirements of the Large Synoptic Survey Telescope. Proc. Of: 33th Annual Coordinate Metrology Society Conference, Utah, USA: 2017.
- Calibration of coordinate measuring machines using laser tracer technology. Proc. Of: Metromeet, Bilbao: 2017.

2.3 Presentation of published works

The following is a brief summary of the research works that comprise this PhD study.

Traceability of On-Machine Tool Measurement: A Review.

The content of this research article is previously presented within the literature review chapter. It was published in July of 2017, so it reports an updated state of the art within the studied field. As previously commented, the aim of this PhD study is to generate new knowledge to close the calibration chain for traceable CMM measurements on MTs. However, there are some key differences between an MMC and an MT, mainly because a CMM is designed for a measurement purpose and an MT is focused on manufacturing production. It means that MT is employed in shop-floor conditions where there are several factors that affect measurement accuracy, such as MT geometric error, temperature variation, probing system, vibrations and dirt. This article presents a detailed qualitative approach of those error sources that contribute to the uncertainty budget of on-MT measurement: the measurement system, the MT itself with the TTP and the measuring software, the component under measurement and the interaction between both of them.

Once all potential error sources are explained in detail, an hypothesis of the potential error budget for small, medium and large size MTs is proposed, considering: a) IK4-TEKNIKER experience in the use and calibration of MTs and CMMs; and b) the information collected on the state of the art of the studied field.

Small and medium-size MTs, from 0.5 m³ to 2 m³, typically offer a positioning accuracy better than 5 µm and repeatability around 2 ÷ 3 µm [171]. However, as stated by Keller at TIM final workshop [172], the geometry variation of a 630 mm × 730 mm × 860 mm MT between 15 ÷ 30 °C could be higher. On this experimental study, the positioning error variation is around 20 µm and the perpendicularity error variation is around 8 µm. While position and squareness errors are dominant and strong contributors to the varying total geometric error due to temperature

2. Presentation of the published work

effects, straightnesses and rotational errors are less prone to temperature effects. Table 2-1 depicts a simple error budget where all major uncertainty contributors are described. The temperature effect is the most important error source unless it is measured and compensated. As demonstrated by Schmitt et al. the uncertainty of a dimensional measurement done on an MT can be around $20 \div 30 \mu\text{m}$ for a small MT [2].

Table 2-1 Error budget for small and medium-size MTs. [6]

Error Source	Significance		
	0–10 μm	10–100 μm	100–1000 μm
Accuracy			
Machine tool geometry	■		
Touch probe	■		
Repeatability			
MT repeatability	■	■	
Temperature effect	■	■	■
Other effects	■	■	
Resolution	■		

The most frequent configurations of large machines are based in serial kinematics and three, four or five motions are located at the machine head. Hence, the part is fixed to the table and a heavy slide to move the part is not required. The dominant serial kinematics configurations for large machines are a movable column, gantry and elevated gantry [55]. The typical positioning accuracy of a high-tech large MT depends on the configuration and volume, could be around $10\text{--}15 \mu\text{m}$ and repeatability could be better than $10 \mu\text{m}$ [173]. As stated by Kortaberria at TIM final workshop [174], while the positioning error variation of a large MT ($6000 \text{ mm} \times 3000 \text{ mm} \times 1500 \text{ mm}$) is around $80 \mu\text{m}$, the squareness and straightness error maintain stable. In addition, as stated by Wennemer [175] a very large MT geometry is extremely sensitive to the temperature influence, a length deviation of $300 \mu\text{m}$ is shown under temperature variation without any length compensation in the beam direction and it is reduced to the half with length deviation. Table 2-2 depicts a simple error budget for a large MT.

Finally, one of the most employed tactile probes nowadays is the OMP400 probe from RENISHAW. It offers repeatability better than $0.5 \mu\text{m}$ and the 3D lobbing error is around $\pm 2 \mu\text{m}$ for a 100 mm stylus length [129]. If a reliable calibration of the tactile probe is performed when mounting it on the MT spindle, it could be neglected on the uncertainty error budget of a large MT. However, for small and medium-size MTs working in a non-controlled shop floor, it shall be considered on the budget.

Table 2-2 Error budget for large size MTs. [6]

Error source	Significance		
	0–10 μm	10–100 μm	100–1000 μm
Accuracy			
Machine tool geometry	■	■	
Touch probe	■		
Repeatability			
MT repeatability	■	■	■
Temperature effect	■	■	■
Other effects	■	■	
Resolution	■		

Traceability of on-machine tool measurement: Uncertainty budget assessment on shop floor conditions

After the qualitative approach presented within the first article, where all potential error sources affecting to the traceable on-MT measurement are explained in detail, this second research article proposes a quantitative approach. Here, a medium size on-MT measurement uncertainty assessment is performed experimentally in shop-floor conditions, according to the ISO 15530-3:2011 technical specification [23]. According to this document, there are four uncertainty contributors that comprise all the systematic and random errors that shall be considered on the uncertainty budget of on-MT measurement:

- u_b standard uncertainty associated with the systematic error of the measurement process.
- u_p standard uncertainty associated with the measurement procedure.
- u_{cal} standard uncertainty associated with the uncertainty of the workpiece calibration.
- u_w standard uncertainty associated with material and manufacturing variations.

Thus, the expanded measurement uncertainty of the complete measurement process (U_{MP}) is assessed by $U_{MP} = k \times u_{MP}$ and the expanded measurement uncertainty of the measurement system (U_{MS}) is assessed by $U_{MS} = k \times u_{MS}$, for a coverage factor of $k=2$, where u_{MP} and u_{MS} are given by the same formula where input information comes from the measurements executed immediately after the machining process and under no-load condition, respectively.

There are different approaches to assessing the uncertainty of the systematic error b . If the measurement result is not corrected by the systematic error, the error fully contributes to the uncertainty, so $u_b = b$. Thus:

$$u_{MP} = \sqrt{u_p^2 + u_{cal}^2 + b} \quad \text{and} \quad u_{MS} = \sqrt{u_p^2 + u_{cal}^2 + b} \quad (1)$$

Variations of form errors and roughness due to the changing manufacturing process and material properties are considered within their required limits, so u_w contribution is considered as insignificant. Additionally, this research article explains in detail how every uncertainty contributor is mathematically obtained from acquisition data [176].

For the experimental exercise, five workpiece replica material standards were manufactured, followed by on-MT measurement in the same chucking using a RENISHAW OMP 400 tactile probe. Each workpiece was measured ten times on the MT to distinguish between systematic and random errors and assess the uncertainty budget of the entire measuring process (U_{MP}). Furthermore, one workpiece was measured on the MT ten times at 20 °C either under no-load or under quasi-static conditions to assess the uncertainty budget of the measuring system (U_{MS}). Figure 2-1 shows on-MT manufacturing and measurement processes [6].

A medium size MT was selected to perform the experimental test. It is a KONDIA MAXIM MT with a cutting stroke of $X = 750$ mm, $Y = 1000$ mm and $Z = 500$ mm. The CNC is a 16i type FANUC controller. A unique cutting tool was employed to machine the "Test piece ISO 10791-7, M1-160" and the total time consumption for workpiece replica standard machining was approximately 2 h [177].

The RENISHAW OMP 400 tactile probe was employed on the MT side to execute the on-MT measurement. The total time consumption for a unique measurement of every feature was 8 min, however, the measurement was repeated ten times, which means a total time consumption of 2 h per measured part. The Power Inspect software was

2. Presentation of the published work

employed for G-code generation and also for the post-processing work of the CMM measurements performed on the MT.

a)



b)

Figure 2-1 On-MT measurement experimental exercise: a) Workpiece manufacturing scenario; and b) on-MT measurement with RENISHAW OMP 400 tactile probe. [176]

The workpiece replica standard selected for the experimental uncertainty assessment exercise is defined at the ISO 10791-7:2014 standard [177]. The selected standard test piece was referenced as “Test piece ISO 10791-7, M1-160”. Figure 2-2 depicts the measured geometry and features on the workpiece replica standard.

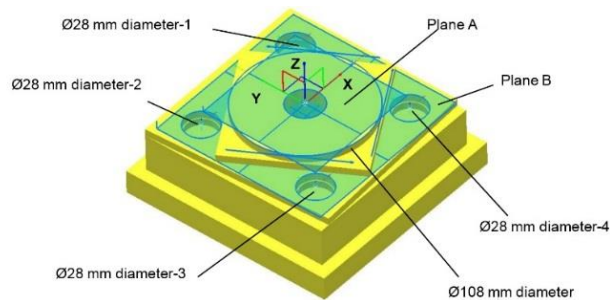


Figure 2-2 The workpiece replica standard with the measured geometry. [176]

A geometric characterisation of the MT was performed under no-load condition aiming to correlate the systematic uncertainty (u_b) of the on-MT measurement with the geometric error of the MT. In this way, the multilateration-based approach was realised on the MT side with laser tracer NG technology from ETALON AG OEM [84], as shown in Figure 2-3.

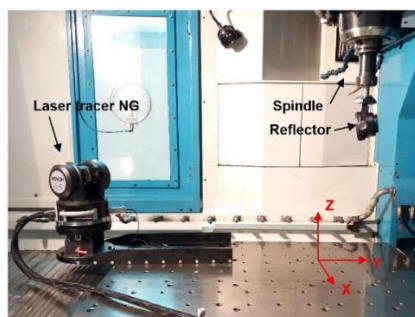


Figure 2-3 Laser tracer NG multilateration exercise on the KONDA MAXIM MT [176]

2. Presentation of the published work

Temperature variation was monitored during the experimental exercise. Figure 2-4 shows how temperature increases either on the MT or the workpiece during the machining process. Workpiece temperature increases to 22.5 °C (on average) immediately after the machining process and it stabilizes to 19.5 °C (on average) after two hours of on-MT measurement acquisition time. In addition, it also illustrates the moment when every workpiece replica standard was measured.

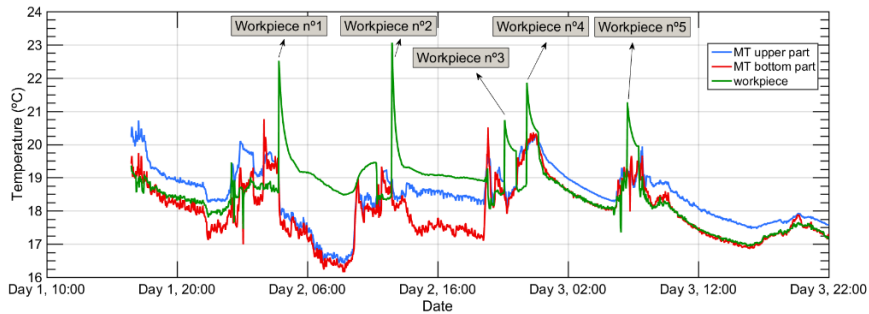


Figure 2-4 Temperature variation during the experimental test. [176]

The uncertainty budget for the experimental test is presented below. A task-specific uncertainty budget assessment was performed, as shown in Figure 2-5. The three major uncertainty contributors were characterized in shop floor conditions: a) For the systematic error (u_b), the mean value of the systematic errors of the individual measurements is taken, b) for the measurement procedure uncertainty (u_p) contributor, the maximum standard deviation of the measurements is considered; and c) for the calibration uncertainty (u_{ca}), it is obtained from the workpiece calibration certificate. It shall be highlighted that in case of the measurement procedure uncertainty (u_p) contributor, repeatability results are shown either for measurements executed immediately after the machining process or measurements executed under no load conditions. Furthermore, the substitution method is applied for diameter measurement result correction to correct the insufficient calibration of the probing system on the MT spindle. It concludes that TTP calibration shall be performed every time it is mounted on the MT spindle after the machining of the workpiece and before the on-MT measurement process.

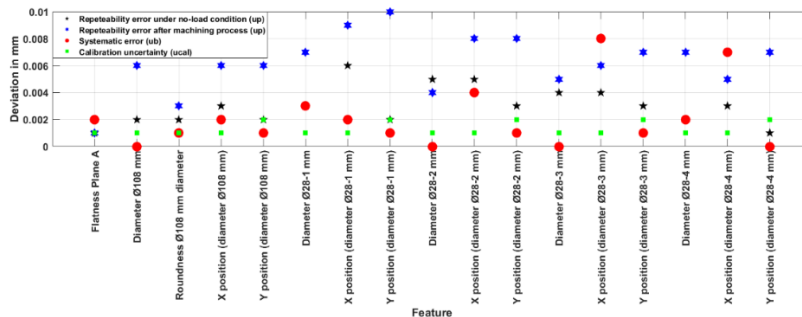


Figure 2-5 On-MT experimental uncertainty budget. [176]

The systematic contributor (u_b) results after values correction show that every mean systematic error is within 10 μm . In addition, results correlate with the geometric error of the MT, particularly with positioning errors in X and Y axes, and squareness between them. Therefore, it seems that the geometric error of the MT is the main error source affecting the u_b major uncertainty contributor.

2. Presentation of the published work

For the measurement procedure uncertainty (u_p) contributor, it is of utmost importance to understand the effect of the temperature gradients on the results. Thus, the experimental test proposes a) on-MT measurements immediately after the machining process; and b) on-MT measurements under the no-load condition when the temperature on the MT side and workpiece side is constant at 20 °C. According to the results depicted in Figure 2-5, the measurement procedure uncertainty (u_p) results show differences between the measurement executed under the no-load condition and the measurements executed immediately after the machining process. All the results show repeatability values within 6 μm for the no-load condition, while the maximum repeatability values for the measurements immediately after the machining process are within 10 μm . Form error feature measurement (flatness and roundness) show better measurement procedure uncertainty results than scale related feature measurement (diameter and positioning values) because these features are more sensitive to the measurement scenario temperature variation.

For the calibration uncertainty (u_{cal}) results, the maximum uncertainty value is up to 2 μm for the CMM positioning error in the Y direction. It shows that this uncertainty contributor shall be considered on a medium size on-MT measurement, but for large scale measurement scenario it could become negligible depending on the magnitude of u_b and u_p .

To sum up, the measurement procedure uncertainty (u_p) contributor is the main contributor to the on-MT measurement uncertainty budget in shop floor condition. Table 2-3 shows that the measurement procedure uncertainty is larger on the measurements executed immediately after the machining process, mainly affected by the dynamically changing temperature conditions of the measurement scenario. For the no-load measurement condition, measurement procedure uncertainty (u_p) is also a few microns larger than the systematic error (u_b) uncertainty, which maintains within 8 μm for every measured feature. In addition, the systematic error (u_b) correlates with the geometric error of the MT, particularly with positioning errors in X and Y axes, and squareness between them. Therefore, it seems that the geometric error of the MT is the main error source affecting the u_b major uncertainty contributor. Uncertainty contribution related to the TTP could be close to the supplier specifications, within 1 μm , but a correct calibration of the TTP is required on the MT side every time it is mounted into the spindle. Table 2-3 depicts expanded measurement uncertainty results (U_{MP} and U_{MS}).

Table 2-3 Expanded measurement uncertainties (U_{MP} and U_{MS} , with $k=2$) of the experimental test. (in μm) [176]

Feature	u_b	$u_{p\text{ no-load}}$	u_p	u_{cal}	u_{MS}	U_{MS}	U_{MP}	U_{MP}
Flatness Plan A	1.7	0.7	0.7	0.7	1.9	3.9	1.9	3.9
$\varnothing 108$ mm	0.2	2.2	5.5	1	2.5	4.9	5.6	11.3
Roundness $\varnothing 108$ mm	1.1	1.9	3.0	0.7	2.3	4.7	3.2	6.5
X position ($\varnothing 108$ mm)	2.1	3.3	5.7	1	4.0	8.0	6.2	12.3
Y position ($\varnothing 108$ mm)	0.7	2.1	5.7	1.7	2.8	5.6	6.0	12.0
$\varnothing 28$ -1 mm	2.6	3.1	7.1	1	4.2	8.4	7.6	15.3
X position ($\varnothing 28$ -1 mm)	2.2	6.1	9.4	1.2	6.6	13.2	9.7	19.4
Y position ($\varnothing 28$ -1 mm)	0.5	2.1	9.5	1.9	2.9	5.7	9.7	19.5
$\varnothing 28$ -2 mm	0.3	5.4	3.9	1	5.5	10.9	4.1	8.1
X position ($\varnothing 28$ -2 mm)	4.4	5.5	8.3	1.2	7.2	14.3	9.5	18.9
Y position ($\varnothing 28$ -2 mm)	1.5	2.7	8.3	1.9	3.6	7.3	8.6	17.2
$\varnothing 28$ -3 mm	0.5	4.0	5.2	1.1	4.2	8.4	5.4	10.7
X position ($\varnothing 28$ -3 mm)	7.6	4.5	5.5	1.2	8.9	17.9	9.5	19.0
Y position ($\varnothing 28$ -3 mm)	1.4	2.6	6.9	1.8	3.4	6.9	7.3	14.6
$\varnothing 28$ -4 mm	1.7	2.1	6.7	1.1	2.9	5.9	7.0	14.1
X position ($\varnothing 28$ -4 mm)	7.2	2.7	5.2	1.4	7.8	15.6	9.0	18.0
Y position ($\varnothing 28$ -4 mm)	0.1	1.3	6.5	1.7	2.2	4.3	6.8	13.5

Uncertainty assessment for on-machine tool measurement: an alternative approach to the ISO 15530-3 technical specification

The previous article presents a traceable on-MT measurement exercise, but it has a strong limitation, it depends on a calibrated workpiece to understand how the systematic error contributor (u_b) performs. Therefore, the scalability of the solution is limited to a medium-size MT. For large scale manufacture, the approach is not affordable because a calibrated workpiece similar to the manufactured part is needed, which makes the solution tedious and expensive. The experimental exercise of the second article shows that the systematic error (u_b) contributor correlates with the geometric error of the MT, so the third article proposes an alternative methodology for traceable on-MT measurement without using a calibrated workpiece. An experimental exercise was performed for a medium size prismatic component according to the VDI 2617-11 guideline [37] and results are compared with the ISO 15530-3 technical specification [23].

Here, the approach is to assess on-MT measurement uncertainty without using a calibrated workpiece, performing the VDI 2617-11 guideline [37]. For this approach, the determination of the on-MT measurement uncertainty is determined with an uncertainty budget. Each uncertainty source and its magnitude on the measurement result shall be contemplated. In this case, error sources are as follows :

- The geometric error of the MT and its repeatability.
- Probing system.
- Temperature: MT structure, surroundings and the workpiece.
- Workpiece under measurement: Temperature and clamping.
- Measurement procedure.
- Geometric error mapping technique.

These error sources comprise systematic and random errors for the on-MT uncertainty budget [41]. The result is the on-MT measurement uncertainty for a 95% confidence level.

Similar to the ISO 15530-3 technical specification, the systematic error contributor on the VDI 2617-11 guideline is affected by the following error sources: the geometric error of the MT, the probing system, the workpiece under measurement, the measurement procedure and the geometric error mapping technique. The random contributor comprises the MT repeatability, the touch probe repeatability and the temperature variation for the measurement scenario.

For the experimental approach presented below, the measurement procedure and the workpiece under measurement were not considered for the uncertainty budget because an easy-to-measure medium-size prismatic component was measured. Moreover, negligible deformations occur during the clamping process. In addition, the probing system characterisation and the uncertainty of the MT volumetric error mapping technique are within $2\ \mu\text{m}$. Thus, the uncertainty budget exercise focuses on major uncertainty contributors. In this manner, the geometric error of the MT is considered as the main error source within the systematic contributor (u_b), and the effect of the temperature on the measurement scenario and MT repeatability are highlighted as the main random error contributors (u_p). However, for a large-scale on-MT measurement scenario some of the discarded uncertainty contributors shall be considered on the uncertainty budget, mainly those related to the workpiece size and clamping process that are affected by temperature variation and gravity effects.

Considering those major uncertainty error contributors, this study adopts the random error characterisation, which performed on the ISO 15530-3 technical specification and which does not require a calibrated workpiece to understand how (u_p) performs. For the systematic error contributor (u_b), Schmitt et al. presented an approach where an MPE value was defined for an MT. Their approach was validated within stable temperature conditions, but they proposed further research for unstable conditions because an unstable status causes gradients inside the structure, and the induced deviations are hard to simulate or predict [2]. Considering such limitations, a volumetric error mapping of the MT was performed immediately before the on-MT measurement process execution for the systematic error characterisation. Thus, the geometric error of each contact point is known, and the systematic error contributor (u_b) can therefore be assessed. This research work does not apply the systematic error value correction, so the error fully contributes to the uncertainty budget.

A new methodology is proposed to perform the on-MT uncertainty assessment without a calibrated workpiece:

- For the systematic error contributor (u_b), a volumetric error mapping of the MT shall be performed immediately before the on-MT measurement. Thus, the geometric error of each point is known for the working volume of the machine, which is the main contributor to the systematic error of the on-MT measurement. Once the on-MT measurement is performed, measurement contact points are registered, and the geometric error of every point is obtained from the volumetric error mapping. Thus, every measured feature is fitted again while considering the geometric error of each contact point. The difference between the feature characteristics before and after the second fitting exercise is the systematic error to be considered on the error budget. Figure 2-6 shows the flow chart for the systematic error characterisation.
- The systematic error originating from the TTP could also be considered for the systematic error contributor (u_b). Thus, as explained by Mutilba et al.[176] if a reliable calibration of the probing system is performed every time the tactile probe is mounted on the MT spindle, this contributor becomes negligible. However, if the calibration process is not executed correctly or if the uncertainty contributor is not sufficiently small ($< 1 \mu\text{m}$ for small MT and $< 3 \mu\text{m}$ for large MT) the TTP systematic error should be added to the u_b value according to the square root of the sum of squares.
- The measurement procedure uncertainty (u_p) is performed on the workpiece to be measured on the MT, similar to the ISO 15530-3 technical specification [23]. Thus, the repeatability of the on-MT measurement shall be performed within the temperature range of the measurement scenario, considering that the temperature variation is critical for this uncertainty contributor. Therefore, several on-MT measurement cycles shall be performed within the complete temperature range of the measurement scenario. For example, consider an eolic hub being machined in a large MT, where the temperature variation on the surrounding air is between $18 \text{ }^\circ\text{C}$ and $23 \text{ }^\circ\text{C}$. The u_p contributor should be assessed by means of repeated measurement cycles (every 15 min) on the workpiece within the working temperature range.
- The u_{cal} contributor is considered as the standard uncertainty associated with the measurement uncertainty on the systematic error characterisation process. The volumetric error mapping approach for the MT geometric characterisation has two additional measurements that are very valuable at this stage: The repeatability and the backlash error of the MT under measurement. The MT volume measurement is performed in two opposite directions so either repeatability and backlash error shall be measured. If

these two values are not good enough, the correlation between the geometric error of the MT and systematic error contributor (u_s) does not exist and therefore, the methodology presented here cannot be applied.

Additionally, the research article explains in detail how every uncertainty contributor is mathematically obtained from acquisition data [178].

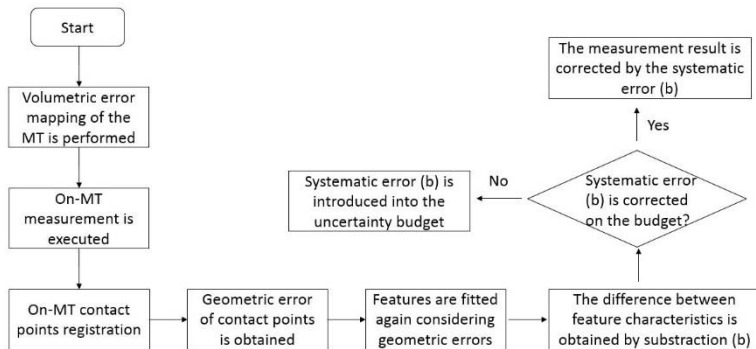
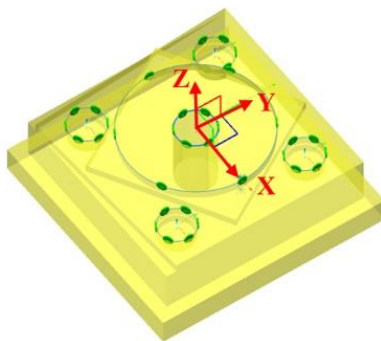


Figure 2-6 The proposed systematic error assessment methodology. [178]

For the experimental exercise, the same workpiece replica standard and MT were employed compared to the experimental exercise presented in the second article. Figure 2-7 shows a) the measured contact points for the experimental on-MT measurement test; and b) the measurement scenario on the MT.

a)



b)

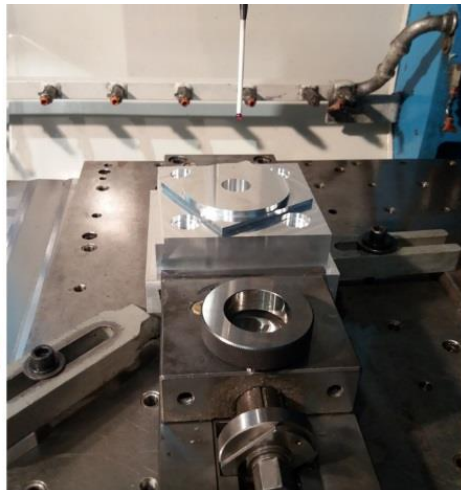


Figure 2-7 On-MT measurement contact points, a) General overview of the measurement strategy (contact points in green), and b) the measurement scenario where the workpiece and the calibrated ring are shown.

[178]

For the systematic error contributor assessment, a volumetric error mapping of the MT was performed immediately before the on-MT measurement. Laser tracer technology from ETALON AG OEM was employed for that purpose. It employs a kinematic model that permits to calculate the geometric error of any point within the measured volume

from the volumetric error mapping information, so the geometric error of the on-MT measurement contacts points was assessed this way. Figure 2-8 shows the volumetric error mapping exercise and the measured point grid (in black) of the MT.

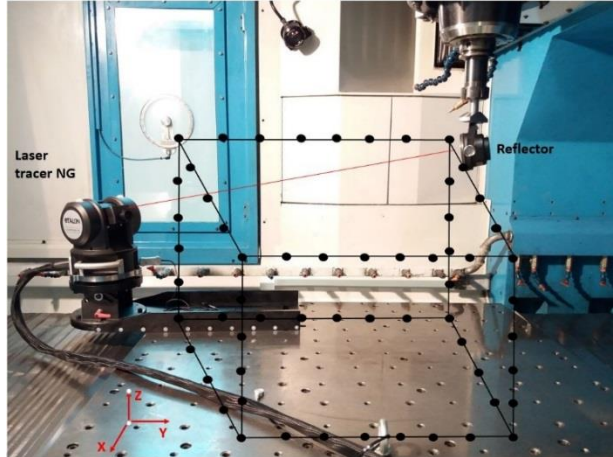


Figure 2-8 Volumetric error mapping of MT and measured point grid. (in black) [178]

Figure 2-9 presents the volumetric error mapping results immediately before the on-MT measurement exercise. Similarly, Table 2-4 shows those results according to the mathematical model output, for a coverage factor of $k=2$. The so-called “reduced” ETALON kinematic model was employed, comprised of 17 components of error. (Component of error notation according to VDI 2617-3 guideline)

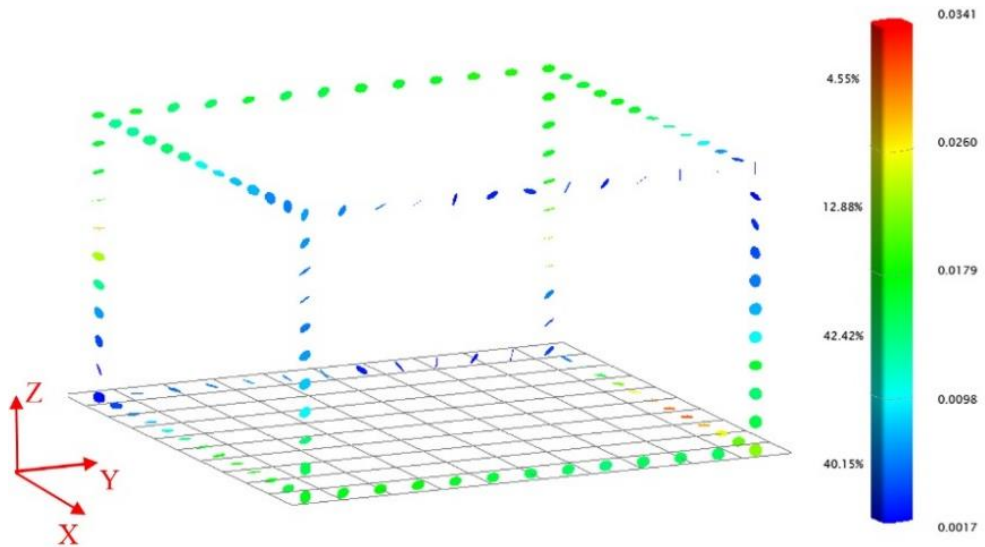


Figure 2-9 MT volumetric error mapping results. (vector mode)

2. Presentation of the published work

Table 2-4 MT volumetric error mapping results. (numerical mode)

Group	Component of error	Deviation (range)	Umax (95%)
Position	EXX	6.4 μm	0.2 μm
	EYY	8.4 μm	0.2 μm
	EZZ	4.2 μm	0.6 μm
Straightness	EYX	1.9 μm	0.1 μm
	EZX	1.7 μm	0.3 μm
	EXY	1.3 μm	0.2 μm
	EZY	2.7 μm	0.5 μm
	EXZ	1.8 μm	0.1 μm
Squariness Pitch / Yaw / Roll	EYZ	3.2 μm	0.1 μm
	ECX	3.4 μrad	0.5 μrad
	EBX	6.5 μrad	0.8 μrad
	EAY	10.5 μrad	0.5 μrad
	EBY	8.0 μrad	0.8 μrad
Squariness	ECY	6.9 μrad	0.3 μrad
	COY	0.4 μrad	0.2 μrad
	BOZ	-57.7 μrad	0.3 μrad
Squariness	AOZ	-11.3 μrad	0.4 μrad

MT volumetric error mapping exercise shows that geometric error is within 20 μm for almost the complete volume of the machine. Moreover, the workpiece replica standard size is 160 mm \times 160 mm, which means that the geometric error on the MT side that applies to the on-MT measurement is within 5 μm .

For the systematic error contributor (u_b) assessment, the proposed methodology depicted in Figure 2-6 was applied. In addition, a reliable TTP calibration was performed prior to the on-MT measurement exercise. The repeatability of the calibrated ring measurement is within 1 μm , which is similar to the MT repeatability. In this manner, it was considered to be within the measurement procedure uncertainty (u_p) on the uncertainty budget. Figure 2-10 shows a comparison of the systematic error assessment for the ISO 15530-3 technical specification and the VDI 2617-11 guideline. The difference between both approaches is within 1.5 μm .

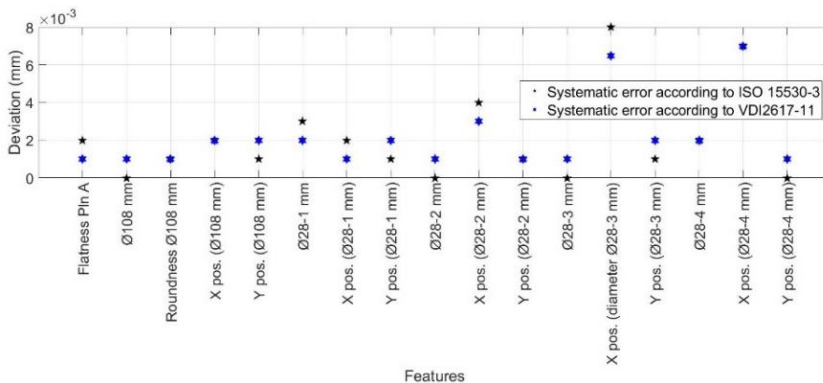


Figure 2-10 Systematic error (u_b) assessment according to ISO 15530-3 technical specification and VDI 2617-11 guideline. [178]

For the measurement procedure uncertainty (u_p), results obtained from the ISO 15530-3 based experimental test were considered, because they do not require a calibrated workpiece.

The uncertainty budget for the experimental test is presented in Figure 2-11 according to VDI 2617-11 guideline. Similar to the ISO 15530-3 technical specification, the expanded measurement uncertainty results are obtained for a coverage factor of $k=2$.

2. Presentation of the published work

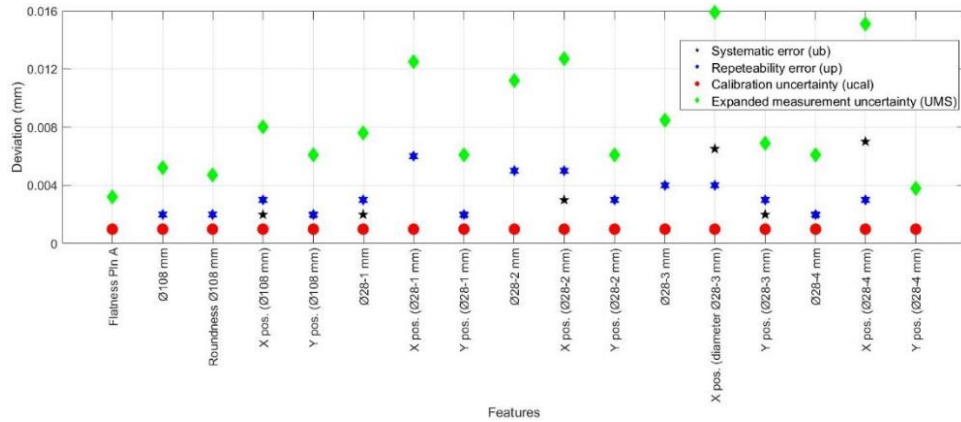


Figure 2-11 Uncertainty budget according to VDI 2617-11 guideline. [178]

Finally, Table 2-5 shows the uncertainty budget assessment within the VDI 2617-11 guideline and results are compared to what obtained with the ISO 15530-3 technical specification.

Table 2-5 Uncertainty budget according to VDI 2617-11 guideline and comparison with ISO 15530-3 technical specification. (results in μm) [178]

Feature	u_b	u_p	u_{ca}	u_{MS}	$U_{MS} - \text{VDI 2617-11}$	$U_{MS} - \text{ISO15530-3}$
Flatness Plan A	1.0	0.7	1.0	1.6	3.2	3.9
Ø108 mm	1.0	2.2	1.0	2.6	5.2	4.9
Roundness Ø108 mm	1.0	1.9	1.0	2.4	4.7	4.7
X position (Ø108 mm)	2.0	3.3	1.0	4.0	8.0	8.0
Y position (Ø108 mm)	2.0	2.1	1.0	3.1	6.1	5.6
Ø28-1 mm	2.0	3.1	1.0	3.8	7.6	8.4
X position (Ø28-1 mm)	1.0	6.1	1.0	6.3	12.5	13.2
Y position (Ø28-1 mm)	2.0	2.1	1.0	3.1	6.1	5.7
Ø28-2 mm	1.0	5.4	1.0	5.6	11.2	10.9
X position (Ø28-2 mm)	3.0	5.5	1.0	6.3	12.7	14.3
Y position (Ø28-2 mm)	1.0	2.7	1.0	3.0	6.1	7.3
Ø28-3 mm	1.0	4.0	1.0	4.2	8.5	8.4
X position (Ø28-3 mm)	6.5	4.5	1.0	8.0	15.9	17.9
Y position (Ø28-3 mm)	2.0	2.6	1.0	3.4	6.9	6.9
Ø28-4 mm	2.0	2.1	1.0	3.1	6.1	5.9
X position (Ø28-4 mm)	7.0	2.7	1.0	7.6	15.1	15.6
Y position (Ø28-4 mm)	1.0	1.3	1.0	1.9	3.8	4.3

Experimental results show that the uncertainty budget according to the VDI 2617-11 guideline obtains similar results to what obtained according to the ISO 15530-3 technical specification, where a calibrated workpiece is employed for the purpose. For the systematic error contributor (u_b), the difference between both approaches is within $1.5 \mu\text{m}$, which agrees with the accuracy of the volumetric error mapping performance, i.e. roughly $1 \mu\text{m}$, and also with the backlash error, which is within the $2 \mu\text{m}$ result that shows the volumetric repeatability. In addition, the calibration component (u_{ca}) is similar in both cases because of the employed reference standards, whether the calibrated workpiece or the volumetric error mapping solution has a similar uncertainty contributor. For the measurement procedure contributor (u_p), the same raw data is employed.

The future research looks for improvement on the proposed measurement procedure in harsh environment shop-floor conditions.

Integrated multilateration for machine tool automatic verification

The fourth article presents an integrated MT volumetric error mapping solution that enables the scaling of traceable on-MT measurement to large-size MTs. The integration of a tracking interferometer measurement device on the MT spindle breaks with the typical multilateration approach, based on sequential measurement scheme, and allows to measure the geometric error of an MT automatically in the complete volume. It reduces the time consumption and the measurement uncertainty for the volumetric error mapping process.

Multilateration-based measurement for MT error mapping requires at least four fixed points for displacement measurement, either absolute or relative, between those fixed points and any moving measuring point. According to this measurement distribution requirement, typically tracking interferometers are set on the MT table in the fixed points' positions and a measuring reflector is attached to the moving spindle to materialize the moving points. This multilateration configuration (hereinafter typical multilateration) is the first barrier to an automated MT calibration solution since manual intervention is needed on fixing tracking interferometers to each measurement station.

Commonly only one tracking interferometer is available, so in practice, multilateration measurements are done in a sequential scheme, as follows: MT movements are repeated several times to the same positions and measurements are taken from different tracking interferometer locations. Consequently, time consumption during measurement realization increases and, therefore, thermal drift between sequential measurements occurs. This becomes the second barrier to an automated solution since this approach requires MT repeatability for suitable multilateration uncertainty results [4].

A third barrier is the wired connectivity of tracking interferometers, which may restrict their movements. However, some new commercial models of laser trackers already offer the possibility to transfer acquired data through integrated wireless LAN communication. This tackles the third barrier so that a tracking interferometer can already be embedded into a large manufacturing system for an automated calibration process.

The idea of integrating a tracking interferometer into the manufacturing system breaks with the typical multilateration approach. Thus, the tracking interferometer moves to every measurement point while reflectors represent the fixed fiducial points. Figure 2-12 shows the integrated multilateration scheme.

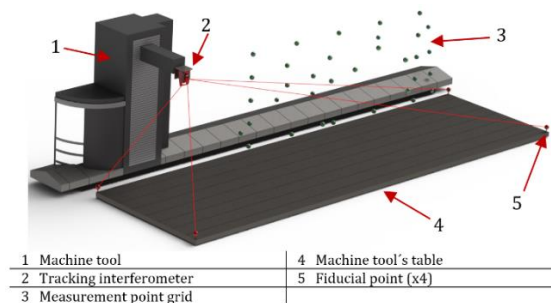


Figure 2-12 Integrated multilateration distribution on an MT. [179]

In this measuring scenario, the volumetric point grid to be measured represent the points to which the tracking interferometer is sequentially moved to acquire distance measurements to the four fiducial reflectors fixed around the manufacturing system. Compared to the typical multilateration approach, where tracking capacity is needed on the tracking interferometer side to track reflector's position in space, this integrated solution presents a totally

different measurement sequence. In this case, tracking interferometer is moved to every measurement point, from which pointing to every fiducial point occurs in sequence. It means that spatial relationship between fiducial points and volumetric point grid shall be established beforehand. Thus, initial automation of the measurement acquisition sequence plays a very important role because the spatial relationship between fiducial points and the point grid needs to be characterized in the MT coordinate system. This is executed in two main steps:

1. MT is moved sequentially to four corner points (one point out of plane) of the point grid volume and the tracking interferometer, working as a laser tracker, measures the 3D position of every fiducial point from every corner point. Best-fit transformation is applied among the four-data set. Thus, the spatial transformation between corner points and fiducial points is solved in a local coordinate system, defined by default at the first laser tracker measuring station.
2. Previous measurement's coordinate system is transformed into the MT coordinate system. To do that, on the previous measurement, the four corner points' coordinates are transformed into the MT coordinate system by means of a second best-fit transformation.

Once that spatial relationship between points is solved in the MT coordinate system, nominal point grid information helps to command the pointing from tracking interferometer to every fiducial point for every measurement position. To do it automatically, MT movement and data acquisition sequence are synchronized. This is done by means of a wireless LAN communication between data acquisition software and the MT's interface. Thus, a measurement trigger is sent from every measurement position to synchronize last fiducial point acquisition with MT next movement.

As previously explained in the literature review, multilateration is an already known mathematical technique that employs pure distance measurements to determine the 3D position of each point. The system to be solved is a non-linear overdetermined system of equations, so that, in addition to the 3D position of every point, length residuals that do not fit to the equation system are also obtained. These residuals provide information about how accurate every length measurement is. The volumetric 3D positioning error of the machine under measurement is thus determined by comparing the real spatial data, obtained by multilateration, versus the nominal data [179].

In this scenario, a Monte-Carlo based simulation was performed to understand that the integrated multilateration could perform similar uncertainty results compared to the well-known sequential multilateration scheme. For this simulation, JCGM 101:2008 guide (Evaluation of measurement data – Supplement 1 to the "Guide to the expression of uncertainty in measurement" – Propagation of distributions using a Monte Carlo method) is employed to determine the measurement uncertainty of the integrated multilateration approach [180]. It involves the propagation of the distributions of the input source of uncertainty by using the laser tracker distance error model to provide the distribution of the output. As a result, the expanded uncertainty for every measured point is assessed.

Different scale measuring volumes were simulated based on length measurements performed by a LEICA AT402 laser tracker. The goal is to show that the integrated multilateration keeps the same uncertainty levels as typical multilateration approach does for different scale measurement scenarios. In a second term, it also demonstrates how the multilateration method improves the 3D measurement accuracy of a single laser tracker. For that purpose, small, medium and large-scale measuring scenarios were simulated, defined by a point grid of 48 points distributed

2. Presentation of the published work

as follows: 4 points in X-axis, 4 points in Y-axis and 3 points in the Z axis (vertical direction). Measurement volumes are defined next (XYZ) [179]:

- Small = 1000 mm × 1000 mm × 1000 mm.
- Medium = 3000 mm × 3000 mm × 3000 mm.
- Large = 8000 mm × 4000 mm × 1000 mm.

Four 3D measurement approaches were tested under simulation to determine their spatial uncertainty assessment:

- Laser tracker measurement.
- Typical multilateration measurement.
- USMN measurement which runs within SA software. [181]
- Integrated multilateration measurement.

Pure length measurement uncertainty for a LEICA AT402 laser tracker is supplied by the OEM according to Equation 2:

$$U_L = U_F + U_M \quad (2)$$

where:

- U_L = Uncertainty of pure length measurement.
- U_F = Uncertainty of fixed length error that applies to all distance measurements. For a LEICA AT402 laser tracker, it is 0.00762 mm (k=1).
- U_M = Uncertainty of additional length error as measurement distance increases. For a LEICA AT402 laser tracker, it is 2.5 $\mu\text{m}/\text{m}$ (k=1).

Monte-Carlo simulation was performed with 500 iterations. Temperature variation was not considered within the simulation. Uncertainty results are expressed in micrometres for a level of confidence of 95% (k=2). Results are shown in Figure 2-13.

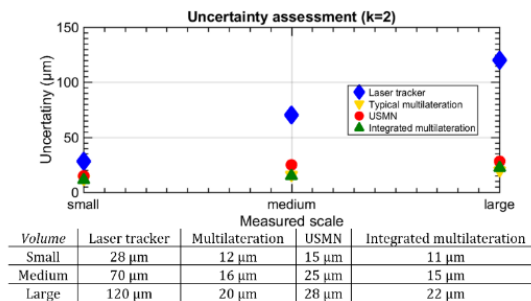


Figure 2-13 Uncertainty values obtained by simulation of four 3D measurement approaches [179]

According to simulated results depicted in Figure 2-13, integrated multilateration uncertainty values are similar to that achieved with either typical multilateration or USMN approaches, which are already validated 3D industrial measurement solutions. Therefore, the next step is to run an initial experimental exercise on an available KUKA industrial robot. In this way, the integrated multilateration performance was evaluated for a small volume point grid. The LEICA AT402 absolute laser tracker was mounted in a KUKA KR60 industrial robot and four fiducial points

2. Presentation of the published work

were fixed surrounding the robot. Figure 2-14 shows the mentioned experimental measurement setup and it also shows the LEICA AT960 laser tracker integration upside-down for a commercial demonstration.

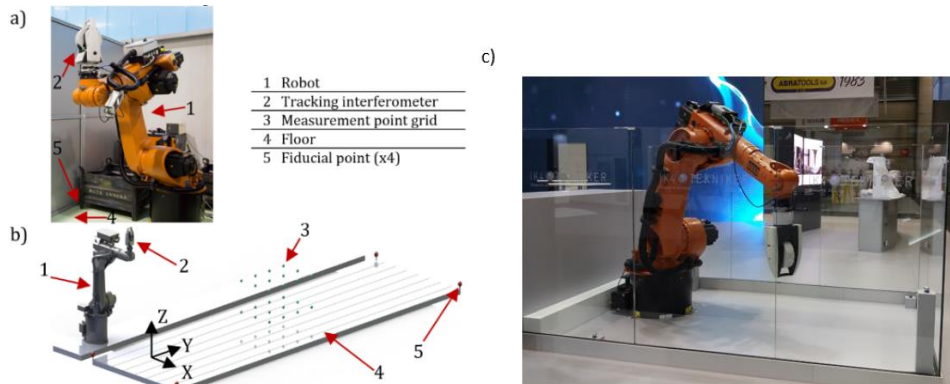


Figure 2-14 Integrated multilateration concept demonstration on a KUKA KR60 industrial robot: a) real setup at IK4-TEKNIKER premises; b) the virtual model and c) the AT960 laser tracker integration upside-down.

A point grid of 24 points divided into 3 points in X-axis, 4 points in Y-axis and 2 points in the Z axis (vertical direction) were measured automatically by the laser tracker. The measurement volume was defined as follows: X = 300 mm; Y = 300 mm and Z = 100 mm. Points 1÷12 comprise XY plane in Z = 100 mm and points 13÷24 comprise XY plane in Z = 0 mm. Firstly, the robot was moved to points 1÷12 depicting the upper XY plane and then, points 13÷24 describe bottom XY plane.

From every measurement point, every fiducial point was measured, so that a total of 96 measurements were sequentially introduced to the Monte-Carlo simulation of the real measurement scenario. 300 iterations were run to determine the expanded measurement uncertainty for every measurement point in X, Y and Z directions (U_x , U_y and U_z , respectively). Figure 2-15 a) shows the measurement uncertainty results for every measured point ($k=2$) and b) depicts uncertainties for fiducial points, for a level of confidence 95% ($k=2$).

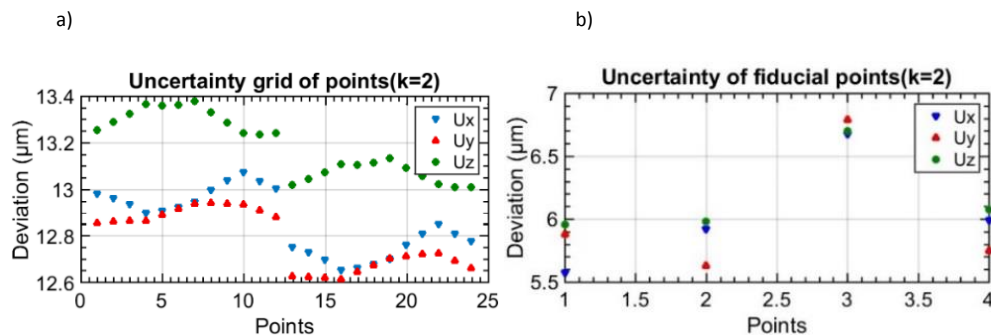


Figure 2-15 a) Uncertainty result for point grid in X, Y and Z directions; and b) Uncertainty result for fiducial point measurements in X, Y and Z directions. (U_x , U_y and U_z respectively) [179]

Results show interesting conclusions:

- Upper XY plane (points 1÷12) and bottom XY plane (points 13÷24) show similar uncertainty distribution, which represents robot measurement sequence in directions +X+Y-X-Y for each XY plane.

2. Presentation of the published work

- Every direction uncertainty in the bottom XY plane is slightly smaller (in average 0.2 μm) since distance measurement between tracking interferometer and fiducial points is 100 mm shorter. The difference is numerically in accordance with U_M parameter defined in Equation 2.
- Concept experimental demonstration uncertainty results are similar to simulation uncertainty results shown in Figure 2-13.
- Uncertainty results for fiducial points are similar to the U_F parameter defined in Equation 2.

In addition to the volumetric point grid uncertainty analysis, there is an extra numerical analysis that allows understanding the quality of the performed pure length measurements. It is based on calculating the length residuals between the real length data and the calculated data, according to Equation 3:

$$L_{res} = D_{ij} - L_{calculated} \quad (3)$$

where:

- L_{res} = Residual of pure length measurement.
- D_{ij} = Actual length measurement taken by the tracking interferometer.
- $L_{calculated}$ = Length measurement for every distance.

Figure 2-16 shows each length residual (L_{res}) defined in Equation 3, either in a plot format or a histogram format.

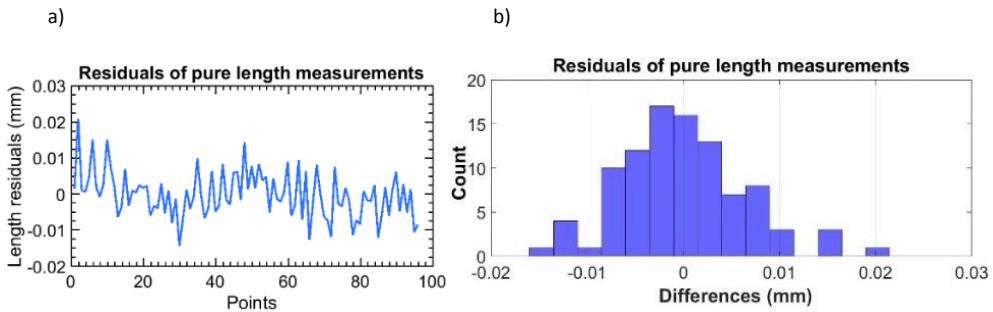


Figure 2-16 Length residuals results for the concept demonstration measurement a) Numerical format; and b) histogram format.

For the concept demonstration measurement, in total 96 length residuals were calculated. Results show that the standard deviation of length residuals is 0.0065 mm, slightly smaller than the uncertainty of fixed error measurement of the employed tracking interferometer (U_F) defined in Equation 2. It means that either length residuals results or uncertainty results that are shown in Figure 2-15 are similar to the accuracy of the employed tracking interferometer. It concludes that thermally induced dimensional drift is smaller than uncertainty results achieved on such a fast measurement acquisition sequence in this case. In fact, the total time consumption for the presented measurement case was 8 min, which means that the LEICA AT402 laser tracker took 20 sec to measure the four fiducial points from every measurement point. Compared to a typical multilateration measurement scheme where point grid measurement is repeated four times, integrated multilateration approach reduces total time consumption to a unique point grid measurement.

In this way, the main advantages compared to the typical multilateration solution are the following:

- Total time consumption during data acquisition is reduced up to 75% since a unique point grid movement is needed.
- Uncertainties for multilateration results are improved because of thermal drift during data acquisition, mainly on the manufacturing system side, is reduced. Thermal drift is somehow proportional to time consumption in a non-controlled shop floor environment.
- No human intervention is needed during the data acquisition process since laser tracker is automatically moved to every measurement position.

The integrated multilateration concept was validated in this work using an industrial robot. However, since its main application will be MT automatic verification, two main considerations have to be highlighted:

- The static stiffness of the KUKA KR 60 robot was measured with a laser tracker, showing values lower than 10 N/ μm . Therefore, for the weight of the employed LEICA AT402 laser tracker (7.3 kg), the vertical deflection could be in the range of more than 10 μm . However, typical static stiffness values are above 100 N/ μm for a gantry type MT and around 30N/ μm for a moving column MT. In these cases, the vertical deflection would be below 0.7 μm and 2.5 μm , respectively, which are even lower than the measurement uncertainty values of the multilateration technique (see Figure 2-15).
- The LEICA AT402 laser tracker used for the experiments could not work properly upside-down, so the measurement volume for concept demonstration was limited by this fact. However, some new models of laser trackers are already able to work upside-down and they will be used for the whole volume measurement of an MT as future work.

Integrated volumetric error mapping for large machine tools: An opportunity for more accurate and geometry connected machines

After the concept presentation and the experimental performance exercise on an available KUKA industrial robot, this article presents the experimental exercise of integrating the multilateration-based measurement solution on a large MT. The work was performed on a ZAYER MEMPHIS large MT and it was executed with a LEICA AT960 laser tracker because it can work upside-down.

For the experimental validation of the integrated volumetric error solution on a large MT, the integrated approach was compared to the typical multilateration approach which was performed with a laser tracer NG [84]. In this case, a unique laser tracer NG was available, so in practice, the multilateration scheme was performed in a sequential mode, as follows: MT movements were repeated several times to the same positions and measurements were taken from different tracking interferometer locations. In practice, the sequential scheme required the MT to move 5 times to every measurement position, so the time consumption during the measurement realization increased and, therefore, thermal drift between sequential measurements occurred. As above-commented, this is the second barrier to an automated solution, since it requires MT repeatability for suitable multilateration uncertainty results. Figure 2-17 shows the classic multilateration approach performed with a laser tracer NG from ETALON AG on a ZAYER MEMPHIS large MT [182].

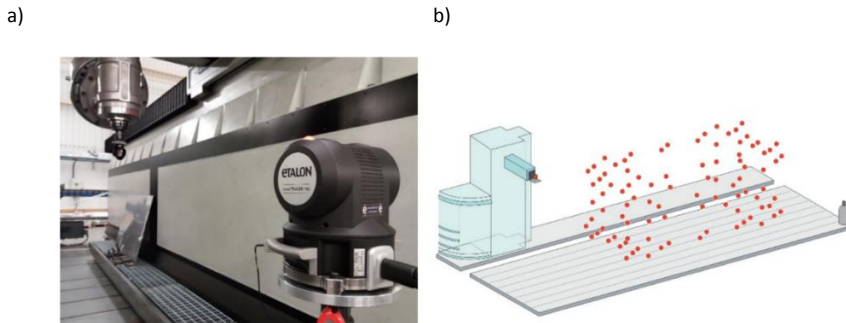


Figure 2-17 Sequential multilateration scheme: a) ZAYER MEMPHIS large MT employing a laser tracer NG; and b) virtual representation of the measurement sequence scheme. (Measurement performed by IK4-TEKNIKER in collaboration with ZAYER) [182]

When four tracking interferometers are available simultaneously, multilateration measurements can be performed according to the simultaneous scheme. Results are not obtained in real-time because mathematical post-processing is needed after data acquisition, but it avoids some of the limitations of the sequential multilateration, such as total time consumption, MT repeatability requirement and MT drift due to thermal variation during the measuring process. The simultaneous approach demands a unique movement to each point comprising the measurement point grid, which enables a reduction of the total acquisition time up to 75%. Measurement uncertainties are also improved because thermal drift during data acquisition, mainly on the manufacturing system side, is reduced. Thermal drift is somehow proportional to time consumption in a non-controlled shop floor environment [6]. However, the total cost for the simultaneous multilateration approach is high because it demands four tracking measurement systems to be working simultaneously and two reflectors on the MT side attached to the spindle. This is the main barrier that prevents this approach from being a common practice to map the volumetric geometric error of MTs.

Figure 2-18 shows a simultaneous multilateration approach on a ZAYER KAIROS large MT where four tracking measurement systems are working simultaneously.

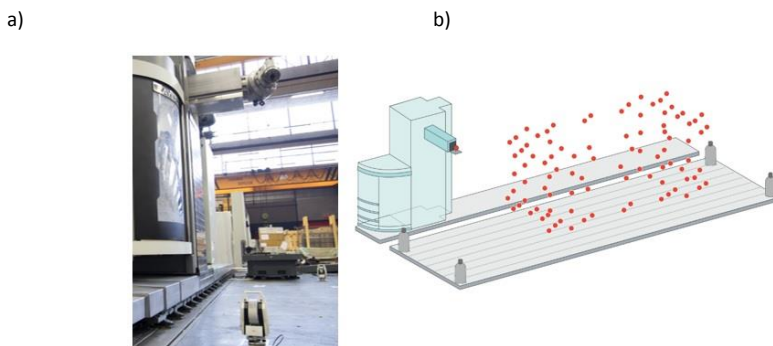


Figure 2-18 Simultaneous multilateration scheme: a) ZAYER KAIROS large MT employing three laser trackers and one laser tracer NG; and b) virtual representation of the measurement scheme. (Measurement performed by IK4-TEKNIKER in collaboration with ZAYER) [182]

Multilateration solution for volumetric error mapping performed either in sequential mode or in simultaneous approach leads to industrial limitations such as cost, total time consumption or thermal drift that prevent an automatic calibration of the MT.

2. Presentation of the published work

The idea of integrating a tracking interferometer into the manufacturing system breaks with the previous multilateration approaches. Thus, the tracking interferometer moves to every measurement point while reflectors represent the fixed fiducial points. The volumetric point grid to be measured represent the points to which the tracking interferometer is sequentially moved to acquire distance measurements to the four fiducial reflectors fixed around the manufacturing system. Compared to the typical multilateration approach, where tracking capacity is needed on the tracking interferometer side to track reflector's position in space, this integrated solution presents a different measurement sequence. In this case, the tracking interferometer is moved to every measurement point, from which pointing to every fiducial point occurs in sequence. It means that spatial relationship between fiducial points and volumetric point grid shall be established beforehand [179]. Figure 2-19 shows the integrated multilateration approach validation on a ZAYER MEMPHIS large MT with a LEICA AT960 laser tracker fixed to the spindle which is similar to the measurement scheme presented in Figure 2-12 [179]. It is working upside-down to improve the visibility between the tracking interferometer and the fiducial points.

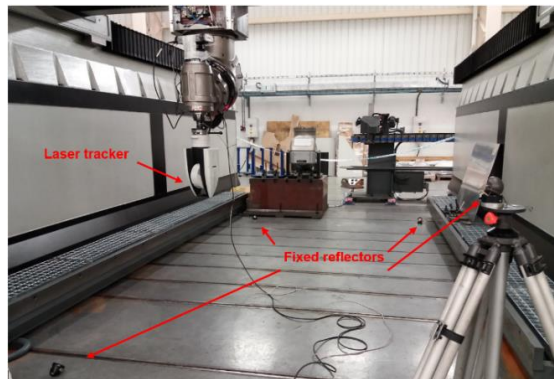


Figure 2-19 Integrated multilateration validation approach on a ZAYER MEMPHIS large MT employing a LEICA AT960 laser tracker. (Measurement performed by IK4-TEKNIKER in collaboration with ZAYER)

The validation of the integrated approach was performed on a MEMPHIS MT at ZAYER MT manufacturer premises. The point grid to be measured was comprised of 64 points. The mapped working range of the MT is: $X = 3000$ mm, $Y = 2300$ mm and $Z = 900$ mm. The performed validation plan is explained next:

- MT volumetric error mapping was performed with the typical approach employing a laser tracer NG from ETALON AG OEM. Four measurement positions were employed and measurement acquisition time was 2 h and 30 min.
- Integrated multilateration scheme is executed with a LEICA AT960 laser tracker fixed to the MT spindle, upside-down. Four cat-eye reflectors define the fiducial points, three of them fixed to the floor and the fourth one fixed out of the floor plane to improve the measurement accuracy on the vertical direction. The total time consumption for the integrated approach was 25 min.

The validation of the integrated multilateration approach against the typical approach is performed comparing four specific results:

- a) The uncertainty values for the fiducial points.
- b) The uncertainty values for the volumetric point grid.

2. Presentation of the published work

- c) The comparison between the point clouds measured with both approaches. Thus, the 3D coordinates are calculated for both measured point clouds and a best-fit transformation is executed to compare them. It shall be highlighted that MT geometry changes between both measurements, so the results also show the MT geometric variation because of the thermal drift effect.
- d) The comparison between the kinematic model outputs according to ETALON AG OEM model.

a) The standard deviation of pure length measurements for the integrated approach is $2.47\ \mu\text{m}$ while the same value for the typical approach is $1.1\ \mu\text{m}$. Therefore, obtained results for the typical approach are better than those obtained with the integrated approach.

b) Figure 2-20 shows the uncertainty results of the fiducial points after the multilateration exercise for both approaches.

c) Figure 2-21 shows the uncertainty values of the volumetric point grid after the multilateration exercise for both approaches.

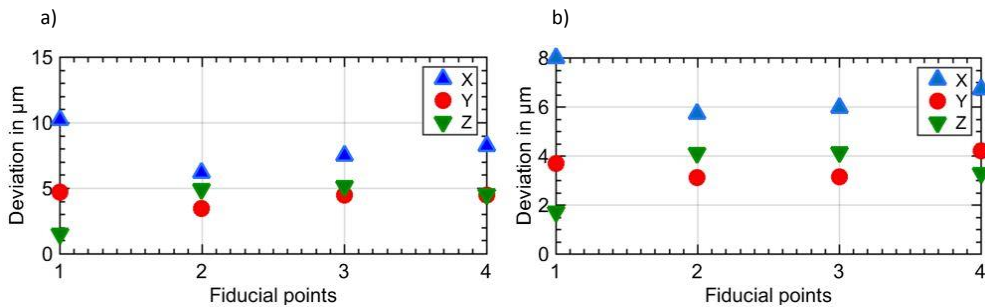


Figure 2-20 Uncertainty results of the fiducial points after the multilateration exercise: a) typical approach and b) integrated approach. [182]

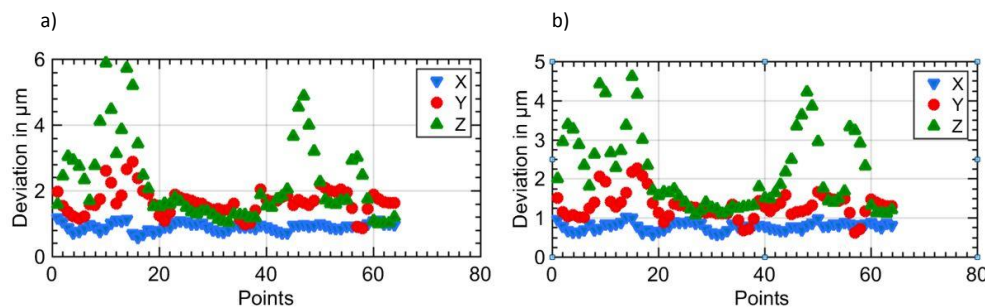


Figure 2-21 Uncertainty results for the point grid after the multilateration exercise: a) typical approach and b) integrated approach. [182]

Figure 2-20 and Figure 2-21 demonstrate that the obtained uncertainty values are better for the integrated approach compared to the typical approach. The measurement scenario is similar, but the measurement time is reduced from 2h 30 min that takes the typical approach to 25 min on the integrated approach. The time consumption is the main reason that better uncertainty results are performed on the integrated approach because the less time-consumption the less thermal drift influence.

Next, a comparison between measured point clouds is executed to understand the difference between both approaches. Figure 2-22 shows the difference in mm at each point comprising the point grid. The standard deviation

2. Presentation of the published work

of the above-mentioned difference is 0.04 mm and there is a vertical axis where deviation is higher between both approaches (points in blue). It shall be remarked that there are three points not properly measured on the integrated approach because the measurement acquisition was performed manually, and this is why results get worse in this line.

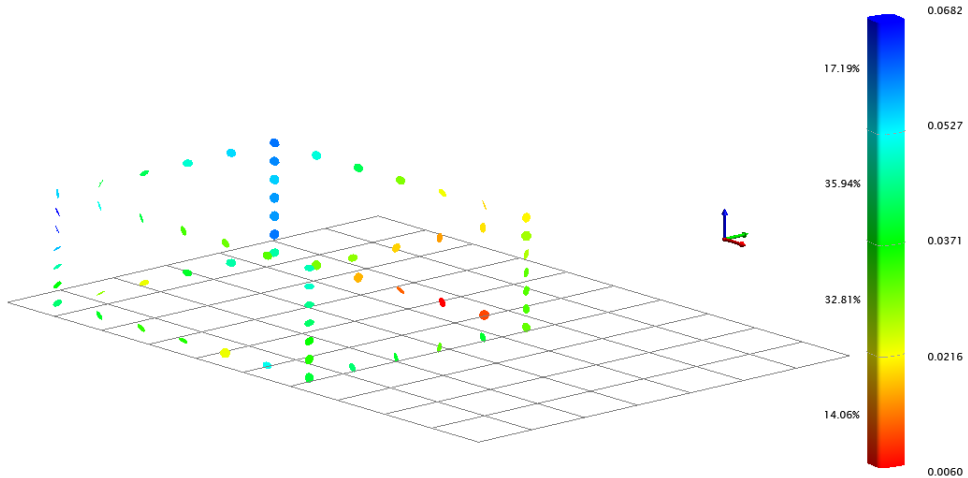


Figure 2-22 3D comparison at the point cloud level between both measurement approaches. [182]

Finally, Figure 2-23 and Figure 2-24 depict the kinematic model output for the typical multilateration approach and integrated multilateration approach respectively.

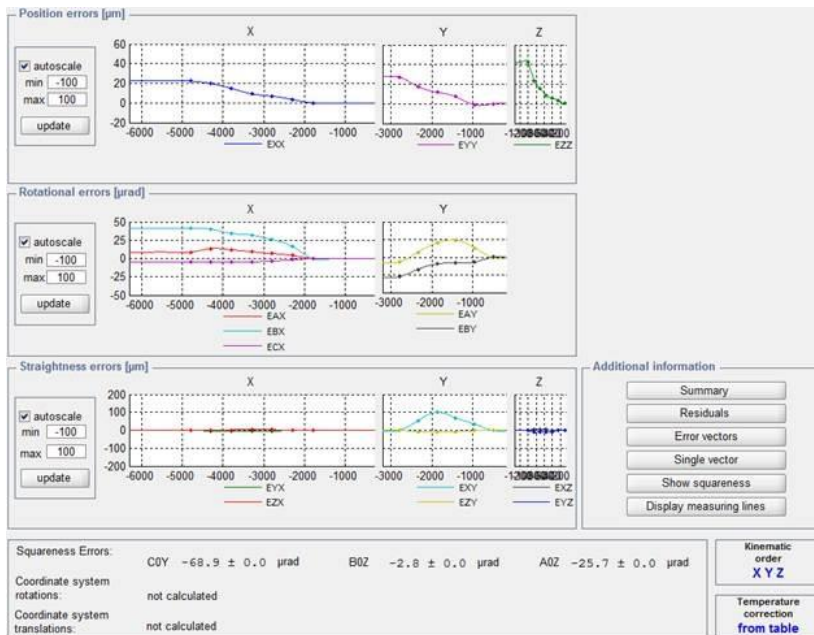


Figure 2-23 Typical multilateration-based kinematic output results.

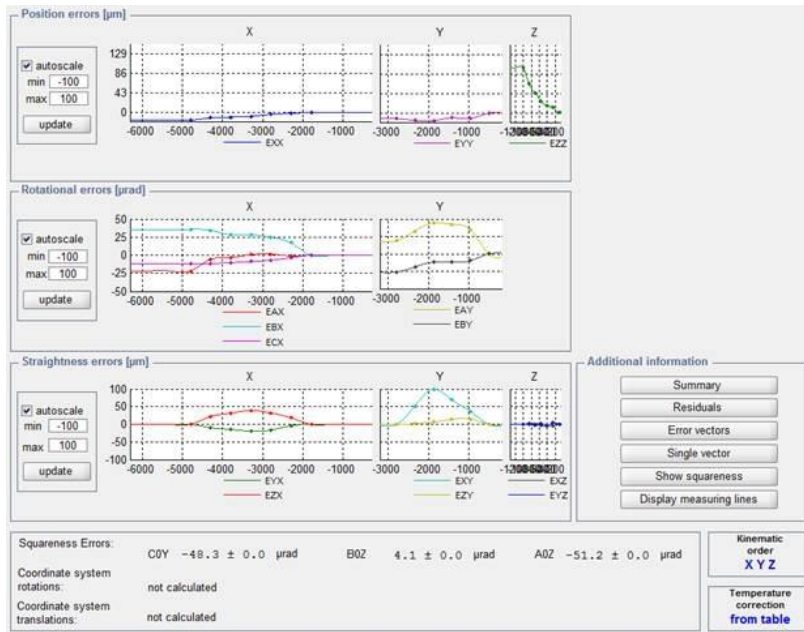


Figure 2-24 Integrated multilateration-based kinematic output results.

Figure 2-23 and Figure 2-24 show that both measurement approaches obtain a similar geometric characterisation of the ZAYER MEMPHIS MT. Rotational and straightness error geometric components are similar for both approaches but positioning and perpendicularity results show a slight variation between them. The MT seems to have 100 µm error in EXY straightness component of error, and both measurement approaches get a similar numerical value.

To sum up, the integration of the volumetric error mapping solution on the MT offers the possibility to enhance several fundamental issues affecting the performance of those manufacturing systems:

- To reduce the total time consumption for a complete volumetric error mapping of a large MT up to 75%. Similarly, it helps to reduce the measurement uncertainty, which is somehow proportional to the time consumption in a non-controlled shop-floor environment.
- To provide an automatic and volumetric MT error mapping process with no human intervention.
- To supply an interim check tool to monitor the volumetric performance of the MT regularly. Diagonal displacement test defined in the ISO 230-6 standard [79] could help to assess the volumetric performance of the MT periodically.
- To provide an active and integrated machine tool geometry error supplier for the industry 4.0 MT platforms. It shall be remarked that current industry 4.0 platforms do not show volumetric and geometric error information during the lifetime of the manufacturing systems.
- To improve the current on-MT measurement state of the art. This integrated solution offers the possibility to perform a volumetric error mapping of the MT immediately after the machining process. It allows distinguishing the error sources affecting the machining and measuring processes, so the systematic error affecting the on-MT measurement could be assessed on a large MT without employing a calibrated workpiece, which was already commented in the second and third articles. In addition, it also shows the information about the volumetric repeatability of the MT and the backlash error.

3D Measurement Simulation and Relative Pointing Error Verification of the Telescope Mount Assembly Subsystem for the Large Synoptic Survey Telescope

The sixth research article proposes a new verification method for the RPE assessment of the TMA subsystem for the LSST project [183]. At this point, this challenge benefits from the generated new knowledge within the LSM field for MTs and looks for a suitable measurement solution for the accuracy assessment of the LSST. The telescope size matches the size of extremely large MTs, and therefore some of the technologies and measurement techniques researched before are adapted for the LSST project.

This new measurement procedure scheme is based on laser tracker technology and several fiducial points fixed to the floor. It was designed and developed thanks to the knowledge generated within the integration of the multilateration scheme on the MT [184]. It demonstrates how the generated knowledge can be transferred horizontally from an industrial sector application to the industry of science sector, where cutting-edge measurement solutions are demanded on the large-scale.

The LSST is a large (8.4 m) wide-field (3.5 degrees) survey telescope, which will be located on the summit of Cerro Pachón in Chile. The TMA subsystem points at and tracks fields on the sky, by providing motions about the azimuth and elevation axes. Therefore, it provides pointing, tracking, and slewing system performance requirements to comply with the space survey mission [185]. The TMA subsystem is currently being assembled in the north of Spain, and the developed measurement procedure aims to assess the RPE requirement of the TMA subsystem [186] in-situ, for the engineering validation of the subsystem.

When observing the sky, it is of great interest to make sure that the telescope is pointing towards the intended location on the sky as accurately as possible, to ensure that it is pointed towards the correct target source and, consequently, to use accurate photometric and astrometric information that is related to that target. It means that the pointing and alignment performance of the LSST will have a very strong influence on the quality of the scientific results obtainable. Thus, a reliable RPE assessment of the TMA subsystem is particularly important. In this scenario, an end-to-end test of the complete LSST, in order to check the pointing performance and the correct alignment of all the elements, is not possible until the final assembly in Chile is complete. For this reason, the TMA subsystem will first be tested, including the RPE requirement, at the factory with surrogate masses, to replace the optical payloads with the aim of avoiding 'late surprises' during the LSST construction in Chile. Thus, the LSST project requires a new RPE verification method based on laser tracker technology for the engineering validation of the TMA subsystem within the complete pointing range of the telescope.

Next, a detailed description of the developed RPE verification method for the LSST is presented [184]:

Measurement scenario: The optical axis of the LSST is defined at the M1M3 primary/tertiary mirrors so that one of the limitations tackled by any RPE measurement procedure is the measurement of the M1M3 mirrors for any pointing motion within the LSST pointing range. Additionally, all the performance requirements must be met for the observing angles between 15 and 86.5 degrees for elevation angles, and from 0 to 360 degrees for azimuth angles. However, for maintenance work, the TMA should be able to point from horizon to zenith (i.e., elevation angles from 0 to 90 degrees) [187].

The measurement of the LSST telescope is an LSM exercise [4] because the dimension of the measurement scenario is up to 40 m of diameter. Thus, the LSM technology proposed for the RPE characterisation is the LEICA AT402 laser

2. Presentation of the published work

tracker technology combined with SA software. Figure 2-25 shows the measurement scenario for the RPE assessment. Figure 2-25a shows the M1M3 measurement plane, where the measurement targets are depicted in red and Figure 2-25b illustrates the complete measurement scenario. Furthermore, it also shows that the engineering validation at the subsystem level is verified with dummies instead of the real optical elements. The real measurement targets are shown in Figure 2-40.

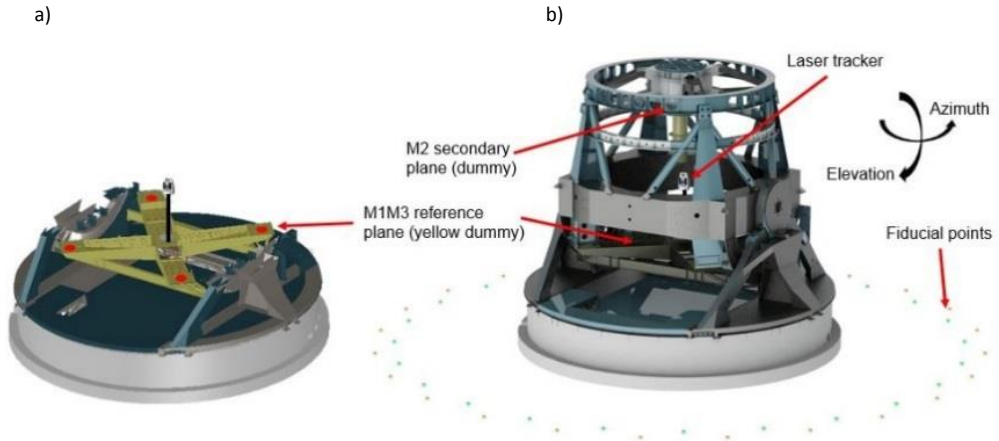


Figure 2-25 Measurement scenario for RPE assessment. (a) M1M3 measurement plane (measurement targets in red); and (b) Complete LSST measurement scenario. [184]

In this measurement scenario, a pointing matrix is defined to characterize the RPE measurement test of the TMA within the pointing range of the LSST. Four elevation angles at four different azimuth positions are defined to represent any pointing direction on the sky, as shown in Figure 2-26.

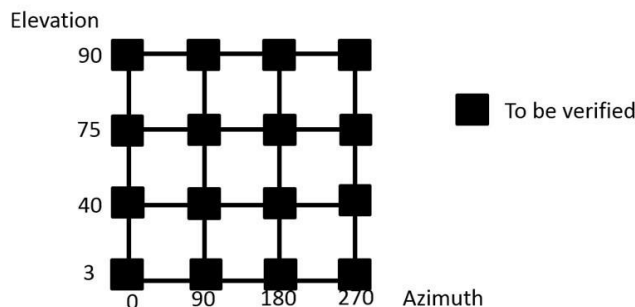


Figure 2-26 Mapping matrix for the RPE test. [184]

Measurement procedure: A new measurement procedure for the RPE assessment is defined as follows: A laser tracker is placed inside of the LSST, close to its origin, and a metrology network comprising a reference point cloud is fixed to the floor, outside and surrounding the LSST telescope. This metrology network is of special importance, as any laser tracker location during the whole measurement process is solved by the measurement of this fiducial metrology network. Thus, the RPE measurement procedure consists of measurements of the metrology network to locate the laser tracker, and afterwards, measurements of the optical axis of the TMA by measuring four target points at the M1M3 reference plane. Thus, by locating the M1M3 reference plane on the earth-fixed reference system, i.e., the floor, each observation angle for TMA is characterized and compared to the input position, which means the RPE assessment. The measurement process is repeated for each of the pointing positions defined in

2. Presentation of the published work

Figure 2-26 and within the pointing range of the LSST [186]. It should be highlighted that the laser tracker position is fixed close to the LSST origin, to nullify the range of the angle of incidence from the laser tracker to the reflectors, as it is shown in Figure 2-34 b. Thus, the laser tracker tilts with the rotation centre of the telescope and incidence angle does not change which means that it will not cause a longer travelling path of the beam inside the prism. For the LSST project, 25 mm hollow corner cube optics are employed, as it is shown in Figure 2-34 a.

An accurate reference point cloud comprised of 48 points is defined on the floor outside and surrounding the telescope. Twenty-four points create a 15 m radius circle, and 24 additional points define a 16 m radius with an offset of 7.5° to the previous one. Its circular shape optimized the visibility challenge for any azimuth-pointing position of the telescope. Additionally, those points are fixed to the floor, minimizing thermal gradients effects. Figure 2-25 b shows the metrology network arrangement around the LSST and the M1M3 reference plane where every measurement shall be executed.

The biggest challenge to meet the RPE measurement specification is to ensure the line of sight between the M1M3 reference plane and the metrology network for any pointing position. Thus, a visibility study is performed within SA software for any elevation axis position. Figure 2-27 visually represents the line of sight for any elevation angle of the TMA. Green lines in Figure 2-27 show the line of sight from the inside-placed laser tracker to the points that comprise the fiducial metrology network. The visibility became worse from the zenith to the horizon on the TMA pointing direction. However, any TMA pointing direction could be assessed by the presented measurement procedure.

The parallelism between M1M3 and M2 optics for any elevation axis is also assessed by the proposed measurement procedure by attaching four measurement reflectors to the M2 plane, as shown in Figure 2-39.

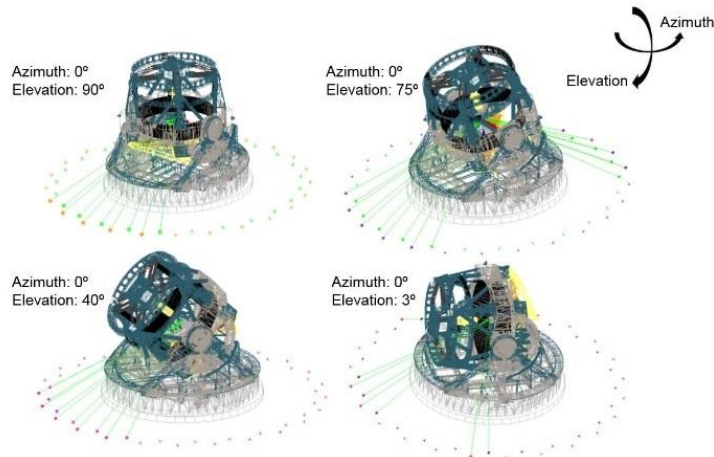


Figure 2-27 Visibility study overview from inside placed laser tracker, from the zenith to the horizon pointing direction. [184]

Measurement simulation: A simulation model, based on the Monte-Carlo technique, is developed to assess the RPE measurement uncertainty according to the developed measurement procedure. The simulation model is developed within SA software, so a commercial tool is employed to code the simulation code [181]. For that simulation, a Gaussian random number generator (utilizing a Box-Muller algorithm) mathematically simulates the measuring scenario with 500 sensitivity samples [188], and the standard deviation parameter is calculated as an uncertainty

2. Presentation of the published work

indicator of the simulated measurement methodology. In addition, the Box-Muller algorithm executes a laser tracker error model according to the specifications of the laser tracker's manufacturer (LEICA) at a 68.3% confidence level ($k = 1$), where: (similar values to that shown in the fourth article)

- U_F = Uncertainty of the fixed length error that applies to all distance measurements. For a LEICA AT402 laser tracker, it is 0.00762 mm.
- U_M = Uncertainty of the additional length error as the measurement distance increases. For a LEICA AT402 laser tracker, it is 2.5 $\mu\text{m}/\text{m}$.
- U_A = Uncertainty of angle measurements. For a LEICA AT402 laser tracker, it is 1 arcsec.

The RPE measurement simulation process has two main stages: a) The first stage is executed to characterize the reference metrology network; and b) the second stage aims to quantify the measurement uncertainty on the RPE assessment measuring the optical reference of the telescope, the M1M3 plane:

a) Metrology network characterisation: The USMN tool is employed to coordinate uncertainty field computation. The laser tracker is fixed to the TMA, as an onboard 3D metrology system and the sixteen TMA pointing positions are performed according to Figure 2-26. Therefore, every fiducial point is measured from different laser tracker locations, which allows locating every fiducial point that is fixed to the floor and that is relative to the TMA. The simulation is performed with 500 samples, according to the above-mentioned LEICA AT402 laser tracker error model, and the standard deviation parameter of every fiducial point coordinate is obtained from the simulation on each axis direction. Thus, the expanded uncertainty of every fiducial point on each axis direction is obtained by multiplying the standard deviation times the coverage factor (k):

$$U_x = k \times s_x ; U_y = k \times s_y ; U_z = k \times s_z \quad (4)$$

where:

- k = coverage factor
- s = standard deviation (s_x = X direction, s_y = Y direction and s_z = Z direction)

According to the executed simulation, every point uncertainty is better than 0.1 mm for a 95% confidence level ($k = 2$), as shown in Figure 2-28.

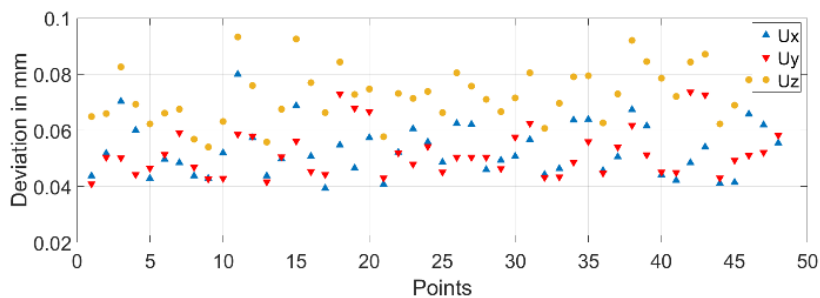


Figure 2-28 Measurement uncertainty for metrology network characterisation. [184]

The simulation result correlates with the research performed by Rakich et al. at the LBT active alignment system with laser tracker technology [189]. Here, Rakich et al. proposed that laser tracker measurement on a 30 m radius shall be performed within 0.1 mm precision.

b) RPE measurement simulation: Once checked that the metrology network allows the location of the laser tracker at any measurement position within the measurement scenario; in fact, any TMA pointing direction could be assessed within the pointing range of the LSST. Thus, the M1M3 reference plane is measured and referenced to the earth-fixed reference system, so that the TMA pointing direction is accurately measured for any pointing direction on the sky. For practical issues, the pointing range of the TMA is discretised as shown in Figure 2-26. Figure 2-29 shows the RPE measurement uncertainty results, for a 95% confidence level ($k = 2$), obtained by the Monte-Carlo simulation according to the mapping matrix represented in Figure 2-26.

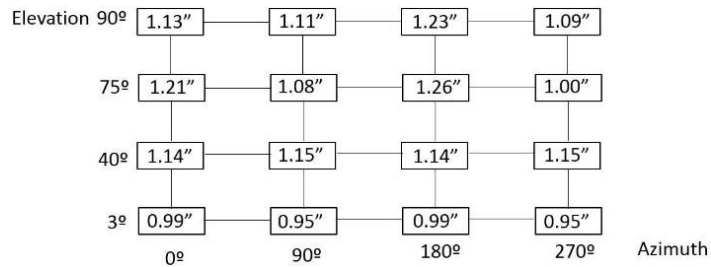


Figure 2-29 RPE measurement uncertainty results. (in arcseconds) [184]

Previous simulations consider an absolute and fixed metrology network, but the floor suffers from dimensional drift because of the ambient temperature variation. Therefore, more realistic simulation is executed to determine the fit for purpose for the presented measurement methodology. A 24-hour measurement is executed on the premises where TMA is being assembled, in the north of Spain. Results provided a more realistic overview of how floor moves. The dimensional drift of the measurement scenario is within 0.5 mm for a temperature change of 4 °C, so a random floor movement with a Gaussian distribution is applied to each simulation sample by means of an additional Monte-Carlo simulation process modelling the floor behaviour. This means that a unique 6 dof transformation is applied onto every single point at each simulation sample, which allows simulating the real behaviour of the floor where the TMA is mounted. Finally, a new RPE measurement simulation is numerically run and realistic uncertainty results for a 95% confidence level ($k = 2$) are achieved. Results are shown in Figure 2-30.

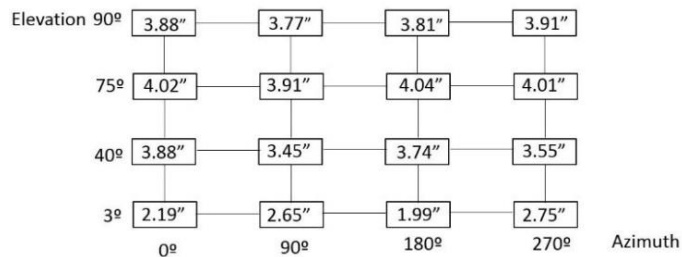


Figure 2-30 RPE measurement uncertainty results with floor movement consideration. (in arcseconds) [184]

In-situ measurement strategy: After simulating the measurement uncertainty for the RPE verification of the LSST, the results make one thing completely clear: the measurement uncertainty for the metrology network characterisation should be kept within 0.1 mm to achieve the RPE measurement uncertainty results better than 2 arcsec (correlation on a stable temperature measurement scenario, e.g., 20 ± 1 °C on the complete LSST volume).

At this point, two main limitations are considered for a successful in-situ implementation of the proposed new verification method for the RPE assessment: a) the laser tracker uncertainty; and b) the temperature effect during

the data acquisition period. a) For the laser tracker uncertainty limitation, the USMN tool is employed within SA software to improve the coordinate uncertainty field computation for the metrology network characterisation [181]. b) For the temperature effect, a fully automatic verification procedure is proposed, to reduce data acquisition time. The laser tracker-based measurement program is interconnected to the LSST control software by the means of a TCP/IP in a private connection, and the USMN is performed during the measurement procedure, so most of the fiducial points are measured for every LSST pointing position. The TCP/IP connection permits the synchronization of the LSST movement with the laser tracker measurement sequence. Figure 2-31 shows the fully automatic verification pointing measurement procedure for the LSST as a flow chart, where the parallelism measurement between M1M3 and M2 is also considered.

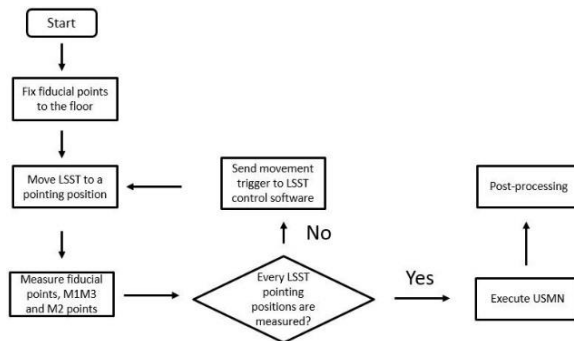


Figure 2-31 The fully automatic RPE verification procedure flow chart. [184]

The fully automatic measurement procedure presented in Figure 2-31 aims to reduce the RPE measurement down to 60–90 min, and it improves the simulation sequence to one stage.

Telescope mount assembly pointing accuracy assessment for the Large Synoptic Survey Telescope: A large-scale metrology challenge

Finally, the last article explains in detail the TMA subsystem in-situ RPE survey. According to the measurement procedure presented in the sixth article, the survey realisation and the remarkable results are presented here.

As it is shown in Figure 2-32, the real measurement scenario was far from being perfect, as considered on the simulation stage. Figure 2-35 shows that there were “obstacles” in the shop floor for being a perfect measurement scenario.



Figure 2-32 The real measurement scenario at ASTURFEITO premises. [190]

2. Presentation of the published work

As above-explained, the laser tracker position was fixed close to the TMA reference system origin, to nullify the range of the angle of incidence from the laser tracker to the reflectors. Thus, the laser tracker tilts with the rotation centre of the telescope and the incidence angle between the laser tracker and the fiducial points did not change which means that it does not cause a longer travelling path of the beam inside the reflector prism. Figure 2-33 shows the laser tracker location in M1M3 when the TMA is pointing to the a) horizon; and b) zenith, it shows how the visibility problem, between the inside placed laser tracker and the fixed reference metrology network, was solved.



Figure 2-33 Laser tracker visibility a) TMA horizon pointing position; and b) TMA zenith pointing position. [190]

Moreover, 25 mm hollow corner cube optics were glued to the floor to define the reference metrology network which helped to the visibility challenge. Figure 2-34 shows a) fiducial point definition and b) laser tracker arrangement at the real measurement scenario.

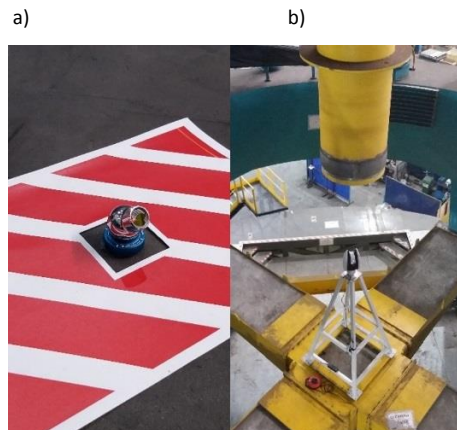


Figure 2-34 a) Fiducial point definition; and b) laser tracker arrangement in M1M3. [190]

The pointing accuracy test was performed during the first week of September of 2018 at Asturfeito premises, in Spain, with a LEICA AT960 laser tracker technology. The automation of the measurement campaign took 3 days. As a result, the time consumption for the pointing accuracy test was 70 min which means that temperature variation of the measurement scenario at floor level was reduced to 1 °C within a unique measurement round. The

2. Presentation of the published work

measurement sequence was repeated five times aiming to assess not just the pointing accuracy of the TMA, but also the repeatability.

Once that measurement was performed, the measurement uncertainty for the pointing accuracy test was updated to the real measurement scenario. It should be highlighted that there were several physical limitations on the real measurement scenario such as, the office box, the stairs of the TMA structure and the shop floor layout that prevent the measurement scenario from being similar to the designed nominal scenario. A new simulation was performed according to the real measurement scenario restrictions depicted in Figure 2-35.

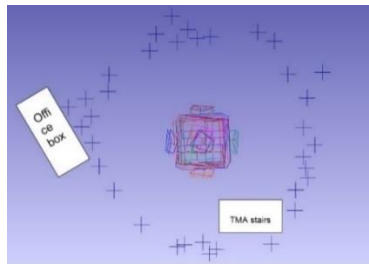


Figure 2-35 Real point distribution for the TMA pointing accuracy test. [190]

Simulation results show that pointing accuracy test uncertainty is worse when the telescope is pointing to the horizon rather than when it is pointing to the zenith. It occurs because point visibility from inside placed laser tracker is much better when the telescope is pointing to the zenith. When pointing to the zenith 18 reflectors are seen, while when pointing to the horizon 5÷6 reflectors are within the line of sight. Pointing accuracy test simulation results (in arcsec) are shown in Figure 2-36 for a 95% confidence level ($k=2$).

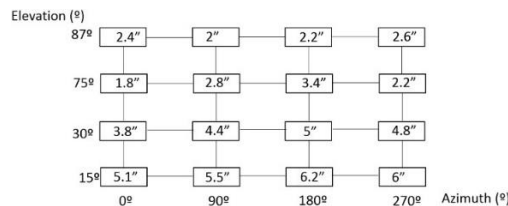


Figure 2-36 Uncertainty assessment for the real measurement scenario. [190]

Uncertainty values are slightly worse than what achieved in simulation mode, mainly because point distribution on the real measurement scenario is not as homogeneous as in the nominal measurement scenario. Additionally, the standard deviation parameter of every fiducial point coordinate on each axis direction is obtained from the updated simulation. Figure 2-37 shows the measurement uncertainty for the metrology network characterisation for a 95% confidence level ($k=2$).

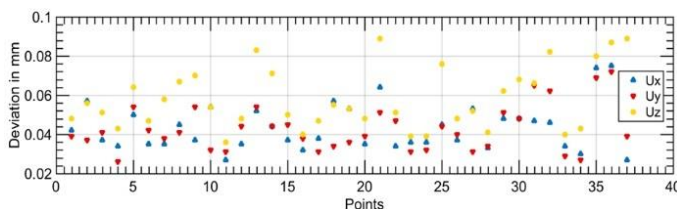


Figure 2-37 Measurement uncertainty for the metrology network characterisation. (real measurement scenario-based simulation) [190]

2. Presentation of the published work

Residual results, the comparison between Figure 2-28 and Figure 2-37, show that uncertainty for X and Y direction (floor plane) are better to that previously simulated with a perfect measurement scenario. In Z direction results are in general better than simulated results but there are some points that are slightly worse for the real measurement scenario. To sum up, the real measurement scenario uncertainty was slightly better than the simulated uncertainty. The main reason is that the real measurement execution was performed with a LEICA AT960 laser tracker which combines two measurement technologies (relative interferometer measurement and absolute distancimeter measurement) compared to the laser tracker employed on the simulation, a LEICA AT402, that uniquely employs distancimeter technology to perform length measurement.

The RPE survey results are obtained as the average result of the five performed pointing accuracy test results. The RPE results are explained in Table 2-6. It shall be remarked that results are within tolerance for every pointing position of the TMA subsystem. Pointing error in azimuth is within 6 arcsec, while pointing error in elevation axis is worse, up to 13.8 arcsec. However, it shall be stated that uncertainty values for those high pointing error pointing positions are also higher than average values, which mean that results shown in Table 2-6 are affected by the uncertainty of the measurement procedure. Therefore, there is a systematic error on the measurement procedure that is within the pointing accuracy test results. The systematic error is not being corrected from the results.

Table 2-6 RPE test results for the TMA subsystem. (Real results obtained on the in-situ survey)

Nominal		Real		Deviation		RPE (arcsec)	Expanded uncertainty (arcsec)
A (°)	E (°)	A (°)	E (°)	A (arcsec)	E (arcsec)		
0	3	0.00004	3.00013	0.144	0.468	0.49	2.4
0	15	0.00081	15.00059	2.916	2.124	3.61	1.8
0	60	0.0017	60.00258	6.12	9.288	11.12	3.8
0	75	0.001	75.00249	3.600	8.964	9.66	5.1
90	3	90	3.00182	5.652	6.552	8.65	2.0
90	15	90.00143	15.0024	5.148	8.640	10.06	2.8
90	60	90.00169	60.00378	6.084	13.608	14.91	4.4
90	75	89.99944	75.00386	2.016	13.896	14.04	5.5
180	3	179.99987	3.00113	0.468	4.068	4.09	2.2
180	15	179.99921	15.00155	2.844	5.580	6.26	3.4
180	60	179.99865	60.00381	4.86	13.716	14.55	5.0
180	75	179.99888	75.00326	4.032	11.736	12.41	6.2
270	3	-89.99857	3.00178	5.148	6.408	8.22	2.6
270	15	-89.99843	15.002	5.652	7.200	9.15	2.2
270	60	-89.9989	60.00289	3.960	10.404	11.13	4.8
270	75	-89.99824	75.00346	6.336	12.456	13.97	6.0

Pointing repeatability measurement tolerance is limited to 1 arcsec, so as depicted in Table 2-7 the laser tracker-based pointing accuracy test cannot perform within the required 1 arcsec accuracy. This is the reason that the pointing repeatability test was repeated with direct measurement methods, a gravity-based level for elevation axis and an autocollimator for the azimuth axis, reducing the measurement uncertainty within 1 arcsec. Figure 2-38

2. Presentation of the published work

shows the measurement approach with the level and the autocollimator. The repeatability results either in azimuth axis or elevation axis are within the required tolerance of 1 arcsec measured with direct measurement approach.

On the RPE test, M2 secondary mirror was also measured for every pointing position within the pointing range of the TMA. It means that parallelism between M1M3 primary-tertiary mirrors and M2 secondary mirror can also be assessed for the pointing matrix depicted in Figure 2-26. Results show that parallelism between M1M3 and M2 maintains within 1 arcsec for the working range of the TMA subcomponent. Figure 2-39 shows three out of four reflectors glued to M2 secondary mirror allowing parallelism requirement assessment. Figure 2-40 depicts the measurement reflectors attached to M1M3 primary mirror.

Table 2-7 TMA repeatability results obtained with laser tracker technology.

NOMINAL				REPEATABILITY (arcsec)	REPEATABILITY (U) (arcsec)
A (°)	E (°)	A (°)	E (°)		
0	87	0	3	0.7	0.1
0	75	0	15	0.8	0.1
0	30	0	60	0.8	0.2
0	15	0	75	0.8	0.2
90	87	90	3	0.7	0.35
90	75	90	15	0.4	0.5
90	30	90	60	0.5	0.55
90	15	90	75	1	1
180	87	180	3	0.9	0.1
180	75	180	15	1	0.1
180	30	180	60	0.3	1
180	15	180	75	1	1
270	87	-90	3	0.5	0.2
270	75	-90	15	0.9	0.2
270	30	-90	60	1	0.3
270	15	-90	75	1.1	1



Figure 2-38 Direct measurement methods for pointing the repeatability test. [190]

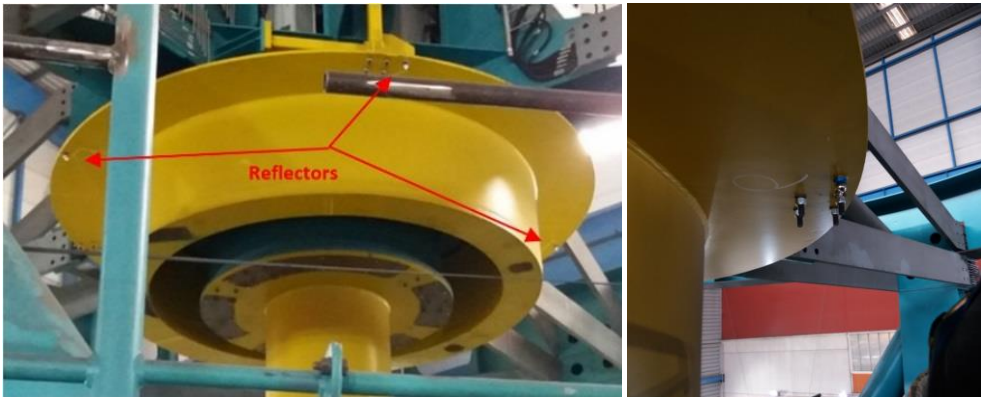


Figure 2-39 Reflectors attached to M2 secondary plane (3 out of 4 reflectors are shown). [190]

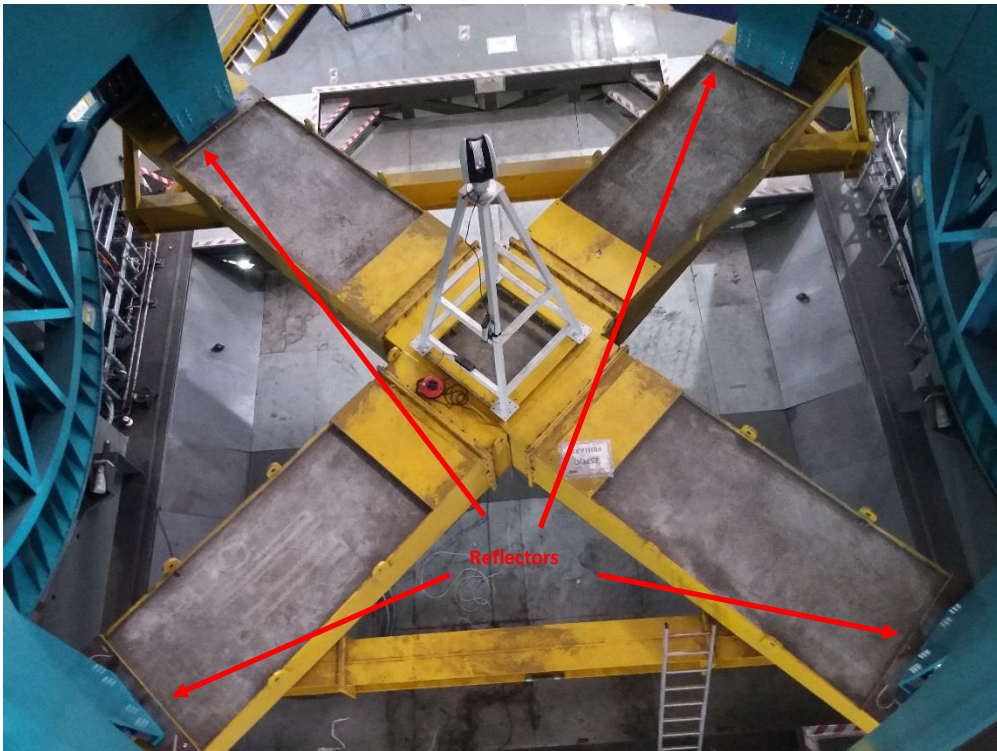


Figure 2-40 Reflectors attached to M1M3 primary plane.

Finally, the last article proposes that the generated knowledge on the development of the customized simulation of the RPE assessment for the LSST could be employed as a laser tracker based LSM simulation tool for similar high-accuracy and large-scale projects. Here, a simulation work is presented for an onboard laser tracker based active alignment system within large telescope applications. The advanced simulation tool permits understanding the best laser tracker arrangement strategy to reduce the survey accuracy to its minimum.

3. RESEARCH ARTICLES



Traceability of On-Machine Tool Measurement: A Review

Review

Traceability of On-Machine Tool Measurement: A Review

Unai Mutilba ^{1,*} , Eneko Gomez-Acedo ¹, Gorka Kortaberria ¹, Aitor Olarra ¹ and Jose A. Yagüe-Fabra ² 

¹ Department of Mechanical Engineering, IK4-Tekniker, Eibar 20600, Spain; eneko.gomez-acedo@tekniker.es (E.G.-A.); gorka.kortaberria@tekniker.es (G.K.); aitor.olarra@tekniker.es (A.O.)

² I3A, Universidad de Zaragoza, Zaragoza 50018, Spain; jyague@unizar.es

* Correspondence: unai.mutilba@tekniker.es; Tel.: +34-636-994-351

Received: 1 May 2017; Accepted: 27 June 2017; Published: 11 July 2017

Abstract: Nowadays, errors during the manufacturing process of high value components are not acceptable in driving industries such as energy and transportation. Sectors such as aerospace, automotive, shipbuilding, nuclear power, large science facilities or wind power need complex and accurate components that demand close measurements and fast feedback into their manufacturing processes. New measuring technologies are already available in machine tools, including integrated touch probes and fast interface capabilities. They provide the possibility to measure the workpiece in-machine during or after its manufacture, maintaining the original setup of the workpiece and avoiding the manufacturing process from being interrupted to transport the workpiece to a measuring position. However, the traceability of the measurement process on a machine tool is not ensured yet and measurement data is still not fully reliable enough for process control or product validation. The scientific objective is to determine the uncertainty on a machine tool measurement and, therefore, convert it into a machine integrated traceable measuring process. For that purpose, an error budget should consider error sources such as the machine tools, components under measurement and the interactions between both of them. This paper reviews all those uncertainty sources, being mainly focused on those related to the machine tool, either on the process of geometric error assessment of the machine or on the technology employed to probe the measurand.

Keywords: machine tool metrology; temperature; uncertainty; traceability; error sources

1. Introduction

“Industry 4.0” represents an initiative for the future development of industrial production [1]. The idea aims to link the manufacturing industry and information technology to make production more flexible, where the flexibility offers the possibility to manufacture customized products through efficient manufacturing processes. As demand fluctuates and batch sizes fall, efficiency in process adjustment and production control operations become crucial. In this context, the importance of measurement technology and its integration in production becomes increasingly significant.

As stated by Imkamp et al. [1], the manufacturing metrology roadmap must address five main challenges: speed, accuracy, reliability, flexibility and holistic measurements. The integration of measurement technology into production processes contributes to cover most of the challenges, where the system works flexibly either for production or measurement purposes. Hence, on-machine tool (MT) measurement shall be applied for machine geometry error monitoring or fast workpiece setup, in-process measurement for flexible manufacturing or post-process measurement for product validation, which leads to a holistic manufacturing system. However, on-MT measurement is influenced by different error sources that are not fully understood yet, which leads to a lack of a

metrological traceability chain [2], which in turn means a lack of reliability. In metrology, the accuracy of a measurement is fully understood quantitatively by specifying a measurement uncertainty [1], and this is what is finally aimed at this work, focused on-MT measurement. Thus, a quantitative approach-based error budget is suggested, where MT is the main error source in a MT measurement process. While systematic errors such as geometric errors or touch probe performance are not crucial because they can be compensated, repeatability [2] becomes the major uncertainty contributor. Both temperature variation and MT repeatability itself turn out to be the effects that limit any uncertainty assessment for on-MT measurement. On the other hand, it is also necessary to take into account the contribution coming from the measurand, mainly in large scale metrology applications.

To sum up, this paper contains a review of the existing technologies and methodologies for traceability [2] assessment on a MT measurement. In addition, uncertainty error sources that affect the measurement are analysed in depth and a quantitative approach-based error budget is suggested for determining major error sources.

2. Benefits and Limits of on-MT Measurement

In order to achieve self-adapting manufacturing processes, dimensional measurements [2] can be employed at different stages of the manufacturing cycle: from the setup and preparation of the MT to be geometrically fitted, to the performance of a final metrology validation of the finished product for final inspection reports and statistical trend analysis. Figure 1 shows the general concept of on-MT measurement.

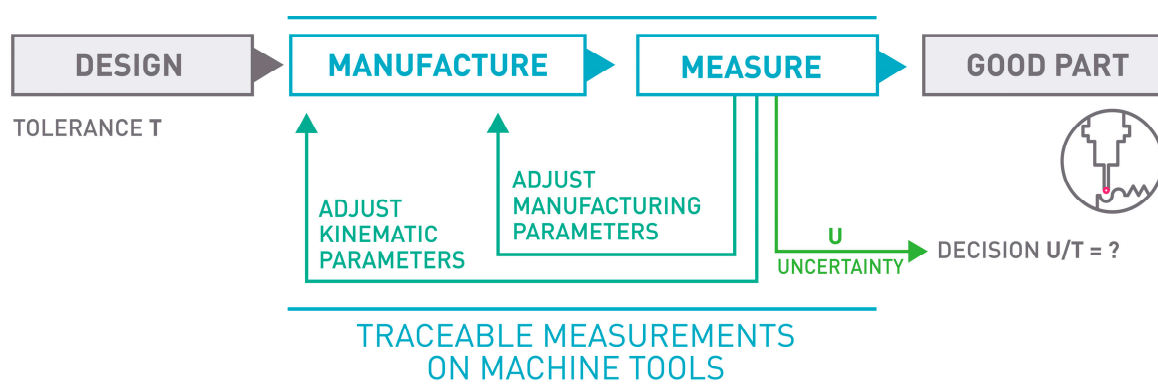


Figure 1. Traceable measurements on machine tools [3].

The top four reasons and benefits of on-MT measurement could be listed as follows [4]:

- **Monitoring MT Performance:** Machine geometry may change during machining operation due to many reasons. By applying an appropriate in-process measurement method with the probe integrated within the MT, geometry changes can be measured. These changes can be monitored to avoid making bad parts and to optimally schedule machine maintenance [4]. Figure 2 shows monitoring of MT performance based on a 3D standard.
- **Part Setup:** Part cutting programs are created based on an assumed workpiece holding coordinate system. Especially for large parts such as the case for aerospace or large parts manufacturing for automotive applications, this process could take a long time. For small part manufacturing and multi-operation processing, precise part locations could be detected automatically. This would reduce both the setup time and the processing time as parts could be cut from optimally sized blocks [4].
- **In-process Measurement:** One of the main reasons for performing a metrological measurement [2] of a manufactured part is to provide correction values to manufacturing parameters based on any deviations from the target dimensions found. Having this capability directly on the machine

tool allows one to feed back these metrological data to the machine tool controller allowing an automatic flexible manufacturing process. This could be done several times during the manufacturing process, and not just at the end, in order to optimize the part cutting process [4]. Figure 3 depicts a tactile MT probing example.

- Post-process Control: Programming and running a manufacturing machine as if it were a coordinate measuring machine (CMM) for in-process measurement generates complete inspection reports without additional effort. For large part manufacturing, moving the part to an external measuring machine may not even be an option. For mass production, just measuring a few control features would not only generate inspection reports for all the parts but also provide a statistical view of the manufacturing process. In addition, it would help to create historical data monitoring for intelligent process control.



Figure 2. Monitoring machine tool performance.

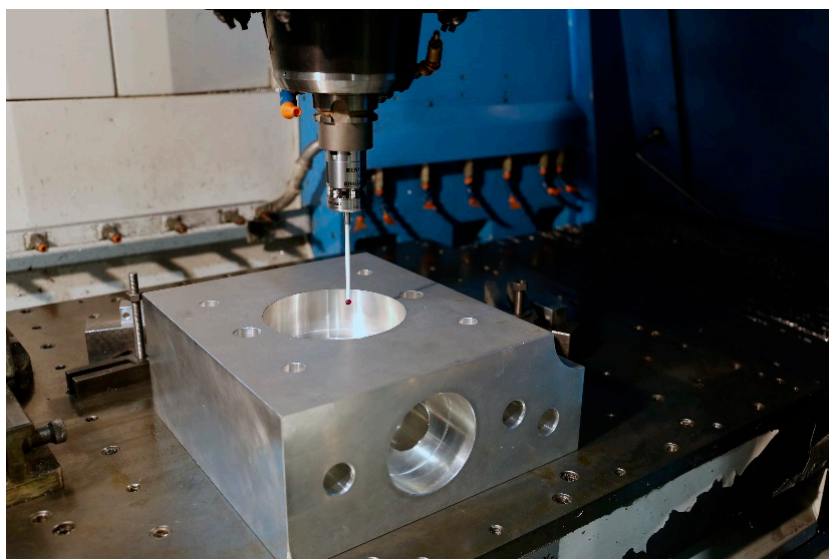


Figure 3. Tactile machine tool probing.

Although on-MT measuring can supply advantages for more flexible and intelligent manufacturing processes, limitations should also be known to make an optimal use of it [5]:

- MT time is more expensive than CMM time: The natural limit of on-MT measurement is given by the time spent on the MT doing measurements. It is known that MT time is more expensive than CMM time, so the measurements done on a MT should clearly add value to the manufacturing process.
- Lack of MT accuracy: MT accuracy is affected by many error sources that change the geometry of the machine's structural loop. As explained in standard ISO TR 16907 [6], there are different compensation possibilities to enhance the geometric accuracy.
- Lack of MT traceability: Another limitation is given by the lack of traceability of the MT as a CMM. Both machining and measurement operations are performed at the same machine, so if the MT's geometric error is repeatable, both processes may observe the same geometric error on the measurand.
- Metrology software insufficiencies: Currently software employed in MT is insufficient for metrology purposes. To perform the complex mathematical calculations required for metrology-based real-time decision making, a powerful metrology software needs to be integrated within the manufacturing system.
- Changing environmental conditions: Industrial environments normally suffer from unstable conditions, so it becomes a challenge not just to reduce measurement uncertainties with unfavourable measuring conditions, but to carry out uncertainty assessment for traceable measurement on-MT.

3. Converting a MT into a Traceable CMM

In 2010 Schmitt et al. suggested that a large MT should be employed as a comparator to measure the geometry of large scale components during the manufacturing process [7]. Since then, several research works have focused on the idea of converting a MT into a CMM [7–11]. In addition, Schmitt et al. presented a work [12] where the main objective is to define a suitable Maximum Permissible Error (MPE) value for the MT working as a CMM, according to ISO 10360-1 [13]. A tracking interferometer is employed to map the volumetric error of the MT and based on a mathematical model, MPE is determined. Currently, ISO 10360 for MT is a under consensus-based draft development process.

For large scale manufacturing where manufactured parts have to be measured in-situ or in-process, the integration of the measurement process into the MT can improve the process efficiency by preventing the workpiece from being carried to a temperature controlled measuring room. For small and medium size parts, there is a real possibility of achieving finished products on the MT, which offers high product quality, lower manufacturing costs, high productivity and prompt and real-life assessment of product quality [11].

Almost every new machine tool is equipped with a probing system nowadays and offers the possibility to measure product features during or after the manufacturing process. Therefore, machining and measuring processes could take place on the same MT. However, there are some key differences between a CMM and a MT, mainly because a CMM is designed for a measurement purpose and a MT is focused on manufacturing production. The main problem of on-MT measurements is that the machining and measuring operations are performed at the same machine. Therefore, both processes may observe the same geometric error on the measurand, which leads to the point that geometric error of the measurand may not be observed if a geometric error characterization of the MT is not performed before the measurement process. In addition, repeatability can also be a big challenge for a traceable on-MT measurement, where non-controlled shop floor environment becomes a major uncertainty source. Researchers have recognized that environmental temperature has a significant impact on the thermal error of the machine tool and, therefore, on any metrology activity performed

on it [14–19]. Hence, time- and space-dependent thermal effects become the dominant uncertainty source for the measurement of large scaled devices [8,20].

Schmitt et al. [12] explain two main approaches to convert a MT into a traceable CMM, a scheme of which is shown in Figure 4. The first approach increases the process capability by a volumetric calibration and compensation. It means that a calibration process is done prior to the manufacturing and measuring processes. However, this approach does not ensure that thermal effects do not affect the compensated machine tool. Achievable accuracy can be compared to large CMMs. The second approach applies an external high precision metrological frame to monitor tool centre point (TCP) position in real time. This option requires a line of sight between the measuring tracking interferometers and the TCP, which cannot be ensured when the workpiece is on the MT. Moreover, this option is very sensitive to dirt and dust. The current cost of the solution is very high, since four tracking interferometers are needed at the same time. However, it offers the possibility of being self-calibrating and represents a scalable measuring solution [12].

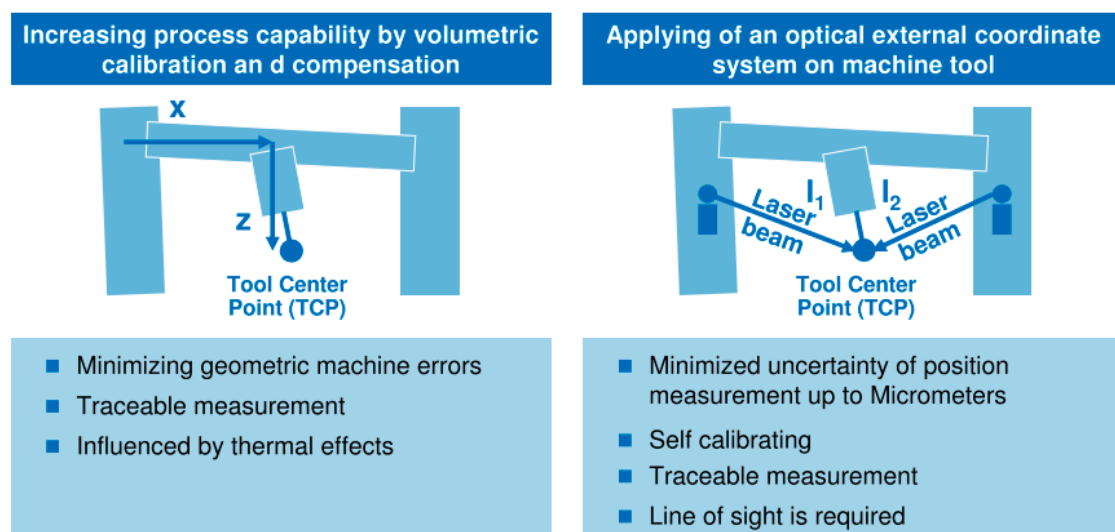


Figure 4. WZL RWTH Aachen approach to convert a MT into a CMM [7].

Currently, the first approach is under research [4], where machine geometric error reduction is of particular importance. Measurement in a shop floor rarely takes place in temperature controlled environment and it means that it is not enough to just measure and compensate geometric errors of the MT, and it must be accompanied by an understanding of how the MT changes. Time- and space- dependent dimensional and gravitational drifts on both MT and the measurand shall be either compensated dynamically or be considered on the uncertainty budget for traceability assessment on-MT measurement.

Although the first approach is being researched in detail, Wendt et al. presented a high accuracy large CMM called M3D3 based on the second approach [21]. In this case, four accurate tracking interferometers are employed for large part calibration directly on-site in production. Schwenke et al. also presented an independent traceable metrology solution for MT measurement based on integrated length monitoring lines on a MT [5].

4. Approaches to Determine Measurement Uncertainty on a Machine Tool

Due to the similarity between a CMM and MT, some of the methods for a correct assessment of uncertainty in CMM are adopted for MT. The general guide for a suitable evaluation of measurement data is given in the ISO Guide 98-3: 2008, on the expression of uncertainty in measurement (GUM) [22]. Three different approaches are considered for an uncertainty assessment on a MT dimensional measurement:

4.1. Substitution Method Based on ISO 15530-3

The first approach as described in ISO 15530-3 is a method of substitution that simplifies the uncertainty evaluation by means of similarity between the dimension and shape of the workpiece and one calibrated reference part. Moreover, the measurement procedure and environmental conditions shall be similar during evaluation of measurement uncertainty and actual measurement [23]. Due to the similarity requirement between the machined workpiece and the calibrated standard, this approach is very arduous and expensive for large scale metrology. However, it is a suitable approach for small and medium size uncertainty assessment where it is affordable to manufacture and calibrate a reference part for uncertainty assessment purposes.

Across the EURAMET research project Traceable In-process Metrology (TIM), high precision and robust material standards have been developed, not just for mapping the geometric errors of machine tools in the harsh environment of the production floor, but for determining the uncertainties associated with task-specific measurements, such as size, form and position measurements for different geometrical shapes such as sphere, cone, cylinder and plane [24–29] by a procedure adopted from ISO 15530-3 [23].

4.2. Numerical Simulation Based on ISO 15530-4

The second approach is based on ISO 15530-4, a method that is consistent with GUM to determine the task specific uncertainty of coordinate measurements. It is based on a numerical simulation of the measuring process allowed for uncertainty influences, where important influence quantities are taken into account [30]. For that purpose, CMM suppliers, research companies and national metrology institutes (NMI) as PTB and NPL created an uncertainty evaluation software (UES) which is based on Monte-Carlo simulation of the error behaviour of a real CMM [31,32]. In recent years, Virtual gear measuring instrument (VCMM-Gear) and Virtual laser tracker (VLT) have been developed but they have not been integrated into a manufacturer software yet [33]. Nowadays, some research activities are focused on transferring the virtual measuring machines (VMM) concept to virtual measuring processes (VMP) [12,34].

4.3. Uncertainty Budget Method Based on VDI 2617-11

The third approach is as stated in GUM and VDI 2617-11. In this case, uncertainty evaluation is done based on an uncertainty budget where the budget should comprise the uncertainty sources that affect the measurement process and the correlation between them [35]. Thus, a correct assessment of the measurement uncertainty requires contributions from the measurement system, from the component under measurement and from the interaction between them [8,35]. Currently, this approach is being considered for large scale uncertainty assessment. Schmitt et al. are developing a software-based solution for uncertainty evaluation on large MT measurement [12].

In conclusion, for small batch production, mainly in large scale manufacture, the substitution method is not an affordable solution because a calibrated workpiece similar to the manufactured part is needed. This requirement makes the solution arduous and expensive. Therefore, the uncertainty budget based solution is being adopted for the machine measurement of large workpieces [12]. For serial production, usually for small and medium size components, the substitution method simplifies uncertainty evaluation. Thus, task specific uncertainty can be assessed.

5. Uncertainty Error Sources

The uncertainty budget for on machine tool metrology should comprise contributions from the measurement system-i.e., the MT itself (Section 6) with the touching probe (Section 7) and the measuring software (Section 8), from the component under measurement (Section 9) and the interaction between both of them [12,36].

International standard ISO 10360-1 [13] defines a CMM as a measuring system with the means to move a probing system and the capability to determine spatial coordinates on a workpiece surface [37]. Due to the similarity between a CMM and MT, some of the methods for a correct assessment of uncertainty in CMM are adopted for MT. However, there are some key differences between a CMM and a MT, mainly because a CMM is designed for measurement purpose and a MT is focused on manufacturing production. For that reason, here an error budget approach will be suggested for machine tool measurement uncertainty assessment.

As stated by Slocum, MT errors can be divided into systematic errors and random errors [2]. While the former can be measured and compensated, the latter is difficult to predict [38]. Therefore, a machine tool should have three main properties: accuracy, repeatability and resolution [2,39]. Figure 5 represents errors sources of a MT according to the described criteria.

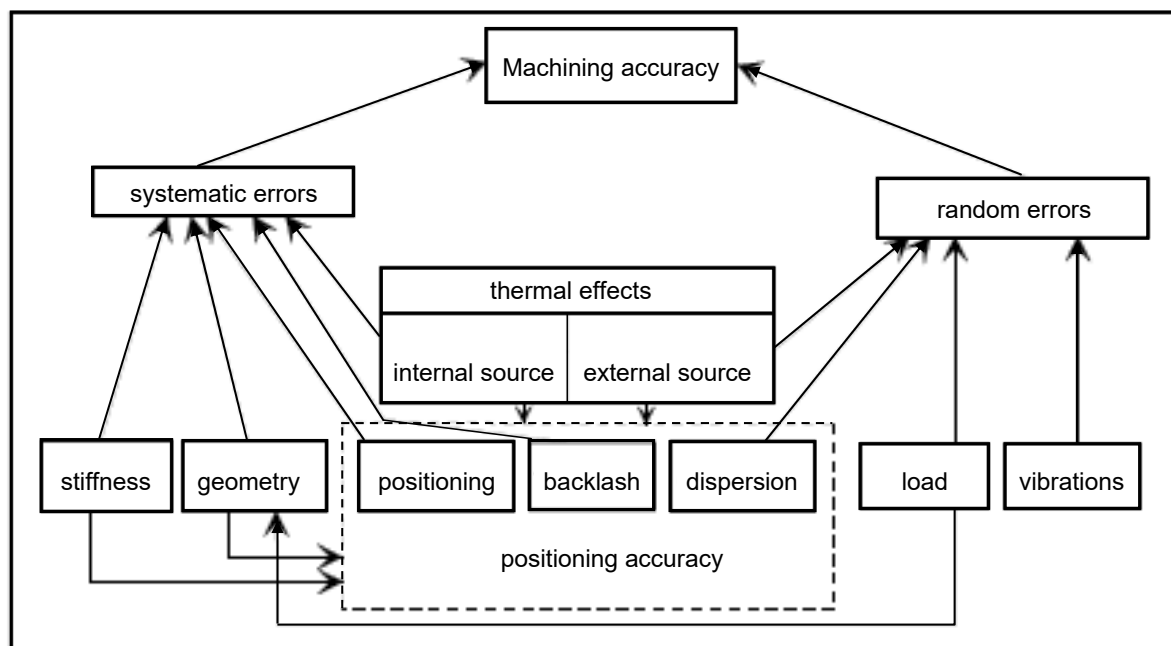


Figure 5. Total error sources of machine tools [40].

In addition, an error budget is a fast and low cost tool to predict the accuracy and repeatability of a MT [39]. Hence, drawing a comparison between design and measurement purposes, an error budget will be established, where each component will be comprised by:

- Accuracy: Systematic geometric errors of the MT (induced by kinematic errors, static loads and control software), touch probe errors and measuring software errors are considered. The accuracy will mean the systematic error of the MT as a CMM, so it can be characterised and compensated.
- Repeatability: Random error sources that affect the repeatability of the MT. Dynamic loads that affect the MT (such as backlash, forces and thermo-mechanical loads) and environmental influences that affect either the MT or the touch probe are considered. Repeatability will mean the random error of the MT as a CMM, so it is difficult to measure and compensate.
- Resolution: Quality of sensors and quality of control system are considered.

6. Error Sources Due to the Machine Tool

6.1. Geometric Errors

Either for a CMM or a MT, geometric errors to be considered are relative motion errors between the end effector and the object under measurement. Geometric errors can be measured and compensated

when both the MT and the measurement procedure have a high repeatability, so that systematic errors can be reduced and not be considered into the uncertainty budget on a -MT measurement [41].

There are several error sources that affect systematically to the accuracy of the relative end-effector position and orientation [41–45]:

- Kinematic errors: Kinematic errors are errors due to imperfect geometry and dimensions of machine components as well as their configuration in the machine's structural loop, axis misalignment and errors of the machine's measuring systems [41,46–53].
- Static loads: In case of static errors, the non-rigid body behaviour has to be considered. Location errors and component errors change due to internal or external forces. The weight of the workpiece and the moving carriages can have a significant influence on the machine's accuracy due to the finite stiffness of the structural loop [41,54].
- Control software: The effect of the control software on the geometric error of the MT can be considerable. Hence, different speed and accelerations can be applied for a known motion path to make control software errors distinguishable. Anyway, the measurement process is usually executed at small feed speeds, so dynamic forces are usually not considered as an uncertainty contributor on machine tool metrology uncertainty budgets [41].

In practice, the interaction between these effects plays an important role in the overall system behaviour. Here the research is focused on the overall system behaviour, which means the systematic geometric error of the MT [41].

6.1.1. Description of Geometric Errors

Under the assumption of rigid body behaviour, each movement of a machine axis can be described by six components of error, three translations and three rotations. As stated in ISO 230-1, the six component errors of a linear axis are the positioning error, straightness errors, roll error motion and two tilt error motions. For a rotary axis, the six component errors are one axial error motion, two radial error motions, two tilt error motions and the angular positioning error. Moreover, location errors are defined as an error from the nominal position and orientation of an axis in the machine coordinate system. In general, for a linear axis three location errors are considered, while for a rotary axis five location errors are considered [41,55].

6.1.2. Mapping of Geometric Errors

Currently, there are different technologies and measurement methods to characterize all the geometrical errors of a serial kinematic configuration machine. As stated by Schwenke et al. [41] "direct" and "indirect" methods can be distinguished. While direct methods allow the measurement of mechanical errors for a single machine axis without the involvement of other axis, indirect measurements require from the movement of multi-axes of the machine under characterisation.

Direct Measurement Methods

As stated by Uriarte et al. [56], direct measurement methods allow to measure component of errors separately regardless of the kinematic model of the machine and the motion of the other axes. Direct measurement can be classified into three different groups according to their measurement principle:

- Standard-based methods, such as straight edges, linear scales, step gauges or orthogonal standards [28,55,57–60]. Such artefacts contribute also to the uncertainty of the measuring results. This is why their own calibration uncertainty should be as low as possible. However, this is not always reachable, mainly when considering the longest ones and the newest highly accurate machines. Nonetheless, as concluded by Viprey et al., most of the existing material standards are developed for CMM calibration, except ball plates, 1D-ball array and telescopic magnetic ball bar [28], which are suitable for MTs.

- Laser-based methods or multidimensional devices, such as interferometers or telescope bars [61–64]. They are usually applied in order to measure principally the machine positioning properties, because the suitability of the laser wavelength for long length measurements, due to its long-coherence length. The most used is the laser interferometer which, with different optics configurations, allows detecting position, geometrical and form errors.
- Gravity-based methods that use the direction of the gravity vector as a metrological reference, such as levels [55,65].

While direct measurement methods are frequently employed in small and medium size MT, they are rarely employed for large MT where they are very time-consuming and have strong limitations for a volumetric performance characterization [56]. However, there are some measuring scenarios where direct methods offer advantages compared with indirect methods, such as:

- In small and medium size working volumes direct measurement of an error can approximate the geometric behaviour of a machine tool.
- Specific error motion shall be checked in a very specific line or position. This is depicted in Figure 6.
- Specific verification protocol shall be applied for a machine's acceptance.
- Iterative “measure and adjust” type of work, which can be needed for component assembly operation.
- Results required in real time.
- High accuracy requirement for a specific application.

For direct measurement of positioning errors, calibrated artifacts (step gauges, gauge blocks, line scales and calibrated encoder system) or laser interferometers are applied as a metrological reference aligned to the axis of interest [41,55,66]. The most accurate/time consuming approach for either short or long machine axis is the use of laser interferometers. Nevertheless, some error sources shall be considered for a correct length measurement [41]:

- Errors in laser wavelength (environmental factors, such as temperature, pressure, humidity and density influence the wavelength compensation).
- Beam deflection shall occur due to temperature changes and gradients.
- Misalignment between interferometer and axis of motion can cause Abbe errors.
- Any movement of the equipment during the measuring process.

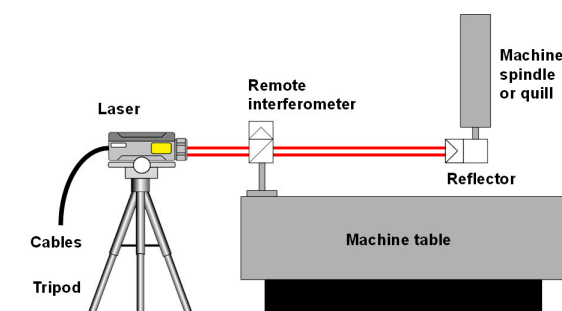


Figure 6. Direct measurement of positioning error through a laser interferometer [67]. (Copyright Renishaw plc. All rights reserved. Image (s) reproduced with the permission of Renishaw.)

Straightness errors of the machine axis can be measured by any of the three measuring principles mentioned before. For large MTs, the most practical way to evaluate straightness is to utilize the direction of the gravity as a reference. Thus, an electronic level is placed on the head of the MT and a

reference level is fixed to a non-moving part to distinguish movements of the machine [41]. Measured angle over the stepwise displacement is integrated to get the straightness as a result. However, the linear propagation of a laser interferometer is the industry leading method for large MT straightness measurement. In this case a Wollaston prism acts as a beam splitter and the lateral displacement is calculated from two separate beams that exit the prism at an angle [66,67]. For small and medium size MT, standard based method is commonly applied. Hence, a displacement indicator (capacitance gauges, electronic gauges or material dial gauges) is fixed to the machine head and it detects lateral displacements along the direction of the axis travel [55].

For large MTs and large volume applications, where straightness reference should be long and flat for a long range, a taut wire technique can be used as a straight reference to overcome the limitations of previously mentioned methods [41,68,69]. Even though it has been an extended applied method for very large MTs and applications such as CERN components and assemblies [70], the main reasons why this method is not widely used at present in accurate large MTs are its low accuracy and inefficient data gathering methods [70]. Another approach under investigation for straightness measurements on large volume applications is the use of a laser beam as a straight reference and a position sensitive device (PSD) as a pointing sensor unit. Generally, the use of a laser beam as a straightness reference is highly critical in normal shop floor environment, because local and global temperature gradients as well as air turbulence may have a high influence on the straightness of the beam. Therefore, this method is mostly used for axes length below 1.5 metres, where the influence in most cases is sufficiently small. Also the pointing stability (thermal drift) of optical straightness setups can be a major source of uncertainty [41,71,72]. Figure 7 shows beam deflection according to measuring conditions.

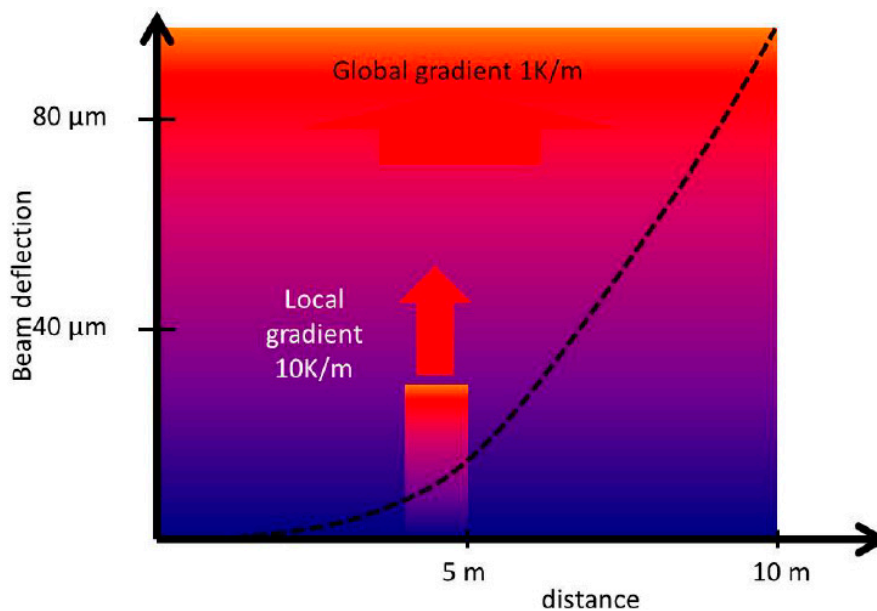


Figure 7. Bending of a straightness reference beam due to local and global gradients [72].

The main approach for squareness measurement in small and medium size MT is to employ granite or ceramic standards with a displacement indicator fixed on the MT head according to the measuring procedure stated in ISO 230-1 [55]. Nevertheless, the main disadvantage of this approach for large MTs is that large and heavy standards are required to verify squareness in large machines. In addition, laser interferometry can also be employed for this purpose but the setup of the laser source and the prism are also very challenging for the squareness error measurement [41].

To measure angular errors in any translation machine axis either the use of electronic levels or laser interferometer based techniques are performed. When applying interferometry, two laser beams are generated with a beam splitter so the angular deviation results in a path length difference of the two

beams, but the setup of the measuring system can be very challenging for a correct error assessment in a large axis. In case of electronic levels, they do not depend on an optical path, so they are suitable for the measurement of long strokes in unstable temperature environments. A limitation of electronic levels is that they cannot measure rotations around the gravity vector. For this purpose, in small and medium size axes, an autocollimator is usually employed. A collimated light beam is aligned to the machine axis where a mirror is fixed. The reflected beam travels back to the autocollimator where rotations are measured either visually or through a PSD. However, the unique direct technique to measure the rotation around the axis of motion is based on the use of electronic levels, since an autocollimator or laser interferometer cannot measure this rotation directly [41].

ISO 230-1 [55] describes an affordable method for the calibration of rotary axes. Displacement indicators are fixed to the centre hole of the rotation axis to measure the radial and axial run-out deviations [41]. For the radial and axial error motions three more sensors are needed to be placed on such a way that errors are measured with a linear indicator. If multiple linear indicators are applied, a single measurement combination can be enough for the measurement of the five degrees of freedom [41,73–75]. For the positioning error of the rotation axis, the most practical approach is to use laser interferometry combined with a self-centring device and the proper optical optics for angle measurement [76]. This approach is commonly employed in large MTs with a rotary table, due to the measuring range of the solution is around ± 10 and the resolution is better than 0.01 arcseconds [76].

Recently, multidimensional laser interferometers have been introduced to measure more than one degree of freedom (dof) simultaneously. Thus, several error components of a machine axis are determined with a unique measurement system setup through direct measurement methods. This multidimensional measuring solutions offer two main possibilities in the near future. On the one hand, measuring time is reduced to a far extent because different setups and measuring systems are not required anymore. On the other hand, the possibility to be embedded into a MT, where TCP position could be monitored in real time by monitoring six dof of each machine movement at the same time, with several measuring systems performing all at once.

In fact, there are two main multidimensional solutions [77–79] and the main difference between them is based on the straightness measurement principle. The first solution is a multi-interferometer based solution, where a unique interferometer source is divided into three beams to get a five dof measurement laser interferometer. The second solution employs the laser beam as a straight reference and a PSD as a pointing sensor unit to measure straightness. Therefore, the second option is suitable for small and medium size MT, but not for large MTs [72]. The principle used by the first solution is explained in Figure 8.

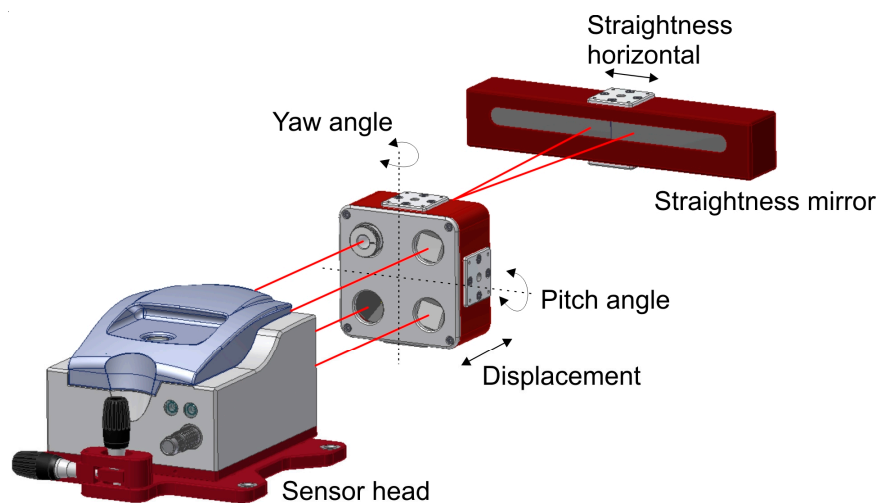


Figure 8. Multidimensional equipment for five dof [78].

As commented before, direct methods are very time-consuming and have strong limitations for large MTs volumetric performance assessment. As explained by Ibaraki et al. [80], for volumetric error compensation, the efficiency of the direct measurement can be a critical issue. In that sense, indirect methods have the advantage of offering fast and reliable volumetric error mapping and compensation possibilities and take less time than direct measurement.

Indirect Measurement Methods

Indirect methods produce a global correction of errors and require less time than direct measurement. They are based on the multi-axis movement of the MT under test and can be broken down into two main possibilities [80]:

- Indirect measurement for orthogonal linear axes.
- Indirect measurement for five axis kinematics with rotary axis.

As stated by Ibaraki et al. [80] there are different procedures and technologies for linear axis indirect characterization:

- Circular tests: The circular test, described in ISO 230-4: 2005 [81] describes a procedure for the characterization of indirect measurement of the geometric accuracy of two orthogonal linear axis. It is usually performed by a ball bar, but it can also be performed by a laser tracer [41] or two dimensional digital scale.
- Diagonal and step-diagonal test: As described in ISO 230-6: 2002 [82], it “allows estimation of the volumetric performance of a machine tool”, but it is not possible to identify 21 geometric error parameter from four body diagonal measurements only. Hence, this test is usually employed for linear scale and squareness error calculation [83]. It is suitable for a fast verification of a MT.
- Measurement of artifacts: The use of calibrated artifacts is widely employed either for MT calibration or CMM calibration. As described by Cauchick-Miguel et al. [60], artifact-based calibration is employed with one dimensional, two dimensional and three dimensional artifacts. The three dimensional artifact is widely employed mainly in CMM calibration for 21 error parameter measurement [84] where pre-calibrated position of spheres are measured by the machine for error characterization. Figure 9 shows a CMM characterization process for virtual coordinate measuring machine error assessment. Since almost every machine tool includes a touch probe nowadays, machine tool builders are looking for fast calibration procedures based on this approach.
- Passive links: Calibrated kinematics of the link mechanism attached to and passively driven by the machine to be measured can be used as a reference [80]. Different link configurations are employed nowadays, either serial links with three orthogonal linear axes or parallel links configurations.
- Tracking interferometer: Tracking interferometers, such as, laser trackers or laser tracers can be employed for indirect error measurement. Laser trackers can directly measure three dimensional position by measuring the distance and direction of a laser beam [80], but angular measurement uncertainty affects the measuring uncertainty of target position and it is rarely employed for MT error measurement. This is the main reason why multilateration based measurement is applied for MT error measurement. In this case, MT position is measured by the distance from at least four tracking interferometers to the target [85,86]. Either laser tracers or laser trackers are usually employed for that purpose. Figure 10 shows a multilateration based scheme, where a tracking interferometer is fixed to the table and the MT or CMM describes a volumetric path through a volumetric point cloud.



Figure 9. 3D artifact for CMM error characterization.

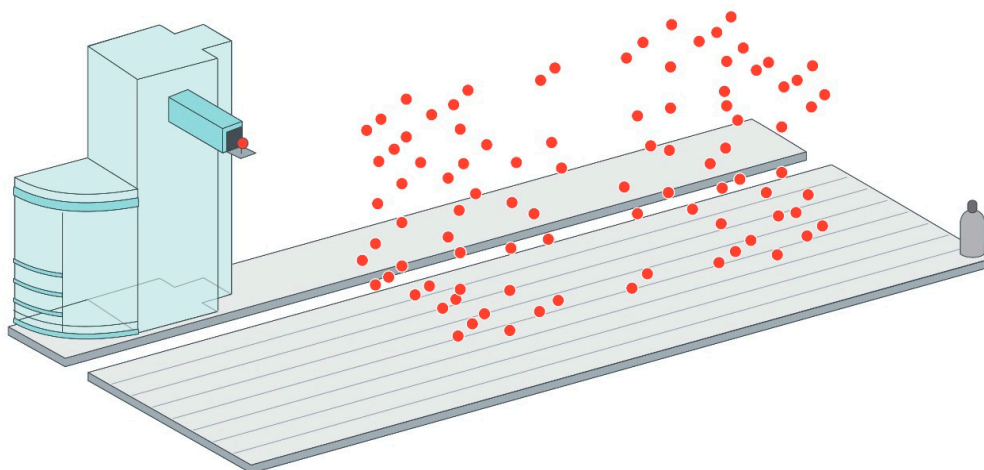


Figure 10. Tracking interferometer and multilateration combination approach.

For indirect measurement for five axis kinematics with rotary axis, there are also different measuring possibilities:

- Ball bar measurement: As described by Ibaraki et al. [80], there are some standards such as ISO 10791-1:2015 [87] and ISO 10791-6:1998 [88] that define measuring procedures for indirect rotary axis calibration. The calibration of rotary axis location with a ball bar is not solved yet and it remains a challenge.
- R-test: Another approach is to employ R-test to measure relative movements between the machine and the workpiece side. A sphere is fixed to the machine table and a measuring sensor, based on three or more length displacement sensors, is coupled to the machine head [89–91]. The measurement consists of a sequence of discrete angles of the rotary table. When moving to the next measurement point the linear axes follow the rotation of the rotary table. At each position the probe head measures the relative displacement of the sphere in X, Y and Z direction simultaneously [91]. Compared to the traditional method that employs “Siemens 996” static cycle to locate a rotary axis in the working volume of a MT, R-test offers the possibility to do static and dynamic measurements [90].

- Measurement of artifacts: As explained for linear axes indirect measurement, any MT has already on machine tool capability. This is why MT probing is being employed for calibration of offset errors of rotary axis [80].
- Machining tests: As explained by Ibaraki et al. [80], MT users are concerned with workpiece's final accuracy rather than MT accuracy. The National Aerospace Standard (NAS) 979 [92] defines the procedure for a five-axis machining test of a cone frustum, which is widely accepted as a final performance test by machine tool builders.

However, multilateration-based approaches are by far the most used techniques to characterise large machine tools nowadays [7,41,85,86,93–98]. The approach relies on interferometric displacement measurements between reference points that are fixed to the machine base and offset points fixed to the machine spindle, near to the TCP [99]. At least four measuring systems are needed for a complete volumetric verification but usually only one measuring device is available, so in practice, multilateration measurements are usually done in a sequential scheme. Thus, machine movements are repeated several times and measurements are taken from different positions. If four measuring devices are available at the same time, simultaneous multilateration avoids some of the limitations of a sequential multilateration, such as total time consumption, MT repeatability requirement and MT drift due to thermal variation during the measuring process.

Several uncertainty sources shall be considered for a complete uncertainty assessment in a sequential multilateration process [95]:

- Volume of the MT.
- Spatial displacement measurement uncertainty of the employed tracking interferometer.
- As stated by Aguado et al. [95], the number of measuring systems to be used and the arrangement of them.
- Repeatability of the measured points does not just depend on the repeatability of the machine itself. As far as the measuring time is extended, environmental influences (e.g., machine shop temperature) generally lead to slow changes of MT temperatures affecting the whole volumetric performance. Therefore, time is a crucial factor.

Currently, three tracking interferometers are being employed on large scale metrology when applying multilateration with different displacement measurement uncertainty:

- Tracking interferometers based on optimized laser trackers. They rely on a high accuracy sphere as optical reference for interferometric measurement. This measurement equipment, called laser tracer [86], was developed by NPL and PTB and commercialised by Etalon AG. It has a spatial displacement measurement uncertainty of $U(k=2) = 0.2 \mu\text{m} + 0.3 \mu\text{m}/\text{m}$ [100]. While laser tracer is a suitable solution for medium and large size MTs, there is a similar solution to the laser tracer, "called laser tracer MT" with a telescopic scheme and employed for maximum measuring volumes of 1 m^3 [101].
- An Absolute Distance Meter (ADM)-based laser trackers has a spatial displacement measurement uncertainty of $U(k=2) = 10 \mu\text{m} + 0.4 \mu\text{m}/\text{m}$ in its whole working range [102].
- An Absolute Interferometer (AIFM)-based laser tracker has a spatial displacement measurement uncertainty of $U(k=2) = \pm 0.4 \mu\text{m} + 0.3 \mu\text{m}/\text{m}$ [102].

The tracking interferometer employed for multilateration shall fit inside the measuring volume in order to execute the measuring procedure. Such a requirement restricts the tracking interferometer to be employed for any size MT. For small size machine tools, the equipment that suitably fits into the measuring volume is the so-called laser tracer MT, it makes use of a metrological beam guiding method of the laser interferometer [101]. For medium and large size MTs, either laser tracers or laser trackers are suitable for the error mapping. However, it should be stated that new laser trackers are portable devices that offer the possibility to be embedded into large manufacturing or measuring

systems and they transfer data through an integrated wireless LAN communication [102] which allows to a wireless employment of the acquisition technology.

In this context, different solutions have been developed based on a tracking interferometer and multilateration combination mainly for large MT geometric characterisation, where the volumetric performance of the MT is of special interest: Olarra et al. [97] showed an intermediate approach where linear components of error are measured with a laser tracker based on sequential multilateration. Hence, by combining the data coming from the different measurement systems, multilateration is applied to measure 3D positions with enough accuracy. Once that measured coordinates are calculated, they are compared with nominal positions and geometric errors of the machine tool are deduced from an analytical solution. Additionally, electronic levels are employed for the measurement of the two rotational errors along the two horizontal axes. A self-developed software makes it easier to synchronise data acquisition for both measurement systems and it allows to run the calculation to achieve the aimed volumetric performance of the MT [97]. This approach is similar to the approach described at ISO 10360-2 standard where a calibrated artefact is employed for volumetric error determination [103,104].

Aguado et al. developed an approach where several commercial laser trackers are employed for sequential multilateration measurement [95]. The adopted technical solution is similar to the solution developed by Olarra et al., where laser trackers are applied to acquire information and multilateration is employed to sort out the mathematical issue. The biggest difference is that Aguado et al. do not use electronic levels for the measurement of the rotational errors of the MT.

Schwenke et al. presented a self-developed hardware and software solution for small to large size MT and CMM volumetric characterisation. The commercial laser tracer [100] is employed for point cloud acquisition and from the error of those points and the kinematic model of the machine it is possible to iterate to minimize the global volumetric error of the machine at considered points. For the measurement of angular errors, different orientation offsets on the spindle side are needed, which makes the verification more time-consuming. Nowadays, new configurations and ways of utilisation are appearing for tracking interferometers for MT and CMM geometric error characterization. Etalon AG presented a solution called "Linecal" where several permanently installed measuring lines replace a motorized tracking and device conversion [105].

To sum up, it seems that interferometer-based non-contact measuring technology will guide large scale metrology into traceable machine tool metrology in the near future, mainly because the absolute distance measurements allow an easy handling in industry where purely interferometric length measurements depending on fringe counting are quite demanding due to the need of an unbroken line-of-sight between the measuring instrument and the reflector [8]. However, it shall be remarked that the technology has some key limitations nowadays, such as [8]:

- Thermal and refractive index distortions: The uncertainty of interferometry technique is proportional to the stability of the refractive index of air. Hence, the correct determination of this parameter is of utmost importance for achieving small measurement uncertainties on interferometer based measurements. However, industrial environments normally suffer from unstable conditions, so it becomes a challenge to reduce measurement uncertainties with unfavourable measuring conditions.
- Real time: Real-time coordinate metrology is a requirement for a factory of the future where metrology and manufacture are integrated into a single engineering process that enables 'zero defects'.
- Dimensional traceability to the SI metre: It shall be ensured for any metrology based solution in a factory environment.
- Automation: For a successful integration of the technology into machine and manufacturing processes, wireless and automation capacity shall be improved.

6.1.3. Compensation of Geometric Errors

Traditionally, the majority of MTs have been compensated along lines parallel to the moving axis and centred in the working volume, which is called positioning error mapping and compensation. The ISO230-2 and VDI/DGQ 3441 standards have been widely employed for that purpose and the most common measuring system for error mapping is the laser interferometer [106,107]. However, due to rotational errors of the machine, it is not enough to compensate positioning errors for linear axis if a volumetric accuracy of the MT is aimed. This is the main reason why volumetric compensation was broadly introduced for CMMs fifteen years ago. Volumetric compensation allows not just positioning error compensation, but also compensation of straightness errors, rotational errors and squareness errors.

Volumetric compensation is now successfully being introduced by main machine tool controller manufacturers on three- or even five-axis machine tools [56]. In general, methodologies based on rigid body kinematics have been proposed [49,108] because the kinematic structure of a MT can be modelled with a kinematic chain and therefore, calculate the position and orientation of the tool in the workpiece coordinate system as the superposition of error motions of each axis [80]. The MT rigid body assumption simplifies the error mapping and compensation because it allows the motion to be implemented by a transformation matrix [109]. Nevertheless, in case of large MTs, due to their size, they suffer from remarkable thermal and mechanical deformations. In order to minimize this effect either on error mapping or compensation, special strategies shall be employed. In compensation, extra compensation factors for the deformation of some parts of the machine, such as column bending and tilt for moving column MT and CMM or table torsion factor for moving table CMMs, are considered [56,72].

Volumetric compensation requires from quantified knowledge of the errors and repeatability from the MT side, as well as time invariant errors. However, changes due to temperature variation play an important role for MT geometry. This is the main reason why limitations must also be known to make a suitable use of compensation. The main limitations are listed next [6,72]:

- Repeatability of the MT: Backlash errors and temperature variation (internal and external) lead to a lack of repeatability. Therefore, long term stability will not be improved.
- Use of long tools: The compensation of orientation requires from three orthogonal rotational axes, which only very few MTs offer. Compensation of angular errors remains a challenge.
- Model conformity: The majority of controllers assume a rigid body model behavior of the machine tool in their compensation models. However, deformations such as column bending and tilt for moving column MTs or table torsion for moving tables CMMs, does not fit to a 21 error model. In these cases, additional parameters shall be included in the compensation model. Therefore, if a model-based compensation is employed, it should be consistent with the machine tool real behavior.

ISO/TR 16907 standard [6] provides information associated with numerical compensation of geometric errors of machine tools. It describes traditional compensation methods such as positioning and straightness compensations and all compensation possibilities within volumetric compensation.

6.2. Dynamic Errors

The repeatability of the machine, usually expressed as a standard deviation, is a part of any uncertainty budget and it is mainly affected by dynamic errors. As stated by Slocum, repeatability is difficult to predict and it is often more important to obtain mechanical repeatability, because accuracy can often be obtained by the sensor and control system [39].

There are different error sources that affect the repeatability of the MT working as a CMM: Dynamic loads that affect the MT (such as backlash, dynamic forces and thermo-mechanical loads) and environmental influences that affect either the MT or the touch probe are considered [39–45].

Between the dynamic loads that affect the MT backlash, dynamic forces and thermo-mechanical loads can be highlighted:

- Backlash: Backlash error is a position dependant error affecting the contouring accuracy. When the axis changes direction from one side to the other, there is a lag before the table starts moving again, that would cause position error- backlash error [110]. Modelling it is challenging, due to multiple sources and complex behaviour. In general, the backlash vector depends on the motion history of all axes. It can result from mechanical play in drives and guideways, cable track forces, and stick/slip effects [72].
- Dynamic forces: Dynamic behaviour of the MT affects the aimed working path. Any varying behaviour, such as, accelerations, varying forces, vibrations or machining forces are hard to measure and compensate. [41,111–113].
- Thermo-mechanical errors: Internal and external heat sources combined with different expansion coefficients of machine part materials generate a thermal distortion of the machine's structural loop which can affect to the accuracy of the measuring process [11,41,114–118]. Expansion coefficient differences may lead to thermal stresses if rules of exact constraint design have not been met carefully.

Apart from dynamic loads affecting the MT, dynamics error sources coming from the touch probe should be also considered. Deviations from the reference temperature of 20 °C lead to thermal expansion or shrinkage of the measuring probe. In addition, temperature variations either inside the workpiece or the stylus, can cause effects like bending. Vibrations may affect the measurement result because it causes a deformation in the metrology loop between probe tip and workpiece. As explained in the previous point, any varying behaviour is hard to measure and compensate, so they contribute directly to the uncertainty of on machine tool metrology [119].

In this scenario, the overall system behaviour is of interest. Some error sources, such as dynamic forces or internal heat sources lead to a fast change of the structural loop that are very hard to measure and compensate [41,111–113]. However, there are other error sources such as environmental temperature or simple backlash errors that induce a quasi-static geometric error of the MT that can be monitored and assessed. In fact, quasi-static errors are one of the most important error sources for large scale precision manufacturing [8].

6.3. Quasi-Static Error Assessment and Monitoring

The aim of some international research projects, such as “Light controlled factory” or the just finished “Large volume unified metrology for industry novel applications & research (LUMINAR)” and “Traceable in-process dimensional measurements (TIM)”, is to tackle several fundamental issues affecting users of large scale metrology (LSM) equipment and techniques in industrial locations [3,120,121] where non controlled environment affects. In particular, a strong evolution of interferometry-based technology seems to trace the roadmap for the future research of LSM in industrial environment.

Peggs et al. [122] rely on ADM technology as distance measurement principle for future error mapping and monitoring technology. Achievable uncertainty with an ADM (typically 10 mm + 0.4 mm/m) is already being reduced so it is becoming similar to the conventional displacement measuring interferometer (IFM) embedded into laser trackers (typically $\pm 0.4 \mu\text{m} + 0.3 \mu\text{m}/\text{m}$) [102]. Consequently, for the built-in displacement device, increasingly absolute distance meters (ADM) are used beside the IFM in commercial laser trackers [8]. While IFM can determine relative distances with accuracies on the nanometer level almost instantaneously, which makes IFM suitable for dynamic measurements, ADM measures absolute distances. However, ADM technology cannot perform dynamic measurements because it must deal with integration times, the time required to perform the operations that determine the target's position [123].

Schmitt et al. [96] mentioned the extension of the application of interferometry-based technology, which is not only used as a dependent measuring unit but also in multilateration applications, for CMM and MT calibration. An external metrological frame is implemented as a virtual reference based on

lengths measured with tracking interferometers. The target positions are calculated using the length measurements with the multilateration principle [21].

Based on ADM technology, multiline technology developed by University of Oxford is a dynamic frequency scanning interferometry (FSI) system scaled up to make many hundreds of measurements for only a small fractional increase in cost compared to laser tracer technology [99], simply by using multiple interferometers whose components are cheap [124]. Despite not having a real time capability (functionality that is under research), this technology allows to monitor large components and structures within an accuracy of $0.5 \mu\text{m}/\text{m}$. Measurement range is up to 20 metres. It is currently being used in LSM for monitoring of long time stability, deformation by temperature; workpiece weight and foundation drift in many applications [124,125]. An example application can be seen in Figure 11.

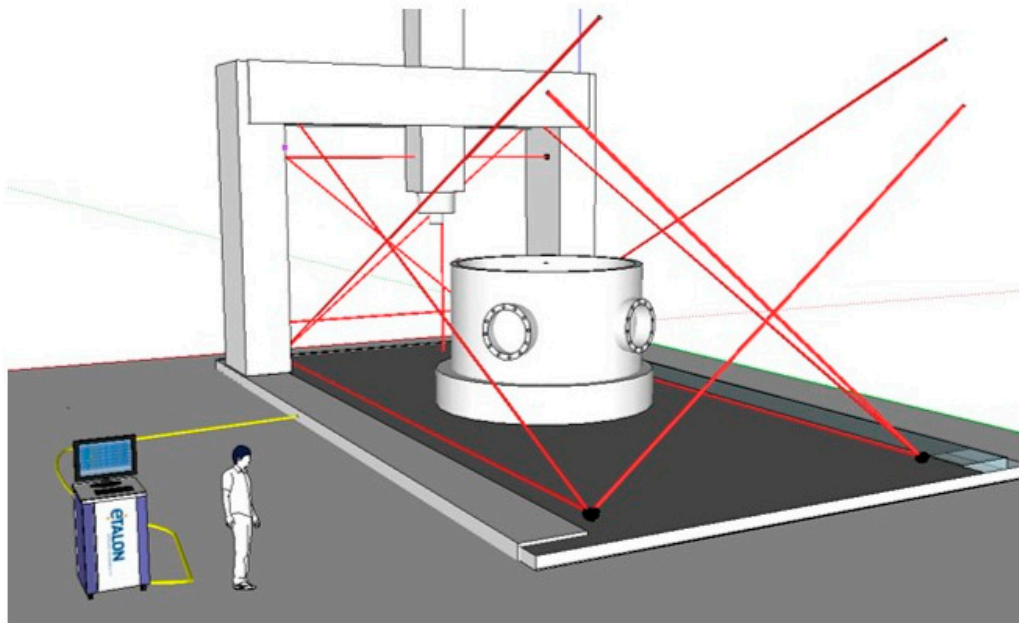


Figure 11. Multiline example on a large MT [125].

As an evolution of the multiline system, a system based on divergent FSI is under development at NPL for real-time coordinate metrology for a factory environment [126]. The measuring system comprises several sensor heads that are placed within the MT volume. Measuring targets, either on the MT or the component under measurement, are defined by spherical retro reflectors. Each sensor head is able to measure absolute distance to multiple targets simultaneously using the mentioned FSI principle. The traceability is ensured through a gas absorption cell embedded into the system and it is used to determine the scale factor for the FSI based distance measurement.

To overcome thermal and refractive index distortions in large volumes, a tracking refractive index compensated interferometer for absolute length measurements, the '3D-Lasermeter', has been developed by PTB and SIOS within LUMINAR European project [121]. The 3D-Lasermeter combines absolute distance measurement by multi-wavelength interferometry, the compensation of the refractive index of air by using the dispersion between two wavelengths, and the tracking capabilities of Laser tracers [8].

More practical approaches are presented nowadays. Schwenke et al. present a multilateration-based continuous data acquisition solution (on the fly) where calibration is speeded up significantly by a continuous measurement at constant speed. This option permits to increase the number of sampling points and reduce drastically the measurement time, allowing the measurement of quasi static errors of MTs [100]. However, the measurement process cannot be automated entirely

because multilateration is executed in sequence and the device is located by hand. Gomez-Acedo et al. suggest an automatic approach for a fast measurement of thermal distortion on large MTs based on an automatic multilateration measuring procedure [127]. A multilateration scheme is conducted using a single laser tracking device positioned on top of the machine table which moves automatically. As depicted in Figure 12, YZ plane is measured with a sampling period of 20 min during a thermal cycle of 5 h. In addition, Ibaraki et al. [128] present a similar approach where the identification of 2D geometric errors of linear axes by single-setup tests is aimed.

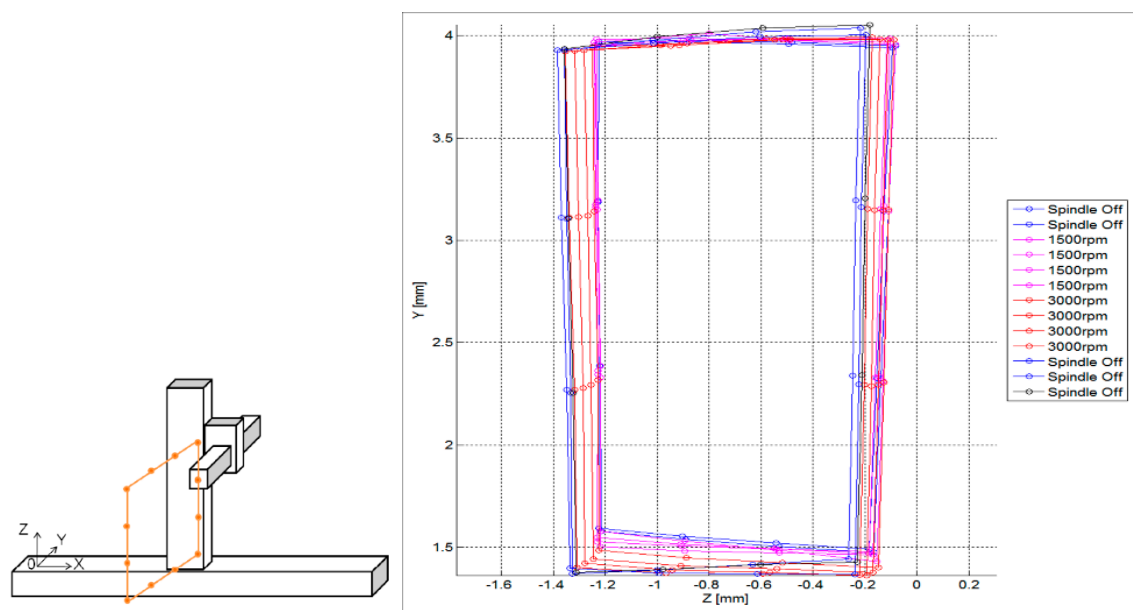


Figure 12. YZ plane measurement and thermal drift assessment on the YZ plane [127].

A mobile climate simulation chamber was developed within the mentioned TIM project in order to simulate the variety of influencing factors related to harsh environmental conditions on shop floors [129]. Thus, it is possible to imitate a variety of environments and investigate the behaviour of MT and on MT measurement under these influences.

7. Error Sources Due to the Touch Probe

Probing has become a vital component of automated production processes on machine tools. The probing system should ensure reproducibility during the sensing process even when any adverse influence appears during the process [119,130]. It is necessary to probe the desired point on the real workpiece surface by touching it with a sensing element or by sensing it in a non-contact way [130–132]. Often the application will dictate the choice due to limitations in the speed or accuracy of each solution.

There are two main options when choosing a probing solution: contact or non-contact. There are major differences between both options. The first is that the accuracy of the individual points in contact measurements is higher to that of non-contact measurements. The second is the amount of collected data: non-contact technology can collect millions of sampled points at high speed without touching the workpiece. The third difference is that some surfaces, due to glossiness or transparency, are not suitable for optical measurement and cause special errors [133].

7.1. Contact Touch Probe

Contact probes can be divided into two general groups—scanning and discrete—based on the type of data being taken, differences are shown in Figure 13. Discrete probes, or touch trigger probes (TTP), are the most prevalent technology available [134,135]. They have the advantage of being less

expensive than some of the other options and are good when fewer data points are needed, such as measurements for position or size [136]. Scanning probes, or analog probes, are continuous contact probes that sense the part as the probe is moved along the expected contour, they are useful in the gathering of high-speed data on a part's form characteristics [137,138].

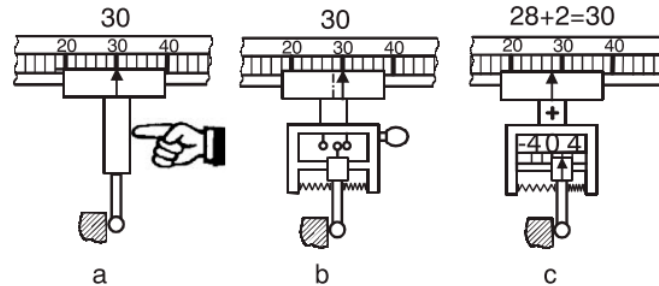


Figure 13. Hard (a), touch-trigger (b) and measuring (c) probe [119].

7.1.1. Touch Trigger Probe

The two main TTP technologies available for MTs are kinematic resistive probes and strain-gage probes [139,140]. As for kinematic resistive probes, most touch trigger probes utilize a kinematic seating arrangement for the stylus. Three equally spaced rods rest on six tungsten carbide balls providing six points of contact in a kinematic location. An electrical circuit is formed through these contacts. The mechanism is spring loaded which allows deflection when the probe stylus makes contact with the part and also allows the probe to reseat in the same position within $1\ \mu\text{m}$ when in free space (not in contact). Under load of the spring, contact patches are created through which the current can flow. Reactive forces in the probe mechanism cause some contact patches to reduce, which increases resistance of those elements. On making contact with the workpiece (touch), the variable force on the contact patch is measured as a change in electrical resistance. When a defined threshold is reached, a probe output is triggered. The probing sequence is explained in Figure 14.

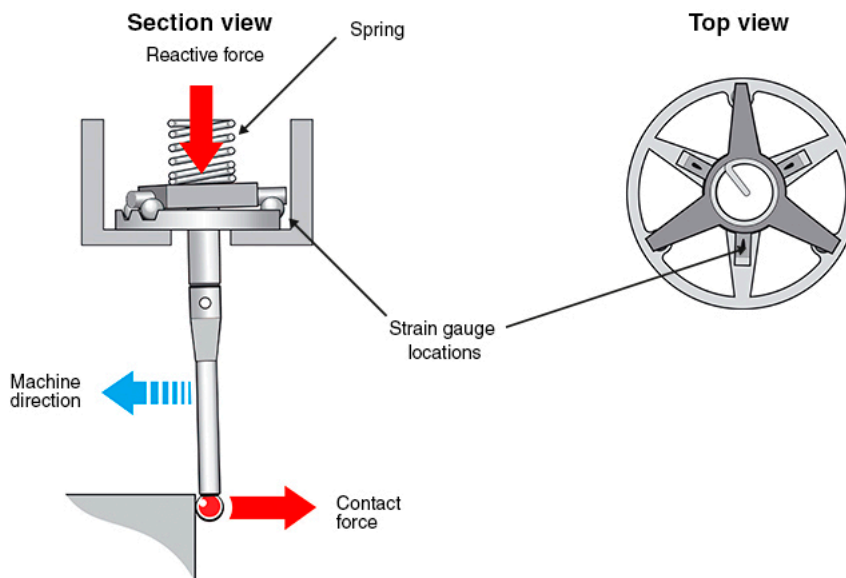


Figure 14. Kinematic resistive probe principle [141]. (Copyright Renishaw plc. All rights reserved. Image (s) reproduced with the permission of Renishaw.)

A number of factors affect the kinematic touch probe measuring performance. From the point at which the stylus ball contacts the workpiece there is bending of the stylus prior to electrical triggering

of the probe. This is known as pre-travel. Pre-travel will vary dependent on the length and stiffness of the stylus and the contact force. Pre-travel variation (PTV)-otherwise commonly known as lobing, probe measuring error or roundness measuring error, can affect measurement performance. Lobing occurs because the pivot distance varies depending on the direction in which the contact force acts in relation to the probe mechanism [141].

On the other hand, strain gauge probe technology has improved the performance limitations of the kinematic resistive probe technology, mainly because modern compact electronics and solid state sensing have been embedded. Thus, kinematic mechanism retains the stylus and strain gauge technology senses the trigger to acquire the measuring point. As a result, a lower trigger force is needed and uniform pre-travel variation is achieved in all directions [141]. Main differences between both probing technologies are explained in Table 1.

Table 1. Comparison table between kinematic and strain gauge probing technology [142].

	Kinematic Resistive Probe	Strain Gauge Probe
Pros	Simple mechanism Low mass (so low inertia at the triggering instant) Cost-effective Easy to retrofit to all types of CMM	Improved repeatability Low and almost uniform pre-travel variations in all directions More accurate measurements Low bending deflection (leading low hysteresis) Low trigger force Support much longer styli
Cons	Directional dependent pre-travel variation Micro-degradation of contact surfaces Exhibit re-seat failures over time Limiting the length of stylus Resistance through the contact elements as the means to sense trigger	Extra mass (filtering circuitry) Expensive

7.1.2. Analog Scanning Probes

Analog scanning probe ensures a permanent and continuous contact between the probe and the component under measurement, so it is particularly suitable for free-form and contoured shaped components as well as for the measurement of large sheet metal assemblies, such as automobile components. Continuous analog scanning (CAS) is a relatively new technology. Its main advantage is the high acquisition speed, which reduces dramatically the measuring time while offers a high density of data acquisition for a full definition of the part's size, position and shape, enabling completely new opportunities for on-machine tool metrology [119]. Nowadays, there are several CAS systems commercially available for machine tools [143,144].

7.1.3. Factors Affecting Probing Performance

There are different factors that affect probing performance of touching probe and therefore, their uncertainty must be considered for the MT accuracy assessment when working as a CMM. They are depicted in Figure 15.

- **Operation principle:** As mentioned in the previous point, contact probes can be broken into two general groups, scanning and discrete, based on the type of data being taken. Based on uncertainty sources, such as pre-travel variation and repeatability, the uncertainty vary according to the contact touch probe selected for the measuring task on the MT.
- **Measurement strategy:** A disadvantage of discrete-point probing is that it may take a long time to measure a free-form shaped part. If CAS technology is employed a continuous data acquisition is ensured so the acquisition time can be reduced considerably.

- Movement during probing: Static probing is executed while the component under measurement is motionless. However, dynamic measurement involves a component movement during data acquisition. With touch-trigger probes there is no possibility for static measurements as the trigger signal can only be generated during movement [119].
- Movement: The suspension can work either passively, with no actuation, or actively with a spring or electro-mechanical actuator. The active acquisition system offers the possibility to ensure a direction-independent probing force. However, the passive system provides better dynamic properties while probing the component and it is also cheaper [119].
- Kinematics: Probing systems can be mechanically fitted in either a parallel or serial configuration. The configuration influences the static and dynamic behaviour of the probe system, since the size and weight of the probe changes considerably. Serial kinematics comprises several self-independent axes, which are frequently mutually orthogonal. Instead, parallel kinematics configuration involves two axis movement with a coordinate, similar to a hexapod structure [145,146]. Serial and parallel kinematics probes are shown in Figure 16.
- Directional response pattern: A probing system can show varying directional sensitivity response [147,148]; mainly affected by asymmetric arrangement of sensors, asymmetric moment of inertia of stylus, tip ball form error or direction dependent sensitivity of sensors [37]. The effect of direction dependent sensitivity has the result that the same displacement of the tip ball leads to different output signals dependent on the direction of the displacement [149]. However, a correct behaviour characterisation offers the possibility to compensate this anisotropic effect through the control software [150–154].
- Environmental influences: The variation of environmental influences affects every metrology measurement. Consequently, it shall be considered as a part of the repeatability of the MT as a CMM.
- Cleanliness of the Surface: The cleanliness of the surface and the tip ball directly affect the measurement result. Therefore, a clean environment helps to uncertainty reduction on the probing process. In addition, if measurement is executed during the machining process, swarf could seriously influence the probing result. In fact, every effect is related to the probing force. If the probing force is near zero and soft surface contaminations (e.g., oil film) are probed, the signal to noise ratio of the probing system will decrease because of attenuation, which can make a reliable surface detection impossible [119].
- Tip ball: It is the contacting element between the MT and the component under measurement, so it is of utmost importance to characterize its position with the lowest uncertainty. The corrected measured point is achieved by correcting the tip ball centre point by adding a tip correction vector of the length of tip ball radius in the direction from the centre point to the probed point [155]. The radius value of the tip ball is measured during a specific measuring process, called qualification procedure of the probing system [156]. If the probing direction is needed for the coordinate correction process, it can be calculated from the probing system, by interpolation (from at least three probed points in the neighbourhood of the surface point) or by estimation (from e.g., CAD model). Usually real surfaces show, in addition to long-wave form deviations, random short-wave deviations known as roughness [157]. For such a surface the measured geometric properties represent a superposition of measurand and touching element [158] leading to a non-linear mechanical filtering effect. This filtering effect has a characteristic similar to a low pass depending on the tip ball diameter, because a smaller tip ball can penetrate smaller roughness valleys than a bigger ball. Because of this effect one gets for measured features different parameter values (size, position, form deviation) dependent on the diameter of the tip ball. As the measurement result is a superposition of tip ball and surface geometry, also form deviations of the ball directly lead to measurement errors. Thus it is necessary to use a tip ball of negligible form deviation compared to the required measurement uncertainty [119].

- Probing force: The probing force not just causes a bending of the stylus, but also has an effect on the elastic deformation of surface and tip ball due to Hertzian stress. Hertzian stress is the elastic deformation of two bodies touching each other [159]. The extent of deformation is dependent on the materials, micro and macro geometrical forms and the force. The effect of elastic deformations can be compensated to a certain extent by the probing system qualification process.
- Wear of tip ball, plastic deformation and wear of the workpiece surface: Wear and plastic deformation may happen during the probing process. This happens because there are some parameters such as probing force or hardness of contact surfaces that affect to the process. Hence, there are three main effects that cause bad probing results (1) Plastic deformation: Roughness peaks [160] of the workpiece at the probed points may be considered as wear of the workpiece surface [161]. The compressive strength of the workpiece material can be exceeded even by the small probing force because of the very small contact area between tip ball and roughness peak leading to high pressure. It affects the appearance of the probed surface (2) Wear of tip ball can occur during the scanning measuring process on a hard rough surface (3) Materials of tip ball and workpiece interact. It may occur that microscopic small particles break out of the surface due to local welding effects. Under normal circumstances, very little pick-up occurs [119].
- Probing system qualification: The position of the tip ball centre point related to the reference point of the probing system, the radius of the tip ball and the lobing error must be characterised to perform low uncertainty measurements [162,163]. These parameters are determined by a measuring procedure called probing system qualification.

ISO 230-10 [164] specifies test procedures to evaluate the measuring performance of contacting probing systems taking into account many of the factors affecting probing performance here presented. Its scope is limited to probing systems used in a discrete-point probing mode, integrated with a numerically controlled machine tool. It does not include other types of probing systems, such as those used in scanning mode or non-contacting probing systems. As this standard explicitly indicates, it does not address the evaluation of the performance of the machine tool, used as a CMM, since such performance evaluation involves traceability issues and is strongly influenced by machine tool geometric accuracy.

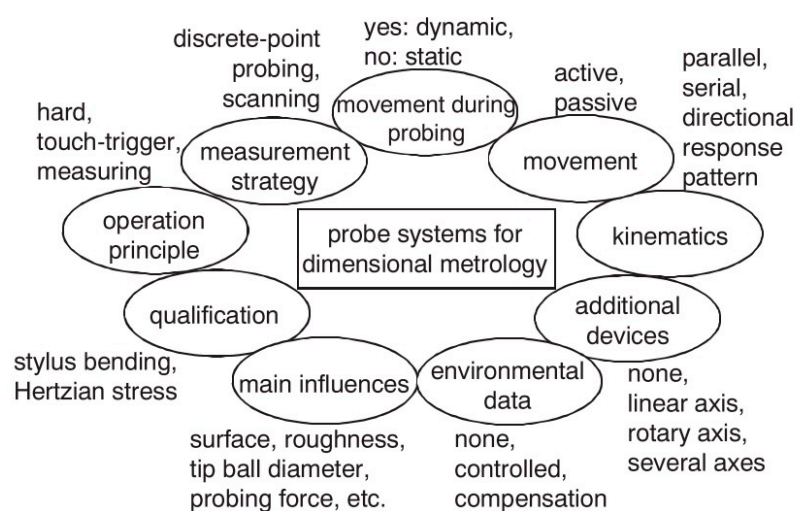


Figure 15. Aspects of probing systems [119].

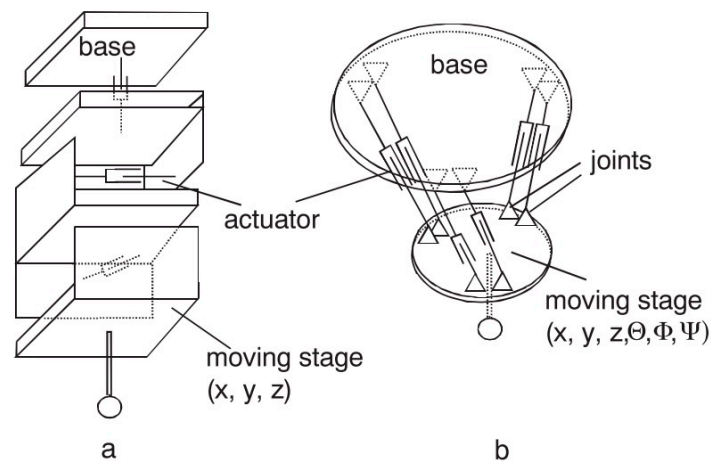


Figure 16. (a) serial and (b) parallel kinematics probes [119].

7.2. Non-Contact Touch Probe

The availability of non-contact 3D data capture systems capable of acquiring dense geometric data from complex surfaces has increased considerably over the past ten years [165]. Optical non-contact inspection techniques have revolutionized CMM inspection applications in the last decade, due to the cost and coverage of the technology. Nevertheless, a very small percentage of applications with non-contact measurement are already established, especially in robot and machine tool industry [166].

In this scenario, where a few approaches of non-contact technology integration are known, Karadayi presented a blue light laser sensor integration within a five axis machine tool, explaining sensor integration and calibration [167]. The laboratory for machine tools and production engineering of the RWTH Aachen University is also exploring the possibility to integrate non-contact sensors into MTs. Hence, de Moraes et al. integrated a 2D laser into a machine tool for an in-process 3D measurement [168].

In the manufacturing industry, there is an increasing need to measure accurately 3D shapes. Freeform shaped parts are of great interest in many applications, either for functional or aesthetical reasons. Their relevance for industry is well-known in the design and manufacturing of products having complex functional surfaces [169–176]. These parts are important components in industries such as automotive, aerospace, household appliances and others. Figure 17 shows measuring requirements for most common free form shaped parts.

Currently there is a wide variety of 3D optical sensing techniques that can be potentially integrated into machine tools to verify the geometry of a manufactured part on a machine tool measurement. Figure 18 comprises a non-contact sensing technology map.

According to CMM non-contact measurement, optical technology offers the greatest potential for a non-contact measurement on machine tool. Figure 19 shows optical non-contact 3D data capture systems map [176].

Considering the usage of CMM-based inspection by tactile probes and the non-contact optical triangulation systems, it seems that machine tool sensing roadmap will follow the CMM current scenario. Hence, triangulation-based technology is prone to be integrated into MT in the near future complementing the usage of tactile probes in MTs.

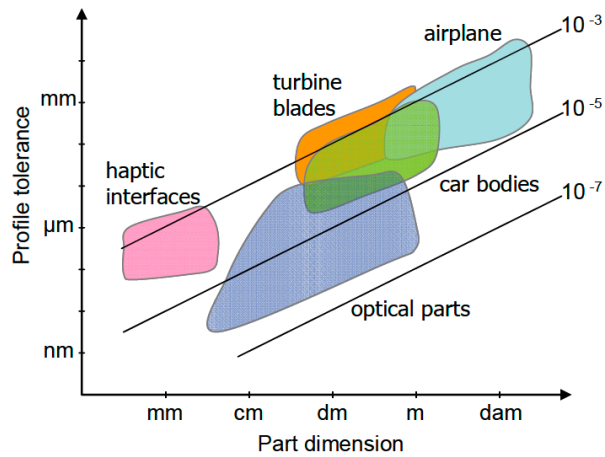


Figure 17. Typical values of tolerances vs. dimensions for most common free form shaped parts [170].

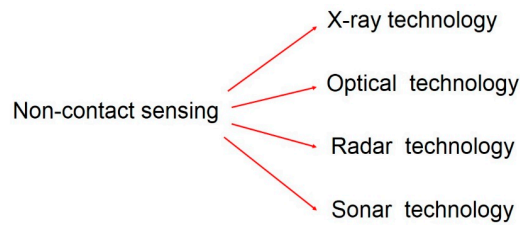


Figure 18. Non-contact sensing technology map.

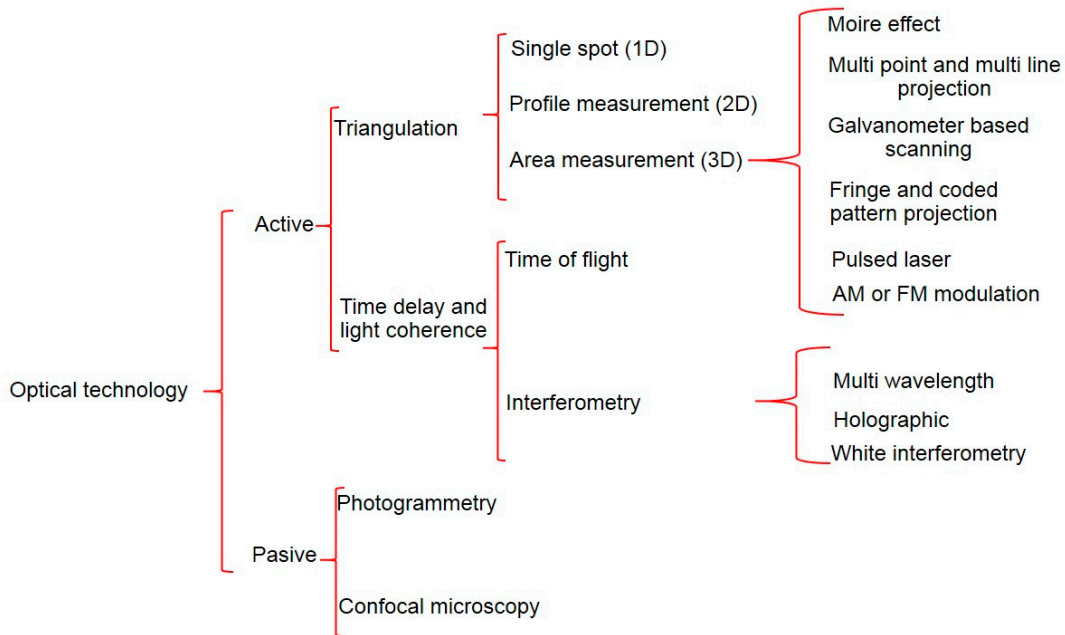


Figure 19. Optical sensing technology map [176].

7.3. Factors Affecting Non-Contact Probing Performance

Additional error sources may appear when using an optical measuring system on a freeform object. The surface characteristic itself dominates the uncertainty of the acquisition process, therefore its variation in terms e.g., of local curvature may add uncertainty. Other common errors are also induced by: the slope of the surface (which may produce direct reflections to the detector), volume

scattering (e.g., for plastic material), or an inhomogeneous surface texture. Secondary reflections, specular reflections, volumetric scattering, colour transitions, or ridges left by machining, may lead to gross systematic measuring errors [177–179].

Post-processing operations of measured data may add further uncertainty. The main difference between discrete and dense point acquisition is the amount and destination of the acquired data. For touch probes the acquired points belong to a single feature, while in scanning acquisition mode the system has no knowledge on which surface or feature the collected points reside. This circumstance is called segmentation and could be the main difference between contact and non-contact technology [180,181]. In fact this is very much like the fundamental problem in computer vision [182,183].

8. Error Sources Due to the Measuring Software

To perform the complex mathematical calculations required for metrology-based real-time decision making, powerful metrology software needs to be integrated within the manufacturing system. Because the system is expected to function by itself without human interaction, it also needs to work autonomously within the manufacturing process. The following characteristics are required from a software program to truly make a machine tool function similar to a CMM [4]:

- **Offline programming:** A computer-aided manufacturing (CAM)-style programming environment with good machine tool virtual modelling, simulation capabilities, automatic path generation with collision avoidance, and complete geometrical fitting and tolerancing functionality is required. Programming languages such as DMIS also allow interfacing and collaborating with CMMs for efficient programming.
- **Bi-directional interface:** A direct and bi-directional interface is a must to analyse data in real time as soon as the measurement of a feature is completed. The calculated metrology characteristics are used as a part of the on-the-fly decision making and written back to the machine tool controller as a part of the adaptive cycle.
- **Ability to handle high-density point cloud data:** When interfacing with a laser to measure large parts, very large amounts of data will be gathered. The software, in addition to offering a live interface with the machine tool, must also be able to handle the display and interaction with such data.
- **Geometric feature extractions:** For on-machine geometrical feature measurements and geometric dimensioning and tolerancing (GD&T) applications, an automatic feature extraction is necessary. Most point cloud systems today are offline and need operator interaction to calculate the required features. An on-machine measurement software that will interface with a laser system should also have a robust automatic feature extraction capability.
- **Ease of operation:** The measurement program must be integrated into the machining centre similar to any other machining program. This allows the measuring to be integrated as a part of manufacturing cycles and can be automatically started by itself. A G-Code NC program is created by post-processing the DMIS measurement routine and resides in the controller.

9. Error Sources Due to the Measured Object

Measurement processes are strongly influenced by the measurement systems and especially for large-scale components, by the object itself under measurement. Temperature fluctuations, either in the environment or during the machining process brings to temperature gradients that sensibly influence the geometry of the part, making a significant contribution to the measurement uncertainty. In addition, gravity affects the geometry of the component under measurement. These influences are evident during the manufacturing process of the component, but mainly when doing on-machine tool metrology [8].

Component temperature variations comprises a significant uncertainty source for on-MT metrology. The uncertainty increases proportionally with temperature differences and component size. Therefore, for large components measured in a thermally unstable production environment, thermal effects can represent a high percentage of the total measurement uncertainty [8,14,16,114,184,185].

Another heat source is the machining process, which creates a transient and non-homogeneous temperature distribution inside the component. Complex or asymmetric workpieces with different wall thicknesses or materials enhance this thermal inhomogeneity. The heat inside the component affects its characteristics (shape, position and size) when compared to their thermal reference state at 20 °C [8].

Additionally, all the geometric measurements done on earth suffer from gravitational deformations. These elastic deformations depend on the positioning and orientation, the material characteristics and the geometry of the component. Moreover, due to variability on the clamping operation during the machining process, object suffers from varying gravity deformations that affect a potential on-machine measurement during the machining process.

When it comes to the object under measurement, quasi-static errors are not as important as they are for large measuring systems, but it is crucial to determine the behaviour of the component according to a specific temperature and gravitational influences at the moment when measurement is executed [8].

To undertake the necessary modelling to understand and predict how large measurand behave under specific thermal and gravitational conditions, FEM software is widely used. It should be noted that any computational method that can accept temperatures and gravitational forces as a load condition to calculate localized displacements could be applied for such an application [186].

The first step is to define with high accuracy the boundary and initial conditions of the simulation. In addition, temperature related information should be characterized, such as, environment temperature information and initial temperature distribution. If the temperature of the part is homogeneous and it is being measured during the manufacturing process, a numerical compensation may be employed for numerical compensation. However, inhomogeneous temperature distributions are difficult to compensate and it should be assigned to the measurement uncertainty [187]. On the other hand, gravity related influences shall be added to the simulation. Information about fixtures that locate and clamp the component on the machine table, clamping orientation related to the gravity vector and detailed information about the component (mass and geometry) are achieved generally from the computer aided design (CAD).

The second step is to run the simulation. Simulation results represent compensation values to be applied as input to the measurement software for compensating thermal geometry and gravitational effects to a certain homogeneous reference temperature and position [8].

Finally, post processing is done to achieve results that can be viewed and analysed depending upon the requirements of the on-machine measurement to be done. Commercially available FEM software for the compensation of thermal and gravitational effects are listed next: Abaqus, Ansys, Comsol and Nastran [188–190].

10. Error Budget Quantitative Approach

The aim at this point is to develop a quantitative approach of a simple error budget [39] on the machine tool side where the weighting factor of each uncertainty source can be distinguished. Hence, main error contributors are detected and future research activities are suggested.

Small and medium size machine tools, from 0.5 m³ to 2 m³, typically offer a positioning accuracy better than 5 µm and a repeatability around 2–3 µm [191]. However, as stated by Keller at the TIM final workshop [10], the geometry variation of a 630 mm × 730 mm × 860 mm MT between 15–30 °C could be higher. On this experimental study, the positioning error variation is around 20 µm and the perpendicularity error variation is around 8 µm. While position and squareness errors are dominant and strong contributors to the varying total geometric error due to temperature effects, straightness

and rotational errors are less prone to temperature effects. Table 2 lists a simple error budget where major error uncertainties are described. Temperature effect is the most important error source, unless it is measured and compensated. As demonstrated by Schmitt et al. the uncertainty of a dimensional measurement done on a MT can be around 20–30 μm for a small MT [12].

Table 2. Error budget for small and medium size MTs.

Error Source	Significance		
	0–10 μm	10–100 μm	100–1000 μm
Accuracy			
Machine tool geometry	█		
Touch probe	█		
Repeatability			
MT repeatability	█		
Temperature effect	█		
Other effects	█		
Resolution	█		

The most frequent configurations of large machines are based in serial kinematics and three, four or five motions are located at the machine head. Hence, the part is fixed to the table and a heavy slide to move the part is not required. The dominant serial kinematics configurations for large machines are: movable column, gantry and elevated gantry [56]. The typical positioning accuracy of a high-tech large machine tool is around 10–15 μm and repeatability is better than 10 μm [192]. As stated by Kortaberria at TIM final workshop [193], while the positioning error variation of a large MT (6000 mm \times 3000 mm \times 1500 mm) is around 80 μm , the squareness and straightness error maintain stable. In addition, as stated by Wennemer [194] a very large MT geometry is extremely sensitive to the temperature influence, a length deviation of 300 μm is shown under temperature variation without any length compensation in beam direction and it is reduced to the half with length deviation. Table 3 depicts a simple error budget for a large MT.

Table 3. Error budget for large size MTs.

Error Source	Significance		
	0–10 μm	10–100 μm	100–1000 μm
Accuracy			
Machine tool geometry	█		
Touch probe	█		
Repeatability			
MT repeatability	█		
Temperature effect	█		
Other effects	█		
Resolution	█		

One of the most employed tactile probes nowadays is OMP400 from Renishaw. It offers a repeatability better than 0.5 μm and the 3D lobing error is around $\pm 2 \mu\text{m}$ for a 100 mm stylus length [130].

11. Outlook and Conclusions

Machine tool measurement has the potential to test product characteristics during or right after the manufacturing process, resulting in improved part quality and reduction of waste material. In addition, the reduction of the production time could also be achieved by preventing the workpiece to be transported to a measuring facility. However, the traceability of the measurement process on a machine tool is not ensured yet and measurement data is still not fully reliable for process control or product validation

On MT measurement, uncertainty should be assessed according to current CMM standards. For serial production, usually in case of small and medium size components, the substitution method based on ISO 15530-3 simplifies the uncertainty assessment by means of using the similarity between the workpiece and the employed standard. The current scenario shows that traceability for on-machine measurement in small size machine tools based on ISO 15530-3 is starting to be introduced as a realistic option [195]. However, for small batch production, mainly in case of large scale manufacture, the substitution method is not an affordable solution due to the size of the part. Thus, uncertainty should be addressed by uncertainty budget solution according to VDI 2617-11.

There are two main error sources, coming from the MT geometric error variation and the measurand that are not fully understood yet, so traceability cannot be ensured. In addition, position and squareness errors are the dominant contributors to the varying total geometric error of the MT due to temperature effects, but they cannot be permanently monitored at the moment. Moreover, the component under measurement makes a significant contribution to the total measurement uncertainty, mainly because of its thermo-mechanical deformation. Errors resulting from the touch probe should be seriously considered for the error budget of small machine tools, while for large machine tools it represents a minor error source.

The future scenario seems to trust in technology based on interferometry to tackle current limitations. A strong evolution of the technology seems to trace the roadmap for the future research of error mapping and monitoring in industrial environment. ADM technology, which offers absolute measurements, is getting affordable and it is already being used in commercial devices, such as laser trackers, for displacement measurement, besides IFM. As soon as ADM technology achieves IFM uncertainty level and performs real time measurements, a new scenario will arise. It means that MTs and components under measurement could be temperature independent systems where any variation could be recorded by ADM technology in absolute scale and therefore, traceability assessment could be done any time. Following this trend of using technology based on interferometry, some facilities have already gone further by applying technologies like the absolute multiline, in the case of NAMRC [72] or the Productive Process Pyramid™ concept [196] as a full approach to control the process from assessing the machine, through pre-production checks and pre-finishing probing to post-production measurement and Statistical Process Control. These approaches can be applied on some specific cases to have a good understanding of their uncertainty and traceability through interferometry, but they cannot be considered yet as general solutions to ensure the traceability of the measurement process on a machine tool.

In spite of all these advances, many challenges still remain, ranging from the need of technology development to the complete knowledge of the error sources that affect the on-MT measuring process. In addition, a complete system of standards supporting the machine integrated traceable measuring process is needed.

Acknowledgments: We would like to show our gratitude to Emilio Prieto from the Spanish National Metrology Institute for comments that greatly improved the manuscript.

Author Contributions: E.G.-A. collected literature related to temperature sensors. A.O. contributed materials to indirect measurement methods review and G.K. contributed materials to quasi-static error assessment and monitoring review (Section 6.3). U.M. wrote the paper and J.A.Y.F. wrote the manuscript. All authors contributed to the editing of the manuscript.

Conflicts of Interest: The authors declare no conflict of interest.

References

1. Imkamp, D.; Berthold, J.; Heizmann, M.; Kniel, K.; Peterek, M.; Schmitt, R.; Seidler, J.; Sommer, K.-D. Challenges and trends in manufacturing measurement technology—the “Industrie 4.0” concept. *J. Sens. Sens. Syst.* **2016**, *83*, 325–335. [[CrossRef](#)]
2. Balazs, A. International vocabulary of metrology—basic and general concepts and associated terms. *Chem. Int.* **2008**, *30*. [[CrossRef](#)]

3. Physikalisch-Technische Bundesanstalt (PTB). Available online: <https://www.ptb.de/emrp/ind62-home.html> (accessed on 20 March 2017).
4. Karadayi, R. In Process Closed Loop Metrology for Adaptive Manufacturing. In Proceedings of the Annual Workshop and Conference, Toronto, ON, Canada, 10–15 March 2014.
5. Schwenke, H. Large parts with critical tolerances: Concepts and possible solutions for traceable CMM measurements on machine tools. In Proceedings of the Traceable in-Process Dimensional Measurement Final Workshop, Physikalisch-Technische-Bundesanstalt (PTB), Braunschweig, Germany, 18 May 2016.
6. *Machine Tools-Numerical Compensation of Geometric Errors*, 1st ed.; ISO/TR 16907:2015; International Organization for Standardization: Geneva, Switzerland, 2015.
7. Nisch, S.; Schmitt, R. Production integrated 3D measurements on large machine tools. In Proceedings of the Large Volume Metrology Conference (LVMC), Chester, UK, 2 November 2010.
8. Schmitt, R.; Peterek, M.; Morse, E.; Knapp, W.; Galetto, M.; Härtig, F.; Goch, G.; Hughes, B.; Forbes, A.; Estler, W. Advances in Large-Scale Metrology—Review and future trends. *CIRP Ann. Manuf. Technol.* **2016**, *65*, 643–665. [[CrossRef](#)]
9. *Industrie 4.0: Aachener Perspektiven: Aachen Machine Tools Colloquium*, 1st ed.; Werkzeugmaschinenkolloquium, A., Ed.; Shaker Verlag: Aachen, Germany, 2014.
10. Keller, F. Traceability of on-machine measurements under a wide range of working conditions. In Proceedings of the Traceable in-Process Dimensional Measurement Final Workshop, Physikalisch-Technische-Bundesanstalt (PTB), Braunschweig, Germany, 18 May 2016.
11. Schmitt, R.; Jatzkowski, P.; Peterek, M. Traceable measurements using machine tools. In Proceedings of the Laser Metrology and Machine Performance X: 10th International Conference and Exhibition on Laser Metrology, Machine Tool, CMM and Robotic Performance, Lamdamap, Buckinghamshire, UK, 20–21 March 2013; pp. 131–139.
12. Schmitt, R.; Peterek, M. Traceable measurements on machine tools-thermal influences on machine tool structure and measurement Uncertainty. *Procedia CIRP* **2015**, *33*, 576–580. [[CrossRef](#)]
13. *Geometrical Product Specifications (GPS)-Acceptance and Reverification Tests for Coordinate Measuring Machines (CMM)-Part 1: Vocabulary, ISO 10360-1:2000*, 1st ed.; International Organization for Standardization: Geneva, Switzerland, 2000.
14. Bryan, J. International Status of Thermal Error Research (1990). *CIRP Ann. Manuf. Technol.* **1990**, *39*, 645–656. [[CrossRef](#)]
15. Bryan, J.; Pearson, J.; Brewer, W.; McClure, E. Thermal effects in dimensional metrology. *Mech. Eng.* **1965**, *87*, 70.
16. Ross-Pinnock, D.; Maropoulos, P.G. Identification of key temperature measurement technologies for the enhancement of product and equipment integrity in the light controlled factory. *Procedia CIRP* **2014**, *25*, 114–121. [[CrossRef](#)]
17. Ross-pinnock, D.; Mullineux, G. Compensating for thermal and gravitational effects in structures and assemblies. In Proceedings of the Luminar Workshop, Bath, UK, 18–19 May 2016.
18. Postlethwaite, S.R.; Allen, J.P.; Ford, D.G. Machine tool thermal error reduction-An appraisal. *Proc. Inst. Mech. Eng. Part B J. Eng. Manuf.* **1999**, *213*, 1–9. [[CrossRef](#)]
19. Mayr, J.; Jedrzejewski, J.; Uhlmann, E.; Alkan Donmez, M.; Knapp, W.; Härtig, F.; Wendt, K.; Moriwaki, T.; Shore, P.; Schmitt, R.; et al. Thermal issues in machine tools. *CIRP Ann. Manuf. Technol.* **2012**, *61*, 771–791. [[CrossRef](#)]
20. Puttock, M. Large Scale metrology. In *Handbook of Measuring System Design*; Wiley: Hoboken, NJ, USA, 1978.
21. Wendt, K.; Franke, M.; Härtig, F. Mobile Multilateration Measuring System for High Accurate and Traceable 3D Measurements of Large Objects. In Proceedings of the 10th International Symposium on Measurement and Quality Control, Osaka, Japan, 5–9 September 2010.
22. *Uncertainty of Measurement-Part 3: Guide to the Expression of Uncertainty in Measurement (GUM:1995)*, 1st ed.; ISO/IEC Guide 98-3:2008; International Organization for Standardization: Geneva, Switzerland, 2008.
23. *Geometrical Product Specifications (GPS)-Coordinate Measuring Machines (CMM): Technique for Determining the Uncertainty of Measurement-Part 3: Use of Calibrated Workpieces or Standards*, 1st ed.; ISO/TS 15530-3:2004; International Organization for Standardization: Geneva, Switzerland, 2004.

24. Widmaier, T.; Kuosmanen, P.; Hemming, B.; Esala, V.; Brabandt, D. New material standards for traceability of roundness measurements of large-scale rotors. In Proceedings of the 58th IWK, Ilmenau Scientific Colloquium Technische Universität, Ilmenau, Germany, 8–12 September 2014.
25. Acko, M.; Klobucar, R.; Milfelener, M. Measurement Standard for Monitoring Performance of Machine Tools in Harsh Environmental Conditions. Available online: https://www.google.es/url?sa=t&rcct=j&q=&esrc=s&source=web&cd=1&ved=0ahUKewicwMm-x_bUAhUL7RQKHdlaCWYQFggoMAA&url=https%3A%2F%2Fpublic.ptb.de%2Ffiles%2Fdownload%2F56d6a9f2ab9f3f76468b4658&usg=AFQjCNEuMQ3SfbhtfaTwuP6ASTt9CXcXIA (accessed on 20 February 2017).
26. Zeleny, J.; Linkeova, I. Design and calibration of free-form standard. In Proceedings of the Laser Metrology and Machine Performance XI, Huddersfield, UK, 17 March 2015; pp. 147–148.
27. Zeleny, J.; Linkeova, I.; Skalnik, P. Calibrated CAD model of freeform standard. In *Proc. XXI IMEKO World Congress 2015*; International Measurement Confederation (IMEKO): Prague, Czech Republic, 2015.
28. Viprey, F.; Nouira, H.; Lavernhe, S.; Tournier, C. Novel multi-feature bar design for machine tools geometric errors identification. *Precis. Eng.* **2016**, *46*, 323–338. [[CrossRef](#)]
29. Woodward, S.; Brown, S.; Dury, M.; McCarthy, M. Producing dimensional transfer material standards for the assessment of workshop machine tool performance. In Proceedings of the Euspen's 16th International Conference & Exhibition, Nottingham, UK, 30 May–3 June 2016.
30. *Geometrical Product Specifications (GPS)—Coordinate Measuring Machines (CMM): Technique for Determining the Uncertainty of Measurement—Part 4: Evaluating Task-Specific Measurement Uncertainty Using Simulation*, 1st ed.; ISO/TS 15530-4:2008; International Organization for Standardization: Geneva, Switzerland, 2008.
31. Trapet, E.; Wäldele, F. A reference object based method to determine the parametric error components of coordinate measuring machines and machine tools. *Measurement* **1991**, *9*, 17–22. [[CrossRef](#)]
32. Trapet, E. *Traceability of Coordinate Measurements According to the Method of the Virtual Measuring Machine*; Physikalisch-Technische Bundesanstalt (PTB): Braunschweig, Germany, 1999.
33. Härtig, F.; Kniel, K.; Schulze, K. *Messunsicherheitsermittlung: Ermittlung Einer Aufgabenspezifischen Messunsicherheit von 3D-Verzahnungsmessungen*; FVA: Freiburg, Germany, 2008.
34. Maropoulos, P.G.; Guo, Y.; Jamshidi, J.; Cai, B. Large volume metrology process models: A framework for integrating measurement with assembly planning. *CIRP Ann. Manuf. Technol.* **2008**, *57*, 477–480. [[CrossRef](#)]
35. *Accuracy of Coordinate Measuring Machines—Characteristics and Their Checking—Determination of the Uncertainty of Measurement for Coordinate Measuring Machines Using Uncertainty Budgets*; Standard: DIN—VDI/VDE 2617 BLATT 11; Verein Deutscher Ingenieure: Düsseldorf, Germany, 2011.
36. García, M. Inspection of Large High Value Components on a Machine Tool Platform. In Proceedings of the 3D Metrology Conference (3DMC), RWTH Aachen University, Aachen, Germany, 22 November 2016.
37. Measurement Good Practice Guide No. 42: CMM Verification. Available online: http://publications.npl.co.uk/npl_web/pdf/mgpg42.pdf (accessed on 18 April 2017).
38. Slocum, A. Precision Machine-Design-Macromachine Design Philosophy and Its Applicability to the Design of Micromachines. In Proceedings of the IEEE Micro Electro Mechanical Systems, New York, NY, USA, 4–7 February 1992.
39. Slocum, A. Fundamentals of Design: Error Budgets. Available online: <http://web.mit.edu/2.75/fundamentals/FUNdaMENTALS%20Book%20pdf/Precision%20Machine%20Design%20Error%20Budget.pdf> (accessed on 4 March 2017).
40. Ispas, C.; Anania, D.; Mohora, C. Contribution concerning machine tool accuracy using software methods for geometrical errors compensation. In Proceedings of the 15th International Conference on Manufacturing Systems-ICMaS, Bucharest, Romania, 26–27 October 2006.
41. Schwenke, H.; Knapp, W.; Haitjema, H.; Weckenmann, A.; Schmitt, R.; Delbressine, F. Geometric error measurement and compensation of machines—An update. *CIRP Ann. Manuf. Technol.* **2008**, *57*, 660–675. [[CrossRef](#)]
42. Hocken, R.J. *Machine Tool Accuracy*. In *Technology of Machine Tools*; California University: Livermore, CA, USA, 1980; Volume 5.
43. Knapp, W.; Matthias, E. Test of the Three-Dimensional Uncertainty of Machine Tools and Measuring Machines and its Relation to the Machine Errors. *CIRP Ann. Manuf. Technol.* **1983**, *32*, 459–464. [[CrossRef](#)]
44. Soons, J. Accuracy Analysis of Multi-Axis Machines. Available online: <https://pure.tue.nl/ws/files/1717013/400139.pdf> (accessed on 23 April 2017).

45. Weekers, W.G.; Schellekens, P.H.J. Compensation for Dynamic Errors of Coordinate Measuring Machines. *Measurement* **1997**, *20*, 197–209. [[CrossRef](#)]
46. Abbe, E. Meßapparate für Physiker. *J. Instrum. Inf.* **1890**, *10*, 446–448.
47. Ibaraki, S.; Sawada, M.; Matsubara, A.; Matsushita, T. Machining tests to identify kinematic errors on five-axis machine tools. *Precis. Eng.* **2010**, *34*, 387–398. [[CrossRef](#)]
48. Dassanayake, K.M.M.; Tsutsumi, M.; Saito, A. A strategy for identifying static deviations in universal spindle head type multi-axis machining centers. *Int. J. Mach. Tools Manuf.* **2006**, *46*, 1097–1106. [[CrossRef](#)]
49. Donmez, M.A.; Blomquist, D.S.; Hocken, R.J.; Liu, C.R.; Barash, M.M. A general methodology for machine tool accuracy enhancement by error compensation. *Precis. Eng.* **1986**, *8*, 187–196. [[CrossRef](#)]
50. Huang, T.; Whitehouse, D. A simple yet effective approach for error compensation of a tripod-based parallel kinematic machine. *CIRP Ann. Technol.* **2000**, *49*, 285–288. [[CrossRef](#)]
51. Hocken, R.J. Three dimensional Metrology. *Proce. CIRP* **1977**, *26*, 403–408.
52. Zhang, G.; Veale, R.; Charlton, T.; Borchardt, B.; Hocken, R. Error Compensation of Coordinate Measuring Machines. *CIRP Ann. Manuf. Technol.* **1985**, *34*, 445–448. [[CrossRef](#)]
53. Soons, J.A.; Theuws, F.C.; Schellekens, P.H. Modeling the errors of multi-axis machines: a general methodology. *Precis. Eng.* **1992**, *14*, 5–19. [[CrossRef](#)]
54. Schellekens, P.; Rosielle, N.; Vermeulen, H.; Vermeulen, M.; Wetzels, S.; Pril, W. Design for Precision: Current Status and Trends. *CIRP Ann. Manuf. Technol.* **1998**, *47*, 557–586. [[CrossRef](#)]
55. *Test Code for Machine Tools-Part 1: Geometric Accuracy of Machines Operating under no-Load or Quasi-Static Conditions*, 1st ed.; ISO 230-1:2012; International Organization for Standardization: Geneva, Switzerland, 2012.
56. Uriarte, L.; Zatarain, M.; Axinte, D.; Yagüe-Fabra, J.; Ihlenfeldt, S.; Eguia, J.; Olarra, A. Machine tools for large parts. *CIRP Ann. Manuf. Technol.* **2013**, *62*, 731–750. [[CrossRef](#)]
57. Weckenmann, A. Comparison of CMM length measurement tests conducted with different 1D, 2D and 3D standards. In Proceedings of the 11th National, 2nd International Scientific Conference Metrology in Production Engineering, Lublin, Poland, 15–17 September 2005.
58. Knapp, W.; Tschudi, U.; Bucher, A. *Vergleich von Prüfkörpern zur Abnahme von Koordinatenmessgeräten*; Technische Rundschau: Bern, Switzerland, 1990.
59. *Test Code for Machine Tools—Part 7: Geometric Accuracy of Axes of Rotation*, 1st ed.; ISO 230-7: 2015; International Organization for Standardization: Geneva, Switzerland, 2015.
60. Cauchick-Miguel, P.; King, T.; Davis, J. CMM verification: A survey. *Meas. J. Int. Meas. Confed.* **1996**, *17*, 1–16. [[CrossRef](#)]
61. Kunzmann, H.; Trapet, E.; Wäldele, F. A Uniform Concept for Calibration, Acceptance Test, and Periodic Inspection of Coordinate Measuring Machines Using Reference Objects. *CIRP Ann. Manuf. Technol.* **1990**, *39*, 561–564. [[CrossRef](#)]
62. Pahk, H.J.A.E.; Kimt, Y.S.A.M.; Moon, J.H.E.E. A New Technique for Volumetric Error Assessment of CNC MTs Incorporating Ball Bar Measurement and 3D Volumetric Error Model. *Int. J. Mach. Tools Manuf.* **1997**, *37*, 1583–1596. [[CrossRef](#)]
63. Zargarbashi, S.H.H.; Mayer, J.R.R. Assessment of machine tool trunnion axis motion error, using magnetic double ball bar. *Int. J. Mach. Tools Manuf.* **2006**, *46*, 1823–1834. [[CrossRef](#)]
64. Knapp, W. Machine Tool Testing Methods: Overview over ISO Standards and other Special Tests for Machine Tool Performance Evaluation and Interim Checking. In Proceedings of the Metroment, Bilbao, Spain, 7–8 April 2005.
65. Belforte, G.; Bona, B.; Canuto, E.; Donati, F.; Ferraris, F.; Gorini, I.; Morei, S.; Peisino, M.; Sartori, S.; Levi, R. Coordinate Measuring Machines and Machine Tools Selfcalibration and Error Correction. *CIRP Ann. Manuf. Technol.* **1987**, *36*, 359–364. [[CrossRef](#)]
66. Knapp, W. Comparison of National and International Standards for Evaluation of Positioning Accuracy and Repeatability of NC Axes. Available online: http://www.google.es/url?sa=t&rc=t=j&q=&esrc=s&source=web&cd=1&ved=0ahUKewiR67_HyfbUAhXFXhQKHaMdCwwQFggjMAA&url=http%3A%2F%2Fwww.amtonline.org%2Farticle_download.cfm%3Farticle_id%3D63300&usg=AFQjCNGIutSKT3NV_EW-A8bbCbTohPDJWQ (accessed on 25 April 2017).
67. *The Benefits of Remote Interferometry for Linear, Angular and Straightness Measurements*; Technical white paper: TE335; Renishaw: Wotton-under-Edge, UK, 2015.

68. Hickman, P.A. Optical tilting viewed in a new light. *Laser Focus* **1968**, *4*, 22.
69. Salsbury, J.G.; Hocken, R.J. Taut Wire Straightedge Reversal Artifact. In *Initiatives of Precision Engineering at the Beginning of a Millennium*; Inasaki, I., Ed.; ICPE: Yokohama, Japan, 2002; pp. 644–648.
70. Quesnel, J.; Durand, H.M.; Touzé, T. Stretched Wire Offset Measurements: 40 Years of Practice of This Technique At Cern. In *Proceedings of the 10th International Workshop on Accelerator Alignment*, KEK, Tsukuba, 11–15 February 2008.
71. Muralikrishnan, B.; Sawyer, D.; Blackburn, C.; Phillips, S.; Borchardt, B.; Estler, W.T. ASME B89.4.19 Performance Evaluation Tests and Geometric Misalignments in Laser Trackers. *J. Res. Natl. Inst. Stand. Technol.* **2006**, *114*, 21. [[CrossRef](#)]
72. Schwenke, H. The latest trends and future possibilities of volumetric error compensation for machine tools. In *Proceedings of the 15th International Machine Tool Engineers' Conference*, IMEC, Tokyo, Japan, 2–3 November 2012; pp. 57–71.
73. CIRP Unification Document Me Axes of Rotation. *Ann. CIRP* **1976**, *25*, 545–564.
74. Chapman, M.A.V.; Holloway, A.; Lee, W.; May, M.; McFadden, S.; Wall, D. *Interferometric Calibration of Rotary Axes*; Technical white paper: TE327; Renishaw: Wotton-under-Edge, UK, 2013.
75. Estler, W.T. Uncertainty Analysis for Angle Calibrations Using Circle Closure. *J. Res. Natl. Inst. Stand. Technol.* **1998**, *103*, 11. [[CrossRef](#)] [[PubMed](#)]
76. Chapman, M.A.V.; Fergusson-Kelly, R.; Holloway, A.; Lock, D.; Lee, W. *Interferometric Angle Measurement and the Hardware Options*; Technical white paper: TE326; Renishaw: Wotton-under-Edge, UK, 2013.
77. XM-60 Multi-Axis Calibrator; Renishaw. Available online: <http://www.renishaw.com/en/xm-60-multi-axis-calibrator--39258> (accessed on 16 April 2017).
78. Calibration Interferometer: SP 15000 C Series; SIOS. Available online: <http://www.sios-de.com/products/calibration-interferometer/> (accessed on 17 April 2017).
79. XD Laser Measuring Solution; Automated Precision Inc. (API). Available online: <https://www.apisensor.com/products/mth/xd-laser/> (accessed on 17 April 2017).
80. Ibaraki, S.; Knapp, W. Indirect Measurement of Volumetric Accuracy for Three-Axis and Five-Axis Machine Tools: A Review. *Int. J. Autom. Technol.* **2012**, *6*, 110–124. [[CrossRef](#)]
81. *Test Code for MTs. Part 4. Circular Tests for Numerically Controlled Machine Tools*, 1st ed.; ISO 230-4:2005; International Organization for Standardization: Geneva, Switzerland, 2005.
82. *Test Code for Machine Tools. Part 6. Determination of Positioning Accuracy on Body and Face Diagonals (Diagonal Displacement Tests)*, 1st ed.; ISO 230-6:2002; International Organization for Standardization: Geneva, Switzerland, 2002.
83. Kruth, J.P.; Zhou, L.; Van den Bergh, C.; Vanherck, P. A Method for Squareness Error Verification on a Coordinate Measuring Machine. *Int. J. Adv. Manuf. Technol.* **2003**, *21*, 874–878. [[CrossRef](#)]
84. Bringmann, B.; Küng, A.; Knapp, W. A Measuring Artefact for true 3D Machine Testing and Calibration. *CIRP Ann. Manuf. Technol.* **2005**, *54*, 471–474. [[CrossRef](#)]
85. Kenta, U.; Ryosyu, F.; Sonko, O.; Toshiyuki, T.; Tomizo, K. Geometric calibration of a coordinate measuring machine using a laser tracking system. *Meas. Sci. Technol.* **2005**, *16*, 2466.
86. Schwenke, H.; Franke, M.; Hannaford, J.; Kunzmann, H. Error mapping of CMMs and machine tools by a single tracking interferometer. *CIRP Ann. Manuf. Technol.* **2005**, *54*, 475–478. [[CrossRef](#)]
87. *Test Conditions for Machining Centres—Part 1: Geometric Tests for Machines with Horizontal Spindle (Horizontal Z-Axis)*, 1st ed.; ISO 10791-1:2015; International Organization for Standardization: Geneva, Switzerland, 2015.
88. *Test Conditions for Machining Centres—Part 6: Accuracy of Speeds and Interpolations*, 1st ed.; ISO 10791-6:2014; International Organization for Standardization: Geneva, Switzerland, 2014.
89. Florussen, G.H.J.; Spaan, H.A.M. Static R-Test: Allocating the Centreline of Rotary Axes of Machine Tools. In *Proceedings of the Laser Metrology and Machine Performance VIII: 8th International Conference on Laser Metrology, Machine Tool, CMM & Robotic Performance*, Cardiff, UK, 26–28 June 2007.
90. Florussen, G.H.J.; Spaan, H.A.M. Determining the machine tool contouring performance with dynamic R-test measurements 3D probe head Masterball C-axis. In *Proceedings of the 12th Euspen International Conference*, Stockholm, Sweden, 4–8 June 2012; pp. 1–5.
91. Florussen, G.H.J.; Spaan, H.A.M. Dynamic R-test for rotary tables on 5-axes machine tools. *Procedia CIRP* **2012**, *1*, 536–539. [[CrossRef](#)]

92. *Uniform Cutting Test—NAS Series. Metal Cutting Equip- Ments*; Standard: AIA/NAS-NAS979; Aerospace Industries Association of America: Arlington, VA, USA, 1969.
93. Hughes, E.B.; Wilson, A.; Peggs, G.N. Design of a High-Accuracy CMM Based on Multilateration Techniques. *CIRP Ann. Manuf. Technol.* **2000**, *49*, 391–394. [[CrossRef](#)]
94. Weckenmann, A.; Jiang, X.; Sommer, K.D.; Neuschaefer-Rube, U.; Seewig, J.; Shaw, L.; Estler, T. Multisensor data fusion in dimensional metrology. *CIRP Ann. Manuf. Technol.* **2009**, *58*, 701–721. [[CrossRef](#)]
95. Aguado, S.; Santolaria, J.; Samper, D.; Aguilar, J.J. Influence of measurement noise and laser arrangement on measurement uncertainty of laser tracker multilateration in machine tool volumetric verification. *Precis. Eng.* **2013**, *37*, 929–943. [[CrossRef](#)]
96. Schmitt, R.; Peterek, M.; Quinders, S. Concept of a Virtual Metrology Frame Based on Absolute Interferometry for Multi Robotic Assembly. Available online: <https://hal.inria.fr/hal-01260735/document> (accessed on 20 March 2017).
97. Olarra, A.; Zubeldia, M.; Gomez-acedo, E.; Kortaberria, G. Measuring positioning accuracy of large machine tool. In Proceedings of the 19th Congress of Machine Tools and Manufacturing Technology, Donostia-San Sebastián, Spain, 12 June 2013.
98. Brecher, C.; Flore, J.; Haag, S.; Wenzel, C. High precision, fast and flexible calibration of robots and large multi-axis machine tools. In Proceedings of the 9th International Conference on Machine Tools, Automation, Robotics and Technology, Prague, Czech Republic, 12 September 2012.
99. Schwenke, H. *Accuracy Improvement of Machine Tool via New Laser Measurement Methods*; The Japan International Machine Tool Fair (JIMTOF), 2015.
100. Schwenke, H.; Schmitt, R.; Jatzkowski, P.; Warmann, C. On-the-fly calibration of linear and rotary axes of machine tools and CMMs using a tracking interferometer. *CIRP Ann. Manuf. Technol.* **2009**, *58*, 477–480. [[CrossRef](#)]
101. LaserTracer-MT: Perfect Geometries through Volumetric Compensation. Available online: <http://www.etalon-ag.com/en/products/lasertracer-mt/> (accessed on 10 January 2017).
102. Hexagon Manufacturing Intelligence. Available online: <http://www.hexagonmi.com/products/laser-tracker-systems/leica-absolute-tracker-at930> (accessed on 23 April 2017).
103. *Geometrical Product Specifications (GPS)—Acceptance and Reverification Tests for Coordinate Measuring Machines (CMM)—Part 2: CMMs Used for Measuring Linear Dimensions*, 1st ed.; ISO 10360-2:2009; International Organization for Standardization: Geneva, Switzerland, 2009.
104. Trapet, E.; Aguilar Martín, J.J.; Yagüe, J.A.; Spaan, H.; Zelený, V. Self-centering probes with parallel kinematics to verify machine-tools. *Precis. Eng.* **2006**, *30*, 165–179. [[CrossRef](#)]
105. Etalon AG. Linecal-Automatic Volumetric Calibration. Available online: <http://www.etalon-ag.com/en/products/linecal/> (accessed on 10 January 2017).
106. *Test Code for Machine Tools-Part 2: DETERMINATION of Accuracy and Repeatability of Positioning of Numerically Controlled Axes*, 1st ed.; ISO 230-2; International Organization for Standardization: Geneva, Switzerland, 2014.
107. *Statistical Testing of the Operational and Positional Accuracy of Machine Tools*; VDI/DGQ 3441; Verein Deutscher Ingenieure (VDI): Dusseldorf, Germany, 1982.
108. Longstaff, A.P.; Fletcher, S.; Myers, A. Volumetric error compensation through a Siemens controller. In Proceedings of the 7th International Conference and Exhibition on Laser Metrology, Machine Tool, CMM & Robotic Performance, Lamdamap 2005, Cranfield, UK, 27–30 June 2005.
109. Duffie, N.A.; Yang, S.M.; Bollinger, J.G. Generation of Parametric Kinematic Error-Correction Functions from Volumetric Error Measurements. *CIRP Ann. Manuf. Technol.* **1985**, *34*, 435–438. [[CrossRef](#)]
110. Liu, H.; Xue, X.; Tan, G. Backlash Error Measurement and Compensation on the Vertical Machining Center. *Engineering* **2010**, 403–407. [[CrossRef](#)]
111. Rehsteiner, F.; Weikert, S.; Rak, Z. Accuracy Optimization of Machine Tools under Acceleration Loads for The Demands of High-Speed-Machining. In Proceedings of the 13th Annual Meeting of American Society for Precision Engineering, Saint Louis, MO, USA, 26–31 October 1998; pp. 602–605.
112. Weikert, S. When five axes have to be synchronized. In Proceedings of the 7th International Conference and Exhibition on Laser Metrology, CMM and Machine Tool Performance, Cranfield, UK, 2005.
113. Weekers, W.G.; Schellekens, P.H.J. Compensation for dynamic errors of coordinate measuring machines. *Precis. Eng.* **1997**, *20*, 197–209. [[CrossRef](#)]

114. Bryan, J. International Status of Thermal Error Research. Available online: <http://emtoolbox.nist.gov/Publications/UCRL-1967-50285-InternationalStatusofThermalErrorResearch.pdf> (accessed on 11 April 2017).
115. Van Den Bergh, C. Reducing thermal errors of CMM located on the shop—Floor. Ph.D. Thesis, Katholieke Universiteit Leuven, Leuven, Belgium, 2001.
116. Delbressine, F.L.M.; Florussen, G.H.J.; Schijvenaars, L.A.; Schellekens, P.H.J. Modelling thermomechanical behaviour of multi-axis machine tools. *Precis. Eng.* **2006**, *30*, 47–53. [[CrossRef](#)]
117. Florussen, G.H.J. Accuracy Analysis of Multi-axis Machines by 3D Length Measurements. Ph.D. Thesis, Eindhoven University of Technology, Eindhoven, Netherlands, 2002.
118. Gruber, R.; Knapp, W. Temperatureinflüsse auf die Werkzeugmaschinen-Genauigkeit. *Werkstatt und Betrieb* **1998**, *131*, S1049–S1052.
119. Weckenmann, A.; Estler, T.; Peggs, G.; McMurtry, D. Probing systems in dimensional metrology. *CIRP Ann. Manuf. Technol.* **2004**, *53*, 657–684. [[CrossRef](#)]
120. Muelaner, J.E.; Maropoulos, P.G. Large volume metrology technologies for the light controlled factory. *Procedia CIRP* **2014**, *25*, 169–176. (In German) [[CrossRef](#)]
121. National Physical Laboratory (NPL). Large Volume Unified Metrology for Industry, Novel Applications & Research (LUMINAR) EMRP Project. Available online: <http://projects.npl.co.uk/luminar/> (accessed on 2 February 2017).
122. Peggs, G.N.; Maropoulos, P.G.; Hughes, E.B.; Forbes, A.B.; Robson, S.; Ziebart, M.; Muralikrishnan, B. Recent developments in large-scale dimensional metrology. *Proc. Inst. Mech. Eng. Part B J. Eng. Manuf.* **2009**, *223*, 571–595. [[CrossRef](#)]
123. Leica Absolute Interferometer, a New Approach to Laser Tracker Absolute Distance Meteres. Leica. Available online: http://www.google.es/url?sa=t&rct=j&q=&esrc=s&source=web&cd=1&ved=0ahUKEwihsanj-vPUAhWDXhQKHdUcC8AQFggrMAA&url=http%3A%2F%2Fwww.hexagonmi.com%2F~%2Fmedia%2FHexagon%2520MI%2520Legacy%2Fm1%2Fmetrology%2Fgeneral%2Fwhite-tech-paper%2FLeica%2520Absolute%2520Interferometer_white%2520paper_en.ashx&usg=AFQjCNE1v4rh9xtmLvH9BePskNh3PgrpNA (accessed on 17 April 2017).
124. Cabral, A.; Abreu, M. Absolute distance metrology for long distances with dual frequency sweeping interferometry. Proceedings of the XIX Imeko World Congress, Fundamental and Applied Metrology, Lisbon, Portugal, 6–11 September 2009.
125. Absolute Multiline Technology. Etalon AG. Available online: <http://www.etalon-ag.com/produkte/absolute-multiline-technologie/> (accessed on 3 March 2017).
126. Hughes, B.; Warden, M.S. Novel Coordinate Measurement System Based on Frequency Scanning Interferometry. *J. Coord. Metrol. Syst. Conf.* **2013**, *8*, 18–24.
127. Gomez-Acedo, E.; Olarra, A.; Zubieta, M.; Kortaberria, G.; Ariznabarreta, E.; de Lacalle, L.N. Method for measuring thermal distortion in large machine tools by means of laser multilateration. *Int. J. Adv. Manuf. Technol.* **2015**, *80*, 523–534. [[CrossRef](#)]
128. Ibaraki, S.; Blaser, P.; Shimoike, M.; Takayama, N.; Nakaminami, M.; Ido, Y. Measurement of thermal influence on a two-dimensional motion trajectory using a tracking interferometer. *CIRP Ann. Manuf. Technol.* **2016**, *65*, 483–486. [[CrossRef](#)]
129. Berger, D.; Brabandt, D.; Lanza, G. Conception of a mobile climate simulation chamber for the investigation of the influences of harsh shop floor conditions on in-process measurement systems in machine tools. *Meas. J. Int. Meas. Confed.* **2015**, *74*, 233–237. [[CrossRef](#)]
130. OMP400 Optical Machine Probe systems. Renishaw. Available online: http://www.google.es/url?sa=t&rct=j&q=&esrc=s&source=web&cd=2&ved=0ahUKEwjQzofc_vPUAhUFRhQKHec8AsoQFgg1MAE&url=http%3A%2F%2Fresources.renishaw.com%2Fen%2Fdownload%2Finstallation-guide-omp400--47616&usg=AFQjCNH8VtRcINKwlpWnhGQu8NZNWn0HRA (accessed on 23 April 2017).
131. Weckenmann, A. Comparability of tactile and optical form measuring techniques with resolution in the nanometre range. In Proceedings of the X. International Colloquium on Surfaces, Chemnitz, Germany, 31 January–2 February 2000; pp. 50–62.
132. Yang, Q.; Butler, C. A 3-D noncontact trigger probe for coordinate measuring machines. *Meas. J. Int. Meas. Confed.* **1996**, *17*, 39–44. [[CrossRef](#)]

133. Lukacs, G.; Lockhart, J.; Facello, M. Non-contact Whole-Part Inspection. Available online: https://www.cmssc.org/stuff/contentmgr/files/0/2bdcf766d9d5daf6e892c46153c591d3/misc/cmssc2011_thur_gh_0830_lockhart_paper.pdf (accessed on 23 April 2017).
134. Marsh, B. An Investigation of Diameter Measurement Repeatability Using A Coordinate Measuring Machine And A Multi-Baseline Repeatability Assessment Methodology. Ph.D. Thesis, University of Northern Iowa, Cedar Falls, IA, USA, 1996.
135. Dove, J. Probe qualification and precision coordinate metrology. *Manuf. Eng.* **2000**, *125*, 18.
136. *Measurement on CMMs*; White paper H-1000-3218-01; Renishaw: Wotton-under-Edge, UK, 2005.
137. Imkamp, D.; Schepperle, K. The Application Determines the Sensor: VAST Scanning Probe Systems. *Innov. Spec. Metrol.* **2006**, *8*, 30–33.
138. Gage R&R Studies on CMM Accuracy. Hexagon Metrology. Available online: http://pcdmiswiki.org/images/0/00/GRR_Studies_on_CMM_Accuracy_Hex.pdf (accessed on 3 March 2017).
139. Ali, S.H.R. Probing System Characteristics in Coordinate Metrology. *Meas. Sci. Rev.* **2010**, *10*, 120–129. [CrossRef]
140. Berisso, K.; Ollison, T. Coordinate Measuring Machine Variations for Selected Probe Head Configurations. *J. Ind. Technol.* **2010**, *26*. Available online: <http://c.ymcdn.com/sites/www.atmae.org/resource/resmgr/articles/berisso010510.pdf> (accessed on 11 July 2017).
141. *Probing Systems for CNC Machine Tools*; Renishaw: Wotton-under-Edge, UK, 2005.
142. Karuc, E. Design of a Touch Trigger Probe for a Coordinate Measuring Machine. Available online: <https://etd.lib.metu.edu.tr/upload/12609112/index.pdf> (accessed on 1 April 2017).
143. *SPRINT High-Speed Scanning System*; White paper: H-5465-8399-03; Renishaw: Wotton-under-Edge, UK, 2014.
144. Digilog Touch Probes. Novotest. Available online: <http://www.blum-novotest.com/en/products/measuring-components/digilog-touch-probes/tc63-tc64-digilog.html> (accessed on 13 March 2017).
145. Weckenmann, A.; Kampa, H. Koordinaten messgeraete, VDI-Z. Available online: <https://de.wikipedia.org/wiki/Koordinatenmesstechnik> (accessed on 26 February 2017).
146. Weckenmann, A.; Krämer, P. Trends in der Koordinatenmesstechnik Multisensorik. Available online: http://www.saq.ch/fileadmin/user_upload/mq/downloads/mq_2012_01_weckenmann.pdf (accessed on 21 April 2017).
147. Aston, R.; Davis, J.; Stout, K. A probing question: A customer's investigation into the directional variability of a coordinate measuring machine touch trigger probe. *Int. J. Mach. Tools Manuf.* **1998**, *38*, 15–27. [CrossRef]
148. Chan, F.M.M.; Davis, E.J.; King, T.G.; Stout, K.J. Some performance characteristics of a multi-axis touch trigger probe. *Meas. Sci. Technol.* **1997**, *8*, 837. [CrossRef]
149. Dobosz, M.; Woźniak, A. Metrological feasibilities of CMM touch trigger probes. *Measurement* **2003**, *34*, 287–299. [CrossRef]
150. Shen, Y.-L.; Zhang, X. Pretravel compensation for vertically oriented touch-trigger probes with straight styli. *Int. J. Mach. Tools Manuf.* **1997**, *37*, 249–262. [CrossRef]
151. Kishinami, T.; Nakamura, H.; Saito, K. Three Dimensional Curved Surfaces measurement using Newly Developed Three Dimensional Tactile Sensing Probe. In Proceedings of the International Symposium on Metrology for Quality Control in Production (ISMQC), Tokyo, Japan, 1984; pp. 288–293.
152. Moons, S.; Shen, Y.-L. Errors in probe offset Vectors of multiple orientations in CMM measurements. *ASPE Proc.* **1998**, *18*, 512–515.
153. Ogura, I.; Okazaki, Y. A Study for Development of Small-CMM Probe detecting Contact Angle. *Proc. ASPE Summer Top. Meet.* **2003**, 74–77.
154. Yang, Q.; Butler, C.; Baird, P. Error compensation of touch trigger probes. *Meas. J. Int. Meas. Confed.* **1996**, *18*, 47–57. [CrossRef]
155. Li, Y.F.; Liu, Z.G. Method for determining the probing points for efficient measurement and reconstruction of freeform surfaces. *Meas. Sci. Technol.* **2003**, *14*, 1280–1288. [CrossRef]
156. Koordinatenmesstechnik. Available online: http://www.google.es/url?sa=t&rct=j&q=&esrc=s&source=web&cd=39&ved=0ahUKEwjzXZzJzPbUAhVMPBQKHRZ-A844HhAWCEYwCA&url=http%3A%2F%2Fapi.vlb.de%2Fapi%2Fv1%2Fasset%2Fmimo%2Ffile%2F7491cffd-5777-4e4c-9c0e-9d269cbc33c1%3Faccess_token%3De047cd7a-ea60-44d5-adc2-59fdaa680c67&usq=AFQjCNHkVQl3FKMBBb5LLx2lwqYBr7wCfA (accessed on 20 March 2017).

157. Uhlmann, E.; Förster, R.; Laufer, J.; Sroka, F. Three-dimensional roughness values for the functional characterization of ceramic surfaces. *X Int. Colloq. Surf.* **2000**, 265–276.
158. Lonardo, P.M.; Lucca, D.A.; De Chiffre, L. Emerging Trends in Surface Metrology. *CIRP Ann. Manuf. Technol.* **2002**, 51, 701–723. [CrossRef]
159. Puttock, M.J.; Thwaite, E.G. Elastic Compression of Spheres and Cylinders at Point and Line Contact. *Natl. Stand. Lab. Tech. Pap.* **1969**, 25, 64.
160. Uhlmann, E.; Oberschmidt, D.; Kunath-fandrei, G. 3D-Analysis of Microstructures with Confocal Laser Scanning Microscopy. Available online: http://aspe.pointinspace.com/publications/Winter_2003/03W%20Extended%20Abstracts/uhlmann.PDF (accessed on 16 February 2017).
161. Zahwi, S.; Mekawi, A.M. Some effects of stylus force on scratching surfaces. *Int. J. Mach. Tools Manuf.* **2001**, 41, 2011–2015. [CrossRef]
162. Edgeworth, R.; Wilhelm, R.G. Uncertainty Management for CMM Probe Sampling of Complex Surfaces. *ASME Manuf. Sci. Eng.* **1996**, 4, 511–518.
163. Aoyama, H.; Kawai, M.; Kishinami, T. A New Method for Detecting the Contact Point between a Touch Probe and a Surface. *CIRP Ann. Manuf. Technol.* **1989**, 38, 7–10. [CrossRef]
164. *Test Code for Machine Tools—Part 10: Determination of the Measuring Performance of Probing Systems of Numerically Controlled Machine Tools*, 1st ed.; ISO 230-10:2016; International Organization for Standardization: Geneva, Switzerland, 2016.
165. Marshall, S.; Gilby, J. New Opportunities in Non-Contact 3D Measurement. *Natl. Meas. Conf.* 2001. Available online: <https://pdfs.semanticscholar.org/fd41/1aa6fdf4dbb324db62b6c66aec61ffb16639.pdf> (accessed on 11 July 2017).
166. Keferstein, C.; Züst, R. Minimizing technical and financial risk when integrating and applying optical sensors for in-process measurement. *Int. Intell. Manuf. Syst. Forum* **2004**, 17. Available online: http://bscw.ntb.ch/pub/bscw.cgi/d8668/OSIS_Publication_IMS_Forum_2004.pdf (accessed on 11 July 2017).
167. Karadayi, R. Blue Light Laser Sensor Integration and Point Cloud Metrology. Available online: <https://www.qualitydigest.com/inside/cm-sc-article/081816-blue-light-laser-sensor-integration-and-point-cloud-metrology.html#> (accessed on 2 February 2017).
168. Paulo de Moraes, J.; Peterek, M. Integration of a Laser Scanner into a Machine Tool for an in-Process 3D Measurement. Master's Thesis, Santa Catarina Federal University, Santa Catarina, Mexico, 2012.
169. Streppel, A.H.; Lutters, D.; ten Brinke, E.; Pijlman, H.; Kals, H.J. Selective measuring of freeform surfaces for quality control and selective maintenance of bending tools. *J. Mater. Process. Technol.* **2001**, 115, 147–152.
170. Savio, E.; Chiffre, L. De; Schmitt, R. Metrology of freeform shaped parts. *CIRP Ann. Manuf. Technol.* **2007**, 56, 810–835. [CrossRef]
171. Brinksmeier, E.; Preuss, W. Diamond Machining of the 3 m Reflector of the KOSMA Submillimeter Telescope by a Single-Point Fly-Cutting Process. Available online: <https://www.tib.eu/en/search/id/BLCP%3ACN019396568/Diamond-Machining-of-the-3m-Reflector-of-the-KOSMA/> (accessed on 23 March 2017).
172. Brinksmeier, E.; Riemer, E.; Glabe, O. Fabrication of Complex Optical Elements. Available online: https://mlecture.uni-bremen.de/ml/index.php?option=com_content&view=article&id=172&template=ml2 (accessed on 7 April 2017).
173. Katahira, K.; Ohmori, H.; Yoshida, K.; Kasuga, H.; Hirai, S. Elid Grinding Effects on Fabrication of Advanced Ceramics Components Riken. Available online: http://aspe.net/publications/Annual_2009/POSTERII/01GRIND/2941.PDF (accessed on 3 March 2017).
174. Klocke, F.; Dambon, O. Precision Machining of Glass for Optical Applications. In Proceedings of the International Workshop on Extreme Optics and Sensors, Tokyo, Japan, 14–17 January 2003; pp. 185–193.
175. Savio, E.; De Chiffre, L. Inspection of free form functional surfaces on fan blades. In Proceedings of the PRIME 2001 International Conference, Sestri Levante, Italy, 20–22 June 2001.
176. Beraldin, J.-A.; Gaiani, M. Evaluating the Performance of Close-Range 3D Active Vision Systems for Industrial Design Applications. *Videometrics VIII Int. SPIE Electron. Imaging* **2005**, 5665, 67–77.
177. Carmignato, S. Traceability of Coordinate Measurements on Complex Surfaces. Ph.D. Thesis, Università di Padova, Dimeg, Italy, 2005.

178. Carmignato, S.; Neuschaefer-Rube, U.; Schwenke, H.; Wendt, K. Tests and artefacts for determining the structural resolution of optical distance sensors for coordinate measurement. In Proceedings of the 6th International Conference European Society for Precision Engineering and Nanotechnology, Baden bei Wien, Austria, 28 May–1 June 2006.
179. Sansoni, G.; Carmignato, S.; Savio, E. Validation of the measurement performance of a three-dimensional vision sensor by means of a coordinate measuring machine. *Conf. Rec. IEEE Instrum. Meas. Technol. Conf.* **2004**, *1*, 773–778.
180. Bartscher, M.; Hilpert, U.; Neuschaefer-Rube, U. Industrielle Computertomographie auf dem Weg zur Koordinatenmesstechnik. *PTB Meet.* **2007**, *117*, 397.
181. Bartscher, M.; Neukamm, M.; Hilpert, U.; Neuschaefer-Rube, U.; Härtig, F.; Kniel, K.; Ehrig, K.; Staude, A.; Goebbels, J. Achieving Traceability of Industrial Computed Tomography. *Key Eng. Mater.* **2010**, *437*, 79–83. [[CrossRef](#)]
182. Sonka, M.; Hlavac, V.; Boyle, R. *Image Processing, Analysis, and Machine Vision*; Springer: Berlin, Germany, 1999.
183. Chen, X.; Golovinskiy, A.; Funkhouser, T. Benchmark for 3D Mesh Segmentation. In Proceedings of the Siggraph, New Orleans, LA, USA, 3 August 2009.
184. Mian, N.S.; Fletcher, S.; Longstaff, A.P.; Myers, A. Efficient estimation by FEA of machine tool distortion due to environmental temperature perturbations. *Precis. Eng.* **2013**, *37*, 372–379. [[CrossRef](#)]
185. Maier, T.; Zaeh, M.F. Modeling of the thermomechanical process effects on machine tool structures. *Procedia CIRP* **2012**, *4*, 73–78. [[CrossRef](#)]
186. Klocke, F.; Lung, D.; Puls, H. FEM-modelling of the thermal workpiece deformation in dry turning. *Procedia CIRP* **2013**, *8*, 240–245. [[CrossRef](#)]
187. Muelaner, J.E. Coping with Thermal Expansion in Large Volume. University of Bath. Available online: <http://projects.npl.co.uk/luminar/publications/luminar-gpg-thermal-expansion-lvm.pdf> (accessed on 3 March 2017).
188. Adams, V.; Askenazi, A. *Building Better Products with Finite Element Analysis*, 1st ed.; OnWord Press: Singapore, 1999.
189. Finite Element Analysis: Theory and Application with ANSYS. Moavani. Available online: <http://ftp.demec.ufpr.br/disciplinas/TM310/livro/Finite%20Element%20Analysis,%20Theory%20and%20application%20with%20ANSYS,%20.pdf> (accessed on 21 April 2017).
190. Nakasone, Y. *Engineering Analysis with ANSYS Software*; Butterworth-Heinemann: Oxford, UK, 2006.
191. Makino Vertical Machining Center-ps-Series-vmc. Available online: [https://www.makino.com/vertical-machining-centers/ps-series-vmc/ps-brochure-\(electronic\).pdf](https://www.makino.com/vertical-machining-centers/ps-series-vmc/ps-brochure-(electronic).pdf) (accessed on 29 April 2017).
192. KAIROS Machine Tool. ZAYER. Available online: <http://www.zayer.com/en/product/movingcolumn/kairos/25> (accessed on 25 April 2017).
193. Kortaberria, G. Characterization of Large Machine Tool Volumetric Behaviour in Workshop. Available online: https://www.ptb.de/emrp/fileadmin/documents/tim/tim-sharepoint/Meetings/2016-05-18%20Final%20Workshop/Presentations/11_TIM_Workshop_Kortaberria_IK4-TEKNIKER.pdf (accessed on 23 February 2017).
194. Wennemer, M. A Case Study on a Very Large Machine Tool: Systematic Deviations and Thermo-Elastic Deformations. Available online: http://downloads.etalon-ag.com/Seminar%20Flyer_en%20Druck.pdf (accessed on 5 February 2017).
195. *Good Practice Guide for Assessing the Fitness for Purpose for Dimensional Measurements on Machine Tool*; PTB: Braunschweig, Germany, 2014.
196. Metrology Solutions for Productive Process Control. Renishaw. Available online: <http://resources.renishaw.com/en/details/brochure-metrology-solutions-for-productive-process-control--47618> (accessed on 23 June 2017).



**Traceability of on-machine tool measurement: Uncertainty budget
assessment on shop floor conditions**



Traceability of on-machine tool measurement: Uncertainty budget assessment on shop floor conditions



Unai Mutilba^{a,*}, Alejandro Sandá^b, Ibon Vega^b, Eneko Gomez-Acedo^a, Ion Bengoetxea^b, Jose A. Yagüe Fabra^c

^a Department of Mechanical Engineering, IK4-Tekniker, Eibar 20600, Spain

^b Department of Production Engineering, IK4-Tekniker, Eibar 20600, Spain

^c I3A, Universidad de Zaragoza, C/María de Luna 3, Zaragoza 50018, Spain

ARTICLE INFO

Article history:

Received 9 July 2018

Received in revised form 12 November 2018

Accepted 16 November 2018

Available online 17 November 2018

Keywords:

Error budget

On-machine tool measurement

Traceability

Uncertainty

ABSTRACT

Almost every new machine tool is equipped with a probing system nowadays, which means that machining and measuring processes could take place on the same machine tool. Thus, the integration of a traceable measurement process into the machine tool is currently one of the main research objectives of production engineering. It provides the traceability of the quality inspection on the machine tool, during or after machining process, which allows the reduction of manufacturing costs and offers high productivity and zero-defect manufacturing processes. Nevertheless, the traceability of a measurement process on a machine tool is not ensured yet and therefore, measurement results are not reliable enough yet for a self-adapting manufacturing process. On-machine tool measurement is affected by multiple uncertainty contributors related to shop floor conditions, such as, machine tool geometric error, temperature variation, probing system, vibrations, dirt, etc that are not fully understood yet, which leads to a lack of a metrological traceability chain, which in turn means a lack of reliability of the manufacturing process. The aim of this paper is to review a medium size on-machine tool measurement uncertainty assessment and give an overview about the significance of each uncertainty contributor on shop floor conditions. For that purpose, an experimental test according to ISO 15530-3:2011 standard is executed for a medium size prismatic component.

© 2018 Elsevier Ltd. All rights reserved.

1. Introduction

High value components, such as aerospace, automotive, nuclear power and science facilities components demand close measurements and fast feedback into their manufacturing processes [1]. Thus, on-machine tool (MT) measurement offers the possibility to flexible manufacturing processes for high quality products at low cost [2]. Particularly, for large scale manufacturing where manufactured parts have to be measured in-situ or in-process, the integration of the measurement process into the MT can improve the process efficiency by preventing the workpiece from being carried to a temperature controlled measuring room [1].

It means that machining and measuring processes could take place on the same MT. However, there are some key differences between a coordinate measuring machine (CMM) and a MT, mainly because a CMM is designed for a measurement purpose and a MT is focused on manufacturing production. The main problem of on-MT measurements is that the machining and measuring processes are

performed at the same machine and therefore some error sources cannot be distinguished if a calibration process is not performed before the measurement process [1].

Several research works have focused on the idea of converting a MT into a CMM. In 2013 Schmitt et al. presented a research work where a specific standard was manufactured and calibrated on a CMM for several on-machine tool measurement experimental tests. The research activities concentrate on different methods for a measurement uncertainty evaluation [3]. In 2015 Schmitt et al. also presented a research work where they tried to assess uncertainty for on-machine tool measurement according to the VDI 2617-11 standard. The work is focused on the hypothesis that temperature induced geometric errors are expected to be the main influence on the achievable measurement uncertainty of the complete measuring process [2]. Holub et al. present a capability assessment for on-machine tool measurement assisted by an external laser interferometer [4]. The EURAMET research project “Traceable In-process Metrology” (TIM) focused on the contribution to the development of appropriate standards and procedures which ensure traceable in-process dimensional measurements on machine tools [5].

* Corresponding author.

E-mail address: unai.mutilba@tekniker.es (U. Mutilba).

This paper presents an approach to understand major uncertainty contributors for on-machine tool measurement on shop-floor conditions. An experimental test is executed according to ISO 15530-3:2011 standard [6], where five workpiece replica material standards have been machined and measured on the same machine tool and afterwards calibrated on a CMM, where task-specific measurement uncertainties have been assessed. Additionally, the MT has been characterised to correlate the resulting uncertainty budget with the expected uncertainty error sources under shop floor conditions.

2. Measurement uncertainty assessment

Due to the similarity between a CMM and MT, some of the methods for a correct assessment of uncertainty in CMM are adopted for MT [1]. The general guide for a suitable evaluation of measurement data (GUM) is given by the ISO Guide 98-3: 2008, on the expression of uncertainty in measurement [7]. Three different approaches are considered for an uncertainty assessment on a MT:

- Substitution method, based on ISO 15530-3: The first approach as described in ISO 15530-3 [6] is a method of substitution that simplifies the uncertainty evaluation by means of similarity between the dimension and shape of the workpiece and one calibrated reference part. Moreover, the measurement procedure and environmental conditions shall be similar during evaluation of measurement uncertainty and actual measurement. Due to the similarity requirement between the machined workpiece and the calibrated standard, this approach is very arduous and expensive for large scale metrology. However, it is a reliable approach for serial production, usually for small and medium size components, because it is affordable to manufacture and calibrate a reference part for uncertainty assessment purposes.
- Numerical simulation, based on ISO 15530-4: The second approach based on ISO 15530-4 [8] is a method that is consistent with GUM to determine the task specific uncertainty of coordinate measurements. It is based on a numerical simulation of the measuring process allowed for uncertainty influences, where important influence quantities are considered. Nowadays, it is employed for CMM uncertainty assessment where all major uncertainty contributors are already characterised. Thus, Monte-carlo type of simulation can be applied for estimation of uncertainty in measurement [9].
- Uncertainty budget method, based on VDI 2617-11: The third approach is as stated in GUM and VDI 2617-11 [10]. In this case, uncertainty evaluation is done based on an uncertainty budget where the budget should comprise the uncertainty sources that affect the measurement process and the correlation between them.

For the presented research, the approach described in ISO 15530-3 has been applied because most of the uncertainty influences during the experimental tests are also present on a real on-machine tool measurement. Additionally, ISO 15530-4 and VDI 2617-11 approaches require understanding the significance of each uncertainty contributor, which is not guaranteed nowadays.

3. On-machine tool measurement uncertainty budget

There are four uncertainty contributors that comprise all the systematic and random errors that shall be considered on the uncertainty budget for on-machine tool measurement [6]:

- u_b standard uncertainty associated with the systematic error of the measurement process;
- u_p standard uncertainty associated with the measurement procedure;
- u_{cal} standard uncertainty associated with the uncertainty of the workpiece calibration.
- u_w standard uncertainty associated with material and manufacturing variations.

Thus, the expanded measurement uncertainty of the complete measurement process (U_{MP}) is assessed by $U_{MP} = 2 \times u_{MP}$ and the expanded measurement uncertainty of the measurement system (U_{MS}) is assessed by $U_{MS} = 2 \times u_{MS}$, for a coverage factor of $k = 2$, where u_{MP} and u_{MS} are given by the same formula where input information come from measurements executed right after the machining process and under no-load condition, respectively.

There are different approaches of assessing the uncertainty of the systematic error b . If the measurement result is not corrected by the systematic error, the error fully contributes to the uncertainty, so $u_b = b$. Thus:

$$u_{MP} = \sqrt{u_p^2 + u_{cal}^2 + b} \quad \text{and} \quad u_{MS} = \sqrt{u_p^2 + u_{cal}^2 + b} \quad (1)$$

Where, five different workpieces ($m = 5$) have been measured ten times ($n = 10$) on the MT directly after the production in the same clamping. The uncertainty u_p is given by the maximum standard deviation of every measurement. For a workpiece's feature that was measured n times (for the same workpiece) one gets the measurement results: mean value and the standard deviation:

$$\bar{y} = \frac{1}{n} \sum_{i=1}^n y_i; \quad s_y = \sqrt{\frac{1}{n-1} \sum_{i=1}^n (y_i - \bar{y})^2} \quad (2)$$

$$u_p = \max_{j=1..m} (s_{y_j}) \quad (3)$$

The calibration of the workpiece's features on a CMM gives the calibration result x_{cal} , with the corresponding expanded uncertainty U_{cal} , so the calibration uncertainty u_{cal} , for every measurement feature is given by: (for a coverage factor of $k = 2$)

$$u_{cal} = U_{cal}/2 \quad (4)$$

There are different approaches of assessing the uncertainty of the systematic error b . If the measurement result is not corrected by the systematic error, the error fully contributes to the expanded measurement uncertainty (U_{MP}). Therefore, the total systematic error for a measured feature is defined as the difference between the mean value of the measurement results on the machine tool and the calibration value:

$$b = \bar{y} - x_{cal} \quad (5)$$

As systematic error of the complete measurement process the mean value of the systematic errors of the individual measurements is taken:

$$\bar{b} = \frac{1}{m} \sum_{j=1}^m b_j \quad (6)$$

Variations of form errors and roughness due to the changing manufacturing process and material properties are considered within their required limits, so u_w contribution is considered as insignificant.

Different error sources that affect to these three major contributors are summarized in Table 1. Uncertainty error sources associated with the measurement procedure (u_p) are classified into two groups: no-load condition (u_{MS}) and right after the machining

Table 1
On-machine tool uncertainty error budget.

Error source	Major uncertainty contributor
Geometric error of the MT	u_b
Systematic error of the probing system	
Scale resolution of the MT	
Probe changing uncertainty	
Errors induced by the procedure (clamping, handling, etc.)	
Errors induced by measurement strategy	
Temperature of the MT Temperature of the workpiece	
Repeatability of the MT	u_p
Random errors of the probing system	
Error induced by dirt	
Geometric drift of the MT*	
Temperature gradients of the MT*	
Geometric drift of the workpiece*	
Temperature gradients of the workpiece*	
Calibration uncertainty of the workpiece	u_{cal}

*Do not affect to the no-load measurement condition (U_{MS}), but yes to the measurements executed right after the machining process (U_{MP}).

process (u_{MP}). Those error sources not affecting to the no-load measurement condition are marked with an asterisk (*) key [6].

For the on-MT experimental test, the aim is to quantify each major uncertainty contributor and identify main error sources on shop floor condition environment. It is expected that the geometric error of the MT could be the main error source for the systematic uncertainty (u_b) and therefore, a volumetric performance test is performed on the MT side. For the uncertainty associated with the measurement procedure (u_p), geometric drift of the MT and temperature variation on the measurement scenario could be main error sources. For the calibration uncertainty (u_{cal}), it depends on the accuracy of the employed CMM on the workpiece calibration.

4. Task specific uncertainty assessment for on-machine tool measurement

By assessing fitness-for-purpose for dimensional measurements of workpieces on-machine tools, it will be determined whether a machine tool is meeting accuracy specifications and is capable of manufacturing as well as inspecting features on a machined part with respect to the required accuracy. This ensures a reliable go or no-go decision based on the obtained measurement result and the achievable measurement uncertainty [11].

When assessing the fitness for purpose for tactile measurements on a MT by using artefacts, one can distinguish between using calibrated material standards, or using workpieces or workpiece replicas, which are produced and measured on the machine tool under investigation and calibrated afterwards, for instance, on a CMM. While the first approach is suitable for assessing the uncertainty budget of the measuring system (U_{MS}), the second approach is used for assessing the uncertainty budget of the entire measuring process including the manufacturing process (U_{MP}). A workpiece replica is a part that has been produced on the machine tool under investigation and allows similar measurement tasks as they are performed on the real workpiece [11].

The presented research work is focused on assessing the expanded measurement uncertainty of the complete measurement process (U_{MP}) because, according to ISO 14253-1 [12], the decision whether a workpiece feature meets its design criteria within the specified tolerance must be based on U_{MP} parameter.

5. Uncertainty budget assessment experimental exercise

5.1. Setup

Five workpiece replica material standards have been manufactured, followed by on-machine tool measurement in the same chucking using a RENISHAW OMP 400 tactile probe. Each workpiece has been measured ten times on the MT to distinguish between systematic and random errors and assess the uncertainty budget of the entire measuring process (U_{MP}). Additionally, one workpiece was measured ten times on the MT at 20 °C operating either under no-load or under quasi-static conditions to assess the uncertainty budget of the measuring system (U_{MS}). Fig. 1 shows on-machine tool manufacturing and measurement processes and Fig. 2 shows the workpiece calibration process.

By a subsequent calibration of these workpieces on a ZEISS UPMC CARAT 850 CMM, the calibration uncertainty for each measurement feature has been assessed by means of the virtual CMM concept [13,14].

5.2. Materials

A medium size MT has been selected to perform the experimental test. It is a KONDIA MAXIM machine tool with a cutting stroke of: X = 750 mm, Y = 1000 mm and Z = 500 mm. The computer numerical control (CNC) is a 16i type FANUC controller. A unique cutting tool has been employed to machine the “Test piece ISO 10791-7, M1-160” and the total time consumption for workpiece replica standard machining is approximately 2 h [15].

RENISHAW OMP 400 tactile probe is employed on the MT side to execute the on-machine tool measurement. The total time consumption for a unique measurement of every feature defined at Table 2 is 8 min, however, the measurement is repeated ten times, which means a total time consumption of 2 h per measured part. Power Inspect software has been employed for G-code generation and performance assessment of the on-machine tool measurement exercise.

The workpiece replica standard selected for the experimental uncertainty assessment exercise is defined at ISO 10791-7:2014 standard [15]. The selected standard test piece is referenced as “Test piece ISO 10791-7, M1-160”. A description of the measured and calibrated features, in addition to the specified tolerances of each workpiece replica standard, are defined in Table 2. Tolerances for diameters are not defined at ISO 10791-7:2014 standard, so a tolerance grade of H7 is employed according to ISO 286 [16]. Additionally, Fig. 3 depicts measured geometry on the workpiece replica standard.

5.3. Machine tool geometric error assessment

A geometric characterization of the machine tool under consideration has been performed under no-load condition to correlate the systematic uncertainty of on-machine tool measurement with the geometric error of the MT. Multilateration based approach [17–19] has been executed on the MT side to characterize the volumetric geometric error of the MT under investigation. The approach to map the geometric error of a machine is based on multiple measurement of displacement between reference points that are fixed to the base of the machine and a reflector which is attached to the machine head or spindle. The employed measurement equipment is a tracking interferometer, the so called Laser tracer NG [20], commercialised by Etalon AG. It has a spatial displacement measurement uncertainty of $U(k=2) = 0.2 \mu\text{m} + 0.3 \mu\text{m/m}$ [21]. Fig. 4 shows laser tracer NG measurement equipment arrangement on the KONDIA MAXIM machine tool table.



Fig. 1. Workpiece replica standard on-machine tool measurement with RENISHAW OMP 400 tactile probe.



Fig. 2. Workpiece replica standard CMM calibration.

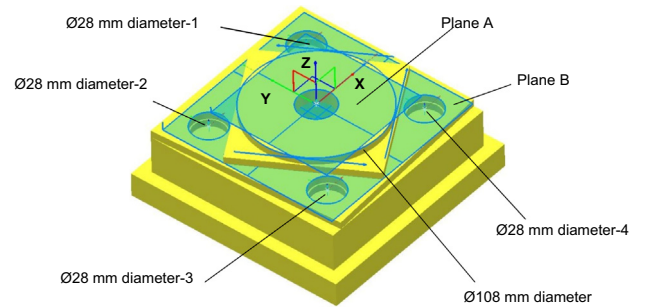


Fig. 3. Workpiece replica standard with measured geometry.

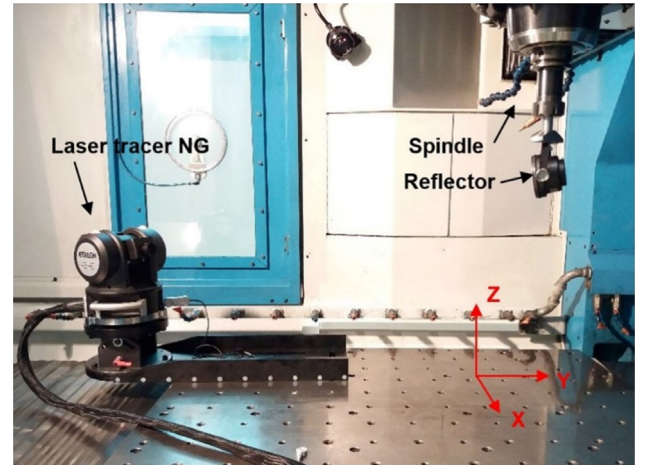


Fig. 4. Laser tracer NG on the KONDIS MAXIM machine tool.

Table 2
Measurement features and specified tolerances for the workpiece replica standard [15].

Feature	Nominal value [mm]	Tol [mm]
Flatness Plane A	0	0.020
Diameter Ø108 mm	108	0.035
Roundness Ø108 mm diameter	0	0.015
X position (diameter Ø108 mm)	52	0.035
Y position (diameter Ø108 mm)	52	0.035
Diameter Ø28-1 mm	28	0.021
X position (diameter Ø28-1 mm)	52	0.035
Y position (diameter Ø28-1 mm)	52	0.035
Diameter Ø28-2 mm	28	0.021
X position (diameter Ø28-2 mm)	52	0.035
Y position (diameter Ø28-2 mm)	52	0.035
Diameter Ø28-3 mm	28	0.021
X position (diameter Ø28-3 mm)	52	0.035
Y position (diameter Ø28-3 mm)	52	0.035
Diameter Ø28-4 mm	28	0.021
X position (diameter Ø28-4 mm)	52	0.035
Y position (diameter Ø28-4 mm)	52	0.035

Table 3 shows geometric error results and expanded measurement uncertainty for each component of error, for a coverage factor of $k = 2$. The simple ETALON kinematic model has been employed, comprised by 17 components of error. (Component of error notation according to ISO 230).

Considering the selected workpiece replica standard and its setup on the MT, the components of error of interest are positioning error in X and Y axis (EXX and EYY) and perpendicularity between X and Y (COY). Positioning errors are within $10 \mu\text{m}$ and perpendicularity is better than $1 \mu\text{radian}$. These results will be

Table 3
Volumetric error mapping of the employed machine tool.

Group	Component of error	Deviation (range)	U _{max} (95%)
Position	E _{XX}	6.4 μm	0.2 μm
	E _{YY}	8.4 μm	0.2 μm
	E _{ZZ}	4.2 μm	0.6 μm
Straightness	E _{YX}	1.9 μm	0.1 μm
	E _{ZX}	1.7 μm	0.3 μm
	E _{XY}	1.3 μm	0.2 μm
	E _{ZY}	2.7 μm	0.5 μm
	E _{XZ}	1.8 μm	0.1 μm
	E _{YZ}	3.2 μm	0.1 μm
Pitch/Yaw/Roll	E _{CX}	3.4 μrad	0.5 μrad
	E _{BX}	6.5 μrad	0.8 μrad
	E _{AY}	10.5 μrad	0.5 μrad
	E _{BY}	8.0 μrad	0.8 μrad
	E _{CY}	6.9 μrad	0.3 μrad
Squareness	C _{OY}	0.4 μrad	0.2 μrad
	B _{OZ}	−57.7 μrad	0.3 μrad
	A _{OZ}	−11.3 μrad	0.4 μrad

compared with the systematic error of the on-machine tool measurement to find a correlation.

5.4. Machine tool drift error assessment

Random errors on-MT measurement are expected to be caused by dynamically changing temperature conditions, vibrations, dirt, high probing forces, etc. However, it is expected that temperature variation could be one major random error source. This is why temperature induced geometric drift error has also been measured on the MT side. It is not only to understand the permanent geometric error of MT, but how it changes with temperature variation and try to correlate it with the random error of on-MT measurement results.

For that purpose, three inductive sensors (eddy current) have been arranged orthogonally on the machine tool spindle and a 2D ball plate has been measured on a unique sphere. Thus, high precision measurement of the sphere centre has been performed during the cooling cycle of the measurement scenario. The test has been performed under no-load condition and right after the machining cycle of an additional workpiece replica standard. Fig. 5 shows inductive sensors based geometric drift measurement, right after machining of the workpiece replica standard.

The geometric drift measurement test has been performed for 2.5 h, similar time consumption to the complete measurement process of a workpiece replica standard. Fig. 6 shows the temperature variation either on the MT side or the workpiece side during the drift assessment test.

Additionally, temperature variation has been monitored during the experimental exercise. Fig. 7 shows how temperature increases either on the MT or the workpiece during the machining process. Workpiece temperature increases to 22.5 °C (in average) right after the machining process and it stabilizes to 19.5 °C (in average) after two hours of on-machine tool measurement acquisition time. Additionally, it also illustrates the moment when every workpiece replica standard has been measured.

5.5. Experimental uncertainty budget assessment

The uncertainty budget for the experimental test is presented below. The three major uncertainty contributors are characterized on shop floor conditions.

5.5.1. Systematic error uncertainty (u_b)

The systematic error (b) of the experimental measurement process is shown in Fig. 8, according to Eqs. (5) and (6). It depicts the mean systematic error of each measured feature and the dispersion of each measured feature.

Results show that the rather big systematic errors occur on diameter measurement, while the mean value for the rest of features is within 0.01 mm. The probing system calibration has been only performed before the first workpiece replica standard measurement, so the systematic error on diameter measurement maintains within 0.01 mm just for the first workpiece replica standard. For the rest of the workpiece replica standards diameter measurement values show a dispersion within 0.045 mm, which is affected by the insufficient calibration of the probing system on the machine tool prior to each measurement process.

On the presented approach, the substitution method is applied for diameter measurement result correction by the systematic error according to Eq. (6). This is an exceptional substitution exercise to correct the insufficient calibration of the probing system on the MT. Workpiece replica standard n°1 measurement values are not introduced into the substitution exercise because probing system calibration has been executed prior to this measurement on the MT.

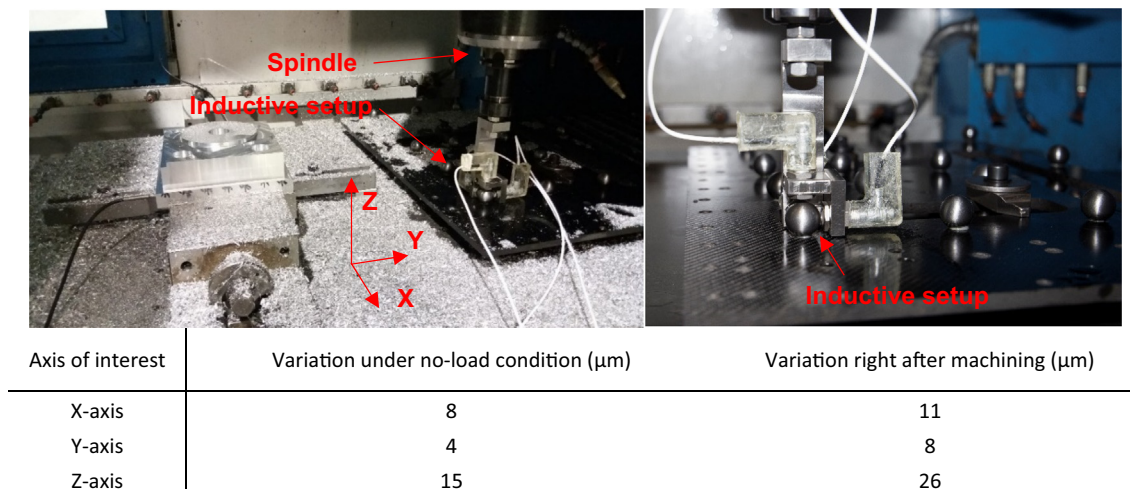


Fig. 5. Temperature induced geometric drift assessment with inductive sensors on the MT side.

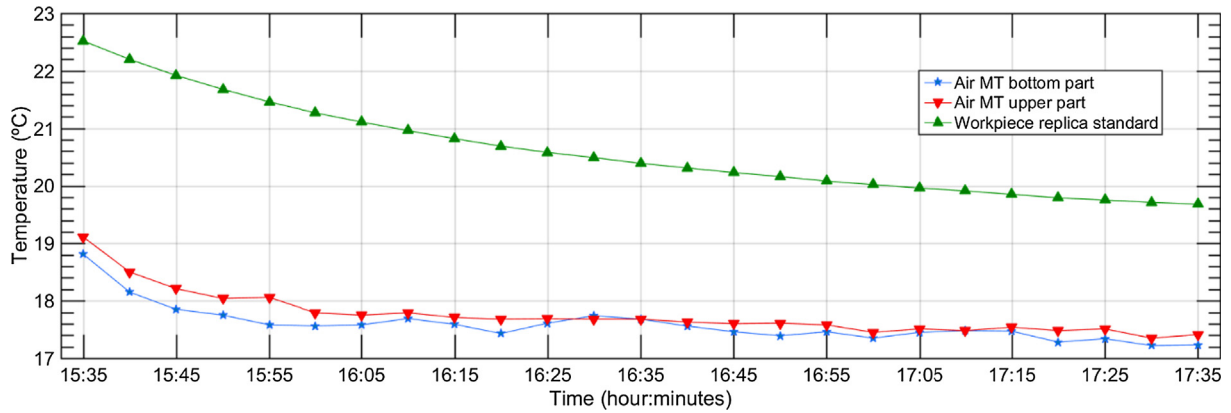


Fig. 6. Temperature variation on the MT side and workpiece side right after the machining process.

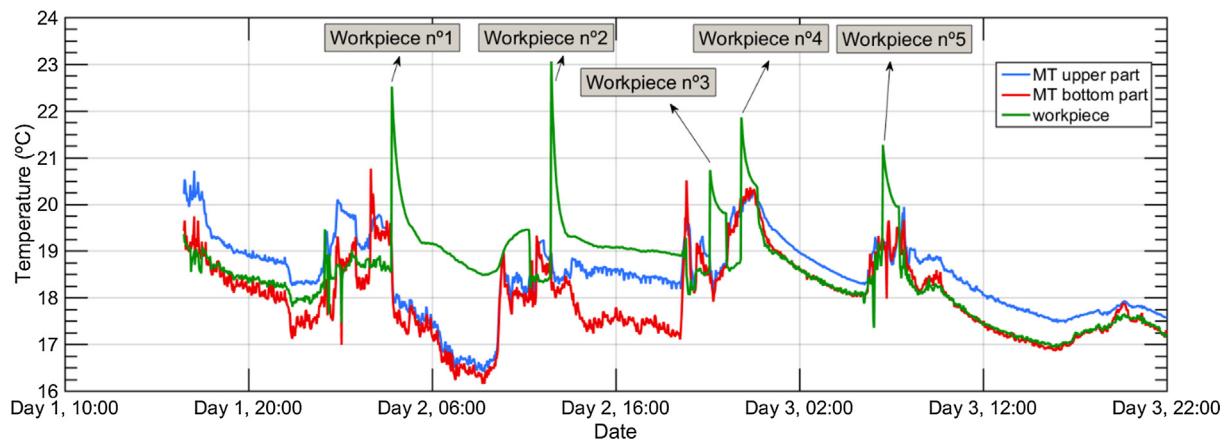


Fig. 7. Temperature variation during the experimental test.

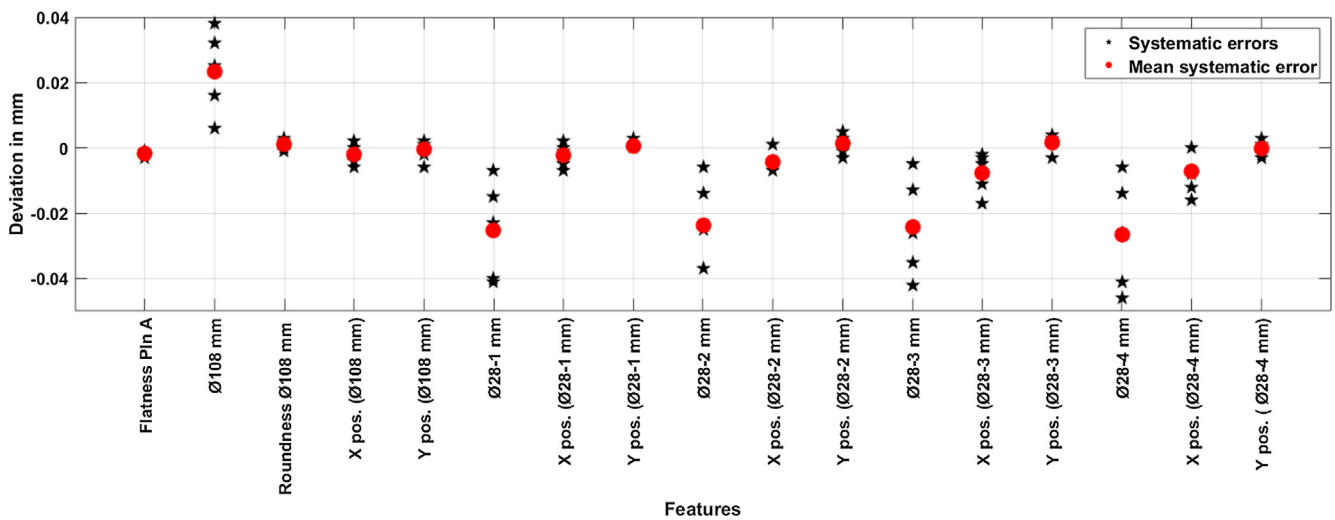


Fig. 8. Systematic error (b) of the measurement process before correction.

Fig. 9 shows the corrected systematic error (u_b) of the measurement process. Systematic error results after correction show that every mean systematic error is within $10 \mu\text{m}$. Additionally, it also highlights the significance of a correct probing system calibration before workpiece replica standard measurement.

Corrected systematic error (u_b) correlates with the geometric error of the MT, particularly with positioning errors in X and Y axes, and squareness between them. Therefore, it seems that geometric error of the MT is the main error source affecting to the u_b major uncertainty contributor.

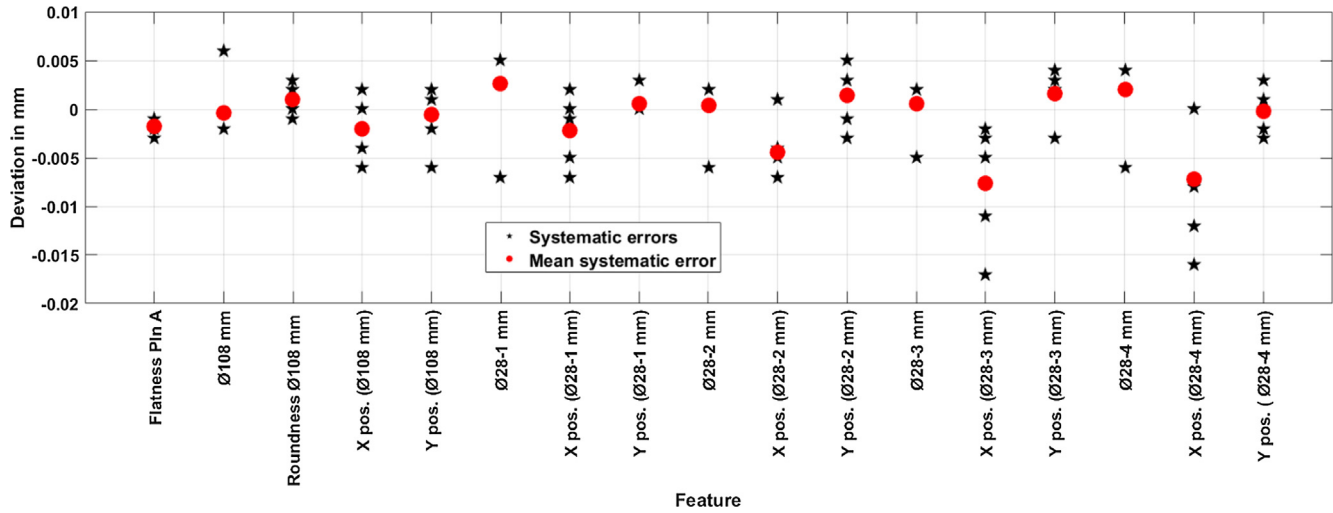


Fig. 9. Corrected systematic error (u_b) of the measurement process.

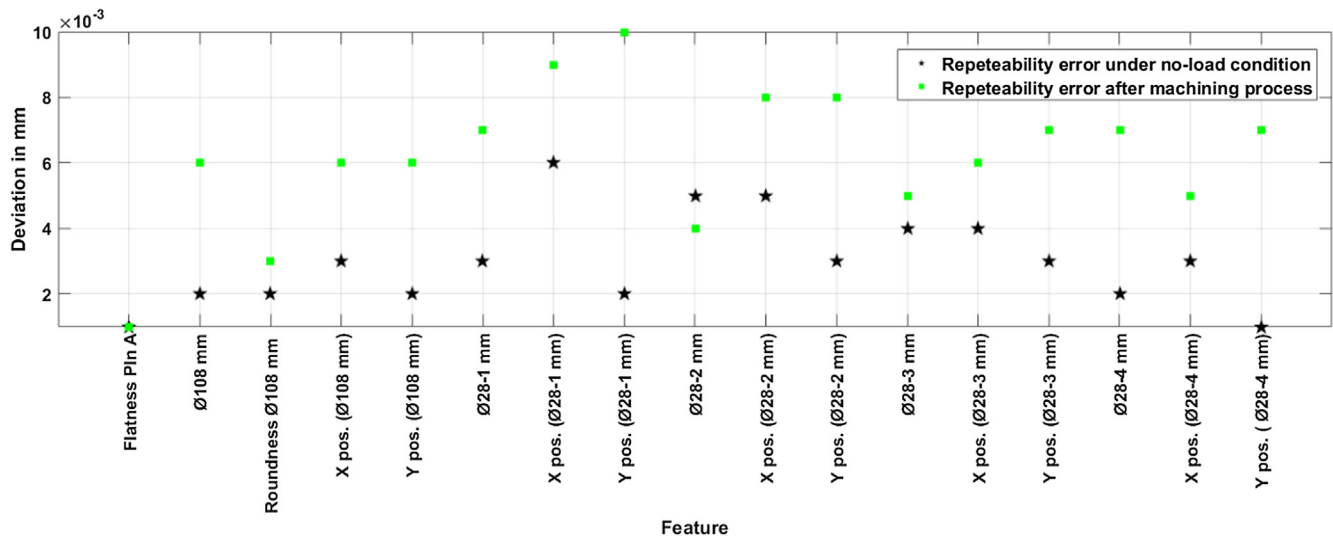


Fig. 10. Measurement procedure uncertainty (u_p) results for the complete measurement process.

5.5.2. Measurement procedure uncertainty (u_p)

For the measurement procedure uncertainty (u_p) contributor, it is of utmost importance to understand the effect of temperature gradients on the results. Thus, the experimental test suggests on-MT measurements right after the machining process when measurement scenario temperature behaviour is as depicted in Fig. 6 and measurements under no-load condition when temperature on the MT side and workpiece side is constant at 20 °C. Fig. 10 shows the measurement procedure uncertainty (u_p) of each measurement feature either for measurements executed right after the machining process or measurements executed under no load conditions. Results are calculated according to Eq. (3).

Measurement procedure uncertainty results show differences between the measurement executed under no-load condition and the measurements executed right after the machining process. Every result shows a repeatability within 6 μm for the no-load condition, while the maximum repeatability values for the measurements right after the machining process are within 10 μm .

Form error feature measurement (flatness and roundness) show better measurement procedure uncertainty results than scale related feature measurement (diameter and positioning values),

because these features are more sensitive to the measurement scenario temperature variation.

5.5.3. Calibration uncertainty (u_{cal})

Fig. 11 shows the calibration uncertainty (u_{cal}) obtained according to Eq. (4). Maximum uncertainty value is up to 2 μm for the CMM positioning error in Y direction.

5.5.4. Uncertainty budget

Fig. 11 shows the uncertainty budget of the task-specific uncertainty assessment on shop floor conditions. For the systematic error (u_b), the mean value of the systematic errors of the individual measurements is taken, according to Eqs. (5) and (6). For the measurement procedure uncertainty (u_p) contributor, the maximum standard deviation of the measurements is considered, according to Eq. (3). Calibration uncertainty (u_{cal}) is obtained from Eq. (4). It shall be remarked that for the measurement procedure uncertainty (u_p) contributor, repeatability results are shown either for measurements executed right after the machining process or measurements executed under no load conditions.

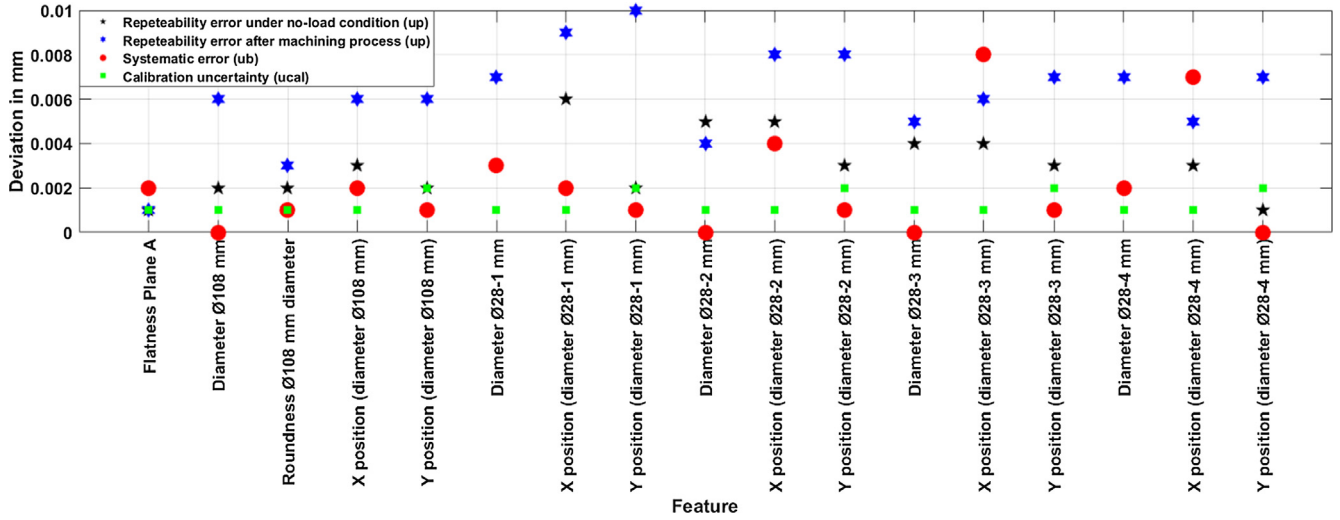


Fig. 11. Uncertainty contributors on shop floor conditions.

Table 4
Expanded measurement uncertainties (U_{MP} and U_{MS} , with $k = 2$) of the experimental test (in μm).

Feature	u_b	$u_{p \text{ no-load}}$	u_p	u_{cal}	u_{MS}	U_{MS}	u_{MP}	U_{MP}
Flatness Plan A	1.7	0.7	0.7	0.7	1.9	3.9	1.9	3.9
Ø108 mm	0.2	2.2	5.5	1	2.5	4.9	5.6	11.3
Roundness Ø108 mm	1.1	1.9	3.0	0.7	2.3	4.7	3.2	6.5
X position (Ø108 mm)	2.1	3.3	5.7	1	4.0	8.0	6.2	12.3
Y position (Ø108 mm)	0.7	2.1	5.7	1.7	2.8	5.6	6.0	12.0
Ø28-1 mm	2.6	3.1	7.1	1	4.2	8.4	7.6	15.3
X position (Ø28-1 mm)	2.2	6.1	9.4	1.2	6.6	13.2	9.7	19.4
Y position (Ø28-1 mm)	0.5	2.1	9.5	1.9	2.9	5.7	9.7	19.5
Ø28-2 mm	0.3	5.4	3.9	1	5.5	10.9	4.1	8.1
X position (Ø28-2 mm)	4.4	5.5	8.3	1.2	7.2	14.3	9.5	18.9
Y position (Ø28-2 mm)	1.5	2.7	8.3	1.9	3.6	7.3	8.6	17.2
Ø28-3 mm	0.5	4.0	5.2	1.1	4.2	8.4	5.4	10.7
X position (Ø28-3 mm)	7.6	4.5	5.5	1.2	8.9	17.9	9.5	19.0
Y position (Ø28-3 mm)	1.4	2.6	6.9	1.8	3.4	6.9	7.3	14.6
Ø28-4 mm	1.7	2.1	6.7	1.1	2.9	5.9	7.0	14.1
X position (Ø28-4 mm)	7.2	2.7	5.2	1.4	7.8	15.6	9.0	18.0
Y position (Ø28-4 mm)	0.1	1.3	6.5	1.7	2.2	4.3	6.8	13.5

To sum up, U_{MP} and U_{MS} values are shown in Table 4. Results are obtained by $U_{MP} = 2 \times u_{MP}$ and $U_{MS} = 2 \times u_{MS}$, for a coverage factor of $k = 2$, where u_{MP} and u_{MS} are given by Eq. (1).

Measurement procedure uncertainty (u_p) contributor is the main contributor to the on-machine tool measurement uncertainty budget on shop floor condition. Fig. 11 and Table 4 show that measurement procedure uncertainty is larger on the measurements executed right after the machining process, mainly affected by the dynamically changing temperature conditions of the measurement scenario. For the no-load measurement condition, measurement procedure uncertainty (u_p) is also few microns larger than systematic error (u_b) uncertainty, which maintains within 8 μm for every measured feature.

6. Methodology for traceable on machine tool measurements according to ISO 15530-3

The main problem of on-MT measurements is that the machining and measuring processes are performed at the same machine and therefore some error sources cannot be distinguished if a calibration process is not performed before the measurement process [1]. The ISO 15530-3 approach relies on a calibrated workpiece to assess traceability according to a previous CMM calibration of the calibrated workpiece. It is a reliable approach for serial production, usually for small and medium size components, where it is afford-

able to manufacture and calibrate a reference part for uncertainty assessment purposes.

To sum up, a methodology for traceable on-machine tool measurements according to ISO 15530-3 is suggested next:

- Run a geometric characterization of the MT under consideration to understand how the geometry of the MT performs under no-load condition (this geometric characterization will correlate with the systematic error of the measurement process (u_b)).
- Establish interim checks on the MT side to validate that the geometry of the MT continues within the geometric boundary conditions to perform on-MT measurement. Diagonal displacement test defined in ISO 230-6 [22] could help to assess that the volumetric performance of the MT continues within specifications.
- Manufacture a unit of the workpiece to be measured afterwards on the MT.
- Set the probing system on the MT side and calibrate it (a new calibration process should be performed on the probing system side for every loading and unloading on the MT spindle).
- Perform continuous on-MT measurements for 24 h to understand how the ambient temperature variation and MT drift after machining process affect to the uncertainty of the measurement procedure (u_p). Results may show that “fast” and “slow” dimensional drifts occur on-MT measurements: “fast” dimensional

drift exists after workpiece machining process and “slow” dimensional drift exists due to ambient temperature variation on shop floor conditions.

- Calibrate the manufactured workpiece on a CMM. It may be desirable to assess calibration uncertainty for each measurement feature to be measured on-MT by means of the virtual CMM concept (u_{cal}).
- Perform workpiece measurement and assess uncertainty according to ISO 15530-3.
- Perform interim checks regularly on the MT side.

7. Conclusions

Reliable on-machine measurements are needed by industry for effective process control and quality assurance of manufactured parts. However, the traceability of the measurement process on a machine tool is not ensured yet because it is affected by multiple error sources associated with shop floor conditions. This research work has contributed to give an overview about the significance of each uncertainty contributor of on-machine tool measurement on shop floor conditions. For that purpose, an experimental test according to ISO 15530-3:2011 standard is executed for a medium size prismatic component.

Experimental test shows that measurement procedure uncertainty (u_p) is the main contributor to the on-machine tool measurement uncertainty budget on shop floor condition. Machine tool repeatability is the main error source for the measurement procedure uncertainty contributor since repeatability results under no-load condition show larger uncertainty values than u_b and u_{cal} contributors. Additionally, it shall be remarked that measurement procedure uncertainty is larger on the measurements executed right after the machining process, mainly affected by the dynamically changing temperature conditions of the measurement scenario, as predicted by Schmitt et al. [2]. Systematic error (u_b) contributor maintains within $4\ \mu\text{m}$ for every measured feature, except for those two features (X position in $\varnothing 28-3$ and $\varnothing 28-4$) that present a systematic error within $8\ \mu\text{m}$. Calibration uncertainty (u_{cal}) maximum value is within $2\ \mu\text{m}$, mainly affected by the CMM positioning error in Y direction.

Systematic error (u_b) correlates with the geometric error of the MT, particularly with positioning errors in X and Y axes, and squareness between them. Therefore, it seems that geometric error of the MT is the main error source affecting to the u_b major uncertainty contributor. Moreover, uncertainty related to the tactile probe could be close to the supplier specifications, within $1\ \mu\text{m}$. However, an insufficient calibration of the probing system can cause the systematic error to become the major uncertainty contributor of the uncertainty budget as shown in Fig. 8. Temperature related error sources represent a minor error source on the presented experimental exercise because measurements are executed on temperature values close to $20\ ^\circ\text{C}$ and the measured prismatic component is small. However, it could represent a major error source on a measurement scenario where large parts are measured on temperature values far to $20\ ^\circ\text{C}$.

Geometric drift assessment test with inductive sensors show larger drift values than the measurement procedure uncertainty (u_p) results obtained on the experimental test. It means that the whole measurement scenario on-machine tool measurement does change different to what measured with inductive sensors. Thus, the suggested drift assessment test doesn't depict the measurement procedure uncertainty (u_p) performance for the on-machine tool measurement.

To sum up, measurement procedure uncertainty (u_p) is the main contributor to the on-machine tool uncertainty budget

on-shop floor condition, followed by the systematic error (u_b) contributor. While the repeatability associated with measurement procedure uncertainty (u_p) is difficult to predict because it depends on variable error sources, the systematic error can be kept under control.

Future work should focus on a permanent calibration of the MT geometric error which would help to keep systematic error under control.

References

- [1] U. Mutilba, E. Gomez-Acedo, G. Kortaberria, A. Olarra, J.A. Yagüe-Fabra, Traceability of on-machine tool measurement: a review, MDPI Sensors 17 (2017) 40, <https://doi.org/10.3390/s17071605>.
- [2] R. Schmitt, M. Peterek, Traceable measurements on machine tools—Thermal influences on machine tool structure and measurement Uncertainty, Procedia CIRP. 33 (2015) 576–580, <https://doi.org/10.1016/j.procir.2015.06.087>.
- [3] R. Schmitt, M. Peterek, Guidelines for traceable measurements on machine tools, in: 11th International Symposium on Measurement and Quality Control 2013, September 11–13, 2013, Cracow-Kielce, Poland, 2013; pp. 11–14.
- [4] M. Holub, R. Jankovych, O. Andrs, Z. Kolibal, Capability assessment of CNC machining centres as measuring devices, Measurement: J. Int. Measurement Confed. 118 (2018) 52–60, <https://doi.org/10.1016/j.measurement.2018.01.007>.
- [5] Traceable in-process dimensional measurements. A Joint Research Project within the European Metrology Research Programme EMRP, 2015.
- [6] ISO 15530-3: 2004. Geometrical Product Specifications (GPS) – Coordinate measuring machines (CMM): Technique for determining the uncertainty of measurement – Part 3: Use of calibrated workpieces or standards, 2004.
- [7] ISO, JCGM 100:2008 (GUM 1995 with minor corrections). Evaluation of measurement data – Guide to the expression of uncertainty in measurement, 2008.
- [8] ISO, ISO/TS 15530-4:2008. Geometrical Product Specifications (GPS) – Coordinate measuring machines (CMM): Technique for determining the uncertainty of measurement – Part 4: Evaluating task-specific measurement uncertainty using simulation, 2008.
- [9] J.C. for G. in M. (JCGM), JCGM 101:2008 – Evaluation of measurement data - Supplement 1 to the “Guide to the expression of uncertainty in measurement” – Propagation of distributions using a Monte Carlo method, 2008.
- [10] Verein Deutscher Ingenieure (VDI), VDI/VE 2617–11–Accuracy of coordinate measuring machines – characteristics and their checking – determination of the uncertainty of measurement for coordinate measuring, Machines Using Uncertainty Budgets (2011).
- [11] G. Lisa, H. Christian, K. Frank, W. Klaus, Good practice guide for assessing the fitness for purpose for dimensional measurements on machine tool, Eur. Metrol. Res. Programme (EMRP) (2014).
- [12] ISO 14253-1: 2017; Geometrical product specifications (GPS) – Inspection by measurement of workpieces and measuring equipment – Part 1: Decision rules for verifying conformity or nonconformity with specifications, 2017.
- [13] M. Trenk, M. Franke, H. Schwenke, F. KG, The “Virtual CMM” a software tool for uncertainty evaluation – practical application in an accredited calibration lab, ASPE Proceedings, Uncertainty Analysis in Measurement and Design. (2004) 6.
- [14] E. Trapet, Traceability of Coordinate Measurements According to the Method of the Virtual Measuring Machine: Part 2 of the Final Report Project MAT1-CT94-0076, 1999.
- [15] ISO 10791-7:2014. Test conditions for machining centres – Part 7: Accuracy of finished test pieces, 2014.
- [16] ISO, Geometrical product specifications (GPS) – ISO code system for tolerances on linear sizes – Part 2: Tables of standard tolerance classes and limit deviations for holes and shafts, 2010.
- [17] S. Nisch, R. Schmitt, Production integrated 3D measurements on large machine tools, in: LVMC Large Volume Metrology Conference 2010, Chester (UK), 2010.
- [18] H. Schwenke, W. Knapp, H. Haitjema, A. Weckenmann, R. Schmitt, F. Delbressine, Geometric error measurement and compensation of machines – an update, CIRP Ann. – Manuf. Technol. 57 (2008) 660–675, <https://doi.org/10.1016/j.cirp.2008.09.008>.
- [19] U. Kenta, F. Ryosyu, O. Sonko, T. Toshiyuki, K. Tomizo, Geometric calibration of a coordinate measuring machine using a laser tracking system, Measurement Sci. Technol. 16 (2005) 2466, <https://doi.org/10.1088/0957-0233/16/12/010>.
- [20] H. Schwenke, M. Franke, J. Hannaford, H. Kunzmann, Error mapping of CMMs and machine tools by a single tracking interferometer, CIRP Ann. – Manuf. Technol. 54 (2005) 475–478, [https://doi.org/10.1016/S0007-8506\(07\)60148-6](https://doi.org/10.1016/S0007-8506(07)60148-6).
- [21] H. Schwenke, R. Schmitt, P. Jatzkowski, C. Warmann, On-the-fly calibration of linear and rotary axes of machine tools and CMMs using a tracking interferometer, CIRP Ann. – Manuf. Technol. 58 (2009) 477–480, <https://doi.org/10.1016/j.cirp.2009.03.007>.
- [22] ISO 230-6: 2002. Test code for machine tools – Part 6: Determination of positioning accuracy on body and face diagonals (Diagonal displacement tests).

Uncertainty assessment for on-machine tool measurement: an alternative approach to the ISO 15530-3 technical specification



ELSEVIER

Contents lists available at ScienceDirect

Precision Engineering

journal homepage: www.elsevier.com/locate/precision

Uncertainty assessment for on-machine tool measurement: An alternative approach to the ISO 15530-3 technical specification

Unai Mutilba^{a,*}, Eneko Gomez-Acedo^a, Alejandro Sandá^b, Ibon Vega^b, Jose A. Yagüe-Fabra^c

^a Department of Mechanical Engineering, IK4-Tekniker, Eibar 20600, Spain

^b Department of Production Engineering, IK4-Tekniker, Eibar 20600, Spain

^c I3A, Universidad de Zaragoza, Zaragoza 50018, Spain

ARTICLE INFO

Keywords:

Uncertainty budget
On-machine tool measurement
Traceability
Uncertainty

ABSTRACT

Touch probes are commonly employed in new machine tools (MTs), and enable machining and measuring processes to occur on the same MT. They offer the potential to measure components, either during or after the machining process, providing traceability of the quality inspection on the MT. Nevertheless, there are several factors that affect measurement accuracy on shop-floor conditions, such as MT geometric errors, temperature variation, probing system, vibrations and dirt. Thus, the traceability of a measurement process on an MT is not guaranteed and measurement results are therefore not sufficiently reliable for self-adapting manufacturing processes. The current state-of-the-art approaches employ a physically calibrated workpiece to realise traceable on-MT measurement according to the ISO 15530-3 technical specification, but it has a significant limitation in that it depends on a physical workpiece to understand the performance of the systematic error contributor (u_b). To this end, the aim of this paper is to propose an alternative methodology for on-MT uncertainty assessment without using a calibrated workpiece. The proposed approach is based on a volumetric error mapping of the MT prior to the measurement process, which provides an understanding of how the systematic error contributor (u_b) performs. An experimental exercise is performed for a medium-size prismatic component according to the VDI 2617-11 guideline, and the results are compared with the ISO 15530-3 technical specification.

1. Introduction

The development of flexible manufacturing processes for high-quality products at low cost is one of the main research objectives in the field of production technology [1]. The quality inspection of high-value components usually takes place on coordinate measuring machines (CMMs), either beside the production line or in an isolated measurement room, so the manufacturing process is interrupted and transportation, handling and the loss of the original manufacturing setup influence the workpiece quality [2] and the overall equipment effectiveness (OEE). The high investment required for a CMM and the above-mentioned limitations show the need for a machine tool (MT) integrated traceable measuring process.

Although on-MT measurement can provide advantages for more flexible and intelligent manufacturing processes, there are also some limitations. The main limitation is that MT time is more expensive than CMM time, so measurements that are executed on an MT should clearly add value to the manufacturing process. Here, it is particularly relevant

to determine critical component dimensions and measure them on the MT in order to ensure zero-defect manufacturing processes [3].

The current manufacturing scenario shows that dimensional measurements are already being employed for on-MT measurements at different stages of the manufacturing cycle, mainly because the technology to perform a measurement, either touch-trigger probes (TTPs) or measurement software, are already available on the MT side. There are four potential measurement scenarios where on-MT measurement adds value to the manufacturing process: a) monitoring of the MT geometry performance by employing a calibrated standard; b) workpiece set up on the MT coordinate system; c) in-process measurements to provide correction values for the manufacturing; and d) the performance of a final metrology validation of the finished product for final quality inspection as well as statistical trend analysis of the manufacturing process. Nowadays, depending on the size of the component, traceable on-MT measurement technology readiness levels (TRLs) are at different stages: While large-scale manufacturing processes employ on-MT measurements to reduce the setup time of large components on the MT

* Corresponding author.

E-mail addresses: unai.mutilba@tekniker.es (U. Mutilba), eneko.gomez-acedo@tekniker.es (E. Gomez-Acedo), alejandro.sanda@tekniker.es (A. Sandá), ibon.vega@tekniker.es (I. Vega), jyague@unizar.es (J.A. Yagüe-Fabra).

<https://doi.org/10.1016/j.precisioneng.2019.03.005>

Received 18 December 2018; Received in revised form 13 March 2019; Accepted 21 March 2019

0141-6359/ © 2019 Elsevier Inc. All rights reserved.

bed, medium-size aeronautic manufacturers are already performing on-MT measurement for the in-process measurement of high-value components such as aircraft engines and components, close to realising a traceable on-MT measurement.

From a technology point of view, the aim is to use an MT as a CMM, but there are some key differences between a CMM and an MT, mainly because CMMs are designed for measurement purposes and MTs are focused on manufacturing production. The main problem when executing a measurement on an MT is that the machining and measuring processes are performed using the same machine, and some error sources therefore cannot be distinguished if a calibration process is not realised before the measurement execution [4]. This is currently the main limitation to close the calibration chain for on-MT measurement.

Over the years, several standards and guidelines [5–10] have been developed in order to verify the accuracy of either MTs [11–16] or CMMs [6,7], but measurement traceability assessments for on-MT measurements are not as developed as is the case for CMMs. In this scenario, owing to the similarity between CMMs and MTs, some of the methods employed for a correct assessment of uncertainty in CMMs are being adopted for MTs. The general guide for a suitable evaluation of measurement data is given in the ISO Guide 98-3: 2008, on the expression of uncertainty in measurement (GUM) [17]. Three different approaches are considered for an uncertainty assessment on an MT [3]: a) an experimental technique according to ISO 15530-3 technical specification [8]; b) a numerical simulation-based approach, as described in the ISO 15530-4 technical specification [9]; and c) an uncertainty budget method based on the VDI 2617-11 guideline [10].

Several research works have focused on the idea of converting an MT into a CMM. In 2010, Schmitt et al. proposed that a large MT should be employed as a comparator to measure the geometry of large scale components during the manufacturing process [18]. In 2013, Schmitt et al. also presented a study in which a specific workpiece was manufactured and calibrated on a CMM for several on-MT measurement experimental tests [1]. In this regard, Mutilba et al. reported that a research work where a calibrated workpiece was employed to assess the on-MT measurement uncertainty on a real manufacturing process for a medium-size prismatic component [4]. In 2015, Schmitt et al. went a step further, presenting an approach to determine the uncertainty assessment for on-MT measurements according to the VDI 2617-11 guideline; they defined a maximum permissible error (MPE) [7] for MTs to assess the systematic error of the on-MT measurement error budget [2]. Recently, Holub et al. presented a capability assessment for on-MT measurement assisted by an external laser interferometer [19]. Similarly, Sladek et al. reported an interesting approach for the systematic error assessment of a CMM based on the use of a laser tracer for the volumetric error mapping and compensation of geometric errors. It is an online accuracy-estimation solution based on the virtual coordinate measuring machine (VCMM) concept for CMMs [9,20–22].

In this context, this paper presents a methodology to perform traceable on-MT measurements without using a calibrated workpiece, performing the VDI 2617-11 guideline [10]. The approach aims to perform the systematic error (u_b) assessment of on-MT measurements by means of a previous volumetric error mapping of the MT using laser tracer technology.

Finally, an experimental exercise was performed on a three linear-axis medium-size MT. It shows that the uncertainty assessment for a medium-size prismatic component can be performed without using a calibrated workpiece. Results have been compared to the ISO 15530-3 technical specification [8].

2. On-machine tool measurement uncertainty budget

Before presenting the new approach, it is interesting to understand those uncertainty contributors that should be considered for on-MT measurement uncertainty budget. The ISO 15530-3 technical specification explicitly presents four uncertainty contributors that consist of

all the systematic and random errors comprising the uncertainty budget for on-MT measurement [8]:

- u_b : Standard uncertainty associated with the systematic error of the measurement process.
- u_p : Standard uncertainty associated with the measurement procedure.
- u_{cal} : Standard uncertainty associated with the uncertainty of the workpiece calibration.
- u_w : Standard uncertainty associated with material and manufacturing variations.

Thus, the standard uncertainty of the measurement system (u_{MS}) is given by the quadrature sum of every uncertainty contributor, according to the formula expressed in Equation (1). In addition, the expanded measurement uncertainty of the measurement system (U_{MS}) is assessed by $U_{MS} = k \times u_{MS}$ for a coverage factor of $k = 2$, as expressed in Equation (2). For the systematic error (u_b) contributor, different approaches are employed to assess it. If the measurement result is not corrected by the systematic error (b), the error fully contributes to the uncertainty, so $u_b = b$. Thus:

$$u_{MS} = \sqrt{u_p^2 + u_{cal}^2 + b^2} \quad (1)$$

$$U_{MS} = k \cdot u_{MS} \quad (2)$$

With respect to the ISO 15530-3 technical specification, the uncertainty u_p is given by the maximum standard deviation of every measurement performed on the workpiece; therefore, it uses the experimental (type A) approach. The systematic error is defined as the difference between the mean value of the on-MT measurement and the calibrated value, and the calibration uncertainty is given by the workpiece's features calibration on a CMM. Both contributors are evaluated using the type B method. Further, if variations of form errors and roughness owing to fluctuating manufacturing processes and material properties are considered within their required limits, the u_w contribution is considered as insignificant [8]. In this case, u_w is considered negligible, so it is not introduced in Equation (1).

For the VDI 2617-11 guideline, the determination of the on-MT measurement uncertainty is determined using an uncertainty budget. Here, each uncertainty source and its magnitude on the measurement result is considered. In this case, the error sources are as follows [2]:

- The geometric error of the MT and its repeatability.
- Probing system.
- Temperature: MT structure, surroundings, and workpiece.
- Workpiece under measurement: Temperature and clamping.
- Measurement procedure.
- Geometric error mapping technique.

Those error sources comprise systematic and random errors for the on-MT uncertainty budget [23]. The result is the on-MT measurement uncertainty for a 95% confidence level.

Similar to the ISO 15530-3 technical specification, the systematic error contributor (u_b) on the VDI 2617-11 guideline is affected by the following error sources: geometric error of the MT, probing system, workpiece under measurement, measurement procedure, and geometric error mapping technique. The random contributor (u_p) comprises the MT repeatability, touch probe repeatability, and temperature variation for the measurement scenario. For the experimental approach presented below, the measurement procedure and the workpiece under measurement have not been considered for the uncertainty budget because an easy-to-measure medium-size prismatic component was measured. Moreover, negligible deformations occur during the clamping process. In addition, the probing system characterisation and the uncertainty of the MT volumetric error mapping technique are within 2 μm . Thus, the uncertainty budget exercise focuses on major

uncertainty contributors. In this manner, the geometric error of the MT is considered as the main error source within the systematic contributor (u_b), and the effect of the temperature on the measurement scenario and MT repeatability are highlighted as the main random error contributors (u_p).

Considering those major uncertainty error contributors, this study adopts the random error characterisation, which performed on the ISO 15530-3 technical specification and which does not require a calibrated workpiece to understand how (u_p) performs. For the systematic error contributor (u_b), Schmitt et al. presented an approach where an MPE value was defined for an MT. Their approach was validated within stable temperature conditions, but they proposed further research for unstable conditions because an unstable status causes gradients inside the structure, and the induced deviations are hard to simulate or predict [2]. Considering such limitations, a volumetric error mapping of the MT is performed immediately before the on-MT measurement process execution for the systematic error characterisation. Thus, the geometric error of each contact point is known, and the systematic error contributor (u_b) can therefore be assessed. This research work does not apply the systematic error value correction, so the error fully contributes to the uncertainty budget, as in Equation (1).

3. Methodology for on-MT uncertainty assessment without a calibrated workpiece

A new methodology is proposed to perform the on-MT uncertainty assessment without a calibrated workpiece:

- For the systematic error contributor (u_b), a volumetric error mapping of the MT is performed immediately before the on-MT measurement. Thus, the geometric error of each point is known for the working volume of the machine, which is the main contributor to the systematic error of the on-MT measurement. Once the on-MT measurement is performed, measurement contact points are registered, and the geometric error of every point is obtained from the volumetric error mapping. Thus, every measured feature is fitted again while considering the geometric error of each contact point. The difference between the feature characteristics before and after the second fitting exercise is the systematic error to be considered on the error budget. Fig. 1 shows the flow chart for the systematic error characterisation.
- The systematic error originating from the tactile probe could also be considered for the systematic error contributor (u_b). Thus, as explained by Mutilba et al. [4] if a reliable calibration of the probing system is performed every time the tactile probe is mounted on the MT spindle, this contributor becomes negligible. However, if the calibration process is not executed correctly or if the uncertainty contributor is not sufficiently small ($< 1 \mu\text{m}$ for small MT and < 3

μm for large MT) the tactile probe systematic error should be added to the u_b value according to the square root of the sum of squares.

- The measurement procedure uncertainty (u_p) is performed on the workpiece to be measured on the MT, similar to the ISO 15530-3 technical specification [8]. Thus, the repeatability of the on-MT measurement is performed within the temperature range of the measurement scenario, considering that the temperature variation is critical for this uncertainty contributor. Therefore, several on-MT measurement cycles shall be performed within the complete temperature range of the measurement scenario. For example, consider an eolic hub being machined in a large MT, where the temperature variation on the surrounding air is between 18°C and 23°C . The u_p contributor should be assessed by means of repeated measurement cycles (every 15 min) on the workpiece within the working temperature range. Equation (3) shows how to calculate the u_p contributor.
- The u_{cal} contributor is considered as the standard uncertainty associated with the measurement uncertainty on the systematic error characterisation process.

$$\bar{y} = \frac{1}{n} \sum_{i=1}^n y_i \quad u_p = \sqrt{\frac{1}{n-1} \sum_{i=1}^n (y_i - \bar{y})^2} \quad (3)$$

where:

- \bar{y} = mean value of the measurement result.
- y = measured value.
- n = number of measurement results.

Fig. 1 shows the flow chart for the systematic error characterisation.

For the geometric fitting of the measured plane and diameters, three dimensional (3D) and two dimensional (2D) fitting equations have been employed in MATLAB [24]. This fitting exercise considers the geometric error information of each contact point obtained in this case from the volumetric error mapping measurement. Results obtained on each fitted feature are compared to the initial fitting value obtained by the on-MT measurement software, so the difference between both fittings is the systematic error to be considered on the error budget according to the VDI 2617-11 guideline. Equation (4) shows the employed algorithm for circumference fitting; the variation of the radius shows the roundness error.

$$r = \sqrt{(x - x_c)^2 + (y - y_c)^2} \quad (4)$$

where:

- r = circumference radius.
- x, y = measured contact points (geometric error in each point is considered).

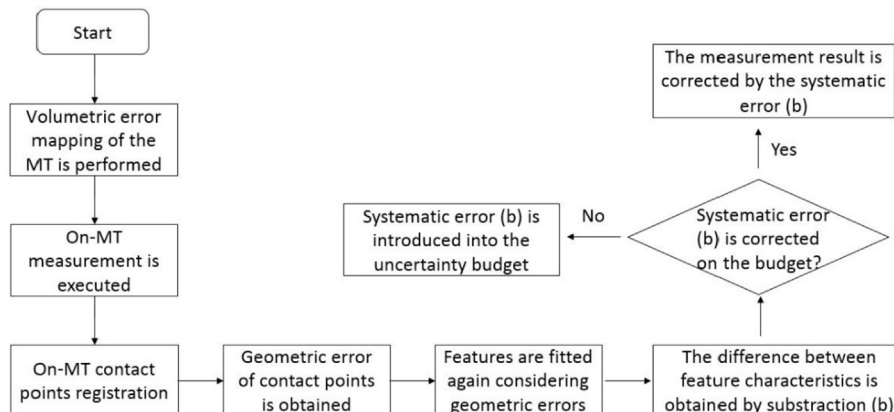


Fig. 1. Systematic error assessment methodology.

- x_c, y_c = circumference centre coordinates (to be obtained).

For the 3D fitting of the plane, Equation (5) shows the algorithm which was employed in this experimental exercise. The least-squares fitting algorithm was employed to compare the flatness error before and after considering the geometric error of the contact points [25].

$$f(x_i, y_i, z_i) = p_1 x_i + p_2 y_i + p_3 z_i + 1 \cong 0 \quad (5)$$

where:

- p = plane feature parameters.
- x_i, y_i, z_i = measured contact points (geometric error in each point is considered)

4. Technology adoption on a machine tool

The presented methodology requires a volumetric error mapping of the MT before performing the on-MT measurement to characterise the geometric error of the MT as the main error source to the systematic error (u_b) of on-MT measurement. In this context, as explained by Nisch et al. [18], there are two main approaches to enable a traceable measurement on MTs: a) the MT geometric error is known at the moment when the measurement is performed through a volumetric error mapping of the MT; and b) an external high precision metrological frame is employed to measure and compensate for the geometric error of the MT in real time [21,22,26,27].

Fig. 2 shows the above-mentioned two alternatives a) an MT volumetric error mapping exercise. It shows an integrated multilateration approach reported by Mutilba et al. [30], and b) an external high-precision metrological frame comprised of four tracking interferometers in simultaneous mode.

The first approach increases the process capability by a volumetric verification and compensation of the MT, as shown in Fig. 2(a). Currently, there are different options for the volumetric error mapping of MTs [28], but they are time-consuming, mainly for large-scale MTs. In this regard, the multilateration approach is suitable for realising such a fast performance. Schwenke et al. reported an approach to continuously monitor the geometric variation of a large MT on shop floor conditions [29], and recently, Mutilba et al. reported an integrated and automatic volumetric error mapping solution for large MTs which is executed within 30 min [30]. For the proposed experimental approach, a volumetric error mapping of the MT under research was performed using laser tracer NG technology in sequential mode.

The second approach applies an external high precision metrological frame to monitor the tool centre point (TCP) position in real time. This option requires a line of sight between the measuring tracking interferometers and the TCP, which cannot be ensured when the workpiece is on the MT. The current cost of the solution is very high

because four interferometers are required simultaneously. However, it offers the possibility of being self-calibrating and represents a scalable measuring solution.

Currently, the first approach is under research, and according to the latest studies, with the continued development of interferometer-based non-contact measuring technology to realise more accurate absolute distance measurements, it will be incorporated into MTs, allowing traceable CMM measurements in MTs [31].

5. Uncertainty budget assessment experimental exercise

An experimental exercise of the proposed methodology was performed using a workpiece replica standard. The obtained results were compared to the ISO 15530-3 technical specification. The workpiece replica standard selected for the experimental uncertainty assessment exercise is defined at the ISO 10791-7:2014 standard [32], and it is referred as a 'Test piece ISO 10791-7, M1-160'. A description of the measured geometry is illustrated in Fig. 3.

A medium-size KONDIA MAXIM MT equipped with a RENISHAW OMP 400 tactile probe and POWER INSPECT on-MT measurement software was selected to run the on-MT measurement experimental test. The MT cutting stroke is: $X = 750$ mm, $Y = 1000$ mm and $Z = 500$ mm. The computer numerical control (CNC) is a 16i-type FANUC controller. For the tactile probe calibration on the MT spindle, a 50 mm-diameter calibrated ring was employed immediately after it was mounted on the MT spindle. Fig. 4 shows a) the measured contact points for the experimental on-MT measurement test and b) the measurement scenario on the MT.

For the systematic error contributor (u_b) assessment, a volumetric error mapping of the MT was performed immediately before the on-MT measurement. To do this, laser tracer technology from ETALON AG was employed [33]. It employs a kinematic model which enables to calculate the geometric error of any point within the measured volume from the volumetric error mapping information, so the geometric error of the on-MT measurement contacts points was assessed in this manner. Fig. 5 shows the volumetric error mapping exercise and the measured point grid (in black) of the MT. The laser tracer NG, which is placed on the MT table, measures the distance to the reflector, which is fixed to the spindle, for every point comprising the point grid under the multilateration scheme [33]. It demonstrates the technology adoption of the above-mentioned first approach where a unique tracking interferometer is employed in sequential mode for the MT volumetric error mapping.

The volumetric error mapping measurement was performed under a no-load condition when the temperature on the MT side was 20 °C, with a temperature variation within 0.5 °C.

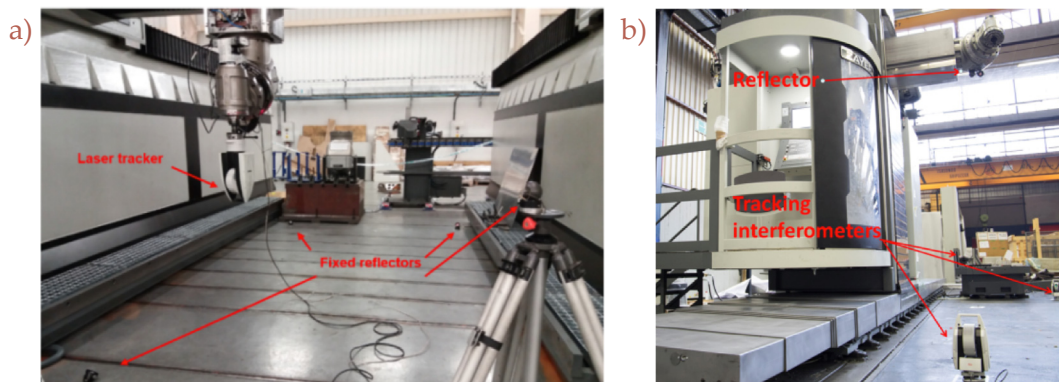


Fig. 2. Multilateration approaches for MT error mapping a) integrated approach, and b) external high-precision frame with four tracking interferometers (Both measurements were performed by IK4-TEKNIKER on a ZAYER large MT).

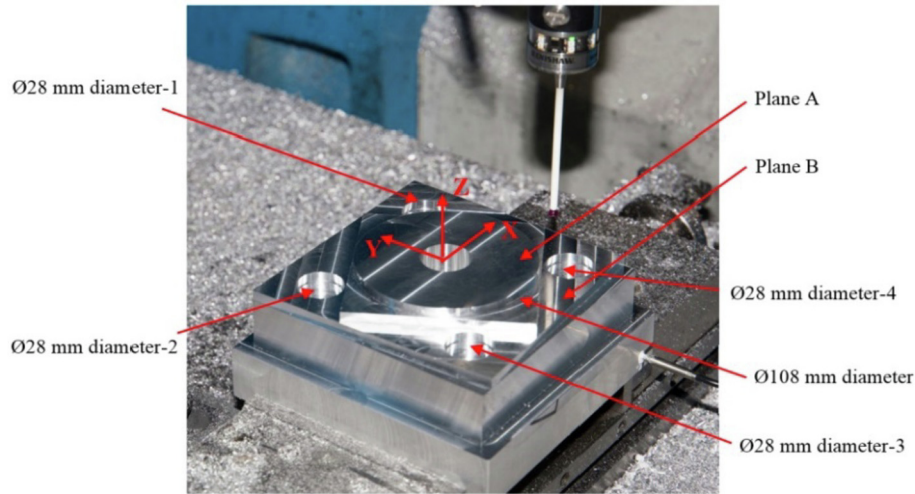


Fig. 3. Workpiece replica standard with measured geometry on the experimental test.

5.1. On-MT measurement results according to ISO 15530-3 technical specification

The experimental on-MT measurement exercise according to the ISO 15530-3 technical specification is explained in detail in the article: 'Traceability of on-MT measurement: Uncertainty budget assessment on shop floor conditions' which was reported by Mutilba et al., in 2018 [4]. Here, the approach is to employ a CMM-calibrated workpiece replica standard to assess the on-MT measurement uncertainty. Fig. 6 shows the absolute value of the systematic error contributor (u_b) assessed using the calibrated workpiece. All of the results are within $8 \mu\text{m}$.

The uncertainty budget of the task-specific uncertainty assessment on shop floor conditions according to the ISO 15530-3 technical specification [4] is shown in Fig. 7. The measurement procedure uncertainty (u_p) is on average a few micrometres larger on than the systematic error (u_b) uncertainty, which is within $8 \mu\text{m}$ for every measured feature. The calibration uncertainty contributor (u_{cal}) is within $2 \mu\text{m}$ for each feature. Expanded measurement uncertainty results are obtained by Equation (2) for a coverage factor of $k = 2$, where u_{MS} is given by Equation (1). As previously mentioned, it should be considered that the systematic error (u_b) contributor is not corrected on the uncertainty

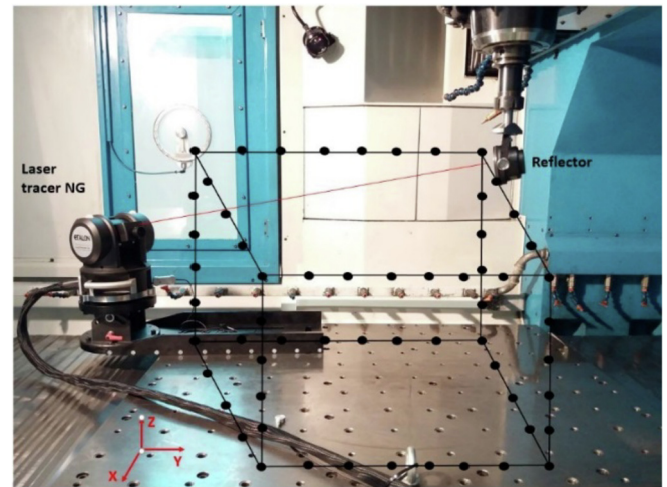


Fig. 5. Volumetric error mapping of MT and measured point grid (in black).

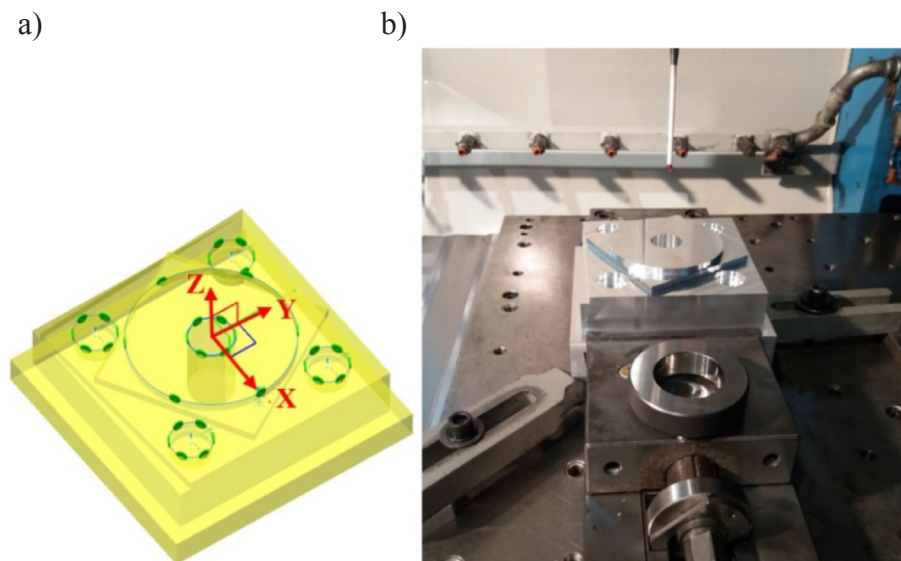


Fig. 4. On-MT measurement contact points, a) General overview of the measurement strategy (contact points in green), and b) the measurement scenario where the workpiece and the calibrated ring are shown.

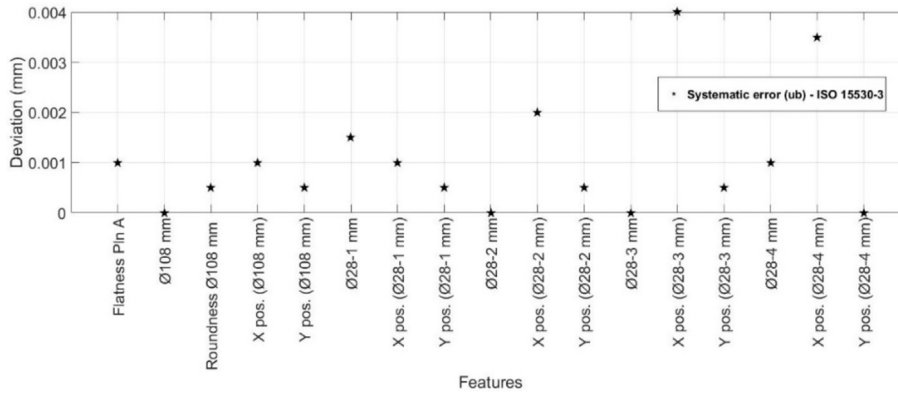


Fig. 6. Systematic error (u_b) according to ISO 15530-3 technical specification [4].

budget, which significantly increases the expanded measurement uncertainty (U_{MS}) result.

5.2. On-MT measurement results according to VDI 2617-11 guideline

The main difference for the VDI 2617-11 approach is that a calibrated workpiece is not employed to assess the systematic error contributor (u_b) on the uncertainty budget. Thus, a volumetric error mapping of the MT was performed immediately before the on-MT measurement exercise, and the TRAC-CAL software from the company ETALON AG, which includes kinematic models for point-error determination, was used to calculate the geometric error of each contact point for the on-MT measurement process. Fig. 5 shows the volumetric error mapping setup on the MT, and Fig. 8 shows the 3D deviation result of each measured point comprising the point grid. The simple ETALON kinematic model was employed, and was performed by 17 components of the error, and the results are depicted in a 3D deviation-type plot. The uncertainty for the geometric error mapping measurement is within 1 μ m. The volume of the point grid depicted in Fig. 8 is similar to the MT cutting stroke, i.e. X = 750 mm, Y = 1000 mm and Z = 500 mm.

The MT volumetric error mapping exercise demonstrates that the geometric error is within 20 μ m for almost the entire volume of the machine. Moreover, the workpiece replica standard size is 160 mm \times 160 mm, which means that the geometric error on the MT side that applies to the on-MT measurement is within 5 μ m. The volumetric error mapping process also measures the MT volumetric repeatability; in this case, the MT volumetric repeatability is within 2 μ m. This means that either the backlash error or the repeatability itself are within this value.

For the systematic error contributor (u_b) assessment, the proposed methodology depicted in Fig. 1 was applied. In addition, a reliable

tactile probe calibration was performed prior to the on-MT measurement exercise to avoid systematic errors due to the probe set-up process. The repeatability of the calibrated ring measurement is within 1 μ m, which is similar to the MT repeatability. In this manner, it was considered to be within the measurement procedure uncertainty (u_p) on the uncertainty budget. Fig. 9 shows a comparison of the systematic error assessment for the ISO 15530-3 technical specification and the VDI 2617-11 guideline. The difference between both approaches is within 1.5 μ m.

For the measurement procedure uncertainty (u_p), results obtained from the ISO 15530-3-based experimental test were considered because they do not require a calibrated workpiece. Here, it is crucial to understand the effect of temperature gradients on the results. Thus, the experimental test suggests on-MT measurements immediately after the machining process of the workpiece replica standard and measurements under a no-load condition when the temperature on the MT side and workpiece side is constant at 20 $^{\circ}$ C. The temperature variation on the on-MT measurement scenario is within 3 $^{\circ}$ C, and the workpiece temperature increases to 22.5 $^{\circ}$ C (on average) immediately after the machining process, after which it stabilises to 19.5 $^{\circ}$ C (on average) after an on-MT measurement acquisition time of 2 h. Fig. 10 shows the measurement procedure uncertainty (u_p) for each measurement feature, both for measurements executed immediately after the machining process as well as measurements executed under no-load conditions [4].

The measurement procedure uncertainty results (u_p) show differences between the measurement executed under the no-load condition and the measurements executed immediately after the machining process. All of the results show repeatability within 6 μ m for the no-load condition, while the maximum repeatability values for the measurements immediately after the machining process are within 10 μ m. The form error feature measurement (flatness and roundness) shows better measurement procedure uncertainty results than the scale-related

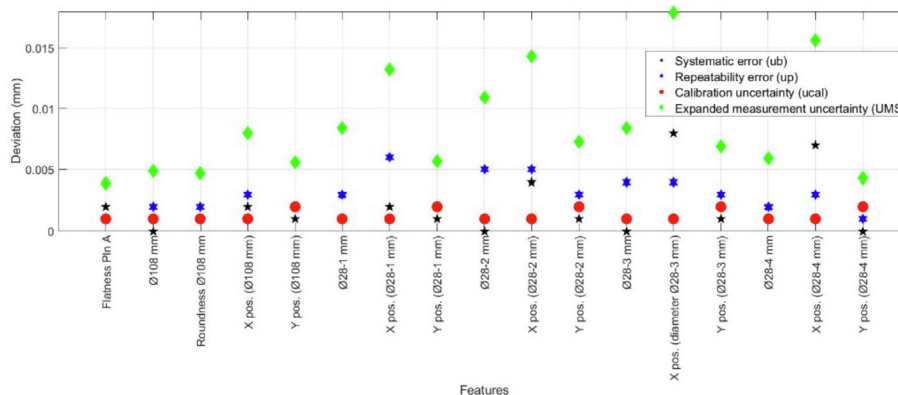


Fig. 7. Uncertainty budget according to ISO 15530-3 technical specification [4].

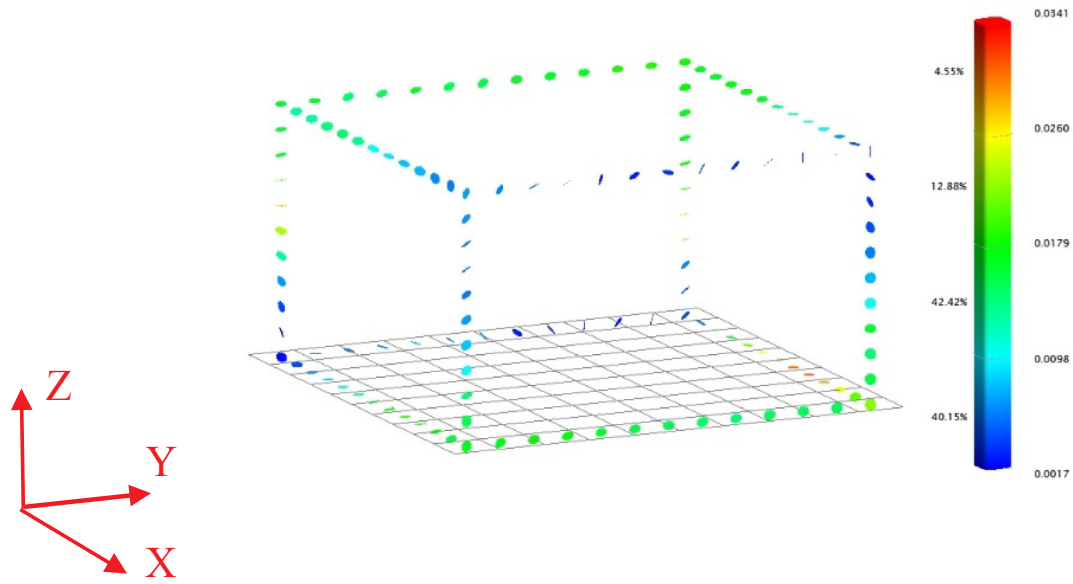


Fig. 8. MT volumetric error mapping results.

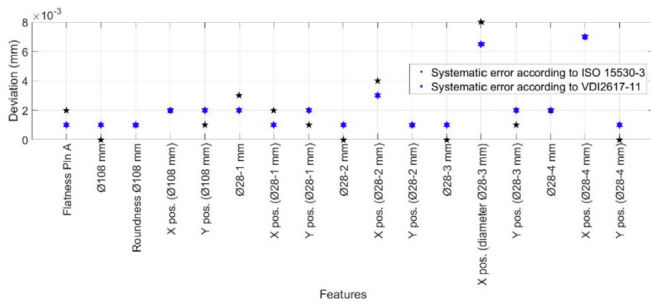


Fig. 9. Systematic error (u_b) assessment according to ISO 15530-3 technical specification and VDI 2617-11 guideline.

feature measurement (diameter and positioning values) because these features are more sensitive to the measurement scenario temperature variation [34]. Here, factors such as the swarf or dirty surfaces should affect the u_p uncertainty result.

For the uncertainty (u_{cal}) contributor, the volumetric error mapping of the MT also indicates the uncertainty of the volumetric measurement exercise; it is obtained using a Monte-Carlo simulation technique considering the spatial displacement measurement uncertainty for the laser tracer NG, $U(k = 2) = 0.2 \mu\text{m} + 0.3 \mu\text{m/m}$ [33]. The obtained uncertainty contributor (u_{cal}) of the volumetric error mapping is within

$1 \mu\text{m}$.

Finally, the uncertainty budget of the task-specific uncertainty assessment in shop floor conditions according to the VDI 2617-11 guideline [3] is depicted in Fig. 11. Similar to the ISO 15530-3 technical specification, the expanded measurement uncertainty results were obtained using Equation (2) for a coverage factor of $k = 2$, where u_{MS} is given by Equation (1). For the measurement procedure uncertainty (u_p), the contribution to the uncertainty budget uncertainty results for the no-load condition were considered.

Finally, Table 1 shows the uncertainty budget assessment within the VDI 2617-11 guideline and it is compared with the result obtained according to the ISO 15530-3 technical specification.

Experimental results show that the uncertainty budget according to the VDI 2617-11 guideline obtains similar results to what obtained according to the ISO 15530-3 technical specification, where a calibrated workpiece is employed for the purpose. For the systematic error contributor (u_b), the difference between both approaches is within $1.5 \mu\text{m}$, which agrees with the accuracy of the volumetric error mapping performance, i.e. roughly $1 \mu\text{m}$, and also with the backlash error, which is within the $2 \mu\text{m}$ result that shows the volumetric repeatability. In addition, the calibration component (u_{cal}) is similar in both cases because of the employed reference standards, whether the calibrated workpiece or the volumetric error mapping solution have a similar uncertainty contributor. For the measurement procedure contributor

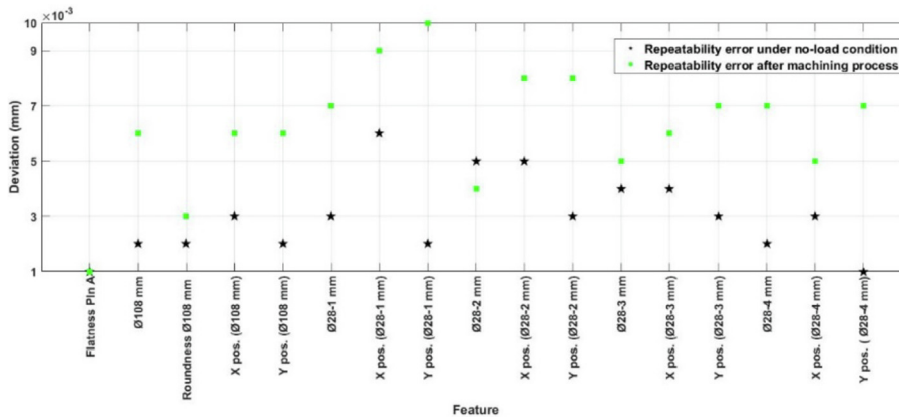


Fig. 10. Measurement procedure uncertainty (u_p) results for both approaches [4].

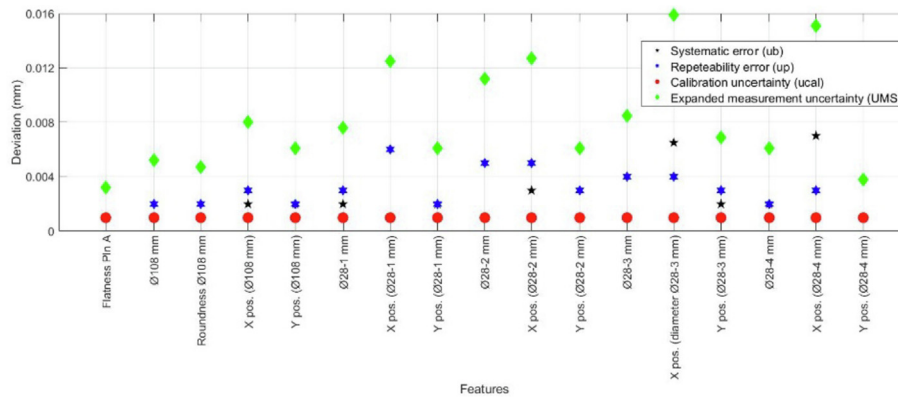


Fig. 11. Uncertainty budget according to VDI 2617-11 guideline (no-load condition).

(u_p), the same raw data is employed.

6. Conclusions and future work

This paper presents an alternative on-MT uncertainty assessment methodology based on the VDI 2617-11 guideline, which could allow scaling traceable on MT measurements to large-size MTs. The current approach, which is based on the ISO 15530-3 technical specification, requires a calibrated workpiece, which is similar to the manufactured part. Therefore, the solution is not very flexible, especially for larger parts, for which it is tedious and expensive. In addition, it also presents the two main alternatives for the adoption of the volumetric error mapping technology to MTs.

An experimental uncertainty budget of on-MT measurement was presented:

- Making a comparison with the ISO 15530-3 technical specification, the systematic error contributor (u_b) on the VDI 2617-11 guideline is shown to be affected by those error sources: the geometric error of the MT, probing system, workpiece under measurement, measurement procedure and the geometric error mapping technique.
- The random contributor (u_p) comprises the MT repeatability, touch probe repeatability, and temperature variation in the measurement scenario. For the experimental approach, the measurement procedure and the workpiece under measurement were not considered in the uncertainty budget because an easy-to-measure medium size prismatic component was measured. Moreover, negligible deformations occur during the clamping process. Furthermore, the probing system characterisation and the uncertainty of the

volumetric error mapping technique are within $2\mu\text{m}$. The former is considered within the procedure uncertainty contributor (u_p) and the latter is considered as the u_{cal} contributor.

The experimental exercise which was performed without a calibrated workpiece shows that the obtained results are similar to what was obtained using a calibrated workpiece. For the systematic error contributor (u_b), the difference between both approaches is within $1.5\mu\text{m}$, which is similar to the volumetric error mapping uncertainty, for which the difference is approximately $1\mu\text{m}$, and also with the volumetric repeatability of the MT, which includes the backlash error within $2\mu\text{m}$. Random errors for both experimental approaches are the same because they were obtained on the ISO 15530-3 approach.

In summary, the methodology offers an opportunity to obtain traceable CMM measurements on MTs without employing a calibrated workpiece as long as interferometer-based technology is developed for MT volumetric error mapping and calibration.

The results obtained were validated on a three linear axis medium-size MT owing to machine availability and other practical issues. The future work will focus on scaling the presented methodology to large MTs similar to those used in large-scale manufacturing; the ISO 15530-3 approach is not affordable because a calibrated workpiece similar to the manufactured part is required, which makes the solution difficult and expensive.

In this scenario, this research work is a gateway to large on-MT traceable measurement.

Table 1

Uncertainty budget according to VDI 2617-11 guideline and comparison with ISO 15530-3 technical specification. (results in μm).

Feature	u_b	u_p	u_{cal}	u_{MS}	$U_{MS} - \text{VDI 2617-11}$	$U_{MS} - \text{ISO15530-3}$
Flatness Plan A	1.0	0.7	1.0	1.6	3.2	3.9
Ø108 mm	1.0	2.2	1.0	2.6	5.2	4.9
Roundness Ø108 mm	1.0	1.9	1.0	2.4	4.7	4.7
X position (Ø108 mm)	2.0	3.3	1.0	4.0	8.0	8.0
Y position (Ø108 mm)	2.0	2.1	1.0	3.1	6.1	5.6
Ø28-1 mm	2.0	3.1	1.0	3.8	7.6	8.4
X position (Ø28-1 mm)	1.0	6.1	1.0	6.3	12.5	13.2
Y position (Ø28-1 mm)	2.0	2.1	1.0	3.1	6.1	5.7
Ø28-2 mm	1.0	5.4	1.0	5.6	11.2	10.9
X position (Ø28-2 mm)	3.0	5.5	1.0	6.3	12.7	14.3
Y position (Ø28-2 mm)	1.0	2.7	1.0	3.0	6.1	7.3
Ø28-3 mm	1.0	4.0	1.0	4.2	8.5	8.4
X position (Ø28-3 mm)	6.5	4.5	1.0	8.0	15.9	17.9
Y position (Ø28-3 mm)	2.0	2.6	1.0	3.4	6.9	6.9
Ø28-4 mm	2.0	2.1	1.0	3.1	6.1	5.9
X position (Ø28-4 mm)	7.0	2.7	1.0	7.6	15.1	15.6
Y position (Ø28-4 mm)	1.0	1.3	1.0	1.9	3.8	4.3

Author contributions

I.V. and E.G.-A. contributed to the MT volumetric error mapping assessment. A.S. contributed to the execution of the on-MT measurement in shop floor conditions. J.A.Y.F contributed to the manuscript. U.M. led the research work and contributed significantly to the paper. All authors contributed to the editing of the manuscript.

Conflicts of interest

The authors declare no conflict of interest.

References

- [1] Schmitt R, Peterek M. Guidelines for traceable measurements on machine tools. 11th int. Symp. Meas. Qual. Control 2013, Sept. 11-13, 2013. Cracow-Kielce, Pol.; 2013. p. 11–4.
- [2] Schmitt R, Peterek M. Traceable measurements on machine tools-Thermal influences on machine tool structure and measurement uncertainty. *Procedia CIRP* 2015;33:576–80. <https://doi.org/10.1016/j.procir.2015.06.087>.
- [3] Mutilba U, Gomez-Acedo E, Kortaberria G, Olarra A, Yagüe-Fabra JA. Traceability of on-machine tool measurement: a review. *MDPI Sens* 2017;17:40. <https://doi.org/10.3390/s17071605>.
- [4] Mutilba U, Sandá A, Vega I, Gomez-acedo E, Fabra JAY. Traceability of on-machine tool measurement: uncertainty budget assessment on shop floor conditions. *Measurement* 2019;135. <https://doi.org/10.1016/j.measurement.2018.11.042>.
- [5] Flack D. Measurement good practice guide No. 42. CMM verification; 2001.
- [6] ISO. ISO 10360-2:2009. Geometrical product specifications (GPS) – Acceptance and reverification tests for coordinate measuring machines (CMM) – Part 2: CMMs used for measuring linear dimensions. 2009.
- [7] ISO. ISO 10360-1. Geometrical Product Specifications (GPS) – Acceptance and reverification tests for coordinate measuring machines (CMM) – Part 1: Vocabulary. 2000.
- [8] ISO. ISO/TS 15530-3: 2004. Geometrical Product Specifications (GPS) — coordinate measuring machines (CMM): technique for determining the uncertainty of measurement — Part 3: use of calibrated workpieces or standards. 2004.
- [9] ISO. ISO/TS 15530-4:2008. Geometrical Product Specifications (GPS) — coordinate measuring machines (CMM): technique for determining the uncertainty of measurement — Part 4: evaluating task-specific measurement uncertainty using simulation. 2008.
- [10] Verein Deutscher Ingenieure (VDI). VDI/VDE 2617-11-accuracy of coordinate measuring machines - characteristics and their checking - determination of the uncertainty of measurement for coordinate measuring machines using uncertainty budgets. 2011.
- [11] ISO. ISO 230-10:2016.. Test code for machine tools – Part 10: determination of the measuring performance of probing systems of numerically controlled machine tools. 2011.
- [12] ISO. ISO 230-7: 2015. Test code for machine tools – Part 7: geometric accuracy of axes of rotation. 2015.
- [13] ISO. ISO 230-2. Test code for machine tools — Part 2: determination of accuracy and repeatability of positioning of numerically controlled axes. 2014.
- [14] ISO (Technical comitee ISO/TC 39/SC 2). ISO 230-4:2005, test code for MTs. Part 4. Circular tests for numerically controlled machine tools. 2005.
- [15] ISO (Technical comitee ISO/TC 39/SC 2). ISO 230-6:2002, test code for machine tools. Part 6. Determination of positioning accuracy on body and face diagonals (diagonal displacement tests). 2002.
- [16] ISO (Technical comitee ISO/TC 39/SC 2). ISO 230-1:2012, Test code for machine tools – Part 1: geometric accuracy of machines operating under no-load or quasi-static conditions. 2012.
- [17] ISO. JCGM 100:2008 (GUM 1995 with minor corrections).. Evaluation of measurement data — guide to the expression of uncertainty in measurement. 2008.
- [18] Nisch S, Schmitt R. Production integrated 3D measurements on large machine tools. LVMC large vol. *Metrol. Conf.* 2010, Chester. 2010.
- [19] Holub M, Jankovych R, Andrs O, Kolibal Z. Capability assessment of CNC machining centres as measuring devices. *Meas J Int Meas Confed* 2018;118:52–60. <https://doi.org/10.1016/j.measurement.2018.01.007>.
- [20] Trapet E. Traceability of coordinate measurements according to the method of the virtual measuring machine: Part 2 of the final report project MAT1-CT94-0076 vol. 35. 1999.
- [21] Kupiec R, Krawczyk M. Virtual coordinate measuring machine built using laser-tracer system and spherical standard. *Metrol Meas Syst* 2013. <https://doi.org/10.2478/mms-2013-007>.
- [22] Sladek J, Gasca A. Evaluation of coordinate measurement uncertainty with use of virtual machine model based on Monte Carlo method. *Measurement* 2012;45:1564–75.
- [23] Slocum A. Precision machine-design - macromachine design philosophy and its applicability to the design of micromachines. *IEEEEMEM'S '92. Proceedings. An investig. Micro struct. Sensors Actuators, Mach. Robot. IEEE;* 1992. <https://doi.org/10.1109/EMEMSYS.1992.187687>.
- [24] Mathworks. Matlab software. 2018.
- [25] Mathworks. Least squares plane fitting code. 2018.
- [26] Schmitt R, Peterek M, Quinders S. Concept of a virtual metrology frame based on absolute interferometry for multi robotic assembly. 2014. p. 79–86.
- [27] Schwenke H. The latest trends and future possibilities of volumetric error compensation for machine tools. 15th int. mach. tool eng. conf. IMEC, Tokyo, Japan, 2-3 Novemb. 2012. p. 57–71.
- [28] Schwenke H, Knapp W, Haitjema H, Weckenmann A, Schmitt R, Delbressine F. Geometric error measurement and compensation of machines—an update. *CIRP Ann - Manuf Technol* 2008;57:660–75. <https://doi.org/10.1016/j.cirp.2008.09.008>.
- [29] Schwenke H, Schmitt R, Jatzkowski P, Warmann C. On-the-fly calibration of linear and rotary axes of machine tools and CMMs using a tracking interferometer. *CIRP Ann - Manuf Technol* 2009;58:477–80. <https://doi.org/10.1016/j.cirp.2009.03.007>.
- [30] Mutilba U, Yagüe-Fabra JA, Gomez-Acedo E, Kortaberria G, Olarra A. Integrated multilateration for machine tool automatic verification. *CIRP Ann* 2018;67:555–8. <https://doi.org/10.1016/j.cirp.2018.04.008>.
- [31] Schmitt R, Peterek M, Morse E, Knapp W, Galetto M, Härtig F, et al. Advances in large-scale metrology – review and future trends. *CIRP Ann - Manuf Technol* 2016. <https://doi.org/10.1016/j.cirp.2016.05.002>.
- [32] ISO 10791-7:2014. Test conditions for machining centres – Part 7: accuracy of finished test pieces. 2014.
- [33] Schwenke H, Franke M, Hannaford J, Kunzmann H. Error mapping of CMMs and machine tools by a single tracking interferometer. *CIRP Ann - Manuf Technol* 2005;54:475–8. [https://doi.org/10.1016/S0007-8506\(07\)60148-6](https://doi.org/10.1016/S0007-8506(07)60148-6).
- [34] Mutilba U, Sandá A, Vega I, Gomez-acedo E, Bengoetxea I, Yagüe JA. Traceability of on-machine tool measurement : uncertainty budget assessment on shop floor conditions. *Measurement* 2019;135:180–8. <https://doi.org/10.1016/j.measurement.2018.11.042>.

Integrated multilateration for machine tool automatic verification



Integrated multilateration for machine tool automatic verification

Unai Mutilba^a, José A. Yagüe-Fabra (2)^{b,*}, Eneko Gomez-Acedo^a, Gorka Kortaberria^a, Aitor Olarra^a

^a Department of Mechanical Engineering, IK4-Tekniker, Eibar 20600, Spain

^b I3A- Universidad de Zaragoza, C/ María de Luna, 3, Zaragoza 50018, Spain

ARTICLE INFO

Article history:

Available online 17 April 2018

Keywords:

Machine tool
Calibration
Multilateration

ABSTRACT

Multilateration based approaches are widely accepted as the most adequate solution for geometric characterisation of medium and large machine tools. However, its application, either in a sequential mode or in a simultaneous approach, leads to industrial limitations such as total time consumption or thermal drift that prevent an automatic calibration. This work presents an integrated multilateration verification procedure where a tracking interferometer is directly attached to the manufacturing system spindle as a tool, which tackles several of the mentioned limitations. Results of both simulations and experimental tests show that levels of uncertainty in the range of micrometres can be guaranteed.

© 2018 Published by Elsevier Ltd on behalf of CIRP.

1. Introduction

Zero defect manufacturing is one of the main objectives in the field of production engineering, so the ability to manufacture accurate parts is a key performance criterion for a modern machine tool (MT). In fact, it is essential for medium and large scale manufacturing processes, where errors during the manufacturing process of high value components are not acceptable [1,2]. Thus, both the repeatability and the absolute accuracy of MTs become crucial. While the repeatability of the machine is a necessary requirement for a well-controlled manufacturing process, the geometric accuracy of the manufactured part can be ensured by using accurately calibrated machine tools [3].

Since the introduction of the volumetric accuracy concept by McKeown and Loxham [4] in 1973, significant research work has been presented [5–7] towards volumetric error mapping and compensation of MTs. A main conclusion of these investigations is that indirect measurement methods have the advantage of offering fast and reliable volumetric error performance assessment for medium and large scale MTs, opposite to direct measurement methods [3] that are very time-consuming and have strong limitations.

In this scenario, multilateration-based approaches are by far the most employed verification solution among indirect measurement methods [1]. Currently, the approach relies on interferometric or absolute displacement measurements between tracking interferometers that are fixed to the machine base and a reflector, fixed to the machine spindle, near to the tool centre point (TCP) [7].

Different multilateration based measurement approaches [5,8,9] have been developed until nowadays, but none of them offers the possibility to execute an automatic self-machine tool verification.

This paper presents an integrated multilateration verification procedure where a tracking interferometer is directly attached to the manufacturing system spindle. The concept has been simulated by means of Monte Carlo method to ensure that achievable uncertainty is in the range of micrometres and finally, it has been validated by mounting a Leica AT402 laser tracker on a Kuka KR60 industrial robot.

As a result, automatic volumetric calibration for manufacturing systems becomes a real possibility that could be applied for medium and large MTs.

2. Multilateration based approach: limitations

Multilateration based measurement for MT error mapping requires at least four fixed points for displacement measurement, either absolute or relative, between those fixed points and any moving measuring point. According to this measurement distribution requirement, typically tracking interferometers are set on the MT table in the fixed points' positions and a measuring reflector is attached to the moving spindle to materialize the moving points. This typical multilateration configuration (hereinafter typical multilateration) is the first barrier to an automated MT calibration solution, since manual intervention is needed on fixing tracking interferometers to each measurement station.

Commonly only one tracking interferometer is available, so in practice, multilateration measurements are done in a sequential scheme, as follows: MT movements are repeated several times to the same positions and measurements are taken from different tracking interferometer locations. Consequently, time consumption during measurement realization increases and, therefore, thermal drift between sequential measurements occurs. This becomes the second barrier to an automated solution, since this

* Corresponding author.

E-mail address: jyague@unizar.es (A. Yagüe-Fabra).

approach requires MT repeatability for suitable multilateration uncertainty results [9].

A third barrier is the wired connectivity of tracking interferometers, which may restrict their movements.

Currently, three kinds of tracking interferometers are being employed on large scale metrology with multilateration purposes. They offer different spatial displacement measurement uncertainties (U) [9]:

1. Laser tracer. $U (k = 2) = 0.2 \mu\text{m} + 0.3 \mu\text{m}/\text{m}$
2. Absolute distance meter (ADM)-based laser tracker. $U (k = 2) = 10 \mu\text{m} + 0.4 \mu\text{m}/\text{m}$
3. Absolute interferometer (AIFM)-based laser tracker. $U (k = 2) = \pm 0.5 \mu\text{m}/\text{m}$ [10]

Some new commercial models of laser trackers already offer the possibility to transfer acquired data through integrated wireless LAN communication. This tackles the third barrier, so that a tracking interferometer can already be embedded into a large manufacturing system for an automated calibration process.

3. Integrated multilateration: workflow and model

The idea of integrating a tracking interferometer into the manufacturing system breaks with the typical multilateration approach. Thus, the tracking interferometer moves to every measurement point while reflectors represent the fixed fiducial points. Fig. 1 shows the integrated multilateration scheme.

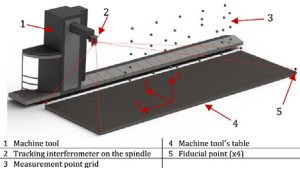


Fig. 1. Integrated multilateration distribution on a MT.

In this measuring scenario, the volumetric point grid to be measured represent the points to which the tracking interferometer is sequentially moved to acquire distance measurements to the four fiducial reflectors fixed around the manufacturing system. Compared to the typical multilateration approach, where tracking capacity is needed on the tracking interferometer side to track reflector's position in space, this integrated solution presents an absolutely different measurement sequence. In this case, tracking interferometer is moved to every measurement point, from which pointing to every fiducial point occurs in sequence. It means that spatial relationship between fiducial points and volumetric point grid shall be established beforehand.

3.1. Automation of the measurement acquisition sequence

For the automation of the measurement acquisition sequence, spatial relationship between fiducial points and point grid needs to be characterized in the MT coordinate system. This is executed in two main steps:

1. MT is moved sequentially to four corner points (one point out of plane) of the point grid volume and the tracking interferometer, working as a laser tracker, measures the 3D position of every fiducial point from every corner point. Best-fit transformation is applied among the four-data set. Thus, spatial transformation between corner points and fiducial points is solved in a local coordinate system, defined by default at the first laser tracker measuring station.
2. Previous measurement's coordinate system is transformed to the MT coordinate system. To do that, on the previous measurement, the four corner points' coordinates are transformed to the MT coordinate system by means of a second best-fit transformation.

Once that spatial relationship between points is solved in the MT coordinate system, nominal point grid information helps to command the pointing from tracking interferometer to every fiducial point for every measurement position. To do it automatically, MT movement and data acquisition sequence are synchronized. This is done by means of a wireless LAN communication between data acquisition software and the MTs interface. Thus, a measurement trigger is sent from every measurement position to synchronize last fiducial point acquisition with MT next movement.

3.2. Multilateration

Multilateration [6–8] is an already known mathematical technique that employs pure distance measurements, D_{ij} , to determine the 3D position of each point. Hence, for each of the N points forming the point grid and for each of the M fiducial points (usually four points), the general Eq. (1) is obtained:

$$(D_{ij} + L_{offset})^2 = (P_{ix} - T_{jx})^2 + (P_{iy} - T_{jy})^2 + (P_{iz} - T_{jz})^2 \quad (1)$$

wherein:

- D_{ij} is a pure distance measurement taken from point i of the point grid to fiducial point j with the tracking interferometer. Therefore, there are $N \times M$ distance measurements, since N is the number of points in the point grid, $1 < i < N$, and M is the number of fiducial points, $1 < j < M$.
- L_{offset} is an initial offset value for any interferometry based measurement, since interferometers measure relative values. If an absolute distance measurement system is used, $L_{offset} = 0$.
- T_j is the position of fiducial point j , $1 < j < M$.
- P_i is the position of point i of the point grid, $1 < i < N$.

The system to be solved is a non-linear overdetermined system of equations, so that, in addition to the 3D position of every point, length residuals that do not fit to the system are also obtained. These residuals provide information about how accurate every length measurement is.

The volumetric 3D positioning error of the machine under measurement is thus determined by comparing the real spatial data, obtained by multilateration, versus the nominal data.

3.3. Monte Carlo simulation

JCGM 101:2008 guide (Evaluation of measurement data – Supplement 1 to the “Guide to the expression of uncertainty in measurement” – Propagation of distributions using a Monte Carlo method) describes a practical guidance on the application of Monte Carlo simulation for the estimation of uncertainty in measurement [11]. For the present work this guide is employed to determine the measurement uncertainty of the integrated multilateration approach. It involves the propagation of the distributions of the input source of uncertainty, D_{ij} , by using the laser tracker distance error model to provide the distribution of the output, T_j and P_i . As a result, the expanded uncertainty for every measured point is assessed.

The coordinate uncertainty simulation process starts defining the uncertainty error model of the laser tracker as a combination of the uncertainty of the pure length measurement (U_L), the uncertainty of the azimuth angular measurement (U_θ) and the uncertainty of the elevation angular measurement (U_δ). Since laser tracker angular measurements are discarded on the multilateration approach, just the U_L uncertainty parameter is considered during the simulation.

A new input variable, DS_{ij} , is defined as the simulated length measurement for every ij distance. It is calculated by Eq. (2):

$$DS_{ij} = D_{ij} + (U_L * f) \quad (2)$$

wherein:

- DS_{ij} = simulated length measurement for ij distance.
- D_{ij} = actual length measurement taken by the tracking interferometer.
- U_L = uncertainty of pure length measurement.
- f = random number generator. For this work, the Box–Muller random generator [12] is applied to sample Gaussian distribute random numbers.

Eq. (1) is updated to Eq. (3) for the Monte Carlo simulation realization:

$$(DS_{ij} + L_{offset})^2 = (P_{ix} - T_{jx})^2 + (P_{iy} - T_{jy})^2 + (P_{iz} - T_{jz})^2 \quad (3)$$

The range of either T_j (fiducial points) or P_i (grid points) as output parameters after Monte Carlo simulation represents the propagation of their respective distributions, so it describes the measurement uncertainty for every point contained in the measurement scenario. As demonstrated by Schwenke et al. in Ref. [7], 20–100 iterations shall be enough to achieve reliable uncertainty results.

4. Concept simulation and experimental demonstration

Integrated multilateration performance has been validated by an experimental demonstration. Previously a Monte Carlo simulation has been carried out to guarantee that it fulfils with the current state of art of industrial multilateration uncertainty.

4.1. Simulation of different scale measurement scenarios

According to Eq. (3), different scale measuring volumes have been simulated based on length measurements performed by a Leica AT402 laser tracker. The goal is to show that integrated multilateration keeps the same uncertainty levels as typical multilateration approach does for different scale measurement scenarios. In second term, it also demonstrates how multilateration method improves the 3D measurement accuracy of a single laser tracker. For that purpose, small, medium and large-scale measuring scenarios have been simulated, defined by a point grid of 48 points distributed as follows: 4 points in X axis, 4 points in Y axis and 3 points in Z axis (vertical direction). Measurement volumes are defined next (XYZ):

1. Small = 1000 mm × 1000 mm × 1000 mm.
2. Medium = 3000 mm × 3000 mm × 3000 mm.
3. Large = 8000 mm × 4000 mm × 1000 mm.

Four 3D measurement approaches have been tested under simulation to determine their spatial uncertainty assessment:

1. Laser tracker measurement.
2. Typical multilateration measurement.
3. Unified spatial metrology network (USMN) measurement which runs in the Spatial Analyzer software [13].
4. Integrated multilateration measurement.

Pure length measurement (U_L) uncertainty for an AT402 laser tracker is supplied by Leica according to Eq. (4):

$$U_L = U_F + U_M \quad (4)$$

wherein:

- U_L = Uncertainty of pure length measurement.
- U_F = Uncertainty of fixed length error that applies to all distance measurements. For a Leica AT402 laser tracker it is 0.00762 mm ($k = 1$).
- U_M = Uncertainty of additional length error as measurement distance increases. For a Leica AT402 laser tracker it is 2.5 $\mu\text{m}/\text{m}$ ($k = 1$).

Thus, pure length measurement error model (U_L) has been introduced in Eq. (2) to calculate DS_{ij} for each D_{ij} length measurement. Finally, Eq. (3) has been solved to calculate T_j and P_i .

Monte Carlo simulation has been performed with 500 iterations. Temperature variation has not been considered in the simulation. Uncertainty results are expressed in micrometres for a level of confidence of 95%, that is within 2 standard deviations for a normal distribution ($k = 2$).

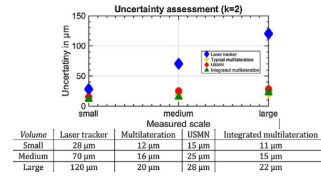


Fig. 2. Uncertainty values obtained by simulation of four 3D measurement approaches.

According to simulated results depicted in Fig. 2, integrated multilateration uncertainty values are similar to what achieved with either typical multilateration or USMN approaches, which are already validated 3D industrial measurement solutions.

4.2. Concept demonstration and results

Integrated multilateration performance has been evaluated for a small volume point grid. Leica AT402 laser tracker was mounted in a Kuka KR60 industrial robot and four fiducial points were fixed surrounding the robot. AT402 laser tracker measured absolute distances, so L_{offset} in Eq. (3) is equal to 0. Fig. 3 shows the measurement setup.

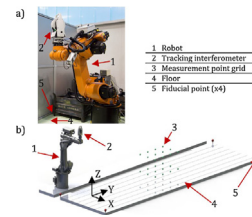


Fig. 3. Integrated multilateration concept demonstration on a Kuka KR60 industrial robot: (a) real setup; (b) virtual model.

A point grid of 24 points divided into 3 points in X axis, 4 points in Y axis and 2 points in Z axis (vertical direction) were measured automatically by the laser tracker. The measurement volume was defined as follows: X = 300 mm; Y = 300 mm; Z = 100 mm. Points 1 ÷ 12 comprise XY plane in Z = 100 mm and points 13 ÷ 24 comprise XY plane in Z = 0 mm. Firstly, robot is moved to points 1 ÷ 12 depicting the upper XY plane and then, points 13 ÷ 24 describe bottom XY plane.

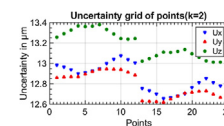


Fig. 4. Uncertainty result for point grid in X, Y and Z directions.

From every measurement point, every fiducial point was measured, so that a total of 96 measurements (D_{ij}) were sequentially introduced in Eqs. (2) and (3) for the Monte Carlo simulation of the real measurement scenario. 300 iterations were run to determine the measurement uncertainty (U) for every measurement point in X, Y and Z directions (U_x , U_y and U_z , respectively). Fig. 4 shows the measurement uncertainty results for every point (P_i) for a level of confidence of 95% ($k = 2$).

Results show interesting conclusions:

- Upper XY plane (points 1 ÷ 12) and bottom XY plane (points 13 ÷ 24) show similar uncertainty distribution, which represents robot measurement sequence in directions +X + Y – X – Y for each XY plane.
- Every direction uncertainty in bottom XY plane is slightly smaller (in average 0.2 μm) since distance measurement between tracking interferometer and fiducial points is 100 mm shorter. Difference is numerically in accordance with U_M parameter defined in Eq. (4).
- Concept experimental demonstration uncertainty results are similar to simulation uncertainty results shown in Fig. 2.

In addition to the volumetric point grid uncertainty analysis, there is an extra numerical analysis that allows understanding the quality of the performed pure length measurements. It is based on calculating length residuals between real length data and calculated data, according to Eq. (5):

$$L_{res} = D_{ij} - L_{calculated} \quad (5)$$

wherein:

- L_{res} = residual of pure length measurement.
- D_{ij} = actual length measurement taken by the tracking interferometer.
- $L_{calculated}$ = length measurement for every ij distance, calculated as the difference between P_i and T_j after solving Eq. (3).

Fig. 5 shows each length residual (L_{res}) defined in Eq. (5).

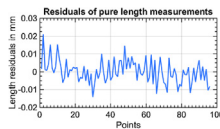


Fig. 5. Length residuals results for the concept demonstration measurement.

For the concept demonstration measurement, in total 96 length residuals were calculated. Results show that standard deviation of length residuals was 0.0065 mm, slightly smaller than uncertainty of fixed error measurement of the employed tracking interferometer (U_F) defined in Eq. (4). It means that either length residuals results or uncertainty results shown in Fig. 4, are similar to the accuracy of the employed tracking interferometer. It concludes that thermally induced dimensional drift is smaller than uncertainty results achieved on such a fast measurement acquisition sequence in this case. In fact, the total time consumption for the presented measurement case was 8 min, which means that AT402 laser tracker took 20 s to measure the four fiducial points from every measurement point. Compared to a typical multilateration measurement scheme where point grid measurement is repeated four times, integrated multilateration approach reduces total time consumption to a unique point grid measurement.

5. Conclusions

This paper presents an integrated multilateration measurement approach for medium and large-scale manufacturing system verification. The research has demonstrated for the first time that volumetric automatic verification and therefore, calibration is a real possibility maintaining levels of uncertainty in the range of micrometres.

Main advantages compared to the typical multilateration solution are the following:

1. Total time consumption during data acquisition is reduced to a 25%, since a unique point grid movement is needed.

2. Uncertainties for multilateration results are improved because thermal drift during data acquisition, mainly on the manufacturing system side, is reduced. Thermal drift is somehow proportional to time consumption in a non-controlled shop floor environment.
3. No human intervention is needed during the data acquisition process, since laser tracker is automatically moved to every measurement position.

The integrated multilateration concept has been validated in this work using an industrial robot. However, since its main application will be machine tool automatic verification, two main considerations have to be taken into account:

1. The static stiffness of the KUKA KR 60 robot has been measured with a laser tracker, showing values lower than 10 N/μm. Therefore, for the weight of the employed Leica AT402 laser tracker (7.3 kg) the vertical deflection could be in the range of more than 10 μm. However, typical static stiffness values are above 100 N/μm for a gantry type MT and around 30N/μm for a moving column MT. In these cases, the vertical deflection would be below 0.7 μm and 2.5 μm, respectively, which are even lower than the measurement uncertainty values of the multilateration technique (see Fig. 2).
2. The Leica AT402 laser tracker used for the experiments could not work properly upside down, so the measurement volume for concept demonstration was limited by this fact. However, some new models of laser trackers are already able to work upside down and they will be used for the whole volume measurement of a MT as future work.

References

- [1] Mutilba U, Gomez-Acedo E, Kortaberria G, Olarra A, Yagüe-Fabra JA (2017) Traceability of On-Machine Tool Measurement: A Review. *MDPI Sensors* 17:40.
- [2] Uriarte L, Zatarain M, Axinte D, Yagüe-Fabra J, Ihlenfeldt S, Eguia J, Olarra A (2013) Machine Tools for Large Parts. *CIRP Annals – Manufacturing Technology* 62:731–750.
- [3] Schwenke H, Knapp W, Haitjema H, Weckenmann A, Schmitt R, Delbressine F (2008) Geometric Error Measurement and Compensation of Machines—An Update. *CIRP Annals – Manufacturing Technology* 57:660–675.
- [4] McKeown PA, Loxham J (1973) Some Aspects of the Design of High Precision Measuring Machines. *Annals of the CIRP* 22.
- [5] Aguado S, Santolaria J, Samper D, Aguilar JJ (2013) Influence of Measurement Noise and Laser Arrangement on Measurement Uncertainty of Laser Tracker Multilateration in Machine Tool Volumetric Verification. *Precision Engineering* 37:929–943.
- [6] Gomez-Acedo E, Olarra A, Zubieta M, Kortaberria G, Ariznabarreta E, de Lacalle LN (2015) Method for Measuring Thermal Distortion in Large Machine Tools by Means of Laser Multilateration. *The International Journal of Advanced Manufacturing Technology* 80:523–534.
- [7] Schwenke H, Franke M, Hannaford J, Kunzmann H (2005) Error Mapping of CMMs and Machine Tools by a Single Tracking Interferometer. *CIRP Annals – Manufacturing Technology* 54:475–478.
- [8] Olarra A, Zubeldia M, Gomez-Acedo E, Kortaberria G (2013) Measuring Positioning Accuracy of Large Machine Tools. *Proceedings of the 19th Congress of Machine Tools and Manufacturing Technology*, Donostia-San Sebastián, Spain, 12 June.
- [9] Schmitt R, Peterek M, Morse E, Knapp W, Galetto M, Härtig F, Goch G, Hughes B, Forbes A, Estler W (2016) Advances in Large-Scale Metrology—Review and future trends. *CIRP Annals – Manufacturing Technology*.
- [10] Leica Absolute Tracker AT930 Brochure. <http://www.hexagonmi.com/products/laser-tracker-systems/leica-absolute-tracker-at930>. (Accessed 20 December 2017).
- [11] Joint Committee for Guides in Metrology JCGM 101:2008—Evaluation of Measurement Data – Supplement 1 to the ‘Guide to the Expression of Uncertainty in Measurement’ – Propagation of Distributions Using a Monte Carlo method; 2008.
- [12] Calkins JM (2002) *Quantifying Coordinate Uncertainty Fields in Coupled Spatial Measurement Systems*. PhD Dissertation, Virginia Polytechnic Institute and State University.
- [13] Muelaner JE, Jamshidi J, Wang Z, Maropoulos PG (2009) Verification of the Indoor GPS System by Comparison with Points Calibrated Using a Network of Laser Tracker Measurements. *Proceedings of the 6th CIRP-Sponsored International Conference on Digital Enterprise Technology* 607–619.

Integrated volumetric error mapping for large machine tools: An opportunity for more accurate and geometry connected machines



8th Manufacturing Engineering Society International Conference

Integrated volumetric error mapping for large machine tools: An opportunity for more accurate and geometry connected machines

Unai Mutilba^{a,*}, Fernando Egaña^a, Gorka Kortaberria^a, Eneko Gomez-Acedo^a, Aitor Olarra^a, Jose A. Yagüe-Fabra^b

^aDepartment of mechanical engineering, IK4-Tekniker, Eibar, 20600, Spain

^bI3A, Universidad de Zaragoza, C/Maria de Luna 3, Zaragoza, 50018, Spain

Abstract

The trend towards intelligent manufacturing processes and zero-defect manufacturing in key industry players such as transport and energy is pushing metrology close to the manufacturing scenario. High-value components, such as those in aerospace, automotive, wind power and large science facilities demand the ability to manufacture accurate parts in well-controlled manufacturing processes, but disturbances like machine tool geometry defects or temperature fluctuations of the surrounding occur. This paper highlights the role of metrology as a key enabling technology for intelligent manufacturing processes and presents the integration of the multilateration technique for a fast and fully automatic volumetric error mapping of large machine tools. The approach does not just reduce the total time consumption up to 75% compared to the current state of the art, but it also improves the measurement uncertainty considerably. This paper explains the integration exercise of the multilateration technique on a large machine tool and compares the obtained results against the classic sequential volumetric error mapping approach.

© 2020 The Authors. Published by Elsevier B.V. This is an open access article under the CC BY-NC-ND license (<https://creativecommons.org/licenses/by-nc-nd/4.0/>)

Peer-review under responsibility of the scientific committee of the 8th Manufacturing Engineering Society International Conference

Keywords: Multilateration; volumetric error mapping; integrated; laser tracker; large machine tool

1. Introduction

As stated by Imkamp et al. [1], the manufacturing metrology roadmap must address five main challenges: speed, accuracy, reliability, flexibility and holistic measurements.

* Corresponding author. Tel.: +34 636 994 351 .
E-mail address: unai.mutilba@tekniker.es

These challenges are also demanded by “Industry 4.0” for the future development of industrial production where the aim is to improve the manufacturing industry with information-rich technology [2]. In this context, the integration of a multilateration solution into the MT contributes to cover most of the challenges, where the solution allows enhancing several fundamental issues affecting to the performance of large manufacturing systems [3].

Since the introduction of the volumetric accuracy concept by McKeown and Loxham in 1973 [4], significant research work has been presented [3, 5–8] towards volumetric error mapping and compensation of MTs. The main conclusion of these investigations is that indirect measurement methods have the advantage of offering fast and reliable volumetric error performance assessment for medium and large scale MTs, opposite to direct measurement methods that are very time-consuming and have strong limitations.

In this scenario, multilateration-based approaches are by far the most employed verification solution among indirect measurement methods for large machine tools. Currently, the classic approach relies on interferometric or absolute displacement measurements between tracking interferometers that are fixed to the machine base and a reflector, fixed to the machine spindle, near to the TCP. However, this approach shows some industrial limitations such as its total time consumption due to sequential measurement scheme or thermal drift that prevent an automatic MT error mapping and calibration [5].

This paper presents an integrated multilateration error mapping approach where a tracking interferometer is directly attached to the manufacturing system spindle. The concept was validated on a large machine tool against the classic multilateration approach and results show that the integrated approach enables more accurate and geometry-connected MTs [5].

Nomenclature

MT	Machine tool
TCP	Tool Centre Point

2. Multilateration technique for MT error mapping

Multilateration [5–10] is an already known mathematical technique that employs pure distance measurements, D_{ij} , to determine the 3D position of each point. Hence, for each of the N points forming the point grid and for each of the M fiducial points (usually four points), the general Eq. (1) is obtained [5]:

$$(D_{ij} + L_{\text{offset}})^2 = (P_{ix} - T_{jx})^2 + (P_{iy} - T_{jy})^2 + (P_{iz} - T_{jz})^2 \quad (1)$$

where:

- D_{ij} is a pure distance measurement taken from point i of the point grid to fiducial point j with the tracking interferometer. Therefore, there are $N \times M$ distance measurements, since N is the number of points in the point grid, $1 < i < N$, and M is the number of fiducial points, $1 < j < M$.
- L_{offset} is an initial offset value for any interferometry-based measurement since interferometers measure relative values. If an absolute distance measurement system is used, $L_{\text{offset}} = 0$.
- T_j is the position of fiducial point j , $1 < j < M$.
- P_i is the position of point i of the point grid, $1 < i < N$.

The system to be solved is a non-linear overdetermined system of equations, so that, in addition to the 3D position of every point, length residuals that do not fit to the system are also obtained. These residuals provide information about how accurate every length measurement is. The volumetric 3D positioning error of the machine under

measurement is thus determined by comparing the real spatial data, obtained from the measurement, versus the nominal data.

Currently, three tracking interferometers are being employed on large-scale metrology when applying multilateration with different displacement measurement uncertainty:

- Tracking interferometers based on optimized laser trackers. They rely on a high accuracy sphere as an optical reference for interferometric measurement. This measurement equipment, called laser tracer [11], was developed by NPL and PTB and commercialized by Etalon AG. It has a spatial displacement measurement uncertainty of $U(k=2) = 0.2 \mu\text{m} + 0.3 \mu\text{m}/\text{m}$. While laser tracer is a suitable solution for medium and large size MTs, there is a similar solution to the laser tracer, "called laser tracer MT" with a telescopic scheme and employed for maximum measuring volumes of 1 m^3 [12].
- Absolute Distance Meter (ADM) based laser tracker has a spatial displacement measurement uncertainty of $U(k=2) = 10 \mu\text{m} + 0.4 \mu\text{m}/\text{m}$ in its whole working range [13].
- Absolute Interferometer (AIFM) based laser tracker has a spatial displacement measurement uncertainty of $U(k=2) = \pm 0.4 \mu\text{m} + 0.3 \mu\text{m}/\text{m}$ [14].

The tracking interferometer employed for multilateration shall fit inside the measuring volume to execute the measuring procedure. Such a requirement restricts the tracking interferometer to be employed for any size MT. For small size machine tools, the equipment that suitably fits into the measuring volume is the so-called laser tracer MT, it makes use of a metrological beam guiding method of the laser interferometer. For medium and large size MTs, either laser tracers or laser trackers are suitable for the error mapping. However, it should be stated that new laser trackers are portable devices that offer the possibility to be embedded into large manufacturing or measuring systems and they transfer data through an integrated wireless LAN communication which allows to wireless employment of the acquisition technology [10].

To understand the quality of the performed measurements on a multilateration approach, there is a numerical analysis that allows understanding the residuals of the pure length measurements. It is based on calculating length residuals between real length data and calculated data, according to Eq. (2):

$$L_{res} = D_{ij} - L_{calculated} \quad (2)$$

where:

- L_{res} = Residual of pure length measurement.
- D_{ij} = Actual length measurement taken by the tracking interferometer.
- $L_{calculated}$ = Length measurement for every ij distance, calculated as the difference between P_i and T_j after solving Equation (1).

3. Multilateration based approach: from the classic approach to the integrated solution

Multilateration based measurement for MT error mapping requires at least four fixed points for displacement measurement, either absolute or relative, between those fixed points and any moving measuring point. According to this measurement distribution requirement, typically tracking interferometers are set on the MT table in the fixed points' positions and a measuring reflector is attached to the moving spindle to materialize the moving points. This classic multilateration configuration (here-in-after classic multilateration) is the first barrier to an automated MT calibration solution since manual intervention is needed on fixing tracking interferometers to each measurement station.

Commonly only one tracking interferometer is available, so in practice, multilateration measurements are done in a sequential scheme, as follows: MT movements are repeated several times to the same positions and measurements are taken from different tracking interferometer locations. Consequently, time consumption during measurement realization increases and, therefore, thermal drift between sequential measurements occurs. This becomes the second

barrier to an automated solution since this approach requires MT repeatability for suitable multilateration uncertainty results [5]. Figure 1 shows the classic multilateration approach performed with a laser tracer NG from ETALON AG on a ZAYER ARION G large MT [7].

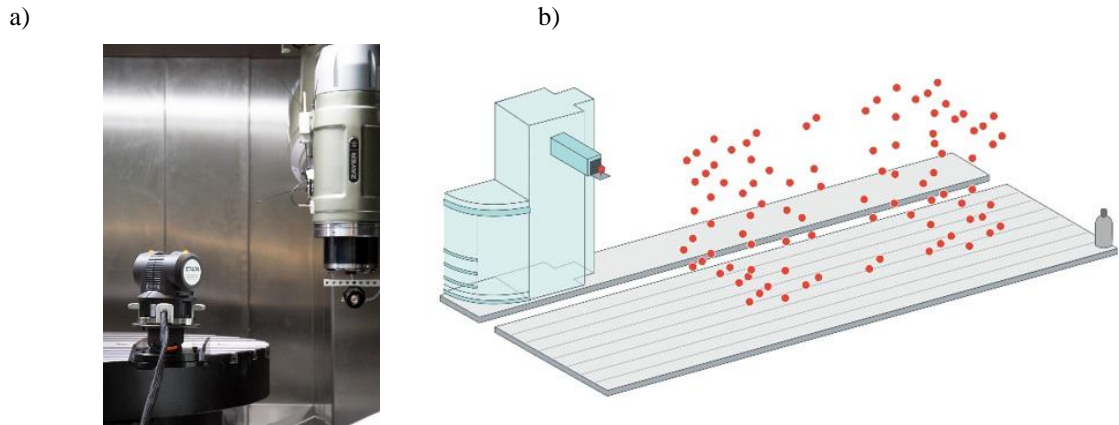


Fig. 1. Sequential multilateration scheme: a) ZAYER ARION G large machine tool employing a laser tracer NG and b) virtual representation of the sequential measurement scheme. (Measurement performed by IK4-TEKNIKER in collaboration with ZAYER)

When four tracking interferometers are available simultaneously, multilateration measurements can be performed according to the simultaneous scheme. Results are not obtained in real-time because mathematical post-processing is needed after data acquisition, but it avoids some of the limitations of the sequential multilateration, such as total time consumption, MT repeatability requirement and MT drift due to thermal variation during the measuring process. The simultaneous approach demands a unique movement to each point comprising the measurement point grid, which enables a reduction of the total acquisition time up to 75%. Measurement uncertainties are also improved because thermal drift during data acquisition, mainly on the manufacturing system side, is reduced. Thermal drift is somehow proportional to time consumption in a non-controlled shop floor environment [5]. However, the total cost for the simultaneous multilateration approach is high because it demands four tracking measurement systems to be working simultaneously and two reflectors on the MT side attached to the spindle. This is the main barrier that prevents this approach from being a common practice to map the volumetric geometric error of MTs. Figure 2 shows a simultaneous multilateration approach on a ZAYER KAIROS large machine tool where four tracking measurement systems are working simultaneously.

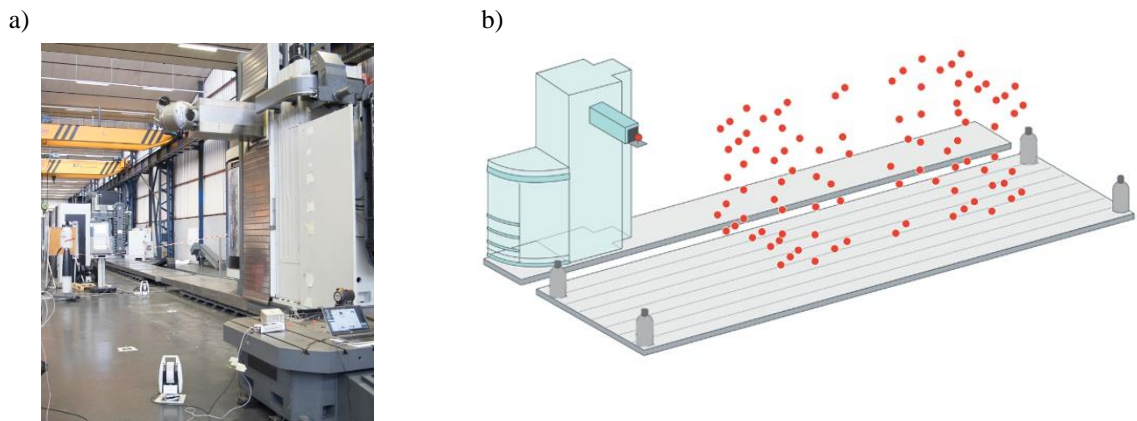


Fig. 2. Simultaneous multilateration scheme: a) ZAYER KAIROS large machine tool employing three laser trackers and one laser tracer NG and b) virtual representation of the measurement sequence scheme. (Measurement performed by IK4-TEKNIKER in collaboration with ZAYER)

Multilateration solution for volumetric error mapping performed either in sequential mode or in simultaneous approach leads to industrial limitations such as cost, total time consumption or thermal drift that prevent an automatic calibration of the MT.

The idea of integrating a tracking interferometer into the manufacturing system breaks with the previous multilateration approaches. Thus, the tracking interferometer moves to every measurement point while reflectors represent the fixed fiducial points. The volumetric point grid to be measured represent the points to which the tracking interferometer is sequentially moved to acquire distance measurements to the four fiducial reflectors fixed around the manufacturing system. Compared to the classic multilateration approach, where tracking capacity is needed on the tracking interferometer side to track reflector's position in space, this integrated solution presents a different measurement sequence. In this case, tracking interferometer is moved to every measurement point, from which pointing to every fiducial point occurs in sequence. It means that spatial relationship between fiducial points and volumetric point grid shall be established beforehand [5]. Figure 3 shows the integrated multilateration scheme.

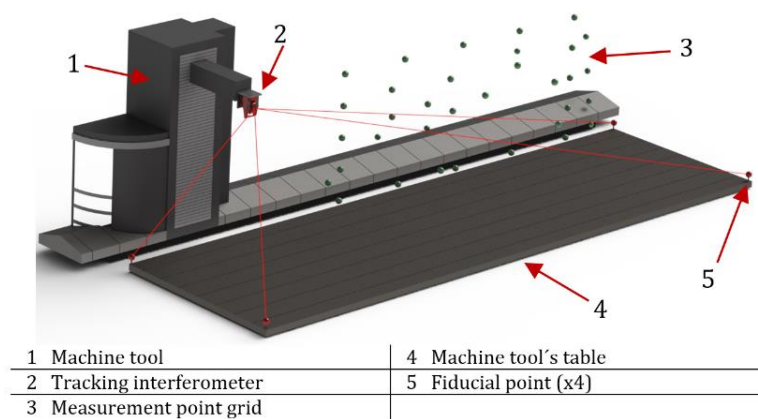


Fig. 3 Integrated multilateration scheme [5].

4. Experimental validation of the integrated multilateration approach

The validation of the integrated approach was performed on a MEMPHIS machine tool at ZAYER MT manufacturer premises. The point grid to be measured was comprised of 64 points. The mapped working range of the MT was: X = 3000 mm, Y = 2300 mm and Z = 900 mm. The validation plan is explained next:

- MT volumetric error mapping was performed with the classic approach employing a laser tracer NG from ETALON AG. Four measurement positions were employed and measurement acquisition time was 2 h and 30 min.
- Integrated multilateration approach was executed with a LEICA AT960 laser tracker fixed to the MT spindle, upside down. Four cat-eye reflectors defined the fiducial points, three of them fixed to the floor and the fourth one fixed out of the floor plane to improve the measurement accuracy on the vertical direction. The total time consumption for the integrated approach was 25 min.

The validation of the integrated multilateration approach against the classic approach was performed comparing three specific results:

- Residuals of pure length measurements, L_{res} parameter according to Eq. (2).
- Uncertainties of volumetric points and fiducial points after multilateration exercise.

c) Comparison between point clouds after multilateration performance, the difference between the point grid measured by both approaches was performed. In this way, the 3D coordinates were calculated from both approaches and a best-fit transformation was executed to compare them.

a) The standard deviation of pure length measurements for the integrated approach was $2.47\ \mu\text{m}$ while the same value for the classic approach was $1.1\ \mu\text{m}$. Therefore, the standard deviation of pure length measurements results obtained by the classic approach were better than those of the integrated approach. The reason is that three points were not correctly measured by the integrated approach (run by hand), which makes the fitting exercise become worse.

b) Figures 4 and 5 present the uncertainty results after multilateration of the fiducial points and the point grid respectively. Results show that uncertainties were better for the integrated approach compared to the classic approach. The measurement scenario was similar, but the measurement time was reduced to 25 min on the integrated approach which is the main reason that better uncertainties were performed since the less time-consumption the less thermal drift influence.

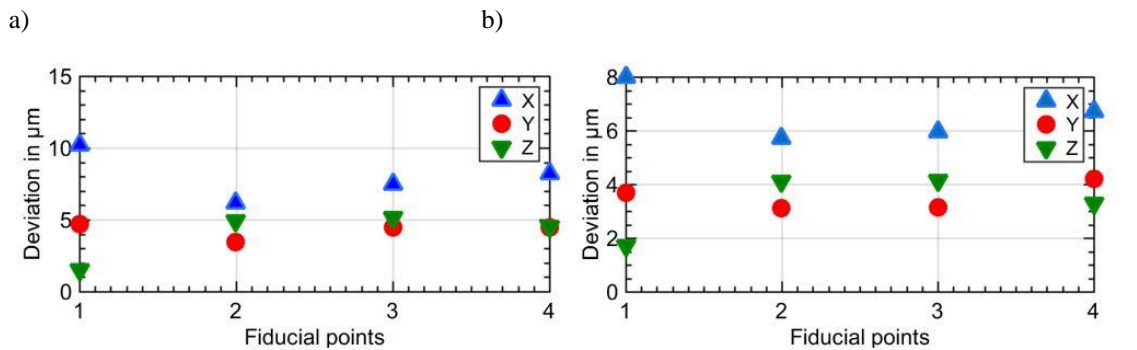


Fig. 4 Uncertainty results of the fiducial points after multilateration exercise: a) classic approach and b) integrated approach

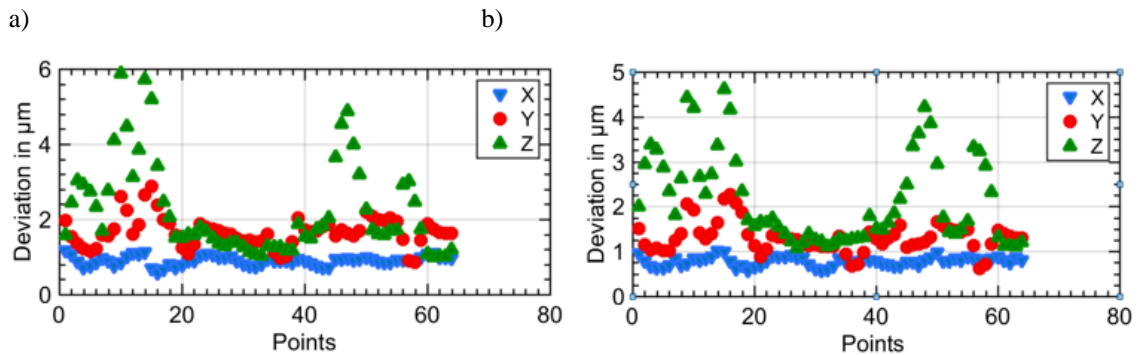


Fig. 5 Uncertainty results for the point grid after multilateration exercise: a) classic approach and b) integrated approach

c) Finally, a comparison between point clouds was executed to understand the difference between both approaches. Figure 6 shows the difference in mm at each point comprising the point grid. The standard deviation was $0.04\ \text{mm}$ and there was a vertical axis where the deviation was higher between both approaches (points in red). It shall be remarked that the three points were not properly measured on that axis, which means that results were getting worse because of this fact.

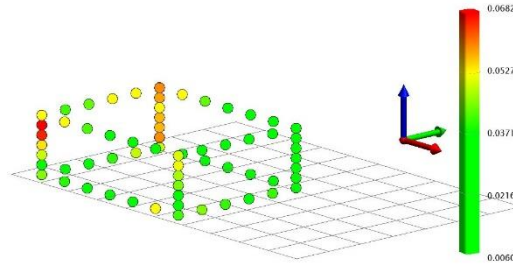


Fig. 6 3D comparison between both approaches. (in mm)

Figure 7 shows the integrated multilateration approach validation on a ZAYER MEMPHIS large machine tool with a LEICA AT960 laser tracker fixed to the spindle. It was fixed upside down to improve the visibility between the tracking interferometer and the fiducial points.

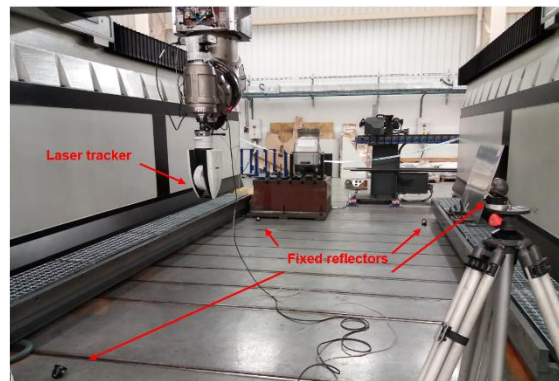


Fig. 7 Integrated multilateration validation approach on a ZAYER MEMPHIS large machine tool employing a LEICA AT960 laser tracker.

5. More accurate and geometry connected machine tools

The integration of an error volumetric mapping solution on an MT offers the possibility to enhance several fundamental issues affecting the performance of those manufacturing systems:

- To reduce the time consumption for a complete volumetric error mapping of a large machine tool, up to 75% of time reduction. Similarly, it helps to reduce the measurement uncertainty, which is somehow proportional to time consumption in a non-controlled shop-floor environment.
- To provide an automatic and volumetric machine tool error mapping process with no human intervention.
- To supply an interim check tool to monitor the volumetric performance of the machine tool regularly. Diagonal displacement test defined in ISO 230-6 [15] could help to assess that the volumetric performance of the MT continues within specifications.
- To provide an active and integrated machine tool geometry error supplier for the industry 4.0 MT platforms. This concept is brand new because current industry 4.0 platforms do not show volumetric and geometric error information during the lifetime of the manufacturing systems.
- To improve the current on-MT measurement state of the art: This integrated solution offers the possibility to perform a volumetric error mapping of the MT right after the machining process. It allows to distinguish the error sources affecting the machining and measuring processes, so the systematic error affecting the on-MT measurement could be corrected and therefore, reduced.

6. Conclusions

This paper presents an integrated multilateration measurement approach for medium and large-scale manufacturing system automatic verification. A validation work was performed on a large MT at ZAYER MT manufacturer premises. A LEICA AT960 laser tracker was integrated on the MT spindle to perform the integrated scheme and obtained results were compared with a previous classic multilateration measurement. Results show that the integrated solution is more accurate than the classic approach, mainly because the time consumption is reduced to 25%, compared to the classic measurement scheme. The total measurement time for the integrated measurement was 25 min for a volumetric point grid comprised of 64 points.

The integration of the solution into the MT offers the possibility to provide an automatic and volumetric machine tool error mapping process with no human intervention. It allows to improve the current volumetric error mapping process but mainly, it permits to perform a regular geometric interim check of the MT. This check could provide to the industry 4.0 machine tool platforms with the geometric information of the MT during its lifetime and this way, ensure the ability of the MT to manufacture high-value components. Additionally, new functionalities such as on-MT measurement or geometrically connected MTs could be a step forward for more intelligent manufacturing processes and zero-defect manufacturing strategy.

Acknowledgement

This research is supported by ZAYER who provided insight and expertise that greatly assisted the experimental research presented here.

References

- [1] Imkamp D, Berthold J, Heizmann M, et al. Challenges and trends in manufacturing measurement technology – the ‘Industrie 4.0’ concept. *Journal of Sensors and Sensor Systems* 2016; 83: 325–335.
- [2] Leach R, Senin N, Feng X, et al. Information-rich metrology : Changing the game.
- [3] Mutilba U, Gomez-Acedo E, Kortaberria G, et al. Traceability of On-Machine Tool Measurement: A Review. *MDPI Sensors* 2017; 17: 40.
- [4] McKeown PA, Loxham J. Some aspects of the design of high precision measuring machines. *Annals of the CIRP*; 22.
- [5] Mutilba U, Yagüe-Fabra JA, Gomez-Acedo E, et al. Integrated multilateration for machine tool automatic verification. *CIRP Annals* 2018; 67: 555–558.
- [6] Olarra A, Zubeldia M, Gomez-acedo E, et al. *Measuring positioning accuracy of large machine tools*. 2012.
- [7] Schwenke H, Franke M, Hannaford J, et al. Error mapping of CMMs and machine tools by a single tracking interferometer. *CIRP Annals - Manufacturing Technology* 2005; 54: 475–478.
- [8] Schwenke H, Knapp W, Haitjema H, et al. Geometric error measurement and compensation of machines—An update. *CIRP Annals - Manufacturing Technology* 2008; 57: 660–675.
- [9] Gomez-Acedo E, Olarra A, Zubieta M, et al. Method for measuring thermal distortion in large machine tools by means of laser multilateration. *The International Journal of Advanced Manufacturing Technology* 2015; 80: 523–534.
- [10] Schmitt R, Peterek M, Morse E, et al. Advances in Large-Scale Metrology – Review and future trends. *CIRP Annals - Manufacturing Technology*. Epub ahead of print 2016. DOI: 10.1016/j.cirp.2016.05.002.
- [11] Etalon AG. Etalon AG laser tracer NG brochure, <https://www.etalon-ag.com/en/products/lasertracer/> (2018).
- [12] Etalon AG. Etalon AG laser tracer MT brochure, <https://www.etalon-ag.com/en/products/lasertracer-mt/> (2018).
- [13] Leica. Leica absolute tracker AT402 brochure, <https://www.hexagonmi.com/products/laser-tracker-systems/leica-absolute-tracker-at403> (2018).
- [14] Leica. Leica absolute tracker AT930 brochure, <http://www.hexagonmi.com/products/laser-tracker-systems/leica-absolute-tracker-at930> (2016).
- [15] ISO. *ISO 230-6: 2002. Test code for machine tools -- Part 6: Determination of positioning accuracy on body and face diagonals (Diagonal displacement tests)*.

**3D metrology simulation and relative pointing error verification of the
Telescope Mount Assembly subsystem for the Large Synoptic Survey
Telescope**

Article

3D Measurement Simulation and Relative Pointing Error Verification of the Telescope Mount Assembly Subsystem for the Large Synoptic Survey Telescope [†]

Unai Mutilba ^{1,*} , Gorka Kortaberria ¹, Fernando Egaña ¹ and Jose Antonio Yagüe-Fabra ² 

¹ Department of Mechanical Engineering, IK4-Tekniker, 20600 Eibar, Spain; gorka.kortaberria@tekniker.es (G.K.); fernando.egana@tekniker.es (F.E.)

² I3A, University of Zaragoza, 50018 Zaragoza, Spain; jyague@unizar.es

* Correspondence: unai.mutilba@tekniker.es; Tel.: +34-636-994-351

[†] This paper is an extended version of the conference paper, Mutilba, U.; Kortaberria, G.; Egaña, F.; Yagüe-Fabra, J.A. Relative pointing error verification of the Telescope Mount Assembly subsystem for the Large Synoptic Survey Telescope. In Proceedings of the 5th IEEE International Workshop on Metrology for Aerospace, Rome, Italy, 20–22 June 2018.

Received: 10 July 2018; Accepted: 5 September 2018; Published: 10 September 2018



Abstract: An engineering validation of a large optical telescope consists of executing major performing tests at the subsystem level to verify the overall engineering performance of the observatory. Thus, the relative pointing error verification of the telescope mount assembly subsystem is of special interest to guarantee the absolute pointing performance of the large synoptic survey telescope. This paper presents a new verification method for the relative pointing error assessment of the telescope mount assembly, based on laser tracker technology and several fiducial points fixed to the floor. Monte-Carlo-based simulation results show that the presented methodology is fit for purpose, even if floor movement occurs due to temperature variation during the measurement acquisition process. A further research about laser tracker technology integration into the telescope structure may suggest that such laser tracker technology could be permanently installed in the telescope in order to provide an active alignment system that aims to detect and correct possible misalignment between mirrors or to provide the required mirror positioning verification accuracy after maintenance activities. The obtained results show that two on-board laser tracker systems combined with eight measurement targets could result in measurement uncertainties that are better than 1 arcsec, which would provide a reliable built-in metrology tool for large telescopes.

Keywords: RPE; large synoptic survey telescope (LSST); telescope mount assembly (TMA); laser tracker; simulation; active alignment system; mirror positioning

1. Introduction

The Large Synoptic Survey Telescope (LSST) is a large (8.4 m) wide-field (3.5 degree) survey telescope, which will be located on the summit of Cerro Pachón in Chile. The Telescope Mount Assembly (TMA) subsystem points at and tracks fields on the sky, by providing motions about the azimuth and elevation axes. Therefore, it provides pointing, tracking, and slewing system performance requirements to comply with the space survey mission [1]. TMA is currently being assembled in the north of Spain, and the presented method will assess the relative pointing error (RPE) of the subsystem [2].

When observing the sky, it is of great interest to make sure that the telescope is pointing towards the intended location on the sky as accurately as possible, to ensure that it is pointed towards the correct target source and, consequently, to use accurate photometric and astrometric information that is

related to that target. To get an overview, while an amateur telescope can reasonably aspire to 30 arcsec, a giant observatory instrument such as the LSST can point to an absolute pointing performance of 1 arcsec [3].

It shall be highlighted that the pointing and alignment performance of the LSST will have a very strong influence on the quality of the scientific results obtainable. There are typically four requirements that are of particular interest on a large telescope for scientists: The absolute pointing error (APE), is defined as the angular separation between the actual direction and the intended telescope line-of-sight. The absolute measurement accuracy (AMA) is defined as the angular separation between the actual direction and the reconstructed direction of the telescope. The absolute pointing drift (APD), defined as the change in the angular separation between the actual direction and the intended direction of the telescope over the observation time. The relative pointing error (RPE) is defined as the angular separation between the actual direction of an axis and a reference axis, over the instrument exposure time [4] and, therefore, it supplies the short term stability for a large telescope. The RPE requirement for the TMA subsystem in the LSST project is limited to 50 arcsec. at a 95% confidence level ($k = 2$) [5].

In this scenario, no telescope structures and control systems are perfect, so the pointing error always exists. Pointing errors include repeatable and non-repeatable errors. Most of the pointing errors are repeatable, and there are different methods to verify those errors and to provide geometric compensation information to the pointing calibration models on the telescope's final working location [6,7]. However, an end-to-end test of the complete LSST, in order to check the pointing performance and the correct alignment of all the elements, is not possible until the final assembly in Chile is complete. For this reason, the TMA subsystem will first be tested, including RPE requirement, at the factory with surrogate masses, to replace the optical payloads with the aim of avoiding 'late surprises' during the LSST construction in Chile. Thus, LSST project requires a new RPE verification method based on laser tracker technology for the engineering validation of the TMA subsystem.

The main way to quantify the absolute pointing error of a telescope is assessed by the "star tracker" method [8]. As star positions in the sky are known with very high precision, the identification of the star signals provides a powerful tool to check the absolute telescope alignment. In practice, guide star catalogue is considered as a measurable point cloud on the sky, and the least square fitting technique provides the solution for the absolute pointing error assessment [9].

There are different techniques to test the RPE of a critical subsystem in a telescope: (a) To employ an optical pointing telescope (OPT) mounted on the subsystem under verification. The pointing verification measurements of the Atacama large millimetre/submillimetre array (ALMA) antenna were performed using an OPT mounted on the antenna backup structure [10]; (b) error budget is also another approach to make error allocations to the relevant subsystems, i.e., structure, thermal, instrument. Thus, a calibration campaign allows verification at an early stage in the programme, when the main parameters of the optical system are within the allocated alignment budget [4]; (c) laser tracker technology that has been previously discussed for defining coordinates for aligning optical systems [11,12] and also have been considered as a built-in alignment tool for various new-generation large telescope projects, such as the Large Binocular Telescope (LBT) [13] and the Extremely Large Telescope (ELT). In this scenario, the LSST project has defined laser tracker technology as a "facility alignment system", and it will be used during the integration to monitor and to position the elements. Additionally, mount pointing and alignment testing will be done on-site before installing the mirrors and the camera with laser tracker technology, using surrogate masses and a small alignment telescope mounted onto the mount structure [14].

Besides the RPE assessment exercise, large telescopes also require on-board 3D metrology systems to align optical mirrors, or to provide an active alignment system in order to allow misalignment correction between optics, either when they deflect due to variations in thermal environment or when gravity-induced structural flexure affects to the mount [15]. Rakich et al. suggest a telescope metrology system (TMS) that incorporates a large number of absolute distance-measuring interferometers to detect misalignments between primary and secondary mirrors for the giant Magellan telescope

(GMT) [15]. Laser tracker technology has also been under research for that purpose, as commented by Sandwith et al. [16] for the LSST. Rakich et al. also suggested to employ a laser tracker for the active alignment of the large binocular telescope (LBT) [13].

In this paper, a new measurement methodology is presented for the RPE assessment of the TMA for any motion that is within the pointing range of the LSST, based on laser tracker technology and fiducial points. In addition, a Monte-Carlo based simulation platform has been built to assess the achievable accuracy with an on-board laser tracker system, either for active alignment or for the mirror positioning activities at the LSST. The aim of the presented research work is to further investigate the application of laser tracker technology on large scale telescopes, and to provide reliable measurement strategies to be compatible with the required mirror positioning accuracy, which is limited to $1 \div 5$ arcsec for large telescopes [3].

2. Relative Pointing Error Verification

A detailed description of the developed RPE verification method for the LSST is presented.

2.1. Measurement Scenario

The optical axis of the LSST is defined at the M1M3 primary/tertiary mirrors, so that one of the limitations tackled by any RPE measurement procedure is the measurement of the M1M3 mirrors for any pointing motion within a LSST pointing range. Additionally, all the performance requirements must be met for the observing angles between 15 and 86.5 degrees for elevation angles, and from 0 to 360 degrees for azimuth angles. However for maintenance work, the TMA should be able to point from horizon to zenith (i.e., elevation angles from 0 to 90 degrees) [5].

The measurement of the LSST telescope was a large-scale metrology (LSM) exercise [17], since the dimension of the measurement scenario was up to 40 m of diameter. Thus, LSM technology was employed for the suggested RPE characterization: The Leica AT402 laser tracker technology combined with Spatial Analyzer (SA) software from New Rivers Kinematics. Figure 1 shows the measurement scenario for the RPE assessment. Figure 1b illustrates the complete measurement scenario. Figure 1a shows the M1M3 measurement plane, where the measurement targets are depicted in red. Additionally, it also shows that the engineering validation at the subsystem level was verified with dummies instead of the real optical elements.

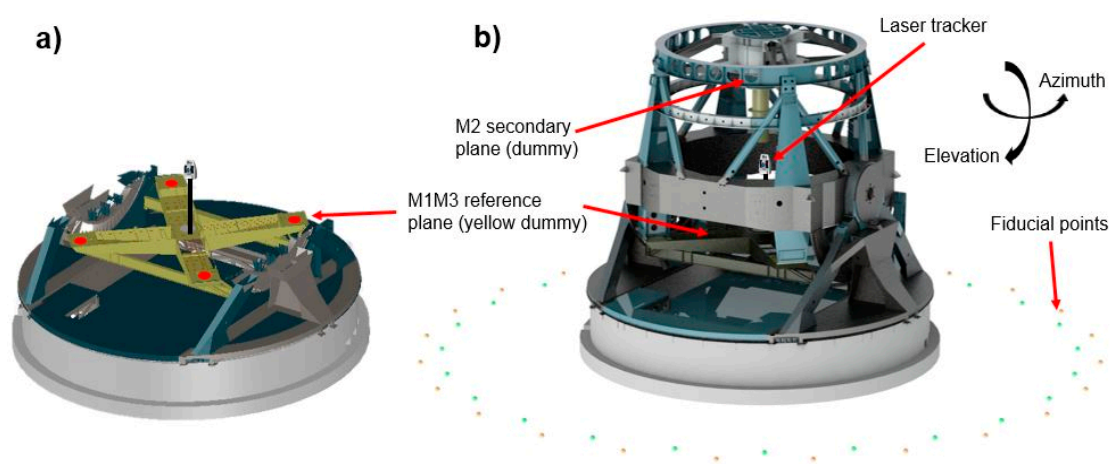


Figure 1. Measurement scenario for RPE assessment. (a) M1M3 measurement plane (measurement targets in red) (b) Complete LSST measurement scenario.

In this measurement scenario, a pointing matrix was defined to characterize the RPE measurement test of the TMA within the pointing range of the LSST. Four elevation angles at four different azimuth positions were defined to represent any pointing direction on the sky, as shown in Figure 2.

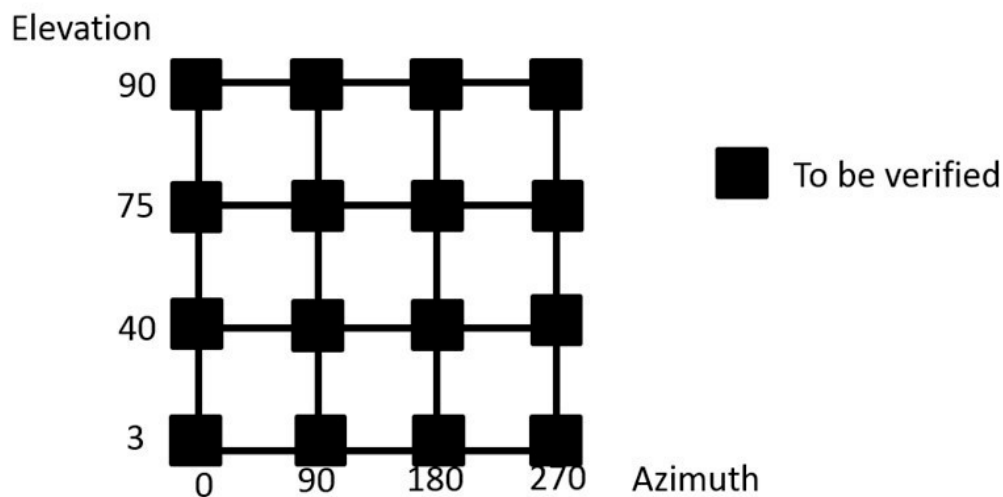


Figure 2. Mapping matrix for the RPE test.

2.2. Measurement Procedure

A new measurement procedure for the RPE assessment was defined as follows: A laser tracker was placed inside of the LSST, close to its origin, and a metrology network comprising a reference point cloud was fixed to the floor, outside and surrounding the LSST telescope. This metrology network was of special importance, as any laser tracker location during the whole measurement process was solved by the measurement of this fiducial metrology network. Thus, the RPE measurement procedure consisted of measurements of the metrology network to locate the laser tracker, and afterwards, measurements of the optical axis of the TMA by measuring four target points at the M1M3 reference plane. Thus, by locating the M1M3 reference plane on an earth fixed reference system, i.e., the floor, each observation angle for TMA was characterized and compared to the input position, which means the RPE assessment. The measurement process was repeated for each of the pointing positions defined in Figure 2, and within the pointing range of the LSST [2]. It should be highlighted that laser tracker position was fixed close to the LSST origin, to nullify the range of the angle of incidence from the laser tracker to the reflectors. Thus, the laser tracker tilts with the rotation centre of the telescope and incidence angle does not change which means that it will not cause a longer travelling path of the beam inside the prism. For the LSST project, 25 mm hollow corner cube optics were employed.

An accurate reference point cloud comprised of 48 points was defined on the floor outside and surrounding the telescope. Twenty-four points created a 15 m radius circle, and 24 additional points defined a 16 m radius with an offset of 7.5° to the previous one. Its circular shape optimized the visibility challenge for any azimuth-pointing position of the telescope. Additionally, those points were fixed to the floor, minimizing thermal gradients effects. Figure 1 shows the metrology network arrangement around the LSST and the M1M3 reference plane where every measurement shall be executed.

The biggest challenge to meet the RPE measurement specification is to ensure that the line of sight between the M1M3 reference plane and the metrology network for any pointing position. Thus, a visibility study was executed within SA software for any elevation axis position. Figure 3 visually represents the line of sight for any elevation angle of the TMA.

Green lines in Figure 3 show the line of sight from the inside-placed laser tracker to the points that comprise the fiducial metrology network. The visibility became worse from the zenith to the horizon TMA pointing direction. However, any TMA pointing direction could be assessed by the presented measurement procedure.

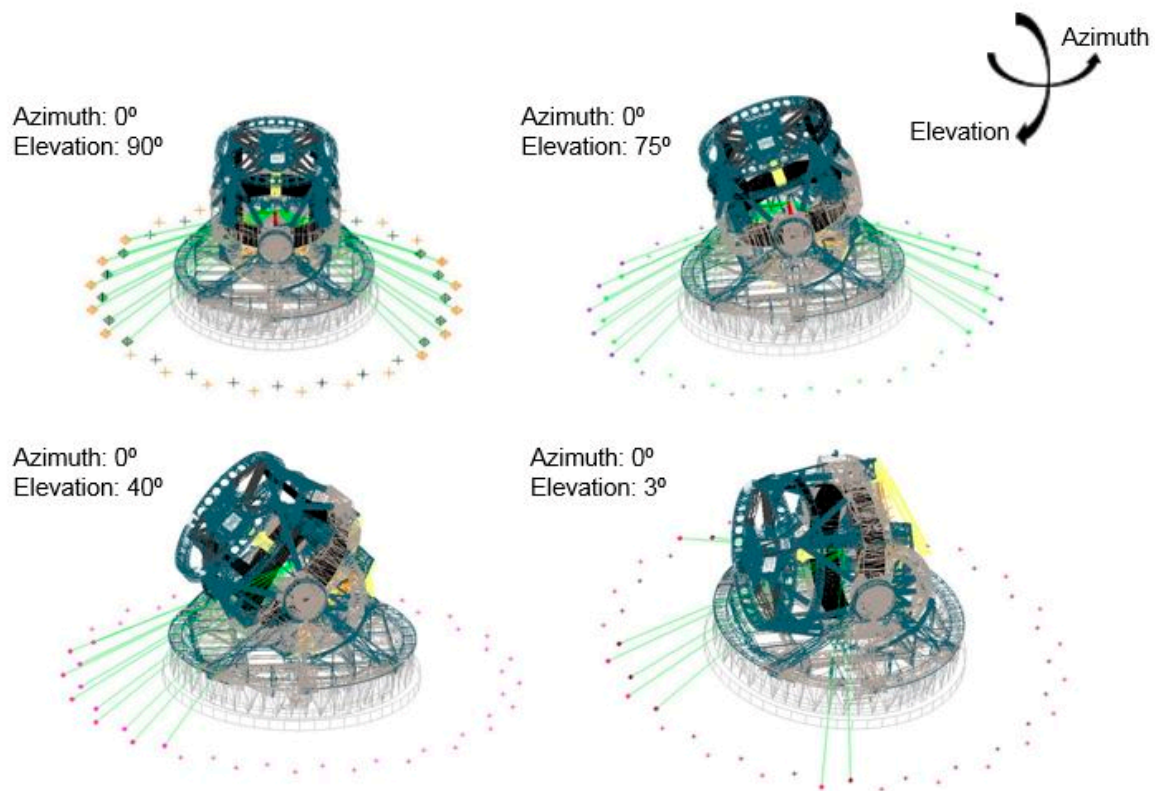


Figure 3. Visibility study overview from inside placed laser tracker, from the zenith to the horizon pointing direction.

2.3. Measurement Simulation

A simulation model, based on the Monte-Carlo technique, was developed to assess the RPE measurement uncertainty according to the developed measurement procedure. The simulation model was developed within SA software, so a commercial tool was employed to code the simulation model [18]. For that simulation, a Gaussian random number generator (utilizing a Box-Muller algorithm) mathematically simulates the measuring scenario with 500 sensitivity samples [19], and the standard deviation parameter was calculated as an uncertainty indicator of the simulated measurement methodology. In addition, the Box-Muller algorithm executed a laser tracker error model according to the specifications of the laser tracker's manufacturer (Leica) at a 68.3% confidence level ($k = 1$), where:

- U_F = Uncertainty of the fixed length error that applies to all distance measurements. For a Leica AT402 laser tracker, it is 0.00762 mm.
- U_M = Uncertainty of the additional length error as the measurement distance increases. For a Leica AT402 laser tracker it is 2.5 $\mu\text{m}/\text{m}$.
- U_A = Uncertainty of angle measurements. For a Leica AT402 laser tracker it is 1 arcsec.

The RPE measurement simulation process had two main stages: The first stage was executed to characterize the reference metrology network, and the second stage aims to quantified the measurement uncertainty on the RPE assessment.

2.3.1. Metrology Network Characterization

The unified spatial metrology network (USMN) tool was employed for coordinate uncertainty field computation [18]. The fundamentals of this technique were that the uncertainty of a particular measurement was simulated using the knowledge of the position of the measurement instrument and the non-isotropic uncertainty of the instrument. The best fitting of all points was weighted, giving less

weight to coordinates with higher uncertainty. Since the uncertainty of measurements taken using a laser tracker is known to be considerably better in range than in angle, the distance measurements were given a greater weight than the angle-derived measurements. The end result of this approach was therefore similar to multilateration. It is not however pure multilateration, since the angle-derived measurements are still used to some extent [20].

For the metrology network characterization, the laser tracker was fixed to the TMA, as an on-board 3D metrology system and the 16 TMA pointing positions were performed. Therefore, every fiducial point was measured from different laser tracker locations, which allowed the characterization of the position of every fiducial point that was fixed to the floor and that was relative to the TMA. The simulation is executed with 500 samples, according to the Leica AT402 laser tracker error model, and the standard deviation parameter of every fiducial point coordinate on each axis direction was obtained from the simulation. Thus, the expanded uncertainty of every fiducial point on each axis direction was obtained by multiplying the standard deviation times the coverage factor (k):

$$U_x = k \times s_x; U_y = k \times s_y; U_z = k \times s_z \quad (1)$$

where:

- k = coverage factor
- s = standard deviation

According to the executed simulation, every point uncertainty was better than 0.1 mm for a 95% confidence level ($k = 2$), as shown in Figure 4.

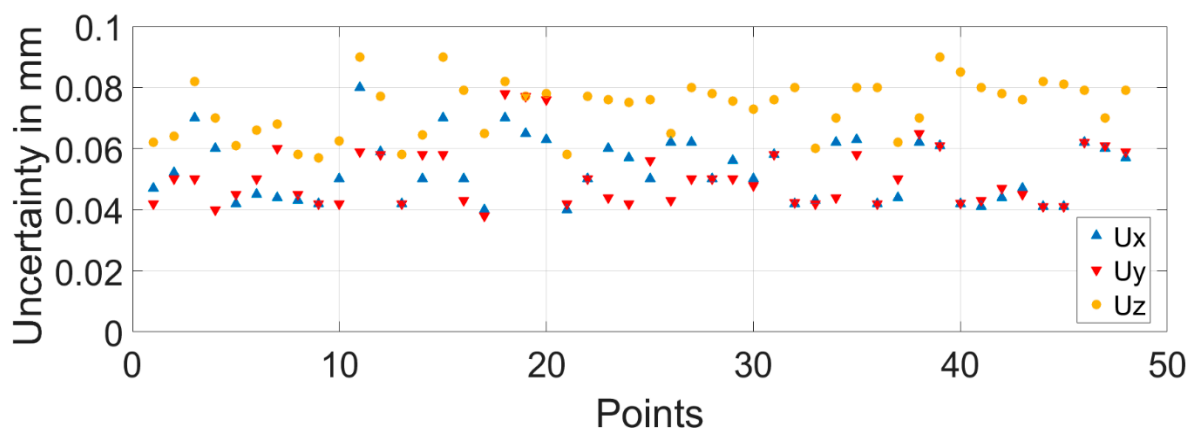


Figure 4. Measurement uncertainty for metrology network characterization.

The simulation result correlated with the research of Rakich et al. at the LBT active alignment system with laser tracker technology [13].

2.3.2. RPE Measurement Simulation

Once checked that the metrology network allowed the location of the laser tracker at any measurement position within the measurement scenario; in fact any TMA pointing direction could be assessed within the pointing range of the LSST. Thus, the M1M3 reference plane was measured and referenced to the earth-fixed reference system, so that the TMA pointing direction was accurately measured for any pointing direction on the sky. For practical issues, the pointing range of the TMA is discretised as shown in Figure 2. Figure 5 shows the RPE measurement uncertainty results, for a 95% confidence level ($k = 2$), obtained by the Monte-Carlo simulation according to the mapping matrix represented in Figure 2.

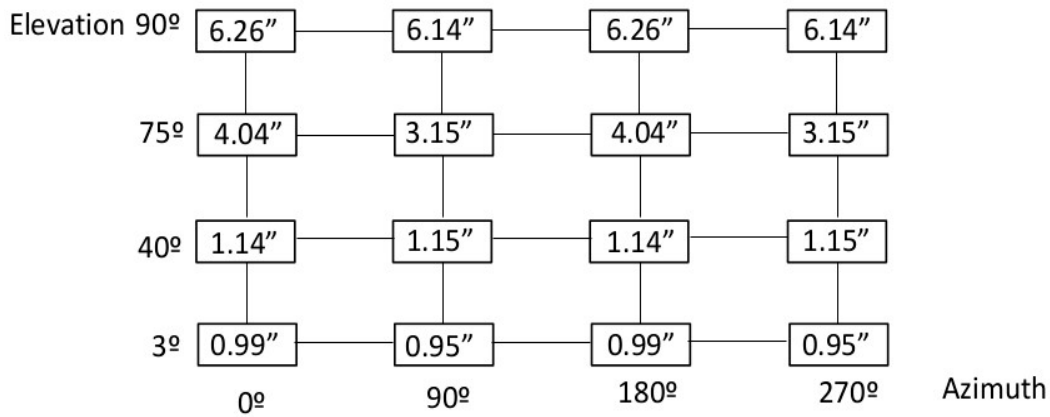


Figure 5. RPE measurement uncertainty results (in arcseconds).

Simulation results showed that uncertainty values were higher when TMA was pointing to the zenith (elevation angle equals 90 degrees). At this pointing position, the normal vector of the M1M3 plane perfectly followed the “z” direction or zenith and, therefore, the uncertainty value was the largest. As the M1M3 plane moved away from the zenith to the horizon, the uncertainty value became smaller.

This means that, for elevation angles near to the zenith pointing position, the plane-based post-processing method showed the highest uncertainty values and, therefore, it seemed that measurement results became worse because of the employed post-processing method. To improve those results, a best-fit based post-processing method was analysed for both 75 degree and 90 degree elevation angles.

While the plane-based post-processing method decomposed the plane vector into 6 degrees of freedom to obtain the rotation angles around the zenith and the elevation axis of the LSST, the best-fit based post-processing method matched the M1M3 points, measured at 75 degree and 90 degree pointing positions respectively, with the M1M3 points measured at the origin, the azimuth at 0 degrees, and pointing to the zenith. The obtained results improved the uncertainty values down to 1 ÷ 2 arcsec for every pointing position of the LSST, which meant that the presented new verification procedure dealt with the RPE requirement, limited to 50 arcsec in a temperature stable measurement scenario (e.g., 20 ± 1 °C on the complete LSST volume).

It is likely that the best-fit based post-processing method will be implemented into the future real measurement scenario, since it could take into account and cope with the real flatness of the mirrors. However, in the current simulation case, the real geometry of the plane did not affect the measurement uncertainty of the RPE assessment.

Figure 6 shows the RPE measurement uncertainty results for a 95% confidence level ($k = 2$), combining plane-based post-processing and best-fit based post-processing methods.

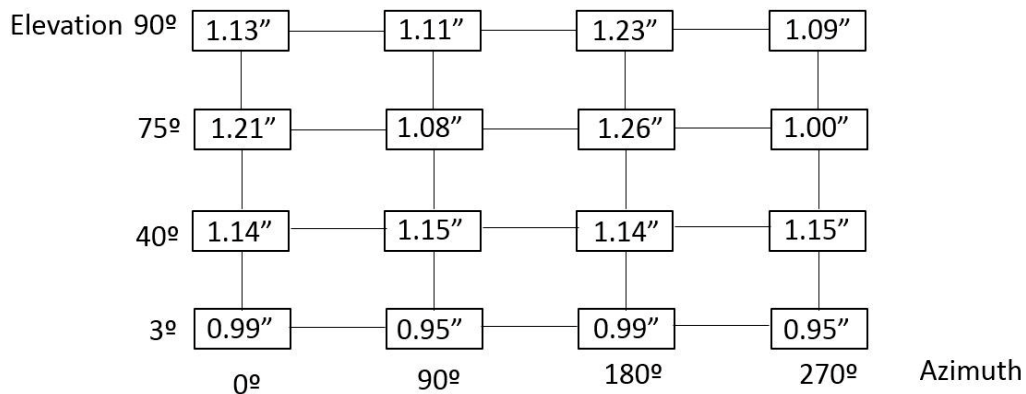


Figure 6. Improved RPE measurement uncertainty results (in arcseconds).

2.4. Floor Movement

Previous simulations consider an absolute and fixed metrology network, but the floor suffers from dimensional drift due to the ambient temperature variation. Therefore, a more realistic simulation was executed to determine the fit for purpose for the presented measurement methodology.

The aim at this point was to quantify the 3D movement of the floor, where fiducial points are fixed, so a 24 h measurement was executed on the premises where TMA was being assembled, in the north of Spain. Results provided a more realistic overview of how floor moved, so a new simulation is performed, considering the floor movement as an input variable for the simulation.

The measurement of the floor was executed with a Leica AT402 laser tracker and five measurement reflectors. They were repeatedly measured, every 5 min, for one day. It was assumed that the laser tracker was fixed to the floor, and that measurement points moved according to the floor drift. Thus, Figure 7 represents the position drift for the five points as the variation of the distance from each of those measurement points to the fixed laser tracker. Measurement results showed that the dimensional drift of every measurement point was within 0.5 mm, for a temperature change of 4 °C. Figure 7 depicts the floor movement assessment for the premises where TMA was being mounted.

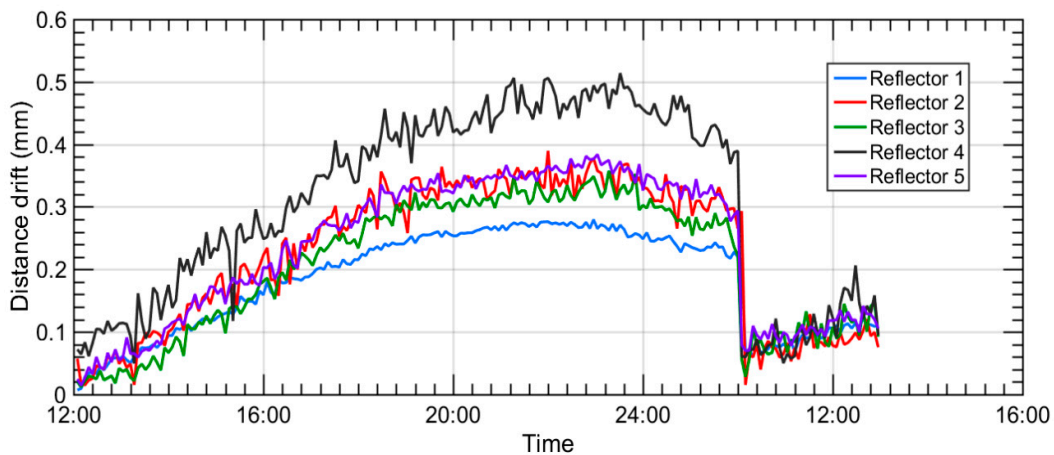


Figure 7. Floor movement assessment for the TMA RPE assessment.

The automatic data acquisition process was interrupted during the first night due to unknown reasons. It was reactivated next morning, and the dimensional drift curves depicted in Figure 7 show that the second morning floor deviation values were similar to the first morning acquired values.

After understanding how the floor movement behaved, the RPE simulation model was completed with floor dimensional drift information. Thus, a random floor movement with a Gaussian distribution was applied to each simulation sample by the means of an additional Monte-Carlo simulation process. This meant that a unique 6 degrees of freedom (d.o.f) transformation was applied onto every single point at each simulation sample, which allowed for the simulation of the real behaviour of the floor where the TMA was mounted. Finally, a new RPE measurement simulation was numerically run and realistic uncertainty results for a 95% confidence level ($k = 2$) were achieved, according to the combined post-processing method mentioned previously, which brought a reduction of the measurement uncertainty. The results are shown in Figure 8.

It should be stated that the simulation model only considered temperature for the floor dimensional drift assessment. The effect of the temperature on the laser tracker measurement system itself was not considered. Additionally, the final workplace of the telescope was environmentally stable because the temperature and pressure would be controlled inside the dome.

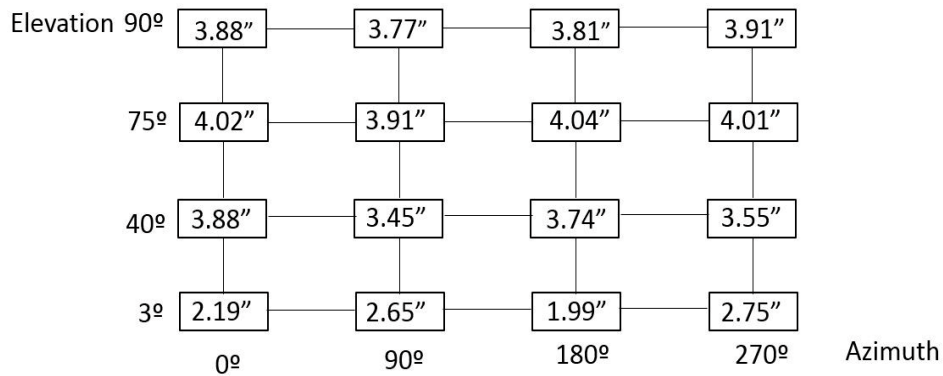


Figure 8. RPE measurement uncertainty results with floor movement consideration (in arcseconds).

2.5. On-Site Measurement Strategy

After simulating the measurement uncertainty for the RPE verification of the LSST, the results made one thing completely clear: the measurement uncertainty for the metrology network characterization should be kept within 0.1 mm to achieve the RPE measurement uncertainty results between 1 ÷ 2 arcsec (correlation on a stable temperature measurement scenario, e.g., 20 ± 1 °C on the complete LSST volume).

At this point, two main limitations were considered for a successful implementation of the suggested new verification method for the RPE assessment: both the laser tracker uncertainty and the temperature effect during the data acquisition period. For the laser tracker uncertainty limitation, the USMN tool was employed within SA software to improve the coordinate uncertainty field computation [18] for the metrology network characterization. For the temperature effect, a fully automatic verification procedure was suggested, to reduce data acquisition time. The laser tracker-based measurement program was interconnected to the LSST control software by the means of a Transmission Control Protocol/Internet Protocol (TCP/IP) in a private connection, and the USMN was applied during the measurement procedure once, so that every fiducial point was measured for every LSST pointing position. The TCP/IP connection permitted the synchronization of the LSST movement with the laser tracker measurement sequence. Figure 9 shows the fully automatic verification pointing measurement procedure for the LSST as a flow chart, where the parallelism measurement between M1M3 and M2 was also considered.

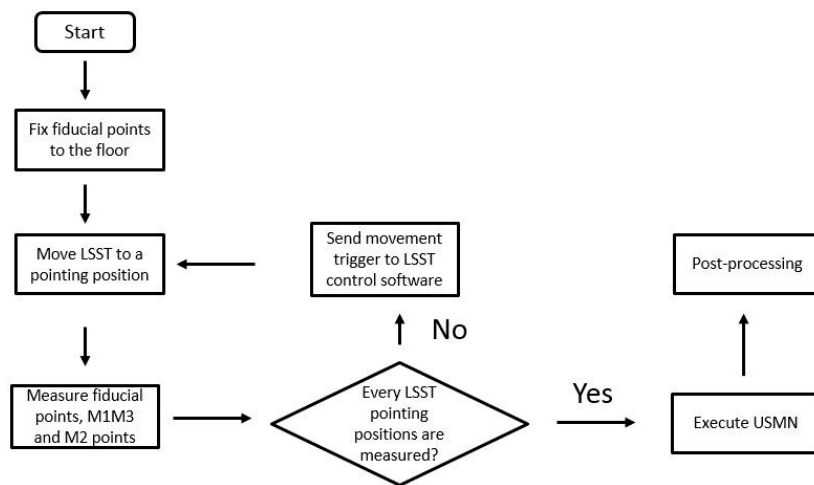


Figure 9. Fully automatic RPE verification procedure flow chart.

The fully automatic measurement procedure presented in Figure 9 aimed to reduce the RPE measurement down to 60–90 min, and it improves the simulation sequence to one stage.

2.6. Validation of Simulated Results—Technological Risk Management

The objective at this point was to validate the developed simulation procedure for the metrology network characterization, considering that its measurement uncertainty should have a maximum of 0.1 mm to achieve the RPE measurement uncertainty results between $1 \div 2$ arcsec. (correlation on a stable temperature measurement scenario).

To do that, the simulation results were compared with real measurement results. A similar shaped 1:2 scale measurement scenario was tested at IK4-TEKNIKER premises, as shown in Figure 10. A Leica AT402 laser tracker has been employed to measure 36 targets distributed on a circular-layout, similar to the real measurement scenario depicted in Figure 1. These targets play the same fiducial role of the metrology network for the LSST measurement scenario.

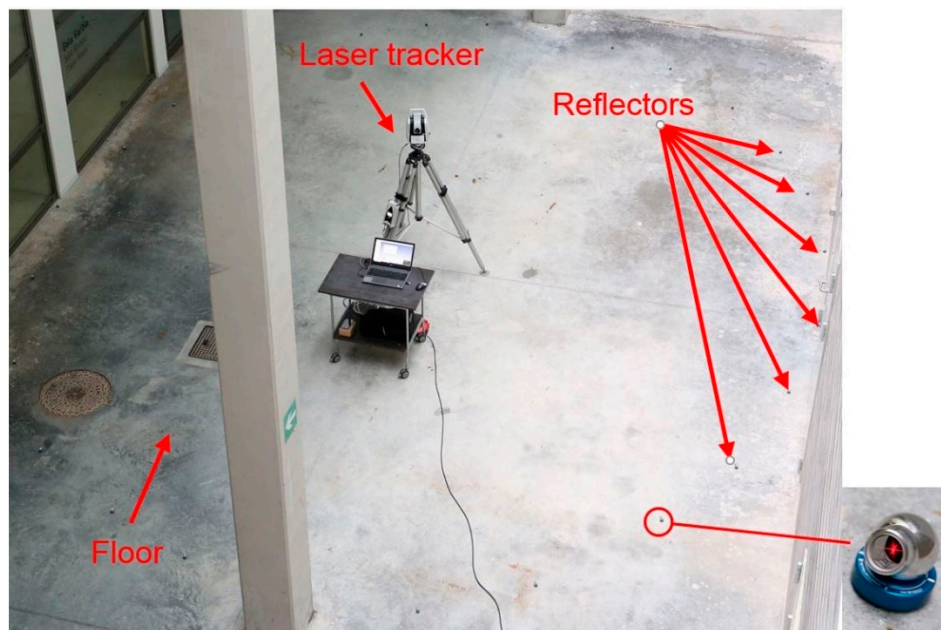


Figure 10. Measurement scenario at IK4-TEKNIKER for simulated results validation.

On the one hand, measurement scenario is simulated with the USMN tool within SA software, with the same simulation code, as described in Section 2.3.1. On the other hand, the measurement scenario was measured 10 times to understand the repeatability contribution of the laser tracker measurement to the obtained uncertainty. After that, simulation-based results are compared to real measurement results on a 1:2 scale LSST measurement scenario. The metrology network characterization results are shown in Figure 11. Here, the combined standard uncertainty value displayed in the vertical axis of the Figure 11 was obtained by summation in the quadrature of each axis uncertainty contribution, obtained by the simulation results. This is defined in Equation (2):

$$U = \sqrt{U_x^2 + U_y^2 + U_z^2} \quad (2)$$

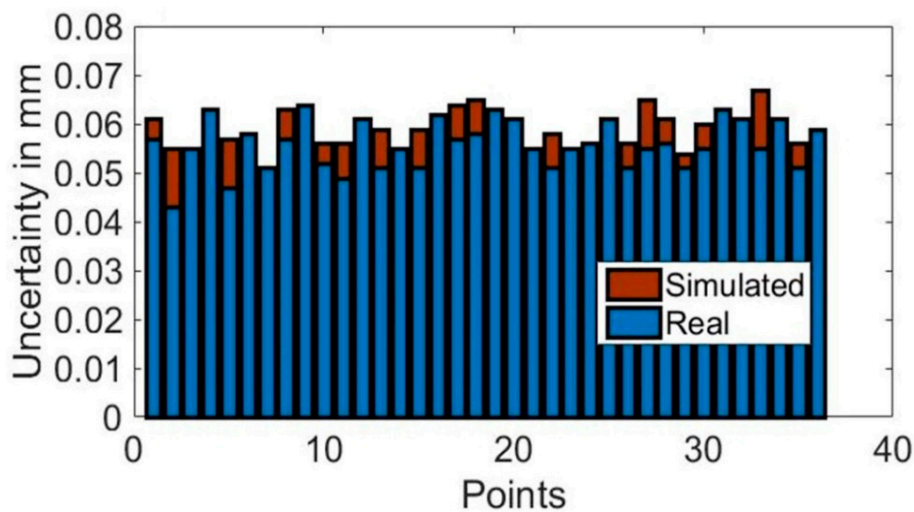


Figure 11. Metrology network characterization validation results.

Experimental test results showed that the simulation-based results and real measurement results were within 0.01 mm in difference, which helps us to understand that the developed measurement procedure tested in the simulation mode resembled its real measurement performance. Thus, the technological risk that was related to the measurement procedure implementation on the real measurement scenario could be reduced and finally managed.

2.7. Relative Pointing Error Calibration

Finally, the RPE calibration will be executed on the TMA with the suggested measurement methodology. For that purpose, a minimum of 10 measurements will be executed to understand the LSST positioning repeatability.

When performing the LSST calibration, three main uncertainty contributors were considered for the uncertainty budget, as described in JCGM 100:2008 guide (Evaluation of measurement data—Guide to the expression of uncertainty in measurement) [21]:

- u_{cal} : standard uncertainty that is associated with the uncertainty of the measurement methodology (measurement technology and measurement procedure). Simulated uncertainties depicted in Figure 6 will be employed for the purpose.
- u_p : standard uncertainty that is associated with the variability of the observed values. It is calculated by the standard deviation of the measured values ($n = 10$).
- u_b : standard uncertainty that is associated with the systematic error of the measurement process for every LSST pointing position.

The expanded measurement uncertainty, U , is calculated for a 95% confidence level ($k = 2$):

$$U = k * \sqrt{u_{cal}^2 + u_p^2 + u_b^2} \quad (3)$$

However, if any other source of uncertainty appears during measurement execution, it will be stated in Equation (3).

3. 3D Metrology Integration into LSST Structure

Various new-generation large telescope projects in the design or early construction stages are considering using laser trackers as a built-in alignment tool that is available to the telescope control system, and that is integral to the basic operation of the telescope [13]. Laser trackers have been historically employed for optical mirror alignment and engineering tasks, and it is interesting to

further investigate the application of on-board laser tracker technology for active telescope alignment. This part of the paper discusses this idea. A metrology simulation tool was presented for the study of the measurement parameters affecting the accuracy of the on-board laser tracker survey and to determine if it was compatible with the required mirror positioning accuracy.

Rakich et al. already tested laser tracker technology on the LBT telescope [13]. They suggest that it is a metrology instrument that is capable of automatically measuring optical element positions with better than 100 μm precision within a spherical volume of 30 m radius centred on the tracker head. They also suggest that the laser tracker is capable of measuring optical component positions during telescope use, with accuracies in the order of 20 microns root mean square (RMS) [13]. These values are considered as a reference for the research work presented in this paper.

Regarding the RPE verification exercise, the simulation code was extended to employ laser tracker technology for the measuring of the alignment between the secondary (M2) and the primary/tertiary (M1M3) mirrors as a part of the active alignment system of the LSST (see Figure 1). Thus, four additional points were added to the M2 mirror, similar to the four that were used for the M1M3 definition shown in Figure 1a, and parallelism measurements were executed between the M1M3 and M2 mirrors for every pointing position depicted in Figure 2. Figure 12 shows the alignment parallelism uncertainty results under stable ambient conditions (e.g., 20 ± 1 °C on the complete LSST volume), where the metrology network is fixed and does not change. The results were based on 2 sigma values (95.46% confidence interval) for the mapping matrix defined at Figure 2.

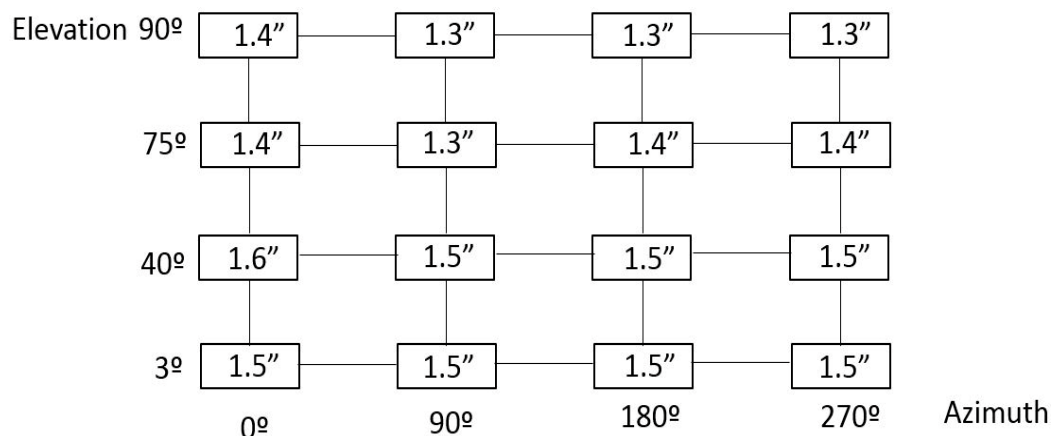


Figure 12. Alignment parallelism uncertainty results under stable floor conditions (in arcseconds).

Results in Figure 12 show that alignment parallelism uncertainty results were similar on every pointing position of the LSST, which makes sense because it was a local measurement between the M1M3 and M2 mirrors. In that sense, the next alignment parallelism simulation was executed to guarantee that parallelism did not change with variations of external conditions, and effectively it was a local measurement. Table 1 shows the simulated uncertainty results for the parallelism between M1M3 and M2 mirrors for different values of floor movement.

Table 1. Floor movement alignment parallelism simulation (in arcseconds).

Floor Movement (mm)	Parallelism Uncertainty (arcsec)
0.05	1.5
0.1	1.6
0.5	1.5
1	1.6
3	1.5
5	1.5

Results certified that alignment parallelism uncertainty did not change according to the floor variation. As previously commented, this made sense, since the measurements were locally executed, and therefore they did not depend on how the floor performed. The results in Table 1 are based on 2 sigma values (95.46% confidence interval).

The main conclusions that were obtained from the simulation of the active alignment system with an on-board metrology system for the LSST are explained next:

- The measurement was locally executed between the M1M3 and M2 mirrors, so that the results did not depend on the accuracy of the fiducial points fixed to the floor.
- The achievable accuracy with a unique on-board laser tracker and that was centred on the telescope structure, was approximately $1.5 \div 1.6$ arcsec. Four measuring points were considered respectively in the M1M3 and M2 mirrors.
- The required mirror positioning accuracy was 1 arcsec. It means that the presented measurement strategy was not yet compatible with the required accuracy.

3.1. Metrology Simulation Tool

Thanks to the knowledge generated on the RPE simulation model construction where laser tracker technology combined with SA software was employed for a Monte-Carlo simulation of the real measurement scenario, a metrology simulation tool was developed for the feasibility assessment of LSM surveying techniques in the LSST. Some key information such as the number and location of the measurement points, and the number and location of the laser trackers, were introduced into the simulation model to understand how they would affect the achievable measurement accuracy. Output information is useful for understanding the feasibility, the anticipated accuracy limits, constraints, the measurement strategy, or the level of effort for the implementation of the suggested survey strategy. Figure 13 presents the metrology simulation tool flow chart.

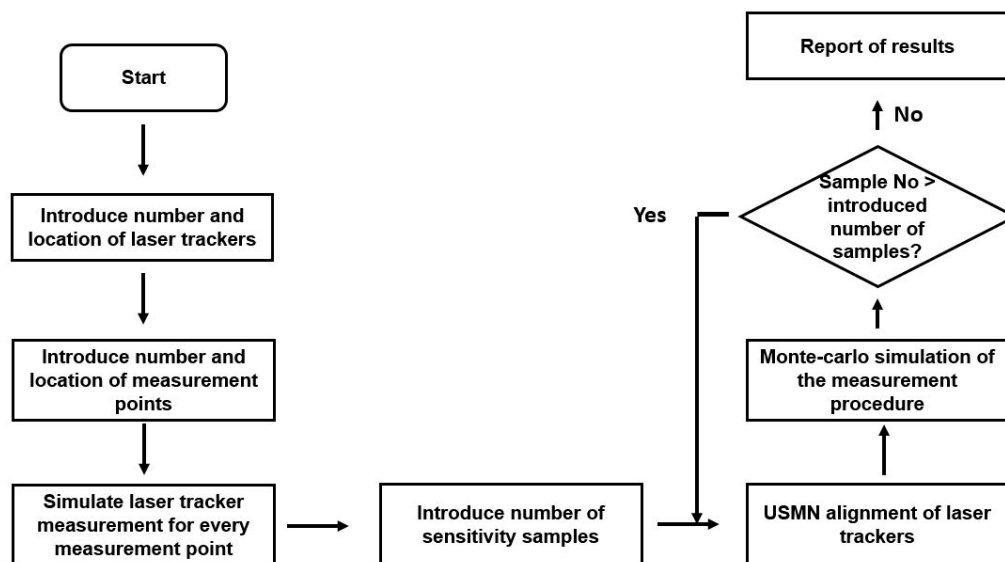


Figure 13. Metrology simulation tool flowchart.

At the present stage, the metrology simulation tool simulates the M1M3 and M2 mirrors measurement. As a result, the centroid that defined their position on the LSST reference system was obtained, as well as the normal vector that defined the pointing direction of each mirror and the angle between them, which showed the parallelism between mirrors.

3.2. On-Board Metrology Simulation Results

The presented metrology simulation tool also aimed to simulate some measurement scenarios on the LSST to understand the influence of the number of laser trackers and the number of the measurement points on the measurement accuracy. Thus, input variables were defined as:

- The number of on-board laser trackers: from 1 to 4. For a permanent installation of laser trackers into the LSST structure, they were located at the M1M3 mirror level with a 7.400 mm radius.
- Number of measurement points: four points or eight points could be selected to define the geometric plane in each mirror.

The simulation tool numerical output provided the standard deviation of each of the six degrees of freedom of a plane. The translation components define the centroid of the plane, and the rotary components define the normal vector. Thus, the combined standard uncertainty of the centroid were obtained by summation in the quadrature of each axis' translation uncertainty contribution, according to Equation (2). Similarly, the combined standard uncertainty of the normal vector was obtained by summation in quadrature of each axis' rotary uncertainty contribution.

Figure 14 shows the combined measurement uncertainty of the normal vector of the M1M3 and M2 mirrors, and the parallelism between them. Figure 15 shows the combined measurement uncertainty of the centroid of the M1M3 and M2 mirrors. The results are based on two sigma values (95.46% confidence interval).

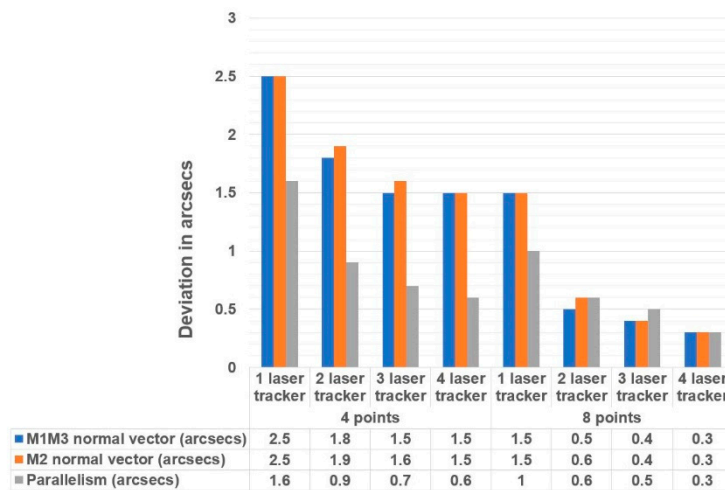


Figure 14. Measurement uncertainty of the normal vector of the M1M3 and M2 mirrors.

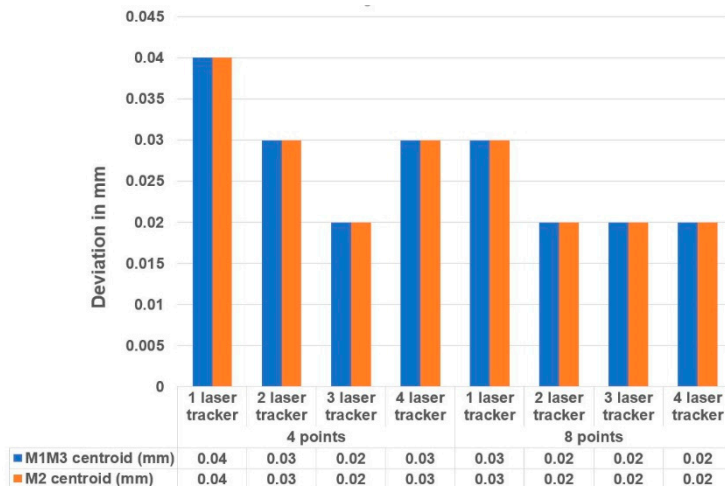


Figure 15. Measurement uncertainty of the centroid of the M1M3 and M2 mirrors.

The simulation results illustrated that the influence of the number of laser trackers was not as important as the number of measurement points employed on the on-board metrology survey. Similar results have been obtained with a unique laser tracker with eight measurement points, compared to three laser trackers with four measurement points. The best price-performance ratio was achieved with a measurement strategy comprised by two laser trackers and eight measurement points where both the normal vector uncertainty and the centroid uncertainty were compatible with the required mirror accuracy.

Obtained uncertainty results also anticipated the accuracy limits for those LSM survey works on large telescopes. As suggested by Rakich et al., it has been demonstrated that the measurement of optical component positions during telescope use can be accomplished with accuracies in the order of 20 microns (RMS) [13]. Additionally, the required mirror positioning accuracy, which is better than 1 arcsec, can also be obtained with a measurement strategy based upon two on-board laser trackers and eight measurement points.

4. Conclusions

A new methodology has been presented and numerically validated for the measurement of the relative pointing error requirement of the TMA subsystem for the LSST. A complete simulation model has been built based upon the Monte-Carlo technique within SA software to anticipate the measurement uncertainty with the suggested methodology. Simulation results show uncertainties better than 5 arcsec for every pointing position within the pointing range of the LSST, which means that the presented methodology is compatible with the RPE requirements, limited to 50 arcsec at a 95% confidence level ($k = 2$). Additionally, a fully automatic RPE verification procedure is presented to reduce the RPE data acquisition down to 60–90 min and, therefore, to reduce the thermal drift of the large-scale measurement scenario.

Regarding the RPE verification exercise, the simulation code has been extended to employ laser tracker technology for the measurement of the alignment between secondary (M2) and primary / tertiary (M1M3) mirrors as a part of the active alignment system of the LSST. Simulated results show that parallelism measurement is a local measurement between the M1M3 and M2 mirrors and therefore the obtained parallelism uncertainty results, better than 1.6 arcsec, can be guaranteed within the pointing range of the LSST.

Based upon the knowledge generated by the RPE simulation model construction, a 3D metrology simulation model has been built to assess the fitness for the purpose of on-board laser tracker technology for performing the alignment of the optical axis and the active telescope alignment. This simulation platform also employs the Monte-Carlo technique to understand how the number and location of the measurement points and laser trackers affect the achievable measurement accuracy. The simulation results show that the best price-performance ratio is achieved with a measurement strategy comprised of two laser trackers and eight measurement points, which is compatible with the required mirror positioning accuracy that is limited to 1 arcsec in the LSST project. This measurement configuration also demonstrates that the measurement of optical component positions during telescope use can be accomplished with accuracies in the order of 20 microns (RMS). Moreover, simulation results conclude that the influence of the number of measurement points is more critical than the number of laser trackers that are employed on the on-board metrology survey.

5. Future Work

The future work is focused on executing the RPE verification on the LSST and on validating the simulation results presented in this research article. In addition, it will be interesting to analyse how the RPE verification results can provide compensation values to the kinematic modelling of the TMA. Thus, the TMA pointing error could be corrected if needed.

Author Contributions: G.K. contributed to the simulation model construction within the SA software. F.E. contributed knowledge to understand how large telescopes behave under real working conditions. J.A.Y.-F contributed to the Monte-Carlo simulation model implementation. U.M. leads the research work and the project execution in collaboration with LSST; he also wrote the paper. All authors contributed to the editing of the manuscript.

Acknowledgments: This material is based upon work supported in part by the National Science Foundation through Cooperative Agreement 1258333 managed by the Association of Universities for Research in Astronomy (AURA), and the Department of Energy under Contract No. DE-AC02-76SF00515 with the SLAC National Accelerator Laboratory. Additional LSST funding comes from private donations, grants to universities, and in-kind support from LSSTC Institutional Members.

Conflicts of Interest: The authors declare no conflict of interest.

References

1. Callahan, S.; Gressler, W.; Thomas, S.J.; Gessner, C.; Warner, M.; Lotz, P.J.; Schumacher, G.; Wiecha, O.; Angeli, G.; Andrew, J.; et al. Large Synoptic Survey Telescope mount final design. In Proceedings of the SPIE Astronomical Telescopes + Instrumentation, Edinburgh, UK, 26 June–1 July 2016; Volume 9906, pp. 1–20. [[CrossRef](#)]
2. Mutilba, U.; Kortaberria, G.; Egaña, F.; Yagüe-Fabra, J.A. Relative pointing error verification of the Telescope Mount Assembly subsystem for the Large Synoptic Survey Telescope. In Proceedings of the IEEE International Workshop on Metrology for AeroSpace, Rome, Italy, 20–22 June 2018.
3. Wallace, P.T. Telescope Pointing. Available online: <http://www.tpointsw.uk/pointing.htm> (accessed on 10 July 2018).
4. Elfving, A.; Bagnasco, G. *The Pointing and Alignment of XMM*; ESTEC: Noordwijk, The Netherlands, 1999.
5. Neill, D.; Sebag, J.; Gressler, W.; Warner, M.; Wiecha, O. *LTS-103 Telescope Mount Assembly (TMA) Specifications*; LSST: Tucson, AZ, USA, 2016.
6. Huang, L.; Ma, W.; Huang, J. Modeling and calibration of pointing errors with alt-az telescope. *New Astron.* **2016**, *47*, 105–110. [[CrossRef](#)]
7. Vaksdal, B. Pointing Calibration for Medium Size Telescopes in the Cherenkov Telescope Array. Master's Thesis, KTH Engineering Sciences, Stockholm, Sweden, 2016.
8. Cheng, J. *The Principles of Astronomical Telescope Design*; Springer: New York, NY, USA, 2009; ISBN 978-1-4419-2785-9.
9. De Donato, C.; Prouza, M.; Sanchez, F.; Santander, M.; Camin, D.; Garcia, B.; Grassi, V.; Grygar, J.; Hrabovský, M.; Řídký, J.; et al. Using stars to determine the absolute pointing of the fluorescence detector telescopes of the Pierre Auger Observatory. *Astropart. Phys.* **2007**, *28*, 216–231. [[CrossRef](#)]
10. Matsuzawa, A.; Saito, M.; Iguchi, S.; Nakanishi, K.; Saito, H. Development of High-Accuracy Pointing Verification for ALMA Antenna. *Proc. SPIE* **2014**, *9145*, 1–7. [[CrossRef](#)]
11. Gallagher, B.B. Optical Shop Applications for Laser Tracker Metrology Systems. Master's Thesis, The University of Arizona, Tucson, AZ, USA, 2003.
12. Burge, J.H.; Su, P.; Zhao, C.; Zobrist, T. Use of a commercial laser tracker for optical alignment. *Proc. SPIE* **2007**, *6676*, 66760E. [[CrossRef](#)]
13. Rakich, A. Using a laser tracker for active alignment on the Large Binocular Telescope. *Proc. SPIE* **2012**, *8444*, 844454.
14. Sebag, J.; Gressler, W.; Neill, D.; Barr, J.; Claver, C.; Andrew, J. LSST telescope integration and tests. *Proc. SPIE* **2014**, *9145*, 91454A. [[CrossRef](#)]
15. Rakich, A.; Dettmann, L.; Leveque, S.; Guisard, S. A 3D metrology system for the GMT. *Proc. SPIE* **2016**, *9906*, 990614. [[CrossRef](#)]
16. Gressler, W.J.; Sandwith, S. Active Alignment System for the LSST. In Proceedings of the Columbia Music Scholarship Conference (CMSC), Orlando, FL, USA, 3–4 February 2006.
17. Schmitt, R.; Peterek, M.; Morse, E.; Knapp, W.; Galetto, M.; Härtig, F.; Goch, G.; Hughes, B.; Forbes, A.; Estler, W. Advances in Large-Scale Metrology—Review and future trends. *CIRP Ann. Manuf. Technol.* **2016**. [[CrossRef](#)]
18. Calkins, J.M. Quantifying Coordinate Uncertainty Fields in Coupled Spatial Measurement Systems. Ph.D. Thesis, Virginia Tech, Blacksburg, VA, USA, 2002.

19. Bindel, D.; Goodman, J. Principles of Scientific Computing Monte Carlo Methods; 2009. Available online: <https://pdfs.semanticscholar.org/9a43/1e7cf68338652b2cbf5aabc3ae88f0949130.pdf> (accessed on 10 July 2018).
20. Muelaner, J.E.; Wang, Z.; Jamshidi, J.; Maropoulos, P.G. Verification of the indoor GPS system by comparison with points calibrated using a network of laser tracker measurements. In Proceedings of the 6th CIRP-Sponsored International Conference on Digital Enterprise Technology, Hongkong, China, 14–16 December 2009; Volume 66, pp. 607–619. [[CrossRef](#)]
21. Joint Committee for Guides in Metrology. JCGM 100:2008—Evaluation of Measurement Data—Guide to the Expression of Uncertainty in Measurement; JCGM: 2008. Available online: https://www.bipm.org/utis/common/documents/jcgm/JCGM_100_2008_E.pdf (accessed on 10 July 2018).



© 2018 by the authors. Licensee MDPI, Basel, Switzerland. This article is an open access article distributed under the terms and conditions of the Creative Commons Attribution (CC BY) license (<http://creativecommons.org/licenses/by/4.0/>).

**Telescope mount assembly pointing accuracy assessment for the Large
Synoptic Survey Telescope: A large-scale metrology challenge**

Telescope mount assembly pointing accuracy assessment for the Large Synoptic Survey Telescope: A large-scale metrology challenge

Unai Mutilba^{1,*}, Gorka Kortaberria¹, Fernando Egaña¹ and Jose Antonio Yagüe-Fabra²

¹ Department of Mechanical Engineering, IK4-Tekniker, 20600 Eibar, Spain.

² I3A, University of Zaragoza, 50018 Zaragoza, Spain.

* Correspondence: unai.mutilba@tekniker.es

Abstract

The Telescope Mount Assembly (TMA) is one of the main subsystems of the Large Synoptic Survey Telescope (LSST), a large (8.4 m) wide-field (3.5 degree) survey telescope, which will be located on the summit of Cerro Pachón in Chile. The TMA provides motions about the azimuth and elevation axes to comply with the space survey mission, so it is of great interest to make sure that the TMA is pointing towards the intended location on the sky as accurately as possible. In this scenario, IK4-TEKNIKER has developed a custom engineered measurement procedure to assess the pointing accuracy error of the TMA, based on laser tracker technology and several fiducial points fixed to the floor. There are several metrology challenges to tackle, such as the large-scale measurement scenario, the visibility to the optical axis of the telescope or the working range of the TMA. A complete simulation model has been built based upon the Monte-Carlo technique within Spatial Analyzer (SA) software to anticipate the measurement uncertainty with the suggested methodology and simulation results show that the presented methodology is fit for purpose. These results show uncertainties better than 2 arcsec for every pointing position within the pointing range of the TMA, which means that the presented methodology is compatible with the pointing accuracy requirements, limited to 50 arcsec at a 95% confidence level ($k = 2$). Finally, the successful implementation of the suggested new verification method is done in situ. A fully automatic measurement procedure is performed reducing the test data acquisition down to 75 minutes and preliminary TMA pointing accuracy results show that the presented measurement procedure has performed according to the simulated performance.

Large Synoptic Survey Telescope, Telescope Mount Assembly, Laser tracker, Spatial Analyzer, Monte-Carlo simulation, Relative Pointing Error

1. Introduction

The Large Synoptic Survey Telescope is one of the biggest and most accurate telescope ever built and will produce the deepest and widest image of the Universe during a 10-year survey of the sky [1]. Thus, the LSST pointing accuracy assessment is a major large-scale metrology challenge. Among the pointing requirements, there are three that are of particular interest to ensure that the telescope is pointing the intended location on the sky: Pointing accuracy or Relative Pointing Error (RPE), pointing repeatability and parallelism between primary-tertiary and secondary mirrors.

To take up the challenge, the aim is to employ an onboard laser tracker system that assesses any pointing position within the pointing range of the telescope. Various new-generation large telescope projects already consider using laser trackers as a built-in measurement system for alignment and engineering tasks [2,3]. Rakich et al. already tested laser tracker technology on the Large Binocular Telescope (LBT). They suggest that it is a metrology instrument capable of automatically measure optical element positions with better than 100 μm precision within a spherical volume of 30 m radius centred on the tracker's head [4]. The Giant Magellan Telescope (GMT) has also considered laser tracker technology for the Telescope Metrology System (TMS) [5].

In this paper, a custom engineered measurement procedure is presented to assess the pointing requirements of the TMA. An end-to-end test of the complete LSST, in order to check the pointing performance and the correct alignment of all the elements, is not possible until the final assembly in Chile is

complete. For this reason, the TMA subsystem will first be tested, including RPE requirement, at the factory with surrogate masses, to replace the optical payloads with the aim of avoiding 'late surprises' during the LSST construction in Chile [6]. Thus, data acquisition is done at Asturfeito company premises, in the north of Spain during the first week of September of 2018.

2. Measurement scenario

The optical axis of the TMA is defined at M1M3 primary/tertiary mirrors, so one of the limitations tackled by any pointing measurement procedure is measuring M1M3 mirror for any pointing motion within the TMA pointing range [7]. Additionally, all the performance requirements must be met for observing angles which are between 15 and 86.5 degrees for elevation angles and from 0 to 360 degrees for azimuth angles [1].

The measurement of the TMA is a large-scale metrology (LSM) exercise [8] since the dimension of the measurement scenario is up to 36 meters of diameter. Thus, LSM technology is employed for the pointing accuracy assessment: A Leica AT960 laser tracker technology combined with Spatial Analyzer (SA) software from New Rivers Kinematics. Figure 1 shows the measurement scenario for pointing accuracy assessment. Figure 1 (b) illustrates the complete measurement scenario. Figure 1 (a) shows the M1M3 measurement plane where measurement targets are depicted in red. Additionally, it also shows that the engineering validation at the subsystem level is verified with surrogate masses instead of the real optical elements.

In this measurement scenario, a pointing matrix has been defined to characterize the pointing accuracy test within the

pointing range of the TMA. Four elevation angles at four different azimuth positions are defined to represent any pointing direction on the sky (zenith pointing occurs when elevation angle is 90°), as shown in Figure 2. Every box on the picture represents a TMA pointing position.

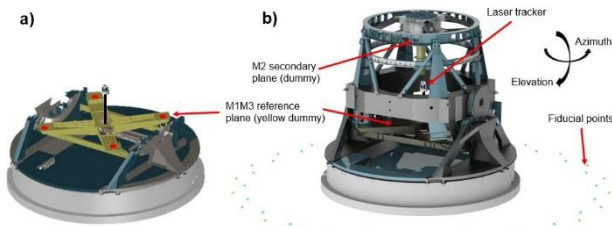


Figure 1. Measurement scenario for RPE assessment. a) M1M3 measurement plane (measurement targets in red) b) Complete LSST measurement scenario.

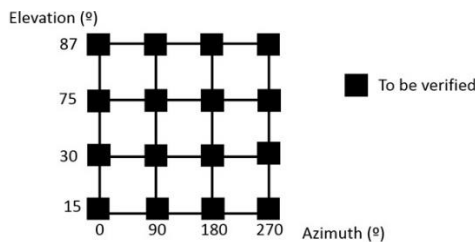


Figure 2. Pointing matrix for the pointing accuracy test.

2.1. Measurement procedure

A custom engineered measurement procedure has been developed to assess the pointing requirements of the TMA. A laser tracker is placed inside of the TMA, close to its origin, and a metrology network comprised of a reference point cloud is fixed to the floor, outside and surrounding the TMA. This metrology network is of special importance, as any laser tracker location during the whole measurement process is located by the measurement of this fiducial metrology network. Thus, the pointing accuracy measurement procedure consists on measuring the metrology network to locate the laser tracker and, afterwards, measure the optical axis of the TMA by measuring five target points at the M1M3 reference plane and measure four targets points at M2 secondary plane. In this way, by locating M1M3 reference plane on earth fixed reference system, i.e. the floor, each observation angle for the TMA is characterized and compared to the nominal input position. The complete measurement process comprises every pointing position defined in Figure 2 and within the pointing range of the TMA. The measurement process for the pointing accuracy test is explained in detail in Figure 3.

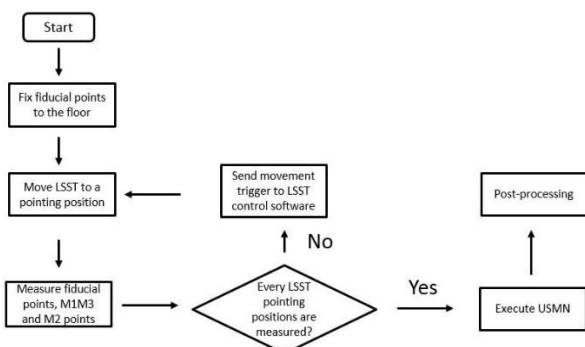


Figure 3. The measurement process for the pointing accuracy test.

A metrology network comprised of 40 points is defined on the floor outside and surrounding the telescope. 20 points create a 15-metre radius circle and 20 additional points define a 16-metre radius with an offset of 7.5° to the previous one. Its

circular shape optimizes the visibility challenge for any azimuth pointing position of the telescope. Additionally, those points are fixed to the floor minimizing thermal gradients effects. Figure 4 shows the real metrology network arrangement around the TMA at shop floor level.



Figure 4. Real metrology network arrangement at Asturfeito premises.

On the other hand, the laser tracker position is fixed close to the TMA reference system origin, to nullify the range of the angle of incidence from the laser tracker to the reflectors. Thus, the laser tracker tilts with the rotation centre of the telescope and the incidence angle between laser tracker and fiducial points does not change which means that it will not cause a longer travelling path of the beam inside the reflector prism. Figure 5 shows laser tracker location in M1M3 when TMA is pointing to the horizon, it shows how the visibility problem, between inside placed laser tracker and TMA outside placed reference metrology network is solved.

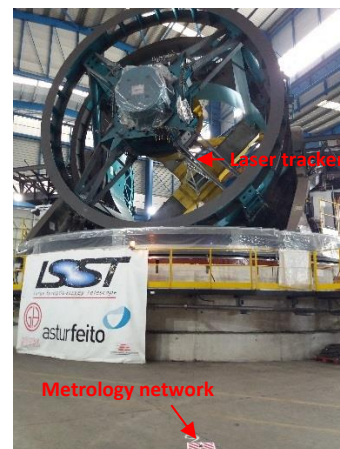


Figure 5. Laser tracker visibility at TMA horizon pointing position.

Additionally, 25 mm hollow corner cube reflectors are glued to the floor to define the reference metrology network which helps to the visibility challenge. Figure 6 shows the fiducial point definition and laser tracker arrangement in M1M3 (right).

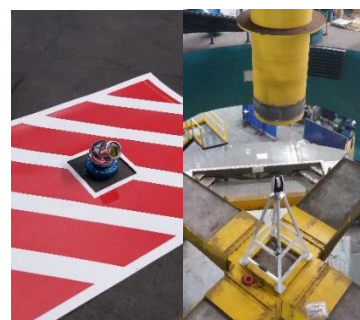


Figure 6. Fiducial point definition (left) and laser tracker arrangement in M1M3 (right).

After conceptually developing the measurement procedure for the pointing accuracy test depicted in Figure 3, a Monte-Carlo based simulation model has been built to anticipate the measurement uncertainty related to the measurement procedure. The simulation model has been developed within SA software, so a commercial tool is employed to code the simulation model [9]. On that simulation, a Gaussian random number generator (utilizing a Box-Muller algorithm) mathematically simulates the measuring scenario with 500 sensitivity samples [9] and the standard deviation parameter is calculated as an uncertainty indicator of the simulated measurement methodology. It shall be highlighted that the Box-Muller algorithm executes a laser tracker error model according to the specifications of the Laser Tracker's manufacturer. In this case, the Leica AT402 absolute laser tracker error model has been employed.

For the metrology network characterization, a total of nineteen laser tracker positions are performed: One laser tracker position per TMA pointing position and 3 additional measurement laser tracker positions for the metrology network characterization improvement. It means that every fiducial point is measured from multiple laser trackers positions, so coordinate uncertainty field computation shall be performed. To do so, the Unified Spatial Metrology Network (USMN) tool within SA software is employed [9]. Thus, the simulation is executed with 500 samples according to the Leica AT402 absolute laser tracker error model and the standard deviation parameter of every fiducial point coordinate on each axis direction is obtained from the simulation. Thus, the expanded uncertainty of every fiducial point on each axis direction is obtained by multiplying the standard deviation times the coverage factor (k).

$$U_x = k * s_x \quad U_y = k * s_y \quad U_z = k * s_z \quad (1)$$

where:

k = coverage factor

s = standard deviation

According to the executed simulation, every point uncertainty is better than 0.1 mm for a 95% confidence level (k=2), as shown in Figure 7.

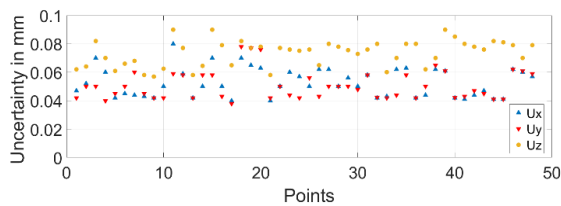


Figure 7. Measurement uncertainty for the metrology network characterisation (nominal simulation).

In addition to the fiducial point uncertainty analysis, the measurement uncertainty for the pointing accuracy test for every pointing position shown in Figure 2 is obtained. Figure 8 shows the measurement uncertainty results (in arcsec) for a 95% confidence level (k=2).

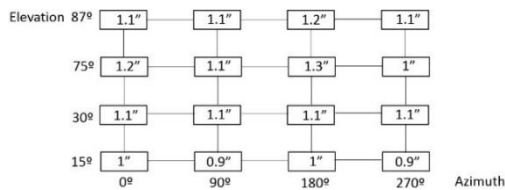


Figure 8. Measurement uncertainty results in simulation mode for the RPE test.

The previous simulation does not consider any floor dimensional drift due to ambient temperature variation.

3. Measurement performance

The pointing accuracy test has been performed during the first week of September of 2018 at Asturfeito premises, in Spain, with a Leica AT960 laser tracker technology. The automation of the measurement campaign has taken 3 days. As a result, the time consumption for the pointing accuracy test is 75 minutes which means that temperature variation of the measurement scenario is reduced to 1°C.

The measurement sequence has been repeated five times aiming to assess not just the pointing accuracy of the TMA, but also the repeatability.

Once that measurement has been performed, the measurement uncertainty for the pointing accuracy test has been updated to the real measurement scenario. It shall be highlighted that there are several physical limitations on the real measurement scenario such as, the office box, the stairs of the TMA structure and the shop floor layout that prevent the measurement scenario from being similar to the designed nominal scenario. A new simulation has been performed according to the real measurement scenario depicted in Figure 9 and in Figure 4.

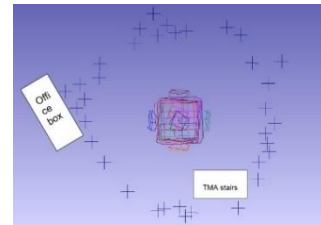


Figure 9. Real fiducial point distribution for the TMA pointing accuracy test.

Simulation results show that pointing accuracy test uncertainty is worse when the telescope is pointing to the horizon rather than when it is pointing to the zenith. It occurs because fiducial point visibility from inside placed laser tracker is much better when the telescope is pointing to the zenith. Pointing accuracy test simulation results (in arcsec) are shown in Figure 10 for a 95% confidence level (k=2).

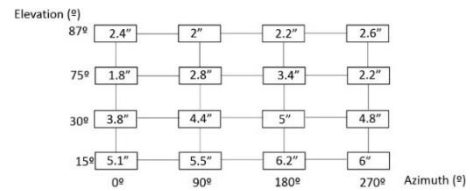


Figure 10. Measurement uncertainty results for the RPE test on the real measurement scenario.

Uncertainty values are slightly worse than what achieved in simulation mode and shown in Figure 8, mainly because fiducial point distribution on the real measurement scenario is not as homogeneous as the nominal measurement scenario. Additionally, the standard deviation parameter of every fiducial point coordinate on each axis direction is obtained from the updated simulation. Figure 11 shows the measurement uncertainty for the metrology network characterisation for a 95% confidence level (k=2).

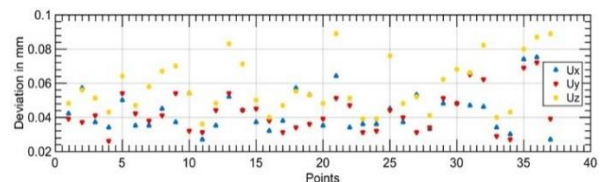


Figure 11. Measurement uncertainty for the metrology network characterisation (real measurement scenario-based simulation).

Residual results comparison between Figure 7 and Figure 11, show that uncertainty for X and Y direction (floor plane) are better to what previously simulated with a perfect measurement scenario. In Z direction results are in general better than simulated results but there are some points that are slightly worse for the real measurement scenario. To sum up, the real measurement scenario uncertainty is slightly better than the simulated uncertainty. The main reason is that the real measurement execution has been performed with a Leica AT960 laser tracker which combines two measurement technologies (interferometry and absolute distancimeter) compared to the simulation Leica AT402 laser tracker, that uniquely employs absolute distance measurement technology to perform length measurement that is not as accurate as absolute distance measurement.

4. Results

Due to confidentiality reasons, the pointing accuracy detailed test results are kept confidential. However, it should be said that obtained results are better than one-fifth of the required tolerance, limited to 50 arcsec.

Pointing repeatability measurement tolerance is limited to 1 arcsec, so as depicted in Figure 10 the laser tracker-based pointing accuracy test cannot perform within the required 1 arcsec accuracy. This is the reason why the pointing repeatability test has been performed with direct measurement methods, a gravity-based level for elevation axis and an autocollimator for azimuth axis, reducing the measurement uncertainty within 1 arcsec. Figure 12 shows the measurement approach with the level and the autocollimator.



Figure 12. Direct measurement methods for the pointing repeatability test.

Repeatability results either in azimuth axis or elevation axis are within the required tolerance of 1 arcsec.

On the pointing accuracy test, M2 secondary mirror has also been measured for every pointing position within the pointing range of the TMA. It means that parallelism between M1M3 primary-tertiary mirrors and M2 secondary mirror can also be assessed for the pointing matrix depicted in Figure 2. Results show that parallelism between M1M3 and M2 maintains within 1 arcsec for the working range of the TMA subcomponent. Figure 13 shows three out of four reflectors glued to M2 secondary mirror allowing parallelism requirement assessment.

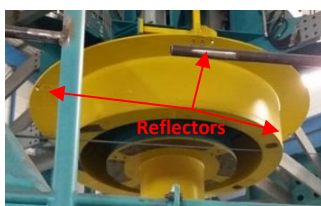


Figure 13. Reflectors attached to M2 secondary plane (3 out of 4 reflectors are shown)

5. Conclusions

A new pointing accuracy test methodology has been successfully implemented on the real TMA measurement scenario at Asturfeito premises, in the north of Spain. From this pointing test, three main pointing requirements are assessed: pointing or RPE accuracy, pointing repeatability and parallelism between primary-tertiary and secondary mirrors.

Pointing accuracy test has been performed after 3 days of automation preparation process where every measurement detail has been carefully analyzed. As a result, a measurement procedure that takes 75 minutes to execute is performed which results in 1°C of temperature variation on the measurement scenario allowing a high quality of measured data. Measurement results show that the accuracy assessment for the metrology network characterisation is better than what achieved previously in simulation mode, mainly because the Leica AT960 laser tracker employs interferometer-based technology to perform length measurement. However, the fiducial point distribution on the real measurement scenario is worse than what designed on the initial simulation stage, which affects to the absolute accuracy of the pointing accuracy test.

The main conclusion of the calibration campaign performed on the real TMA measurement scenario is that every pointing requirement is within the defined tolerance value.

Acknowledgement

This material is based upon work supported in part by the National Science Foundation 390 through Cooperative Agreement 1258333 managed by the Association of Universities for Research in Astronomy 391 (AURA), and the Department of Energy under Contract No. DE-AC02-76SF00515 with the SLAC National 392 Accelerator Laboratory. Additional LSST funding comes from private donations, grants to universities, and in-393 kind support from LSSTC Institutional Members.

References

- [1] S. Callahan, W. Gressler, S.J. Thomas, C. Gessner, M. Warner, P.J. Lotz, G. Schumacher, O. Wiecha, G. Angeli, J. Andrew, B. Schoening, J. Sebag, V. Krabbendam, D. Neill, E. Hileman, Large Synoptic Survey Telescope mount final design, 9906 (n.d.) 1–20. doi:10.1117/12.2232996.
- [2] J.H. Burge, P. Su, C. Zhao, T. Zobrist, Use of a commercial laser tracker for optical alignment, 6676 (2007) 66760E. doi:10.1117/12.736705.
- [3] B.B. Gallagher, Optical Shop Applications for Laser Tracker Metrology Systems, (2003) 205.
- [4] A. Rakich, Using a laser tracker for active alignment on the Large Binocular Telescope, in: Proceedings of SPIE 7733, 2012: p. 844454. doi:10.1117/12.928706.
- [5] A. Rakich, L. Dettmann, S. Leveque, S. Guisard, A 3D metrology system for the GMT, 9906 (2016) 990614. doi:10.1117/12.2234301.
- [6] J. Sebag, W. Gressler, D. Neill, J. Barr, C. Claver, J. Andrew, LSST telescope integration and tests, 9145 (2014) 91454A. doi:10.1117/12.2055241.
- [7] U. Mutilba, G. Kortaberria, F. Egaña, J. Yagüe-Fabra, U. Mutilba, G. Kortaberria, F. Egaña, J.A. Yagüe-Fabra, 3D Measurement Simulation and Relative Pointing Error Verification of the Telescope Mount Assembly Subsystem for the Large Synoptic Survey Telescope, Sensors 2018, Vol. 18, Page 3023. 18 (2018) 3023. doi:10.3390/S18093023.
- [8] R. Schmitt, M. Peterrek, E. Morse, W. Knapp, M. Galetto, F. Härtig, G. Goch, B. Hughes, A. Forbes, W. Estler, Advances in Large-Scale Metrology – Review and future trends, CIRP Annals - Manufacturing Technology. (2016). doi:10.1016/j.cirp.2016.05.002.
- [9] J.M. Calkins, Quantifying coordinate uncertainty fields in coupled spatial measurement systems, 2002.

4. SUMMARY



4. SUMMARY

4.1 Objectives

The overall purpose of this PhD study is to provide new knowledge for traceable CMM measurements on MTs and present a closed calibration chain for on-MT measurement as the main scientific outcome of the research. In addition, there are several specific objectives that break down the general objective into specific and allows to systematically address the various aspects of this thesis:

The first objective is to understand the strategic relevance of performing traceable CMM measurements on MTs. Product features such as precision and accuracy are far more important than unit labour costs in a technology-intensive sector such as MTs, as a source of competitive advantage. High-tech MT builders seek for differentiation and sources of uniqueness by creating value for their customers through the development of new processes, functionalities and services which help achieve high productivity levels, meet the precision needs of their customers and help lower their costs, looking for a positive impact on the OEE indicator of their customers, the MT users. Nowadays, the quality inspection of high-value components usually takes place on a CMM, either beside the production line or in an isolated measurement room, so the manufacturing process is interrupted and transportation, handling and the loss of the original manufacturing setup influence the workpiece quality. The high invest for a CMM and the mentioned influences show the need for an MT integrated traceable measuring process for product's quality assurance. In fact, the technology to run an MT working as a CMM already exists, such as touch TTPs and measurement software for MTs, but there are several factors that affect the on-MT measurement which leads to a lack of a metrological traceability chain, which in turn means a lack of reliability of the manufacturing processes

From the research point of view, the initial objective of this thesis is to identify the uncertainty contributors of a traceable on-MT measurement and it is also to understand the significance of each uncertainty contributor to the final uncertainty budget. No less important is to find out the available methods and standards for a correct assessment of uncertainty in CMMs that could be adopted for traceable on-MT measurement. At this stage, it is also helpful to target the current main limitations of using an MT as a CMM to understand the challenges that this PhD study faces to assess traceability for MTs working as CMMs in shop floor conditions.

After the first qualitative approach that provides an updated state of the art, the objective at this point is to contrast the theoretical weight of each uncertainty contributor with an experimental exercise. Here, the goal is to perform a medium-size on-MT measurement uncertainty assessment in shop floor conditions. A complete experimental test, combining manufacturing and measurement processes, should be performed employing a calibrated workpiece on a medium size available MT. At this point, it should be clear the weight of each uncertainty contributor and the limitations of the calibrated workpiece approach according to the ISO 15530-3 technical specification.

As commented in the introduction, this PhD study focuses on making a special effort towards large scale manufacturing scenarios, where high-value components require fast and reliable feedback on the manufacturing scenario. Thus, the next milestone is to scale the traceable on-MT measurement solution to large-scale MTs. Here, there are two main limitations that are highlighted on the initial review: a) the lack of integrated and automatic error

mapping solutions on-MTs; and b) the strong limitation that implies the use of a calibrated workpiece to understand the systematic error contributor on an MT measurement.

In this way, the objective at this point is to propose an alternative methodology to enable traceable measurements on large-scale MTs. The approach does not employ a calibrated workpiece as recommended on the ISO 15530-3 technical specification but it proposes an MT volumetric error mapping exercise immediately before to the on-MT measurement to assess the systematic error contributor.

Considering the lack of integrated and automatic error mapping solutions on-MTs, the initial review makes a special effort to breakdown the currently available error mapping techniques for MTs. It is of particular importance to understand available technologies and techniques for large scale volumetric error mapping. In this way, after considering the current state of the art where it is highlighted that interferometer-based non-contact measuring technology will guide the LSM filed in shop floor conditions in the near future, this PhD study aims to develop an integrated and automatic volumetric error mapping solution for medium and large size MTs, which permits either the volumetric error mapping measurement for volumetric compensation or a fast geometry-health tool to monitor the MT geometry over time. This solution would enable to improve the accuracy of MTs, to maintain the required accuracy during the MT life-cycle and it would also allow scaling the previously proposed methodology for traceable on-MT measurement to large scale MTs.

In parallel, this thesis aims to develop a customized error mapping solution for a cutting-edge large telescope, the LSST project. The objective at this point is to benefit from the generated new knowledge within the LSM field for MTs and find a suitable measurement solution for the accuracy assessment of the LSST. The telescope size matches the size of extremely large MTs, and therefore some of the technologies and measurement techniques could be adapted for the LSST project. Thus, a new measurement procedure is aimed at this stage based on laser tracker technology and several fiducial points fixed to the floor. Once that the measurement procedure is designed, the target is to develop a complete simulation scenario within SA software to a) understand if the proposed procedure is fit for purpose and b) employ the simulated results to improve the measurement procedure aiming to reduce real survey time-consumption and uncertainty. Finally, the objective is to perform the in-situ survey of the LSST accuracy assessment.

4.2 Scientific contribution

The main contributions of this PhD study to the scientific community are:

- An updated review of the state of art of traceable CMM measurements on MTs. A qualitative approach of the uncertainty contributors that comprise the uncertainty budget is presented in detail. It highlights not just the main uncertainty contributors and its error sources, but also the significance of each uncertainty contributor on the final uncertainty budget.
- A quantitative approach to the uncertainty budget for on-MT measurement. The study demonstrates the realisation of a traceable CMM measurement on an MT and it also remarks the order of magnitude of the obtained expanded uncertainty for a medium size component, breaking down the significance of each uncertainty contributor.
- A new methodology for traceable CMM measurements on MTs without using a calibrated workpiece. A volumetric error mapping of the MT is proposed immediately before the measurement execution. In this

way, the systematic error contribution is assessed without using a calibrated workpiece so the main limitation presented by the ISO 15330-3 technical specification is overtaken and the on-MT measurement methodology could be scaled to large-size MTs.

- An integrated MT volumetric error mapping solution. The integration of a tracking interferometer into the MT spindle allows measuring the geometric error of an MT automatically in the complete volume, reducing the measurement time up to 75% of the total time consumption compared to the sequential scheme. In this way, it permits to scale traceable on-MT measurement to large-size MTs.
- A new survey procedure for the RPE assessment of the TMA subsystem for the cutting-edge LSST project. This new measurement procedure is developed within the LSM field and is based on laser tracker technology and several fiducial points fixed to the floor. Monte-Carlo-based simulations within SA software demonstrate that it is fit for purpose before performing the in-situ survey.
- The TMA subsystem RPE survey for the LSST project. It was performed within 70 min and obtained uncertainty results are better than 0.1 mm on a 40 m diameter measurement scenario. It improves that current state of the art of the LSM in shop-floor conditions for a large telescope [189].

4.3 Methodology

Dimensional measurements on MTs are already being employed at different stages of the manufacturing cycle because the technology to perform a measurement, either a TTP or measurement software, are already available on MTs. There are four potential measurement scenarios where on-MT measurement adds value to the manufacturing process: a) monitoring of the MT geometry performance by employing a calibrated standard; b) workpiece setup on the MT coordinate system; c) in-process measurements to provide correction values for the manufacturing; and d) the performance of a final metrology validation of the finished product for final quality inspection as well as statistical trend analysis of the manufacturing process. Nowadays, depending on the size of the component, the on-MT measurement TRL is at different stage: While large-scale manufacturing processes are employing on-MT measurements to reduce the setup time of large components on the MT bed, medium-size aeronautic manufacturers are already performing on-MT measurements for in-process measurement of high-value components, closer to realise traceable measurements on MTs. Nevertheless, any CMM measurement performed on an MT in shop-floor conditions is affected by several factors, such as MT geometric error, temperature variation, probing system, vibrations and dirt. Thus, the traceability of a measurement process on an MT is not guaranteed and measurement results are therefore not sufficiently reliable for self-adapting manufacturing processes. In this scenario, the aim of this PhD study is to generate new knowledge to assess traceable CMM measurements on MTs towards metrology enhanced zero-defect manufacturing processes.

The idea of converting an MT into a CMM is not new. Schmitt et al. from the RWTH Aachen University presented the guidelines for a traceable on-MT measurement [2,3]. Here, they proposed that a large MT could be employed as a comparator to measure the geometry of large-scale components. They also presented some experimental tests for a previously calibrated workpiece CMM measurements on an MT. In this context, there are several approximations for traceable on-MT measurements [12,13] where the systematic error contributor to the on-MT measurement uncertainty budget is corrected by an external metrology framework.

The main problem for traceable CMM measurements on MTs is that the machining and measuring processes are performed using the same machine, and some error sources therefore cannot be distinguished if a calibration

process is not realised before the measurement execution [176]. This is currently the main limitation to close the calibration chain for on-MT measurement.

In this scenario, there are two main approaches to perform traceable CMM measurements on an MT:

- MT calibration is performed by fitting measured data to a kinematic model of the MT. This calibration data shall reduce the mechanical inaccuracies of the MT so the systematic error of the MT performing as a CMM is reduced and considered on the uncertainty budget. The calibration process on the MT side should be performed immediately before the measurement stage.
- Closed loop control uses an external metrology framework to monitor and control the automation in real-time. This has several challenges, many of which are unique to the automation and controller. The line of sight requirement and the cost of the metrology equipment for the external metrology frame are the main barriers to this approach.

Owing to the similarity between CMMs and MTs, some of the methods employed for a correct assessment of uncertainty in CMMs are being adopted for MTs. The general guide for a suitable evaluation of measurement data is given in the ISO Guide 98-3: 2008, on the expression of uncertainty in measurement (GUM) [22]. Three different approaches are considered for an uncertainty assessment on an MT [6]: a) an experimental technique according to the ISO 15530-3 technical specification [8]; b) a numerical simulation-based approach, as described in the ISO 15530-4 technical specification [32]; and c) an uncertainty budget method based on the VDI 2617-11 guideline [37]. Thus, for small batch production, mainly in large scale manufacture, the substitution method is not an affordable solution because a calibrated workpiece similar to the manufactured part is needed. This requirement makes the solution tedious and expensive and therefore, the uncertainty budget-based solution according to the VDI 2617-11 guideline is being adopted. For serial production, usually, for small and medium-size components, the substitution method according to the ISO 15530-3 technical specification simplifies the uncertainty evaluation, because a calibrated masterpiece could be stored beside the MT preventing the manufactured workpiece from being carried to a temperature-controlled measuring room.

As stated by Slocum, MT errors can be divided into systematic errors and random errors [41,42]. While the former can be measured and compensated, the latter is difficult to predict. Therefore, an MT should have three main properties: accuracy, repeatability and resolution. Thus, for the on-MT traceability assessment an error budget is established, and the budget should comprise contributions from the measurement system—i.e. the MT itself (Section 1.2.5) with the touching probe (Section 1.2.6) and the measuring software (Section 1.2.7), from the component under measurement (Section 1.2.8) and the interaction between both of them. Considering the proposed MT main properties, every on-MT measurement error source is rearranged next:

- Accuracy: Systematic geometric errors of the MT (induced by kinematic errors, static loads and control software), TTP errors and measuring software errors are considered. The accuracy will mean the systematic error of the MT as a CMM, so it could be characterised and compensated to a high extent.
- Repeatability: Random error sources that affect the repeatability of the MT. Dynamic loads that affect the MT (such as backlash, forces and thermo-mechanical loads) and environmental influences that affect either the MT or the TTP are considered. Repeatability will mean the random error of the MT as a CMM, so it is difficult to measure and compensate.

- Resolution: Quality of sensors and quality of control system are considered.

The literature review describes a detailed description of every potential error source affecting the on-MT measurement. In summary, the MT is the main error source compared to the component under measurement or the measurement technology itself, i.e. TTP or software. Thus, the geometric error of the MT and its repeatability become the main uncertainty contributors to the on-MT measurement uncertainty budget. As far as the measurement scenario approaches to the large-scale, the geometric error of the MT becomes worse and the MT and the measured object become extremely sensitive to environmental influences such as temperature and gravity. Here the component under measurement becomes a major uncertainty contributor. On the other hand, TTP contribution becomes negligible on the large-scale measurement scenario because the TTP uncertainty is within 1 ± 2 μm , according to OEM specifications. However, for medium and small-size on-MT measurement it shall be considered on the uncertainty budget [6].

To sum up, a qualitative approach of the uncertainty contributors that comprise traceable CMM measurements on MTs is presented, considering not just the error sources but the significance of each uncertainty contributor on the uncertainty budget.

After the introduction to the state of art of traceable CMM measurements on MTs, the methodology adopted for the developing of the core knowledge of this PhD study is based on experimental work, initially in simulation mode and afterwards in real experimental-measurement mode to validate the uncertainty budget assumptions proposed on the literature review.

For serial production, usually, for small and medium-size components, some of the most important players on the aircraft supply chain are already performing traceable CMM measurements on-MTs for medium-size engine manufacturing processes. Thus, a medium size on-MT measurement uncertainty exercise is performed in shop floor conditions with a calibrated prismatic part according to the ISO 15530-3 technical specification [23].

According to this technical specification, there are four uncertainty contributors that comprise all the systematic and random errors that should be considered on the uncertainty budget for CMM measurements on MTs:

- U_b standard uncertainty associated with the systematic error of the measurement process.
- U_p standard uncertainty associated with the measurement procedure.
- U_{cal} standard uncertainty associated with the uncertainty of the workpiece calibration.
- U_w standard uncertainty associated with material and manufacturing variations.

The expanded measurement uncertainty of the complete measurement process (U_{MP}) is assessed by $U_{MP} = k \times u_{MP}$ and the expanded measurement uncertainty of the measurement system (U_{MS}) is assessed by $U_{MS} = k \times u_{MS}$, for a coverage factor of $k=2$, where u_{MP} and u_{MS} are given by the same formula where input information comes from measurements executed immediately after the machining process and under no-load condition, respectively.

For the experimental exercise performed on a medium size KONDIA MT available at IK4-TEKNIKER premises, five workpiece replica material standards were manufactured, followed by on-MT measurement in the same chucking using a RENISHAW OMP 400 tactile probe. Each workpiece was measured ten times on the MT to distinguish between the systematic and the random errors and assess the uncertainty budget for the entire measuring process

(U_{MP}). In addition, one workpiece was measured ten times on the MT at 20 °C operating either under no-load or under quasi-static conditions to assess the uncertainty budget of the measuring system (U_{MS}). The workpiece replica standard selected for the experimental uncertainty assessment exercise was defined at ISO 10791-7:2014 standard [177] and it is referenced as “Test piece ISO 10791-7, M1-160”. Every workpiece was calibrated on a high-accuracy ZEISS CMM, using the VCMM tool for the task-specific uncertainty assessment [176].

Apart from this quantitative approach, the aim of this experimental test is to understand how the geometric error of the MT affects to the systematic error contributor to the on-MT measurement uncertainty budget. Thus, a geometric characterisation of the MT under consideration was performed under a no-load condition. The sequential multilateration-based approach was executed with a laser tracer NG technology from ETALON AG OEM.

During the experimental test, the workpiece temperature increases to 22.5 °C (on average) immediately after the machining process and it stabilizes to 19.5 °C (on average) after two hours. During this time interval, on-MT measurements are performed every ten minutes so the measurement procedure uncertainty contributor can be assessed.

Before obtaining the values for each uncertainty contributor, the substitution method is applied for diameter measurement result correction to amend the insufficient calibration of the probing system on the MT spindle. It highlights the significance of a correct probing system calibration before the on-MT measurement performance. Consequently, the uncertainty budget according to the ISO 15530-3 technical specification comprises the three major uncertainty contributors:

For the systematic contributor (u_b), results after the diameter correction show that every mean systematic error is within 10 μm . In addition, results correlate with the geometric error of the MT, particularly with positioning errors in X and Y axes, and squareness between them. Therefore, it seems that geometric error of the MT is the main error source affecting to the u_b major uncertainty contributor, which means that an MT geometric error characterisation could supply the information for the systematic contributor assessment, without the use of a calibrated workpiece.

For the measurement procedure uncertainty contributor (u_p), it is of utmost importance to understand the effect of the temperature gradients on the result. Thus, the experimental test proposes on-MT measurements immediately after the machining process and measurements under a no-load condition when the temperature on the MT side and workpiece side is constant at 20 °C. Thus, measurement procedure uncertainty results show differences between the measurement executed under the no-load condition and the measurements executed immediately after the machining process. Every result shows repeatability within 6 μm for the no-load condition, while the maximum repeatability values for the measurements immediately after the machining process are within 10 μm . Form error feature measurement (flatness and roundness) show better measurement procedure uncertainty results than scale related feature measurement (diameter and positioning values) because these features are more sensitive to the measurement scenario temperature variation.

For the calibration uncertainty (u_{cal}) results, the maximum uncertainty value is up to 2 μm for the CMM positioning error in the Y direction.

To sum up, the measurement procedure uncertainty contributor is the main contributor to the on-MT measurement uncertainty budget in shop floor conditions. It is larger on the measurements executed immediately after the machining process, mainly affected by the dynamically changing temperature conditions of the measurement scenario. For the no-load measurement condition, the measurement procedure uncertainty contributor is also a few

microns larger than the systematic error uncertainty contributor, which maintains within $8\ \mu\text{m}$ for every measured feature. In addition, the systematic error correlates with the geometric error of the MT, particularly with positioning errors in X and Y axes, and in the squareness between them. Therefore, it seems that the geometric error of the MT is the main error source affecting the systematic error contributor. Uncertainty contribution related to the tactile probe could be close to the supplier specifications, within $1\ \mu\text{m}$ [176].

According to the performed experimental test, the geometric error of the MT is the main error source for the systematic error contributor to traceable on-MT measurement. This conclusion opens the door to a new potential measurement procedure to realise traceable on-MT measurements. The ISO 15530-3 technical specification has a strong limitation, it requires a calibrated workpiece to understand the systematic error of an MT when performing as a CMM. It means that a calibrated standard is required beside the MT to close the calibration chain, which does not make sense for high-value components at large-scale manufacturing scenarios. It concludes that the ISO 15530-3 technical specification-based approach is fit for purpose for medium-size components manufactured in series production, but for small batch production, mainly in large scale manufacture, the substitution method makes the solution expensive. For that reason, a new measurement procedure is proposed to perform traceable large-scale on-MT measurements without employing a calibrated workpiece to assess the systematic error contributor on the uncertainty budget.

The idea here is to perform the VDI 2617-11 guideline [37]. For this approach, the determination of the on-MT measurement uncertainty is determined with an uncertainty budget. Here, each uncertainty source and its magnitude on the measurement result should be contemplated. In this case, error sources are as follows [178]:

- The geometric error of the MT and its repeatability.
- Probing system.
- Temperature: MT structure, surrounding and workpiece
- Workpiece under measurement: Temperature and clamping.
- Measurement procedure.
- Geometric error mapping technique.

Making a parallel with the previously presented exercise according to ISO 15530-3 technical specification, the systematic error contributor on the VDI 2617-11 guideline is affected by those error sources: The geometric error of the MT, the probing system, the workpiece under measurement, the measurement procedure and the geometric error mapping technique. The random contributor comprises the MT repeatability, the touch probe repeatability and the temperature variation on the measurement scenario.

At this stage, the most suitable methodology to demonstrate the proposed methodology is to perform a new experimental test on the same MT with the same workpiece replica standard used on the ISO 15530-3 approach. Here, the calibrated workpiece is not employed for the systematic error assessment of the MT performing as a CMM but for the validation of the proposed new measurement procedure. A volumetric error mapping of the MT was performed immediately before the on-MT measurement with laser tracer NG technology for the assessment of the systematic error contributor. It employs a kinematic model that permits to calculate the geometric error of any point within the measured volume from the volumetric error mapping information, so the geometric error of the on-MT measurement contacts points was assessed this way. In this uncertainty budget, the measurement procedure and

the workpiece under measurement are not considered on the because an easy-to-measure medium-size prismatic component was measured. Furthermore, negligible deformations occur during the clamping process. In addition, the probing system characterisation and the uncertainty of the volumetric error mapping technique were within 2 μm [178].

The experimental test was performed under the no-load condition when the temperature on the MT side and workpiece side is constant at 20 °C with a temperature variation within 0.5 °C. In addition, a reliable tactile probe calibration was performed prior to the on-MT measurement exercise, the repeatability on the calibrated ring measurement is within 1 μm , which is within the on-MT repeatability obtained values. In this way, it is considered negligible on the uncertainty budget. For the measurement procedure uncertainty, results obtained from the ISO 15530-3 technical specification based experimental test are considered, because they do not require a calibrated workpiece. For the systematic error contributor assessment, the proposed methodology, depicted in Figure 2-6, was applied. Results show that difference in the systematic error assessment comparison between the ISO 15530-3 technical specification and the VDI 2617-11 guideline is within 1.5 μm .

Finally, experimental results show that the uncertainty budget according to the VDI 2617-11 guideline obtains similar results to what obtained according to the ISO 15530-3 technical specification, where a calibrated workpiece is employed for the uncertainty assessment. For the systematic error contributor, the difference between both approaches is within 1.5 μm which fits with the uncertainty of the volumetric error mapping performance, roughly 1 μm . In addition, the calibration uncertainty is similar in both cases, because of the employed reference standards, either the calibrated workpiece or the volumetric error mapping solution, have a similar uncertainty contributor. For the measurement procedure uncertainty contributor, the same raw data is employed [178].

The MT volumetric error mapping processes on the previous experimental exercises were sequentially performed by a qualified technician. It shows that technically a traceable on-MT measurement can be performed without employing a calibrated workpiece but is far from being an industrial solution.

To tackle this limitation, the next milestone of this PhD study proposes the integration of a volumetric mapping error measurement solution within the MT. In this way, the volumetric error mapping of MTs can be performed in a short period of time and automatically, without no-human intervention. The methodology here is to perform an initial simulation of the suggested integration exercise and execute it on a real MT once that simulation shows that it could be fit for purpose.

The idea of integrating a tracking interferometer into the MT breaks with the typical multilateration approach that requires at least four fixed points for displacement measurement, either absolute or relative, between those fixed points and any moving measuring point. According to this measurement distribution requirement, typically tracking interferometers are set on the MT table in the fixed points' positions and a measuring reflector is attached to the moving spindle to materialize the moving points [179].

Thus, the integrated tracking interferometer moves to every measurement point while reflectors represent the fixed fiducial points. This new configuration breaks the barrier to an automated MT calibration solution because manual intervention is avoided on fixing tracking interferometers to each measurement station on the MT table.

This integrated solution presents a totally different measurement sequence. In this case, the tracking interferometer is moved to every measurement point, from which pointing to every fiducial point occurs in sequence. It means that

spatial relationship between fiducial points and volumetric point grid shall be established beforehand. Thus, initial automation of the measurement acquisition sequence plays a very important role because the spatial relationship between fiducial points and the point grid needs to be characterized in the MT coordinate system. A characterisation procedure is proposed to deal with the spatial relationship between the fiducial points and volumetric point grid [179].

Once that spatial relationship between points is solved in the MT coordinate system, nominal point grid information helps to command the pointing from the tracking interferometer to every fiducial point for every measurement position. To do it automatically, MT movement and data acquisition sequence are synchronized. This is done by means of a wireless LAN communication between data acquisition software and the MT's interface. Thus, a measurement trigger is sent from every measurement position to synchronize the last fiducial point acquisition with the MT next movement.

The integrated measurement procedure was initially simulated within SA software, results in Figure 2-13 show that the uncertainty with this approach is similar to the typical multilateration approach which makes sense because mathematics behind the measurement procedure is the same.

Finally, two experimental exercises were performed: a) A first experimental exercise executed on an available KUKA KR60 industrial robot where a Monte-Carlo based simulation was performed with the real measurement scenario information; and b) an integration of a typical multilateration scheme on a ZAYER MEMPHIS large-scale MT, comparing the integrated approach results with the typical multilateration scheme.

a) For the KUKA KR60 experimental exercise, a LEICA AT402 laser tracker was mounted on the robot spindle and four fiducial points were fixed surrounding the robot. The spatial relationship between fiducial points and volumetric point grid was successfully tested and data acquisition sequence was synchronized with robot movement. Thus, a movement trigger command was sent from the laser tracker to the robot for every measurement position.

From the simulation results point of view, a total of 96 measurements were sequentially introduced within the Monte-Carlo simulation model of the real measurement scenario. 300 iterations were run to determine the expanded measurement uncertainty for every measurement point in X, Y and Z directions (U_x , U_y and U_z , respectively). Results show that the standard deviation of length residuals is 0.0065 mm, slightly smaller than the uncertainty of the fixed error measurement of the employed tracking interferometer (U_f). It means that either length residuals results or uncertainty results are similar to the accuracy of the employed tracking interferometer. It concludes that thermally induced dimensional drift is smaller than uncertainty results achieved on such a fast measurement acquisition sequence in this case. In fact, the total time consumption for the presented measurement case was 8 min, which means that LEICA AT402 laser tracker took 20 sec to measure the four fiducial points from every measurement point.

b) For the MT integration exercise, the integrated approach was compared to the typical multilateration approach. Thus, the typical multilateration approach was performed on a large ZAYER MT with laser tracer NG technology. In this case, only one laser tracer NG was available, so in practice, multilateration measurements were performed in a sequential scheme. The integrated multilateration approach validation was performed with a LEICA AT960 laser tracker fixed to MT spindle. The validation of the integrated approach was performed on the ZAYER MT manufacturer premises.

The point grid to be measured was comprised of 64 points. The mapped working range of the MT was: X = 3000 mm, Y = 2300 mm and Z = 900 mm. The validation plan is explained next:

- MT volumetric error mapping was performed with the typical multilateration approach employing a laser tracer NG. Four measurement positions were employed and measurement acquisition time was 2 h and 30 min.
- Integrated multilateration approach was executed with a LEICA AT960 laser tracker fixed to the MT spindle, upside-down. Four cat-eye reflectors defined the fiducial points, three of them fixed to the floor and the fourth one fixed out of the floor plane to improve the measurement accuracy on the vertical direction. The total time consumption for the integrated approach was 25 min.

For the validation of the integrated multilateration approach against the typical approach several comparisons were performed: a) The uncertainty values of the fiducial points; b) the uncertainty values of the volumetric point grid; c) the comparison between the measured point clouds for both approaches; and d) the comparison between the kinematic model output for both approaches. The measurement execution demonstrates a time reduction of up to 75% of the total time consumption compared to the typical approach. Similarly, the integrated approach helps to reduce the measurement uncertainty, which is somehow proportional to the time consumption in a non-controlled shop-floor environment [182].

This PhD study focuses on the development of new knowledge for traceable CMM measurements on MTs where the MT accuracy improvement is required to reduce the systematic error of the MT working as a CMM. The knowledge generated within the integration of the multilateration scheme on the MT is being horizontally transferred from an industrial sector application to the industry of science sector to develop a new measurement procedure for the LSST project. In this way, this PhD study also comprehends the accuracy assessment of the cutting-edge LSST. The LSST is a wide-field survey reflecting telescope with an 8.4-meter primary mirror [183] currently under construction, that will photograph the entire available sky every few nights.

IK4-TEKNIKER is playing an outstanding role in this unique scientific project. Among other tasks, IK4-TEKNIKER aims to develop and perform the so-called RPE assessment of the TMA subsystem. The LSST should be considered as a high accuracy sky measurement machine within the scope of this thesis, so, both, an MT and a large telescope have a measurement error that shall be performed with an uncertainty budget. As any measurement device, the uncertainty budget is comprised of systematic and random components of error that should be assessed as accurately as possible. The problem here is that the LSST meets the current state of the art of the LSM field. Therefore, the challenge is to develop a new measurement procedure within the LSM with commercial measurement equipment to assess the accuracy requirement of the TMA subsystem in shop-floor conditions.

In this case, the methodology employed for the development of the new measurement procedure is based on the development of a complex simulation platform within SA software to understand the measurement scenario and its uncertainty contributors. Simulation results allow to improving the measurement procedure until is fit for purpose and finally it shall be employed on the real in-situ survey of the TMA subsystem.

There are two main challenges that make the LSST measurement scenario unique: a) the coordinate uncertainty shall be within 0.1 mm on a 40 m diameter measurement scenario in shop-floor conditions; and b) any pointing motion within the LSST pointing range shall be characterised considering that every measurement shall be

performed on the M1M3 reference of the TMA. The latest point presents a huge challenge due to the reduced visibility between the outside and the inside volume of the telescope. Thus, the aim here is to develop a customized survey procedure to assess the pointing accuracy of the TMA subsystem within these demanding requirements.

In fact, there is a unique possible arrangement of the measurement system to perform the pointing accuracy survey of the telescope. The measurement system should be fixed inside of the TMA subsystem to execute the TMA positioning matrix, shown in Figure 2-26, that depicts the complete pointing range of the telescope. In this way, the new measurement procedure for the RPE assessment of the TMA subsystem is defined as follows: A laser tracker is placed inside of the LSST, close to its origin, and a circular shape metrology network comprising a reference point cloud is fixed to the floor, outside and surrounding the LSST telescope. This metrology network is of special importance, as any laser tracker location during the whole measurement process is solved by the measurement of this fiducial metrology network. Thus, the RPE measurement procedure consists of measurements of the metrology network to locate the laser tracker, and afterwards, measurements of the optical axis of the TMA by measuring four target points at the M1M3 reference plane. As a result, the M1M3 reference plane is located on an earth-fixed reference system, i.e., the floor, so each observation angle for the TMA is characterized and compared to the input position, which means the RPE assessment. The measurement process is repeated for each of the pointing positions defined in the positioning matrix and within the pointing range of the LSST. It should be highlighted that the laser tracker position is fixed close to the LSST origin, to nullify the range of the angle of incidence from the laser tracker to the reflectors. Thus, the laser tracker tilts with the rotation centre of the telescope and incidence angle does not change which means that it will not cause a longer travelling path of the beam inside the prism. For the LSST project, 25 mm hollow corner cube optics are employed [184].

However, it is not clear that the measurement procedure will meet the accuracy challenge, so there is an important previous simulation work to understand how the new survey procedure performs. For that reason, an advanced simulation model was built within SA software to understand that the measurement procedure was or not fit for purpose. Based on the Monte-Carlo technique, the simulation model aimed to assess the coordinate uncertainty for the fiducial metrology grid, the RPE measurement uncertainty and the parallelism between M1M3 and M2 according to the developed measurement procedure. For that simulation, a Gaussian random number generator (utilizing a Box-Muller algorithm) mathematically simulates the measuring scenario with 500 sensitivity samples and the standard deviation parameter is calculated as an uncertainty indicator of the simulated measurement methodology. The Box-Muller algorithm executes the laser tracker error model according to the specifications of the OEM LEICA at a 68.3% confidence level ($k = 1$). It shall be stated that the simulation model also considers how the floor behaves in real shop floor conditions, considering that the reference fiducial metrology network behaves according to the floor movement. Up to now, when performing a laser tracker measurement, it was supposed that fiducial points do not move, but it cannot be assumed in such a high accuracy application. Depending on temperature variation, measurement time-consumption and the shop floor construction, the floor moves and therefore fiducial points do accordingly. This error source was introduced on the simulation model, so obtained results demonstrate how this movement affect the targeted RPE measurement [184].

Simulation results show that the coordinate uncertainty for fiducial metrology network is within 0.1 mm, which means that RPE assessment can be performed within 5 arcsec uncertainty. These simulation results correlate with

the uncertainty results obtained at the LBT active alignment system with laser tracker technology on a similar LSM measurement scenario [189].

In addition, simulation results also permit to understand that: a) the TMA repeatability cannot be assessed with the proposed survey procedure because results cannot perform within 1 arcsec of uncertainty ;and b) the parallelism between M1M3 and M2 could be performed within 2 arcsec with laser tracker technology for the complete pointing range of the telescope.

At this point, once that the new survey procedure seems to be fit for purpose, there is one main challenge to deal with for the successful in-situ performance on the TMA subsystem: the temperature effect on the measurement network. The real laser tracker performance could also be considered as a challenge on the in-situ survey, but it was already tested in the simulation mode and the USMN tool was employed to improve the poor encoder accuracy performance. For the temperature significance on the final accuracy result, the best approach to reduce its effect is to keep the acquisition time to the minimum. In this way, a second major challenge arises on how to automate the full measurement execution of the RPE test. Here, a fully automatic verification procedure is proposed. The laser tracker-based measurement program is interconnected to the LSST control software by the means of a TCP/IP in a private connection, and the USMN tool is applied during the measurement procedure, so most of the fiducial points are measured for every LSST pointing position. The TCP/IP connection permits the synchronization of the LSST movement with the laser tracker measurement sequence so the time consumption can be reduced, down to 60 ÷ 90 min. It means that temperature variation effect either on the laser tracker performance or the fiducial metrology network drift shall be reduced improving the final accuracy result.

Finally, the survey was performed in-situ on the TMA subcomponent. There are several challenges on the real survey execution that should be highlighted to understand the complexity of such an LSM measurement exercise: a) laser tracker was placed close to the LSST origin by means of a vertical physical support and therefore, laser tracker working orientation varies according to the TMA pointing position. When the telescope is pointing to the horizon, laser tracker working orientation is 90 degrees as shown in Figure 2-33a. For that reason, a LEICA AT960 laser tracker was employed on the in-situ survey, which apparently performs similarly for any laser tracker working orientation; b) the shape of the measurement scenario is far from the simulated one: the available area in the shop floor, the stairs that connect the floor with the telescope and the office building place beside the TMA disrupt the simulated measurement scenario so the fiducial metrology network is adapted to the real measurement layout; and c) the automation process of the complete measurement sequence implies a complex in-situ work.

After three days of preparation (laser tracker and fiducial metrology network definition, measurement strategy, code of the automatic measurement program...) the survey was performed. The measurement acquisition and results obtaining processes were automatically performed within 70 min, which means that results were obtained almost in real time for the in-situ decision-making process. RPE results show that the measurement uncertainty is within 2 arcsec which improve the simulated results, mainly because the LEICA AT960 cutting-edge laser tracker was employed. Furthermore, it also means that TMA repeatability cannot be assessed within the 1 arcsec requirement. In this way, the repeatability measurement was repeated with direct measurement methods, i.e. autocollimator and mirror for the azimuth axis assessment and electronic levels for the elevation axis assessment, respectively. In addition, the parallelism between M1M3 and M2 for every pointing position of the telescope is ensured to perform

within 1.5 arcsec, which means that the structure of the telescope does not suffer from rigidity variation for different elevation axis pointing positions.

Finally, a huge LSM simulation knowledge was developed at this stage of the PhD study, there is a real possibility to develop an advanced LSM simulation tool for LSM complex measurement scenarios.

4.4 Conclusions

The overall purpose of this PhD study has been fulfilled, considering that new knowledge for traceable CMM measurements on MTs is provided. This thesis presents traceable on-MT measurements realisation for medium-size components according to the standards and guidelines that rule current traceable CMM measurements and propose new measurement procedures for the large scale on-MT measurement challenge.

An increasing number of MT users perceive traceable on-MT measurement functionality as an opportunity to improve their manufacturing processes and move forward to the zero-defect paradigm. Some of them, involved in the manufacturing of high-value components have already started performing the MT as a CMM but they cannot assess the traceability of their on-MT measurements yet. For serial production, usually, for small and medium-size components, some of the most important players on the aeronautics supply chain are already performing traceable on-MT measurements for medium-size engine manufacturing processes, according to the ISO 15530-3 technical specification. In this way, the substitution method simplifies the uncertainty evaluation because it is affordable to manufacture and calibrate a reference part for uncertainty assessment purposes. This PhD study shows that the main uncertainty contributors for this small and medium-size on-MT measurement are: a) the measurement procedure uncertainty contributor; and b) the systematic error contributor mainly affected by the geometric error of the MT.

When it comes to large-scale manufacturing scenario, traceability of on-MT measurement faces similar challenges to what the LSM does. Large-size on-MT measurements are extremely sensitive to environmental influences such as temperature and gravity, which influence the measurement procedure uncertainty contributor. Moreover, the systematic error contributor can also be a major contributor if the geometric error of the MT is not previously calibrated. In this scenario, this PhD study presents an integrated volumetric error mapping approach into the MT spindle. It allows improving the time-consumption and accuracy of the typical multilateration approach, as well as automating the volumetric error mapping process. Thus, the complete volumetric error mapping process can be performed within 30 min and the volumetric compensation of the MT can be executed, compensating the geometric error of the MT and reducing the systematic error component of the on-MT measurement uncertainty budget. However, there is a strong barrier to industrialize the integrated solution nowadays because the economic cost of the commercial tracking interferometer to be integrated on the MT is relatively high. Anyway, technologically speaking, a volumetric error mapping of the MT immediately before the measurement process execution could help to distinguish the systematic error contribution between the machining and measuring processes performed at the same MT. This is the foundation of the new methodology for on-MT uncertainty assessment that is presented within this thesis for large-size traceable on-MT measurements. Compared to the ISO 15530-3 technical specification that considers a calibrated workpiece to close the traceability chain, the new methodology can be performed on a large MT without a calibrated workpiece.

Experimental results show that traceable on-MT measurements can be performed, either based on the use of a calibrated workpiece or based on a volumetric error mapping of the MT immediately before the measurement process execution. Owing to the availability of a medium size MT at IK4-TEKNIKER premises, on-MT measurement experimental tests were performed on a medium size prismatic component. Considering the ISO 15530-3 technical specification, an experimental test comprised of five workpiece replica standards were manufactured and subsequently measured on an MT. Results show expanded uncertainty results within 20 μm and the significance of each uncertainty contributor on the uncertainty budget. Here, the measurement procedure uncertainty is the main contributor and the geometric error of the MT is the main error source for the systematic error contributor. For the VDI 2617-11 guideline, an experimental test without a calibrated standard was performed and the volumetric error mapping of the MT immediately before the measurement process execution assessed the systematic error contributor performance. Results demonstrate that traceable on-MT measurement can be realised without a calibrated workpiece, obtaining results that are similar to those obtained with the ISO 15530-3 technical specification.

This PhD study also considers a unique opportunity to contribute to the state of art of the LSM field within the LSST project. The LSST is a unique and cutting-edge worldwide project that will address several profound questions, such as: What is the mysterious dark energy that is driving the acceleration of the cosmic expansion? What is dark matter, how is it distributed, and how do its properties affect the formation of stars, galaxies, and larger structures?...[183].

Behind this exciting scientific project, the pointing and alignment performance of the telescope will have a very strong influence on the quality of the scientific results obtainable, so the importance of the LSM assessment is remarkable. In this scenario, a new survey method for the RPE assessment of the LSST is proposed within this PhD study. From the concept design to the real survey performance of the telescope, the new measurement procedure offers a reliable LSM survey solution for large telescopes. The survey method was performed in-situ on the TMA subcomponent within 70 min and it assesses uncertainty results better than 0.1 mm on a 40 m diameter measurement scenario. It clearly states the current state of the art of the LSM in shop-floor conditions.

To sum up, it is worth remarking that metrology can leverage the competitiveness of the MT industry and the advanced manufacturing industry in general, including the industry of science sector where accurate survey methods are required to meet with the accuracy-related specifications. In this way, it is a KET for MT manufacturers that aim to develop precise and accurate MTs with new technologies and services that are major determinants of the competitive advantage in the sector. It is also remarkable that the LSM field should help to execute major scientific projects such as the cutting-edge LSST project. Thus, metrology is increasingly being recognised for its role as a KET of Industry 4.0 in data-driven manufacturing and industrial digitalisation.

4.5 Future work

The research performed within this PhD thesis provides some prospective points for the future research of LSM for MTs and large scientific projects.

Before performing traceable CMM measurements on an MT, the aim should be to improve the geometric performance of the MT during its lifetime. Thus, this thesis proposes an integrated and automatic volumetric error mapping approach that could be performed continuously on the MT. It technically fits the purpose of verifying the geometric error of an MT in the complete volume reducing the measurement uncertainty and time consumption,

but from the point of view of technology access, the available commercial technology has a high investment cost nowadays. Therefore, the recommended future work in this line is to develop a cheaper absolute and CNC guided measurement device, reducing the measurement functionalities of current commercial tracking interferometer to what is needed on the proposed integrated measurement procedure. This potential measurement device could allow improving the ROI to MT manufacturers and the massive adoption of the technology.

For the traceability of large-size on-MT measurements, the lack of available large-size MTs during this PhD study has conditioned the experimental part of the thesis. It is strongly recommended that every experimental test performed within this thesis shall be scaled to a large on-MT measurement scenario. It shall contribute to understanding the performance of a large-MT working as a CMM and the significance of each error contributor on the large scale.

From the LSM field point of view, the LSST project has been a state of the art challenge on this PhD study. A customized simulation code has been developed for the project to understand how laser tracker technology performs on such an LSM measurement scenario. This simulation code could become on an LSM metrology simulation tool that shall be employed on high accurate large-scale projects. The article presented by Mutilba et al. already commented that possibility [184] and presented some simulation results for a potential onboard laser tracker metrology solution. It seems that this measurement simulation tool could become in a general laser tracker based LSM simulation active for IK4-TEKNIKER research centre.

5. RESUMEN



5. RESUMEN

5.1 Objetivos

El objetivo principal de esta tesis doctoral es generar nuevo conocimiento para realizar el ejercicio de asignación de incertidumbre a la medición por coordenadas realizada en una MH y así, demostrar que la medición por coordenadas trazable en MH es realizable. Con este gran objetivo en el horizonte, esta tesis doctoral propone hitos intermedios que se presentan en las siguientes líneas.

El punto de partida es entender el valor estratégico de los potenciales resultados de esta tesis doctoral. En un escenario de competitividad donde la diferenciación del producto en términos de nuevas funcionalidades y servicios son determinantes para garantizar la productividad, la calidad y la reducción de costes del usuario final, la funcionalidad de la medición por coordenadas trazable en MH podría suponer una ventaja competitiva para el sector de la MH. Actualmente, la medición en MH ya está siendo empleada por los fabricantes de componentes de alto valor añadido. Es el caso de los proveedores de las piezas de motor mecanizadas para el sector aeronáutico. Aquí, se realizan mediciones en la MH para verificar que las cotas críticas del componente han sido bien fabricadas y así evitar volver a introducir la pieza en máquina tras el control de calidad dimensional que habitualmente se realiza en planta, al lado del medio productivo. Para los fabricantes de componentes de gran tamaño, como por ejemplo, los proveedores de componentes del sector eólico y/o aeronáutico, la medición en MH se está empleando para optimizar el alineamiento inicial de la pieza en la mesa de la MH. A diferencia de los anteriores, donde por el tamaño medio de la pieza se puede emplear una pieza patrón para realizar el ejercicio de asignación de incertidumbre en la MH, los fabricantes de componentes de gran tamaño no pueden emplear una pieza patrón por el alto coste y gran tamaño de los componentes.

En realidad, la tecnología para realizar mediciones en MH ya está disponible, como son los palpadores de contacto y los softwares de medición. Sin embargo, hay varios factores que impiden asegurar la trazabilidad de la medición por coordenadas en MH realizada en condiciones de taller, que no permiten emplear las medidas realizadas para controlar el proceso de fabricación o validar la pieza en la propia MH, asegurando un proceso de fabricación cero-defectos.

El primer hito de la tesis doctoral presenta el estado del arte actual de la medición por coordenadas trazable en MH. Aquí, se realiza un estudio cualitativo de los componentes de incertidumbre que afectan a la trazabilidad de estas mediciones. Se emplea una aproximación basada en el balance de incertidumbres donde se deben considerar las diferentes fuentes de la incertidumbre, que son: el sistema de medición compuesto por la MH, el palpador y el software de medición, el mensurando y la interacción entre ambos. Desde el punto de vista de la normativa aplicable, se realiza un estudio de las normas que se aplican en la actualidad para la asignación de incertidumbre en las MMC y que podrían ser aplicables a la medición por coordenadas en las MH. Este estudio del arte también identifica las limitaciones principales de emplear una MH como una MMC, y estas limitaciones a su vez, se convierten en los retos principales de esta tesis doctoral.

El siguiente hito presenta un estudio cuantitativo para caracterizar cuantitativamente el balance de incertidumbres de forma experimental. Según el documento técnico ISO 15530-3, se ha realizado un estudio experimental en condiciones de taller sobre una pieza prismática de tamaño medio y los resultados muestran que la medición por

coordenadas trazable en MH es realizable. Además, se muestran las principales componentes de incertidumbre y sus fuentes de error que afectan al balance de incertidumbres. Aquí, la incertidumbre del proceso de la medición se muestra como la principal componente del balance de incertidumbres y el error geométrico de la MH se presenta como la principal fuente de error del componente de incertidumbre asociada al error sistemático. Sin embargo, el procedimiento que describe el documento técnico ISO 15530-3 presenta una gran limitación: el uso de una pieza patrón para asignar la componente de incertidumbre asociada al error sistemático. Esto limita el uso de este procedimiento a MH de tamaño medio y pequeño.

Como se describe en la introducción, esta tesis doctoral identifica que la medición por coordenadas trazable en MH es de especial interés para escenarios de fabricación de componentes de gran tamaño y alto valor añadido, donde los costes asociados al proceso de fabricación no admiten piezas no-conformes. Por lo tanto, el reto aquí es escalar la solución de medición por coordenadas trazable a MH de gran tamaño y se propone una nueva metodología para superar la limitación que presenta el documento técnico ISO 15530-3, basando la medición del componente asociado al error sistemático en una caracterización volumétrica previa de la geometría de la MH.

El siguiente objetivo trata de demostrar experimentalmente que la nueva metodología propuesta en el párrafo anterior puede realizar el ejercicio de asignación de incertidumbre para una medición por coordenadas en una MH con garantías y que por lo tanto, se puede prescindir de una pieza patrón para asegurar la trazabilidad de las mediciones. Los resultados obtenidos son muy positivos pero destacan que la caracterización geométrica previa de la MH limita la industrialización de la solución por el excesivo tiempo que conlleva realizar la verificación volumétrica de la MH.

En este escenario, el reto aquí se centra en desarrollar una solución de verificación geométrica y volumétrica integrada en la MH, de tal forma que la verificación se pueda realizar de forma automática y en un espacio de tiempo reducido. Esta nueva metodología supera las barreras técnicas del proceso de multilateración secuencial que se emplea en la actualidad y por lo tanto, se convierte en una tecnología habilitadora para el nuevo procedimiento de medición por coordenadas trazable en MH de gran tamaño. Además, su integración en la propia MH permitiría asegurar la precisión de la MH en todo su ciclo vida, habilitando verificaciones periódicas de la MH para asegurar su precisión.

Para finalizar, esta tesis doctoral asume el reto de desarrollar un nuevo procedimiento para la caracterización de la precisión de apunte del telescopio LSST. Con el conocimiento generado en la integración de la solución geométrica en la MH, se ha desarrollado un procedimiento de medición automático para verificar el requisito de apunte dentro de todo el rango de trabajo del telescopio y en un espacio reducido de tiempo para minimizar el efecto geométrico negativo de la temperatura. Este nuevo procedimiento se basa en integrar un sistema de medición láser tracker en el telescopio LSST y en fijar puntos de control fiduciales en el suelo y alrededor del telescopio. El procedimiento de medición se ha modelizado en el software SA y una simulación previa de tipo Monte-Carlo ha permitido determinar que el procedimiento es adecuado para cumplir con el objetivo. Para finalizar, el último objetivo es realizar la verificación in-situ de la precisión de apunte del telescopio LSST.

5.2 Contribución científica

Las principales contribuciones científicas de esta tesis doctoral se describen a continuación:

- Un estado del arte actualizado sobre la medición por coordenadas trazable en MH. Se presenta un estudio cualitativo de las componentes de incertidumbre que condicionan la trazabilidad de estas mediciones. Aquí, se destacan no solo las principales componentes de incertidumbre y sus fuentes de error, sino también la importancia de cada componente en el balance de incertidumbres.
- Un estudio cuantitativo del balance de incertidumbres de la medición por coordenadas en MH. Este trabajo demuestra que la medición por coordenadas trazable en MH para piezas de tamaño medio es realizable y muestra un desglose en detalle de las componentes de incertidumbre que forman el balance de incertidumbres.
- Un nuevo procedimiento para realizar el ejercicio de asignación de incertidumbre a una medición por coordenadas en MH sin emplear una pieza patrón. Aquí, se plantea una verificación volumétrica previa de la MH para conocer su error geométrico y así, determinar la componente asociada al error sistemático de la medida en MH sin emplear una pieza patrón, superando la limitación del documento técnico ISO 15530-3.
- Un nuevo procedimiento para realizar la verificación volumétrica de una MH mediante una solución integrada en la propia máquina, de forma automática y en un espacio de tiempo reducido. De esta forma, se reduce el consumo de tiempo hasta en un 75 % comparado con la aproximación secuencial que se emplea actualmente, permitiendo escalar la medición por coordenadas trazable en MH a componentes gran tamaño.
- Un nuevo procedimiento para la verificación de la precisión de apunte del telescopio LSST. Este nuevo procedimiento se enmarca dentro del campo de la metrología de alto-rango y se materializa con la integración de un sistema láser tracker en el propio telescopio y con varios puntos de control fiduciales fijos en el suelo. Una simulación previa de tipo Monte-Carlo ha permitido optimizar el procedimiento y determinar que es adecuado para cumplir con su objetivo.
- La verificación in-situ de la precisión de apunte del telescopio LSST. La duración de cada tanda de medición fue de 70 minutos y la incertidumbre de medición para los puntos fiduciales que describen un diámetro de 40 m es mejor que 0.1 mm. Esta actuación iguala o incluso mejora el estado del arte actual de la verificación de un telescopio de gran tamaño en condiciones de taller [189].

5.3 Metodología

La medición por coordenadas en MH ya está siendo empleada en diferentes fases de un proceso de fabricación porque la tecnología para realizar mediciones en MH ya está disponible, como son los palpadores de contacto y los softwares de medición. Hay cuatro potenciales usos de la medición por coordenadas en MH que aportan valor al proceso de fabricación: a) La monitorización de la geometría de la MH en base a la medición de un patrón dimensional con la propia máquina; b) la optimización del alineamiento inicial de la pieza a mecanizar en la MH; c) la medición por coordenadas en MH durante el proceso de fabricación empleando las medidas realizadas para darle feedback al proceso de fabricación; y d) la validación de la pieza en la propia MH asegurando un proceso de fabricación cero-defectos, garantizando que la pieza que sale de la MH es conforme y generando información metrológica para el control de los procesos productivos en lo que se denomina “data-driven manufacturing processes”.

Actualmente, en función del tamaño del componente a medir, la trazabilidad de la medición por coordenadas en MH está a un nivel de madurez diferente. Para los componentes de gran tamaño, el uso actual de la medición en MH se limita a la realización del alineamiento inicial de la pieza en la mesa de la MH y para los componentes de tamaño pequeño y medio, la asignación de incertidumbre se está materializando en base al documento técnico ISO 15530-3, donde se emplea una pieza patrón previamente caracterizada para asegurar la trazabilidad de las medidas en MH. Sin embargo, cualquier medición por coordenadas realizada en un ambiente de taller está condicionada por diferentes factores como el error geométrico de la MH, la variación de la temperatura, el sistema de palpado o la suciedad de la pieza, que afectan y limitan la realización del ejercicio de asignación de incertidumbre. Resumiendo, la trazabilidad de la medición por coordenadas en una MH no está resuelta por el momento, y el objetivo principal de esta tesis doctoral es generar nuevo conocimiento que permita hacerlo y así habilitar procesos de fabricación cero-defectos.

La idea de convertir una MH en una MMC no es nueva. Schmitt et al. de la Universidad RWTH de Aachen propusieron una guía práctica para la realización de la medición por coordenadas trazable en MH [2,3]. Su propuesta se basa en emplear la MH como un sistema de medición, tipo comparador, para la medición en MH de componentes de gran tamaño. A su vez, Schmitt et al. también presentaron varios ensayos experimentales donde se emplea una MH como una MMC [191]. En este contexto, se conocen varias aproximaciones [12,13] donde se emplea una pieza patrón o un marco metrológico externo para caracterizar y corregir la componente de incertidumbre asociada al error sistemático de la medición por coordenadas en MH.

La mayor barrera que presenta la medición en MH está en la dificultad de separar los errores geométricos que afectan al proceso de mecanizado y al proceso de medición. Ambos procesos se ejecutan en una misma MH y en un intervalo de tiempo reducido, lo que conlleva a que sea realmente complejo caracterizar y separar los componentes de error que afecta a cada proceso [176]. Esta es actualmente la gran limitación que muestra la medición por coordenadas en MH y que se pretende estudiar mediante esta tesis doctoral.

En este escenario, hay dos posibles aproximaciones para tratar de convertir una MH en una MMC:

- Se realiza la verificación volumétrica de la geometría de la MH justo antes de realizar la medición en MH. De esta forma, se conoce el error geométrico de la MH en el momento de realizar la medición por coordenadas y se consigue caracterizar el componente de incertidumbre asociado al error sistemático de la medida en MH.
- Se emplea un marco metrológico externo que sea capaz de monitorizar y controlar la posición de la MH en tiempo real. Esta aproximación tiene dos barreras importantes: a) el coste de los equipos de medición que se necesitan para materializar la solución; y b) la línea de visión ininterrumpida entre los sistemas de medición ubicados fuera del volumen de trabajo de la MH y el cabezal.

Gracias a la similitud entre las cinemáticas de una MMC y una MH, algunos de los procedimientos empleados para realizar el ejercicio de la asignación de incertidumbre en MMC están siendo adaptados a las MH. Actualmente, son tres las aproximaciones que se están valorando para la asegurar la trazabilidad de la medición por coordenadas en MH [6]: a) la aproximación experimental basada en el documento técnico ISO 15530-3 donde se emplea una pieza patrón para caracterizar el componente de incertidumbre asociada al error sistemático [23]; b) la aproximación basada en simulación que se describe en el documento técnico ISO 15530-4 [32]; y c) la aproximación basada en el

balance de incertidumbres según la guía VDI 2617-11 [37]. En este sentido, para la producción en serie de componentes de tamaño pequeño y medio, la asignación de incertidumbre se está materializando en base al documento técnico ISO 15530-3, donde el empleo de una pieza patrón similar al componente que se está fabricando en serie es una alternativa práctica y económica. Para los componentes de gran tamaño, el ejercicio de asignación de incertidumbre se está materializando según la guía VDI 2617-11, ya que el empleo de piezas patrón de gran tamaño conlleva un coste económico elevado.

Según Slocum, los errores geométricos de una MH se pueden clasificar en: a) errores sistemáticos; y b) errores aleatorios [41,42]. Mientras que los errores sistemáticos se pueden caracterizar y por lo tanto, compensar en gran parte; los errores aleatorios son difíciles de predecir. Además, Slocum predice que una buena MH debería de tener tres grandes características: precisión, repetibilidad y resolución. De esta forma, se establece que el balance de incertidumbres de una medición por coordenadas en MH debería contemplar las siguientes fuentes de error: a) la MH (sección 1.2.5), el sistema de palpado (sección 1.2.6) y el software de medición (sección 1.2.7); b) el componente sobre el que se realizará la medición en MH (sección 1.2.8); c) la interacción entre ambos sistemas. Además, haciendo una analogía con la clasificación de Slocum para las principales características de una MH, el balance de incertidumbres y las fuentes de error que la componen quedaría así:

- **Precisión:** Aquí se recogen las fuentes de error que inducen un error sistemático en la medición en MH: los errores geométricos de la MH, los errores del sistema de palpado y los errores asociados al software de medición.
- **Repetibilidad:** Aquí se recogen las fuentes de error que inducen un error aleatorio en la medición en MH: las cargas dinámicas y los efectos medioambientales que afectan a la MH y al componente de medición.
- **Resolución:** Depende en gran parte de los sensores y actuadores que incorpora la MH y el sistema de palpado para realizar la medición por coordenadas.

El estado del arte que se recoge en esta memoria describe todas las potenciales fuentes de error que afectan a la medición por coordenadas en MH independientemente de la escala en la que se produzca [6]. En concreto, la MH es la principal fuente de error comparada con la tecnología que se emplea para realizar el palpado de los puntos o el software elegido para gestionar los datos de adquisición. En caso de que el ejercicio de la medición en MH se realice sobre un componente de gran tamaño, el propio componente se convierte en una fuente de incertidumbre principal ya que los efectos de la temperatura y la gravedad afectan negativamente a la estabilidad del componente. Por otro lado, la componente de incertidumbre asociada al sistema de palpado se convierte en despreciable para la medición de componentes de gran tamaño ya que el error del sistema de palpado estaría entre $1\pm 2\ \mu\text{m}$, según las especificaciones del fabricante. Sin embargo, para la medición por coordenadas de componentes de tamaño pequeño y medio esta componente se debería de tener en cuenta, ya que el orden de magnitud se iguala al resto de las componentes de incertidumbre [6].

En conclusión, el estado del arte presenta las fuentes de error que afectan a la medición por coordenadas en MH desde un enfoque cualitativo. Además, no solo se describen las potenciales fuentes de error sino que se trata de destacar aquellas que pueden tener más peso para los diferentes tamaños de pieza. En la parte final del estado del arte [6], se presenta una primera estimación, en forma de hipótesis, del balance de incertidumbres de la medición en MH para diferentes tamaños de pieza.

Tras la introducción y análisis del estado del arte de la medición por coordenadas en MH, gran parte del trabajo realizado en esta tesis doctoral está basado en la materialización de pruebas experimentales que permitan entender y caracterizar las fuentes de error asociadas a la medición en MH. Para el desarrollo de nuevos procedimientos, primero se trabaja en modo simulación para posteriormente validar los resultados con pruebas experimentales.

Para la producción en serie de componentes de tamaño pequeño y medio, algunos de los proveedores de la cadena de suministro de las piezas de motor mecanizadas para el sector aeronáutico ya están realizando la medición por coordenadas de las cotas críticas de sus componentes en MH. Aquí, el ejercicio de asignación de incertidumbre se realiza empleando una pieza patrón de características similares a la pieza mecanizada y según el documento técnico ISO 15530-3 [23]. Según esta especificación técnica, son cuatro las componentes de incertidumbre que se deben contemplar en el balance de incertidumbres para la medición trazable de coordenadas en MH:

u_b	incertidumbre típica asociada al error sistemático de la medición.
u_p	incertidumbre típica asociada al proceso de medición.
u_{cal}	incertidumbre típica asociada a la incertidumbre de calibración del patrón.
u_w	incertidumbre típica asociada a las variaciones del material y las condiciones del proceso de fabricación.

La incertidumbre expandida del proceso de medición (U_{MP}) es igual a $U_{MP} = k \times u_{MP}$ y la incertidumbre expandida del sistema de medición (U_{MS}) es igual a $U_{MS} = k \times u_{MS}$, para un factor de cobertura de $k=2$. Las incertidumbres típicas u_{MP} y u_{MS} , tienen su origen en la misma fórmula matemática pero los datos empleados en su cálculo tienen su origen en las mediciones en MH realizadas después del proceso de mecanizado y en vacío, respectivamente.

El trabajo experimental de esta tesis doctoral se ha realizado en gran parte en una MH de marca KONDIA de tamaño medio disponible en las instalaciones de IK4-TEKNIKER. En la primera prueba experimental, se han fabricado y posteriormente medido cinco componentes prismáticos de tamaño medio empleando una sonda RENISHAW OMP 400 instalada en la MH. Cada componente se ha medido diez veces con la propia MH para caracterizar la componente de incertidumbre asociada al proceso de medición. Además, uno de los componentes se ha medido a una temperatura estable de 20 °C donde la MH opera sin carga, con el objetivo de caracterizar la incertidumbre típica asociada al sistema de medición (u_{MS}). La pieza prismática elegida para realizar el ensayo experimental es una pieza tipo NAS definida en la norma ISO 10791-7:2014 [177] y denominada como "Test piece ISO 10791-7, M1-160". Cada uno de los cinco componentes se ha calibrado posteriormente en una MMC ZEISS de gran precisión, empleando el módulo VCMM para realizar el ejercicio individual de la asignación de incertidumbre de las cotas medidas [176].

Durante la prueba experimental, la temperatura de la pieza ha alcanzado una temperatura máxima de 22.5 °C (de media) durante el proceso de mecanizado de los componentes y se ha estabilizado a una temperatura de 19.5 °C (de media) tras dos horas. Durante este intervalo de tiempo, donde todo el sistema se está enfriando, se han realizado mediciones en MH cada diez minutos para entender el componente de incertidumbre asociada al proceso de medición.

Antes de realizar el ejercicio de la asignación de incertidumbre, se han corregido los resultados obtenidos para las cotas de diámetro de los diferentes agujeros que componen la geometría de la pieza. El proceso de medición se ha realizado tras el proceso de mecanizado y esto requiere montar el sistema de palpado en el cabezal para cada uno

de los componentes medidos en MH. Sin embargo, solo se ha realizado la calibración de la sonda de palpado en MH para el primer componente. Esto ha inducido un error sistemático en la medición de las cotas de los diámetros de los agujeros y para evitar la insuficiente calibración de la sonda de palpado, estos valores han sido corregidos por el método de la sustitución [23]. Estos resultados muestran la necesidad de calibrar la sonda cada vez que es montada en el cabezal de la MH.

El balance de incertidumbres de la prueba experimental según el documento técnico ISO 15530-3 queda compuesto por las tres principales fuentes de incertidumbre que se describen a continuación:

La componente asociada al error sistemático (u_b): los resultados obtenidos tras la corrección de los diámetros muestran que la media de los valores de diámetro medidos es mejor que $10\ \mu\text{m}$ para todos los casos. Además, los resultados de posición de los diámetros tienen una correlación directa con el error geométrico de la MH, sobre todo, con sus componentes de error de posicionamiento en los ejes X e Y, y la perpendicularidad entre ellos. Por lo tanto, se deduce que el error geométrico de la MH es la principal fuente de error de la componente de incertidumbre asociada al error sistemático (u_b), lo que representa la primera gran conclusión de este trabajo experimental: una caracterización previa de la geometría de la MH podría predecir la componente de incertidumbre asociada al error sistemático de la medición en MH pudiendo prescindir del empleo de una pieza patrón.

La componente asociada al proceso de medición (u_p): es importante entender el efecto de la temperatura en esta componente de incertidumbre. Por este motivo, el trabajo experimental plantea la medición en MH: a) tras un proceso de mecanizado; y b) en condiciones de vacío y a una temperatura estable en torno a $20\ ^\circ\text{C}$. Para la medición en MH del componente en condiciones de vacío, los resultados de repetibilidad son mejores que $6\ \mu\text{m}$ en todos los casos, y sin embargo, para las mediciones realizadas tras el proceso de mecanizado del componente los resultados de repetibilidad no superan las $10\ \mu\text{m}$. En este análisis también se observa que las cotas de tipo geométricas, como la planitud o la redondez, tienen una repetibilidad mejor que las cotas tipo-escala, como los diámetros o las cotas de posición, que son más sensibles a la variación de la temperatura.

La componente asociada a la incertidumbre del patrón (u_{cal}): Los resultados de incertidumbre obtenidos en la MMC ZEISS son mejores que $2\ \mu\text{m}$. Los resultados de mayor incertidumbre se obtienen en el eje más largo de la MMC, el eje Y.

Resumiendo, la componente de incertidumbre asociada al proceso de medición es la principal componente de incertidumbre del ensayo experimental realizado en condiciones de taller. Aquí, la repetibilidad de las mediciones en MH es menor para las mediciones realizadas justo después del proceso de mecanizado, que para las mediciones realizadas en vacío. La componente de error asociada al error sistemático muestra una correlación directa con el error geométrico de la MH, sobre todo, en las componentes del error de posicionamiento de los ejes X e Y y la perpendicularidad entre estos ejes. La incertidumbre asociada al sistema de palpado es de aproximadamente $1\ \mu\text{m}$, lo que sería acorde con la especificación del fabricante [176].

La conclusión más importante de esta prueba experimental es la correlación entre el error geométrico de la MH y la componente de incertidumbre asociada al error sistemático. Esta conclusión es el punto de partida a la realización de la medición por coordenadas trazable en MH sin emplear una pieza patrón, siendo ésta la gran limitación del documento técnico ISO 15530-3. Este procedimiento es práctico y económicamente asequible para la medición en MH de piezas de tamaño pequeño y medio, fabricados en serie; pero para componentes de gran tamaño supone una gran limitación. En este punto, esta tesis doctoral propone un nuevo procedimiento para realizar el ejercicio de

la asignación de incertidumbre a la medición por coordenadas en MH sin emplear una pieza patrón y en base a la caracterización previa de la geometría de la MH en todo su volumen de trabajo [178].

La propuesta aquí consiste en plantear un balance de incertidumbres acorde a la guía VDI 2617-11 [37]. Aquí, es importante conocer cada componente de incertidumbre y sus fuentes de error, así como su magnitud para que el presupuesto de errores que se plantea sea preciso. En este caso se contemplan las siguientes fuentes de error:

- El error geométrico y la repetibilidad de la MH.
- El sistema de palpado.
- El efecto de la temperatura en la MH y el componente.
- El efecto de la gravedad sobre el componente.
- El procedimiento de medición.
- La técnica empleada en la verificación de la geometría de la MH y su incertidumbre.

Haciendo un paralelismo entre la aproximación que plantea el documento técnico ISO 15530-3 y la guía VDI 2617—11, las fuentes de error que se describen en el párrafo anterior se clasifican de la siguiente manera en cada una de las componente de incertidumbre principales:

- Componente de incertidumbre asociada al error sistemático (u_b): El error geométrico de la MH, el sistema de palpado, el componente y el procedimiento de medición.
- Componente de incertidumbre asociada al proceso de medición (u_p): La repetibilidad de la MH, la repetibilidad del sistema de palpado y la variación de la temperatura en el escenario de la medición.
- Componente de incertidumbre asociada a la incertidumbre de calibración del patrón (u_{cal}): La incertidumbre de la verificación de la geometría de la MH.

En este punto, se realiza una nueva prueba experimental para demostrar que este nuevo procedimiento para materializar el ejercicio de asignación de incertidumbre sin pieza patrón es adecuado. Para esta prueba, se utiliza el mismo componente que el empleado para la prueba experimental realizada según el documento técnico ISO 15530-3. Sin embargo, en este caso el rol de la pieza patrón es diferente, es decir, esta pieza patrón no se emplea para conocer el error sistemático de la medición en MH, sino que se emplea para validar la obtención de esta componente con el nuevo procedimiento. Como punto de partida, se ejecuta la verificación geométrica de la MH en todo su volumen de trabajo antes de realizar la medición por coordenadas en MH, esta verificación se realiza con la tecnología láser tracer NG del fabricante ETALON AG. La multilateración matemática de todas las medidas de longitud se procesan en un software del mismo fabricante y se ajustan a un modelo matemático que representa la cinemática de la MH. De esta forma, se determina el error geométrico de la MH en cualquier punto dentro del volumen de medición y conociendo los puntos de palpado sobre la pieza, se puede obtener el error geométrico de los puntos de palpado en el momento de realizar la medición en MH.

En este balance de incertidumbres, las fuentes de error asociadas al procedimiento de medición y al componente se han despreciado porque el componente prismático de tamaño medio no conlleva una estrategia de medición compleja. Por otro lado, se considera que el componente no sufre deformaciones en su amarre en la MH, por lo que el efecto de la gravedad ha sido descartado. Por último, las incertidumbres asociadas al procedimiento de verificación volumétrica y al sistema de palpado respectivamente son mejores que $2 \mu\text{m}$ [178].

Esta prueba experimental se ha ejecutado en condiciones de vacío a una temperatura estable de 20 °C, la variación de la temperatura durante el ensayo no supera los 0.5 °C. Además, se ha realizado la calibración del sistema de palpado tras ser montado en el cabezal de la MH, evitando así los problemas surgidos en la anterior prueba experimental. La repetibilidad durante el proceso de calibración del sistema de palpado sobre el anillo patrón es menor que 1 µm, lo que está dentro de la repetibilidad de la propia MH.

En cuanto a la caracterización de las componentes de incertidumbre. Para la componente de incertidumbre asociada al proceso de medición, se han empleado los resultados obtenidos según el documento técnico ISO 15530-3, donde no se precisa de una pieza patrón para la caracterización de esta componente. Para la componente de incertidumbre asociada al error sistemático de la medición en MH, se ha ejecutado el nuevo procedimiento que se propone en esta tesis doctoral y que se describe en la Figure 2-6. Los resultados obtenidos con este nuevo procedimiento para esta componente de incertidumbre muestra una diferencia máxima de 1.5 µm respecto al ejercicio de incertidumbre realizado según el documento técnico ISO 15530-3, donde se emplea una pieza patrón. En cuanto a la componente asociada a la incertidumbre del patrón, la incertidumbre de la verificación geométrica de la MH en todo su volumen de trabajo es menor que 2 µm, lo que resulta similar al empleo de una pieza patrón calibrada en una MMC de alta precisión [178].

Como conclusión, el nuevo procedimiento que se propone en esta tesis doctoral según la guía VDI 2617-11 permite materializar el ejercicio de asignación de incertidumbre de forma similar al procedimiento que plantea el documento técnico ISO 15530-3. Sin embargo, en este nuevo procedimiento no se emplea una pieza patrón para caracterizar la componente de incertidumbre asociada al error sistemático, lo que ofrece la posibilidad de escalar la medición por coordenadas en MH a componentes de gran tamaño. La industrialización del nuevo procedimiento que se plantea aquí está limitada por la duración del proceso de verificación de la MH, que al ser ejecutado de forma secuencial requiere que la MH repita el volumen de medición al menos cuatro veces. Para la prueba experimental que se presenta aquí, la verificación volumétrica se ha ejecutado en 3h 30 min. Por lo tanto, este nuevo procedimiento requiere que la parada de MH sea larga duración.

Para superar esta limitación y escalar la medición por coordenadas a componentes de gran tamaño, esta tesis doctoral propone un procedimiento de verificación volumétrica integrada en MH, de tal forma, que la verificación se pueda realizar de forma automática y en un espacio de tiempo reducido, sin intervención humana. La metodología que se ha seguido en esta fase de la tesis doctoral es realizar la simulación del procedimiento en base a la técnica de Monte-Carlo y posteriormente se ha realizado el ejercicio de integración en una MH.

Este nuevo procedimiento de multilateración integrada en MH mejora en gran parte la aproximación de medición secuencial que se emplea actualmente. En esta nueva metodología, se integra un sistema interferométrico en el cabezal de la MH y se definen cuatro puntos fiduciales fijos y alrededor de la MH, de esta forma, el sistema interferométrico se mueve junto con el cabezal de la MH y se materializa la nube de puntos que describe el volumen de medida de la MH [179]. Aquí, desde cada uno de los puntos que compone la nube de puntos, el sistema interferométrico realiza la medición de distancia a cada uno de los cuatro puntos fiduciales, de tal forma que la nube de puntos que describe la MH solo se debe ejecutar una sola vez, reduciendo el tiempo de adquisición en un 75% comparado con la aproximación secuencial y mejorando a su vez la incertidumbre de medida, ya que la MH sufre una deriva geométrica menor por una menor variación de la temperatura ambiente.

Este nuevo procedimiento rompe con una de las grandes barreras del procedimiento secuencial, ya que el procedimiento no requiere de intervención humana y se puede ejecutar de forma automática. Sin embargo, este requiere de una automatización previa del escenario de la medición, donde es necesario localizar la posición de los puntos fiduciales fijos en el sistema de coordenadas de la MH. Para ello, se propone un procedimiento de caracterización que requiere mover la MH a varias posiciones de la nube de puntos a medir posteriormente. Una vez que los puntos fiduciales están localizados, la información nominal de la nube de puntos permite asegurar la automatización del proceso de medición y realizar el apunte correcto desde cada posición de MH a cada uno de los puntos fiduciales [179]. La capacidad de los nuevos láser tracker de trabajar sin cables, mediante una conexión LAN, permite sincronizar el trigger de la medición del sistema interferométrico con el próximo movimiento de la MH.

Inicialmente, este procedimiento fue simulado mediante el software SA. Los resultados que se muestran en la Figure 2-13 indican que los resultados de esta solución integrada son similares a los resultados que se obtienen con el procedimientos secuencial, lo que habilita la realización de una primera prueba experimental donde ensayar la automatización y la captura de datos de este nuevo procedimiento.

Aquí, se han realizado dos pruebas experimentales: a) se integra el láser tracker AT402 en un robot industrial KUKA KR60 y se fijan varios puntos fiduciales alrededor del robot; y b) se integra un láser tracker AT960 en una MH de gran tamaño de la marca ZAYER y los resultados se han comparado con los resultados obtenidos mediante la aproximación secuencial.

a) Se ha integrado un láser tracker AT402 en el cabezal de un robot industrial KUKA KR60 y se han definido cuatro puntos fiduciales alrededor del robot, uno de ellos fuera del plano para mejorar la precisión en la dirección vertical como muestra la Figure 2-14 a. La automatización de la secuencia de medición se ha realizado con éxito y se ha realizado la sincronización del trigger del láser tracker con el siguiente movimiento del robot.

Para la simulación del escenario real de medición, el escenario de medición conlleva la medición de 96 longitudes para el láser tracker integrado en el robot. Con las longitudes reales de la medición y empleando el modelo de error de este láser tracker en el software SA, se ha realizado una simulación con la técnica de Monte-Carlo para un total de 300 muestras. Como resultado, se ha obtenido la incertidumbre expandida de los datos residuales del ejercicio de multilateración, donde la desviación estándar máxima de este parámetro no supera un valor de 0.0065 mm, lo que supera ligeramente el componente de error fijo (U_f) del modelo de error de este láser tracker en el software SA. De estos resultados, se concluyen que la incertidumbre obtenida es proporcional al sistema de medición empleado y que la deriva geométrica del escenario de medición por variación de temperatura es menor que la incertidumbre de medida del sistema de medición. El tiempo total de medición para ejecutar la nube de puntos de medida es de 8 min, lo que significa que cada punto de medición requiere un tiempo de medición aproximado de 20 segundos.

b) Se ha integrado un láser tracker AT960 en el cabezal de una MH de gran tamaño marca ZAYER y se han definido cuatro puntos fiduciales alrededor de la MH, uno de ellos fuera del plano para mejorar la precisión en la dirección vertical de la MH como muestra la Figure 2-19. En paralelo, se ha realizado la verificación volumétrica de la MH con la aproximación secuencial y con la tecnología láser tracer NG. El ejercicio experimental se realizó en las instalaciones de ZAYER.

Se ha definido una nube de puntos compuesta por 64 puntos y que define el volumen de trabajo completo de la MH. $X = 3000$ mm, $Y = 2300$ mm y $Z = 900$ mm. El plan de validación de los resultados se describe a continuación de forma cronológica:

- Se realiza la verificación volumétrica de la MH con la aproximación secuencial empleando la tecnología láser tracer NG. En la prueba experimental, se emplearon 4 posiciones del sistema de medida y el tiempo completo de la medición fue de 2 h y 30 min.
- Se realiza la verificación volumétrica de la MH con el sistema de medida láser tracker AT960 integrado en el cabezal de la MH, boca-abajo. En la prueba experimental, se definieron cuatro puntos fiduciales alrededor de la MH, uno de ellos fuera del plano para mejorar la precisión en la dirección vertical de la MH. El tiempo completo de la medición fue de 25 min.

Para analizar los resultados obtenidos con el nuevo procedimiento, se han comparado estos resultados contra los resultados de la aproximación secuencial de la siguiente forma: a) la incertidumbre de los puntos fiduciales; b) la incertidumbre de los puntos que componen la nube de puntos; c) la comparación entre las nubes de puntos medidas con ambas aproximaciones; y d) la comparación de los resultados del ajuste del modelo cinemático del software de ETALON. Como resultado, se ha reducido el consumo de tiempo hasta en un 75 % comparado con la aproximación secuencial y la incertidumbre de medida, que es proporcional a la variación de temperatura y por lo tanto, al tiempo de adquisición, también muestra un resultado más favorable [182].

El objetivo principal de esta tesis doctoral es generar nuevo conocimiento para realizar la medición por coordenadas trazable en MH. Sin embargo, el conocimiento generado en el ejercicio de integración de la verificación volumétrica en la MH, ha permitido abordar un reto en el campo de la metrología de alto rango para el proyecto LSST. El objetivo aquí es desarrollar un nuevo procedimiento de verificación para caracterizar la precisión de apunte del telescopio en todo su rango de trabajo. Este telescopio que será un telescopio de 8,4 metros capaz de examinar la totalidad del cielo visible se construirá en el norte de Chile entrando en funcionamiento en el año 2022 [183,192].

IK4-TEKNIKER está participando en varias fases del proyecto LSST. Entre otros, uno de los objetivos de IK4-TEKNIKER es desarrollar un nuevo procedimiento para realizar la verificación de la precisión de apunte del telescopio LSST. Esta tesis doctoral trata de realizar el ejercicio de asignación de incertidumbre para el nuevo procedimiento desarrollado, considerando que el telescopio es un instrumento de medición en el campo de la metrología de alto rango. De forma similar al trabajo realizado para MH, el balance de incertidumbres para la verificación de la precisión de apunte del telescopio está compuesto por: a) la componente de incertidumbre asociada al error sistemático de la medida en el apunte del telescopio; b) la componente asociada al proceso de la medición, es decir, la repetibilidad del telescopio en el proceso de apunte; y c) la componente asociada al patrón empleado en la verificación.

El escenario de la medición es complejo, no solo por el tamaño del telescopio sino por el acceso al interior del mismo y la dificultad de hacer pruebas in-situ. Por esto, gran parte del trabajo para el desarrollo del nuevo procedimiento de verificación se ha desarrollado en un entorno de simulación que se ha habilitado con el software SA. Las ventajas de trabajar en simulación son muchas, pero destacan: a) la capacidad de predecir si el nuevo procedimiento de verificación que se propone es capaz de cumplir con su objetivo; y b) la capacidad de mejorar el procedimiento de medición en base a los resultados que se obtienen cambiando la configuración de algunos parámetros de la simulación.

El telescopio LSST propone un escenario de medición que tiene varios retos que igualan el nivel del estado del arte de la metrología de alto rango [189]: a) la incertidumbre de los puntos fiduciales fijos en el suelo no debería de ser superior a 0.1 mm en un diámetro de medición de 40 m; y b) la verificación del apunte del telescopio se debe realizar para todo su rango de actuación, además, todas las verificaciones se deben realizar sobre el eje óptico del telescopio que es el espejo primario-terciario M1M3. Este último punto presenta un gran reto ya que la visibilidad es reducida entre la parte interior y exterior del telescopio, sobre todo en la zona central del rango del eje de elevación donde el anillo central del cuerpo del subcomponente TMA se interpone en la mitad, ver Figure 2-32. Por lo tanto, el reto aquí es desarrollar un procedimiento de medición que ofrezca una solución adecuada para satisfacer ambos requisitos [192].

El entorno de simulación indica que en realidad solo existe una única configuración que asegure la visibilidad de medida dentro de todo el rango de trabajo del telescopio: el sistema de medición se debe colocar dentro del telescopio y centrado con el origen de los ejes de giro de azimuth y elevación. Como se muestra en la Figure 2-27, desde esta posición se asegura la visibilidad entre el sistema de medición y los puntos fiduciales fuera del telescopio para cualquier posición de apunte del eje de elevación.

El nuevo procedimiento para la verificación de apunte del telescopio se describe a continuación: Un sistema de medición láser tracker se ubica dentro del telescopio, en el origen de giro de los ejes de azimuth y elevación, y los puntos fiduciales se fijan en el suelo, formando un círculo fuera del telescopio. Estos puntos fiduciales tienen un rol importante en el procedimiento de medición ya que permiten localizar la posición del láser tracker para cualquier posición de apunte del telescopio. Por esto, para cada posición de apunte del telescopio primero se miden los puntos fiduciales visualmente disponibles desde esa posición y posteriormente se miden los puntos de medición que definen las geometrías de los espejos M1M3 y M2 respectivamente. La Figure 2-25 muestra la distribución de los puntos de forma esquemática y la Figure 2-40 muestra el escenario real de la medición en el plano M1M3. De esta forma, se consigue localizar de forma muy precisa la posición y orientación de los espejos M1M3 y M2 en un sistema de coordenadas fijo y solidario a la Tierra. Siguiendo este procedimiento se ejecutan todas las posiciones de apunte que se define en la Figure 2-26 y se comparan los resultados obtenidos con las posiciones nominales de apunte del telescopio, la diferencia entre ambos representa el error de apunte del telescopio para cada posición. Aquí, se debe destacar que el láser tracker se ha fijado en el origen de giro de los ejes de azimuth y elevación para reducir la variación del ángulo de entrada del haz de medida del sistema láser tracker sobre los puntos fiduciales, de esta forma, ya que la posición del láser tracker no cambia para cualquier posición de apunte del telescopio el ángulo de entrada del haz sobre los reflectores es siempre idéntico. En este caso, se han empleado 48 reflectores de 25 mm de diámetro con una óptica del tipo “hollow corner cube” [184].

En este punto, no está del todo claro que el nuevo procedimiento de medición sea capaz de cumplir con los requisitos de medición que demanda el proyecto LSST. Por esto, se ha modelizado no solo el entorno de verificación sobre el telescopio LSST sino el propio procedimiento que se plantea en estas líneas. Todo esto se ha realizado en el software de metrología conocido como SA. Se ha empleado la técnica de Monte-Carlo para simular la incertidumbre de medición de: a) los puntos fiduciales; b) del apunte del telescopio; y c) del paralelismo entre M1M3 y M2 para las posiciones de apunte del telescopio que se presentan en la Figure 2-26. En esta simulación se ha empleado un modelo, tipo Box-Muller, para generar los pares de números aleatorios independientes con distribución normal para alimentar el modelo de error que emplea el software SA para un sistema láser tracker LEICA AT402. En concreto en

esta simulación se han empleado 500 muestras y la incertidumbre típica de los resultados obtenidos es el parámetro que se muestra como el resultado de la simulación. La modelización del escenario de la medición también contempla la deriva geométrica del suelo por la variación de la temperatura ambiente que se produce en el pabellón industrial donde se ubica el telescopio. De esta forma, se ha modelizado el comportamiento del nuevo procedimiento según la variación de temperatura que se produce en el escenario de la medición. Los resultados muestran que el procedimiento de medición es apto por debajo de una deriva geométrica del suelo de hasta 4 mm. Una medición preliminar del suelo del pabellón industrial durante 24 h muestra una deriva geométrica de hasta 0.5 mm para una variación de temperatura de 4 °C [184].

Los resultados de la simulación muestran que la incertidumbre de medición es mejor que 0.1 mm para la medición de los puntos fiduciales, lo que se traduce en una incertidumbre de medición para la posición de apunte del telescopio mejor que 0.5 arcsec. Los resultados obtenidos en la simulación correlan con el nivel del estado del arte que se presenta en el telescopio LBT donde se emplea un sistema de medición láser tracker para realizar el ejercicio de metrología de alto rango que requiere el telescopio [189].

Además, el entorno de simulación permite entender que: a) la repetibilidad de la posición de apunte del telescopio no se puede asegurar con el nuevo procedimiento porque la incertidumbre que se obtiene, en torno a $1 \div 2$ arcsec, está por encima de la tolerancia para este requisito, que es de 1 arcsec; y b) la verificación de paralelismo entre los espejos M1M3 y M2 se puede realizar con una incertidumbre de medición mejor que 2 arcsec para cualquier posición de apunte del telescopio, ya que es una medida local y no depende de la precisión obtenida en la verificación de los puntos fiduciales [184].

Una vez validado que el nuevo procedimiento de medición es apto para cumplir con su objetivo, el reto aquí es reducir en la medida de lo posible el efecto negativo de la temperatura en la verificación in-situ del telescopio LSST. Aquí, solo existe una alternativa que es reducir el tiempo de la verificación mediante la automatización de todo el proceso de adquisición de datos. La automatización se realiza conectando el sistema de medición láser tracker al controlador del telescopio mediante una conexión privada de tipo TCP/IP que permite sincronizar el disparo de la medición con el láser tracker con el siguiente movimiento del telescopio. De esta forma, el tiempo de adquisición se reduciría hasta un tiempo de adquisición que oscila entre $60 \div 90$ min.

Finalmente, se ejecuta la verificación in-situ de la precisión de apunte del componente TMA del telescopio LSST. Esta verificación se realiza entre los meses de septiembre y octubre del año 2018 en las instalaciones de ASTURFEITO, en Asturias. El escenario real de la medición presenta varios retos adicionales que no se pueden contemplar en la simulación y deben ser resueltos in-situ antes de ejecutar el procedimiento automático de la medición: a) se coloca un láser tracker en el origen de giro de los ejes de azimuth y elevación mediante un soporte de longitud 2.500 mm fijado al dummy M1M3. Esto hace que el láser tracker trabaje en diferentes orientaciones de su cabezal y por eso, se ha elegido el láser tracker LEICA AT960 que asegura un funcionamiento similar para cualquiera que sea la orientación de trabajo. La Figure 2-33 se muestra el láser tracker en su posición más vertical, cuando el telescopio apunta al zenith, y en su posición más horizontal, cuando el telescopio apunta al horizonte; b) el espacio disponible en el suelo del pabellón industrial donde se encuentra el telescopio está lejos de ser perfecto como lo es en la simulación. Aquí, existen varios obstáculos como la cabina de control, las escaleras de acceso al subcomponente TMA y el acceso restringido a un lateral del telescopio que obligan a adaptar el layout de los puntos fiduciales a las condiciones reales del pabellón industrial; y c) la preparación de la automatización del proceso de adquisición de los

datos de la verificación conlleva un trabajo importante a realizar in-situ antes de proceder con la adquisición de los datos.

Después de tres días de preparación (preparación del láser tracker en la posición de medida, preparación de los puntos fiduciales fijos en el suelo, definición de la estrategia de medición con el layout real del pabellón industrial, automatización del procedimiento de medición...) se ha realizado la verificación in-situ. Los procesos de adquisición y procesado de los datos se realizaron de forma automática en un tiempo inferior a 70 min, lo que permitió tener los resultados de la verificación en tiempo real y así, se facilitó la toma de decisiones sobre el proceso de la verificación de la precisión de apunte. La incertidumbre de medición ha sido inferior a 2 arcsec, lo que ha mejorado los resultados obtenidos en la fase de simulación, en parte porque se ha empleado un láser tracker LEICA AT960 que dispone de dos tecnologías de medición de longitud, interferometría relativa y distanciómetro absoluto, que permiten que la medición de distancia sea más precisa que los resultados obtenidos en simulación. Estos resultados muestran que el requisito de repetibilidad, con una tolerancia de 1 arcsec, no puede ser verificado con este procedimiento de verificación. Por este motivo, el requisito de repetibilidad se ha verificado mediante dos tecnologías directas de medición: a) autocolimador y un espejo para la verificación del posicionamiento del eje de azimuth; y b) nivel electrónico para la verificación de posicionamiento del eje de elevación. Los resultados de la verificación del paralelismo entre los espejos M1M3 y M2 están por debajo de 1.5 arcsec para todas las posiciones de apunte del telescopio LSST, lo que significa que no se produce un cambio de rigidez de la estructura del subcomponente TMA para las diferentes posiciones de apunte del telescopio.

Finalmente, se ha generado mucho conocimiento en esta última fase de la tesis doctoral para el campo de la metrología de alto rango, lo que podría traducirse en el desarrollo de una herramienta de simulación avanzada para escenarios de verificación de gran escala y visibilidad reducida, donde sea necesario realizar un trabajo previo de simulación importante para definir la estrategia óptima de medición [184].

5.4 Conclusiones

Se ha cumplido con el objetivo principal de esta tesis doctoral en la que se ha creado nuevo conocimiento para la medición por coordenadas trazable en MH. Esta tesis doctoral presenta la materialización del ejercicio de asignación de incertidumbre para la medición en MH para piezas prismáticas de tamaño medio según las normas que se aplican en la actualidad para la asignación de incertidumbre en las MMC y propone nuevos procedimientos de medición para la asignación de incertidumbre en componentes de gran tamaño.

Cada vez un número mayor de usuarios de MH percibe que la capacidad de realizar la medición por coordenadas en la propia MH les permitiría mejorar la eficiencia de sus procesos de fabricación y avanzar hacia lo que el sector de fabricación avanzada denomina cero-defectos. De hecho, en la actualidad muchos de estos usuarios de MH ya están empleando la medición con la MH para la fabricación de componentes de alto valor añadido. Sin embargo, estas mediciones están limitadas ya que en muchos casos no vienen acompañadas de su asignación de incertidumbre.

Para la producción en serie de componentes de tamaño pequeño y medio, algunos de los proveedores de la cadena de suministro de las piezas de motor mecanizadas para el sector aeronáutico ya están realizando la medición por coordenadas de las cotas críticas de sus componentes en MH. Aquí, el ejercicio de asignación de incertidumbre se realiza empleando una pieza patrón de características similares a la pieza mecanizada y según el documento técnico ISO 15530-3.

Para los componentes de gran tamaño, el uso actual de la medición en MH está más restringida, en parte porque el tamaño de la pieza impide disponer de piezas patrón que en coste y volumen suponen una gran limitación. Aquí, las MH y los componentes son especialmente sensibles a los efectos negativos de la temperatura y la gravedad, que se pueden convertir en las principales fuentes de incertidumbre para la medición por coordenadas en MH. Además, el error geométrico de la MH, en caso de no haber sido previamente calibrado, también se puede convertir en una fuente de error de primer orden ya que en las MH de gran tamaño el error geométrico de la MH puede llegar a ser importante. Así, el uso actual de la medición en MH para componentes de gran tamaño se limita a la realización del alineamiento inicial de la pieza en la MH ya que la trazabilidad estas medidas no está suficientemente caracterizada.

Por todo esto, esta tesis doctoral propone una solución de verificación volumétrica de MH integrada en la propia máquina, lo que permitiría que la verificación se pueda realizar de forma automática y en un espacio de tiempo reducido. Esta nueva metodología supera las barreras técnicas del proceso de multilateración secuencial que se emplea en la actualidad donde es necesario que la MH repita al menos cuatro veces el volumen de medida para que la multilateración se pueda materializar. De esta forma, el proceso de verificación volumétrica se realizaría en un tiempo inferior a 30 minutos, mejorando no solo el tiempo de adquisición sino también la incertidumbre de la medición.

Este procedimiento integrado en MH habilita el desarrollo de una nueva metodología para realizar la medición por coordenadas trazable en MH sin emplear una pieza patrón. El procedimiento que se propone en esta tesis doctoral se basa en una verificación previa de la geometría de la MH en todo su volumen de trabajo para caracterizar el componente de incertidumbre asociada al error sistemático de la medición en MH, superando las limitaciones que plantea el uso del documento técnico ISO 15530-3.

Los resultados de los ejercicios experimentales realizados en esta tesis doctoral, demuestran que la medición por coordenadas trazable en MH es realizable tanto con el uso de una pieza patrón o bien con la caracterización previa de la geometría de la MH. La ejecución de esta tesis doctoral está marcada por la falta de disponibilidad de MH de gran tamaño, lo que conlleva a que todas las pruebas experimentales se hayan realizado sobre una pieza prismática de tamaño medio. En el ensayo experimental realizado según la ISO 15530-3 se han mecanizado y posteriormente medido cinco componentes en la MH y los resultados muestran que la incertidumbre expandida de las mediciones es de 20 μm . En este balance de incertidumbres, la componente de incertidumbre asociada al proceso de la medición es la principal fuente de error y el error geométrico de la MH es la principal fuente de error que afecta a la componente de incertidumbre asociada al error sistemático de la medición. Por otro lado, para el ensayo experimental realizado según la guía VDI 2617-11, el ejercicio de asignación de incertidumbre se ha materializado sin emplear una pieza patrón. En este caso, se ha realizado una verificación volumétrica previa de la MH con tecnología láser tracer NG para caracterizar la componente de incertidumbre asociada al error sistemático de la medición. Los resultados obtenidos en este ensayo proponen que la asignación de incertidumbre de la medición por coordenadas en MH se puede realizar sin emplear una pieza patrón, ya que los resultados obtenidos son similares a los obtenidos según el documento técnico ISO 15530-3.

Esta tesis doctoral ha asumido el reto de desarrollar un nuevo procedimiento para la caracterización de la precisión de apunte del telescopio LSST y así contribuir al estado del arte de la metrología de alto rango. Este telescopio que será un telescopio de 8,4 metros capaz de examinar la totalidad del cielo visible y que se construirá en el norte de

Chile entrando en funcionamiento en el año 2022, permitirá entre otros: a) reconocer objetos pequeños, tipo asteroides, en el sistema solar; b) detectar novas y supernovas; y c) realizar un mapa de la vía láctea [183].

En este proyecto científico de gran envergadura, la precisión del alineamiento y apunte del telescopio tendrán una gran influencia en la calidad de las imágenes que se obtengan con el telescopio LSST. Por este motivo, se ha desarrollado un nuevo procedimiento automático para la caracterización de la precisión de apunte del telescopio dentro de todo el rango de trabajo del y en un espacio de tiempo reducido para minimizar el efecto geométrico negativo de la temperatura. El procedimiento de medición se ha programado en el software SA y una simulación previa de tipo Monte-Carlo ha permitido determinar que el procedimiento es adecuado para cumplir con el objetivo. Así, la verificación in-situ se realizó sobre el componente TMA en menos de 70 minutos y se obtuvo una incertidumbre de medida mejor que 0.1 mm para los puntos fiduciales que describen un diámetro de 40 m, igualando o incluso mejorando el actual estado del arte de la verificación dimensional de un telescopio de gran tamaño.

Resumiendo, esta tesis doctoral pretende destacar la importancia de la metrología en un entorno industrial cada vez más digital donde los datos recogidos no solo de los procesos de fabricación sino de los medios productivos pueden servir para mejorar la eficiencia y digitalizar los procesos industriales. En este escenario, la metrología pretende mejorar la precisión de las MH, habilitando nuevas funcionalidades que permitan realizar un control de calidad más rápido e in-situ, en el propio medio productivo, facilitando la fabricación de componentes de alto valor añadido y cero-defectos. Es por eso que la metrología es una tecnología habilitadora para la mejora de la competitividad del sector de la MH. Además, esta tesis doctoral también muestra el rol de la metrología de alto rango para habilitar la ejecución de grandes proyectos científicos como es el proyecto LSST.

5.5 Trabajo futuro

La investigación desarrollada en esta tesis doctoral plantea varias líneas de trabajo futuras en el campo de la metrología de alto rango para la mejora de la precisión de las MH y telescopios de gran tamaño.

Para las MH de gran tamaño, uno de los grandes objetivos del sector es mejorar la precisión volumétrica de estas máquinas en todo su ciclo de vida. Esto no solo permitiría mejorar la calidad de las piezas mecanizadas, sino que permitiría reducir la incertidumbre de las mediciones realizadas con la propia MH. En esta tesis doctoral se propone integrar un sistema interferométrico en la MH para ejecutar el procedimiento de medición de forma automática y en un espacio de tiempo reducido. Desde el punto de vista tecnológico, se ha demostrado que la solución funciona y que supone una ventaja considerable en precisión y tiempo respecto a la aproximación secuencial que se emplea en la actualidad, pero desde el punto de vista económico, no resulta sencillo justificar el retorno de la inversión considerando que los únicos equipos que se pueden integrar en la actualidad son sistemas de medición láser tracker. Es aquí, donde se abre una línea futura de investigación para el desarrollo de un sistema de medición interferométrico e integrable en las MH que permita materializar varias de las funcionalidades que ofrece un láser tracker pero evitando muchas otras funcionalidades que ofrecen estos equipos y que encarecen la solución.

La ejecución de esta tesis doctoral ha estado marcada por la falta de disponibilidad de MH de gran tamaño, lo que ha supuesto que todas las pruebas experimentales se hayan realizado sobre un componente de tamaño medio. Una línea de trabajo futura consiste en repetir las pruebas experimentales realizadas en esta tesis doctoral con MH y

componentes de gran tamaño, contrastando así que las componentes de incertidumbre en el balance de incertidumbres tienen una distribución similar a lo obtenido con componentes de tamaño medio.

En el campo de la metrología de alto rango, esta tesis doctoral propone un nuevo procedimiento para la verificación de la precisión de apunte del telescopio LSST, lo que supone todo un reto a nivel del estado del arte. Aquí, se ha desarrollado un código de simulación con la técnica de Monte-Carlo que permite conocer por adelantado si el procedimiento y la tecnología de medición son adecuados para cumplir con su objetivo. Esta herramienta también permite mejorar los parámetros del procedimiento en base a los resultados de la simulación y así reducir la incertidumbre de la medición. Por lo tanto, una línea de trabajo futura propone desarrollar esta herramienta de simulación para facilitar la planificación de las óptimas estrategias de verificación en el campo de la metrología de alto rango.

APPENDIX



APPENDIX

A.1 The impact factor of the published work

The JCR of each publication is presented below:

The article "Traceability of On-Machine Tool Measurement: A Review" was published in the journal "SENSORS", volume 17, issue 7, pages 40, year 2017. The journal JCR index at the year of publication was 2.475, which ranks the journal on position 16 out of 61 (quartile Q2) within the category "Instruments and Instrumentation".

The article "Traceability of on-machine tool measurement : Uncertainty budget assessment on shop floor conditions" was published in the journal "MEASUREMENT", volume 135, pages 9, year 2018. The journal JCR index in 2017 was 2.218, which ranks the journal on position 22 out of 86 (quartile Q2) within the category "Engineering, multidisciplinary".

The article "Uncertainty assessment for on-machine tool measurement: an alternative approach to the ISO 15530-3 technical specification" was published in the journal "PRECISION ENGINEERING", volume 57, pages 14, year 2019. The journal JCR index in 2017 was 2.582, which ranks the journal on position 20 out of 87 (quartile Q1) within the category "Engineering, multidisciplinary".

The article "Integrated multilateration for machine tool automatic verification" was published in the journal "CIRP ANNALS", volume 67, pages 4, year 2018. The journal JCR index in 2017 was 3.333, which ranks the journal on position 8 out of 47 (quartile Q1) within the category "Engineering, industrial".

The article "3D Measurement Simulation and Relative Pointing Error Verification of the Telescope Mount Assembly Subsystem for the Large Synoptic Survey Telescope" was published in the journal "SENSORS", volume 18, Issue 9, pages 17, year 2018. The journal JCR index in 2017 was 2.475, which ranks the journal on position 16 out of 61 (quartile Q2) within the category "Instruments and Instrumentation".

A.2 Author's contribution to the published work

The contribution of the author either to the research or the preparation of the published work is explained next.

Traceability of On-Machine Tool Measurement: A Review.

- To collect the literature related to the previously published studies about traceable CMM measurements on MTs.
- To collect the literature related to the guidelines, technical specifications and standards within the CMM field that could be adapted for MTs.
- To collect the literature related to the state of the art of geometric errors of MTs.
- To prepare the initial error budget quantitative approach.
- To get the main outlook and conclusions of the published work.
- To write and edit the article.

Traceability of on-machine tool measurement : Uncertainty budget assessment on shop floor conditions.

- To collect the literature related to the state of the art.

- To perform the complete experimental research work at IK4-TEKNIKER premises in collaboration with machine-tool technicians.
- To process the experimental data and to execute the uncertainty budget assessment exercise.
- To propose the methodology described in the article to perform traceable CMM measurements on MTs according to the ISO 15530-3 technical specification.
- To get the main outlook and conclusions of the published work.
- To write and edit the article.

Uncertainty assessment for on-machine tool measurement: an alternative approach to the ISO 15530-3 technical specification.

- To collect the literature related to the state of the art.
- To propose a new methodology for traceable CMM measurements on MTs without a calibrated workpiece.
- To perform the complete experimental research work at IK4-TEKNIKER premises in collaboration with machine-tool technicians.
- To process the experimental data and to execute the uncertainty budget assessment exercise.
- To get the main outlook and conclusions of the published work.
- To write and edit the article.

Integrated multilateration for machine tool automatic verification.

- To collect the literature related to the state of the art.
- To describe the limitations of the currently employed approach.
- To propose a new methodology for the integration of the multilateration approach into the MT spindle (in collaboration with the research group within IK4-TEKNIKER).
- To perform the simulation-based research work.
- To perform the concept demonstration on an industrial robot.
- To get the main outlook and conclusions of the published work.
- To write and edit the article.

Integrated volumetric error mapping for large machine tools : An opportunity for more accurate and geometry connected machines.

- To collect the literature related to the state of the art.
- To perform the complete experimental research work at ZAYER OEM premises in collaboration with machine-tool technicians.
- To process the experimental data and to draw the comparison between the integrated and typical multilateration approaches.
- To get the main outlook and conclusions of the published work.
- To write and edit the article.

3D Measurement Simulation and Relative Pointing Error Verification of the Telescope Mount Assembly Subsystem for the Large Synoptic Survey Telescope.

- To collect the literature related to the state of the art.
- To propose a new methodology for the RPE assessment within the LSST project.
- To perform the simulation-based research work: From the code development within SA software to the processing of the simulated data.
- To execute previous temperature and laser tracker measurement in-situ, at ASTURFEITO premises.
- To perform the concept demonstration on a similar 1:2 scale measurement scenario at IK4-TEKNIKER premises.
- To develop a metrology simulation tool for LSM scenarios.
- To perform the simulation-based research work related to the most suitable configuration related to the number of laser trackers and measurement points within the LSST project.
- To get the main outlook and conclusions of the published work.
- To write and edit the article.

Telescope mount assembly pointing accuracy assessment for the Large Synoptic Survey Telescope : A large-scale metrology challenge.

- To perform the simulation-based research work.
- To improve and customize the above-proposed new RPE measurement methodology to the in-situ measurement scenario.
- To perform the real measurement in-situ.
- To process the experimental data and to execute the uncertainty budget assessment exercise.
- To get the main outlook and conclusions of the published work.
- To write and edit the article.

A.3 Acceptance letters for the pending publishing work

Telescope mount assembly pointing accuracy assessment for the Large Synoptic Survey Telescope : A large-scale metrology challenge. EUSPEN 19th International Conference & Exhibition 2019;1:9–12.

Mutilba U, Egaña F, Kortaberria G, Gomez-Acedo E, Olarra A, Yagüe-Fabra JA. Integrated volumetric error mapping for large machine tools : An opportunity for more accurate and geometry connected machines. Procedia Manufacturing 2019;1:1–8.



European Society for Precision Engineering & Nanotechnology

euspen
Cranfield University Campus
Building 90, College Road
Cranfield
Bedfordshire MK43 0AL
UK

Tel: +44 (0)1234 754023
www.euspen.eu

To whom it may concern

10 April 2019

Dear Sirs,

Re: Letter of Acceptance for Publication

This letter is to confirm that the following paper has been accepted for publication in euspen's 19th International Conference proceedings.

Telescope mount assembly pointing accuracy assessment for the Large Synoptic Survey Telescope: A large-scale metrology challenge

Unai Mutilba¹, Gorka Kortaberria¹, Fernando Egaña¹, Jose Antonio Yagüe-Fabra²

¹ *Department of Mechanical Engineering, IK4-Tekniker, 20600 Eibar, Spain.*

² *I3A, University of Zaragoza, 50018 Zaragoza, Spain.*

Please do not hesitate to contact me should you require any further information.

Yours sincerely,

A handwritten signature in black ink, appearing to read "Dishi Phillips", followed by a horizontal line.

Mrs Dishi Phillips
Business Development Manager



Madrid 22th April 2019

Dear Mr. Mutilba,

I am pleased to inform you that your communication entitled 'Integrated volumetric error mapping for large machine tools: An opportunity for more accurate and geometry connected machines' has been accepted for its presentation at the 8th MESIC (Manufacturing Engineering Society International Conference) to be held in Madrid from 19th to 21st June 2019. Congratulations!

As soon as possible, we will indicate you the oral/poster format of the presentation, trying to meet your preferences expressed in the pre-registration. Likewise, an abstract of the communication will be published in the Book of Abstracts of the Conference. (ISBN 978-84-09-10387-4)

I am looking forward to welcome you personally on June in Madrid. Best regards.

Alfredo Sanz
Chair of Scientific Committee

A handwritten signature in blue ink, consisting of several overlapping loops and a long horizontal stroke extending to the right.

BIBLIOGRAPHY



BIBLIOGRAPHY

- [1] CECIMO. Study on competitiveness of the European machine tool industry. 2011.
- [2] Schmitt R, Peterek M. Traceable measurements on machine tools-Thermal influences on machine tool structure and measurement Uncertainty. *Procedia CIRP* 2015;33:576–80. doi:10.1016/j.procir.2015.06.087.
- [3] Schmitt R, Peterek M. Guidelines for traceable measurements on machine tools. 11th International Symposium on Measurement and Quality Control 2013, September 11-13, 2013, Cracow-Kielce, Poland, 2013, p. 11–4.
- [4] Schmitt R, Peterek M, Morse E, Knapp W, Galetto M, Härtig F, et al. Advances in Large-Scale Metrology – Review and future trends. *CIRP Annals - Manufacturing Technology* 2016. doi:10.1016/j.cirp.2016.05.002.
- [5] Karadayi R. Adaptive manufacturing with metrology feedback. 2012.
- [6] Mutilba U, Gomez-Acedo E, Kortaberria G, Olarra A, Yagüe-Fabra JA. Traceability of On-Machine Tool Measurement: A Review. *MDPI Sensors* 2017;17:40. doi:10.3390/s17071605.
- [7] Imkamp D, Berthold J, Heizmann M, Kniel K, Peterek M, Schmitt R, et al. Challenges and trends in manufacturing measurement technology – the “Industrie 4.0” concept. *Journal of Sensors and Sensor Systems* 2016;83:325–35. doi:10.1515/teme-2015-0081.
- [8] Schwenke H, Knapp W, Haitjema H, Weckenmann A, Schmitt R, Delbressine F. Geometric error measurement and compensation of machines—An update. *CIRP Annals - Manufacturing Technology* 2008;57:660–75. doi:10.1016/j.cirp.2008.09.008.
- [9] Schwenke H. Large parts with critical tolerances: Concepts and possible solutions for traceable CMM measurements on machine tools, Traceable in-process dimensional measurement Final Workshop 2016.
- [10] ISO. ISO/TR 16907 Machine tools - Numerical compensation of geometric errors 2015.
- [11] Nisch S, Schmitt R. Production integrated 3D measurements on large machine tools. *LVMC Large Volume Metrology Conference 2010, Chester (UK), 2010*.
- [12] Uekita M, Takaya Y. On-machine dimensional measurement of large parts by compensating for volumetric errors of machine tools. *Precision Engineering* 2016;43:200–10. doi:10.1016/j.precisioneng.2015.07.009.
- [13] Holub M, Jankovych R, Andrs O, Kolibal Z. Capability assessment of CNC machining centres as measuring devices. *Measurement: Journal of the International Measurement Confederation* 2018;118:52–60. doi:10.1016/j.measurement.2018.01.007.
- [14] Bryan J. International Status of Thermal Error Research (1990). *CIRP Annals - Manufacturing Technology* 1990;39:645–56. doi:10.1016/S0007-8506(07)63001-7.
- [15] Bryan J. International Status of Thermal Error Research 1967. doi:10.1016/S0007-8506(07)63001-7.
- [16] Mayr J, Jedrzejewski J, Uhlmann E, Alkan Donmez M, Knapp W, Härtig F, et al. Thermal issues in machine tools. *CIRP Annals Manufacturing Technology* 2012;61:771791. doi:10.1016/j.cirp.2012.05.008.
- [17] Postlethwaite SR, Allen JP, Ford DG. Machine tool thermal error reduction - An appraisal. *Proceedings of the Institution of Mechanical Engineers, Part B: Journal of Engineering Manufacture* 1999;213:1–9. doi:09544054.
- [18] Ross-Pinnock D, Maropoulos PG. Identification of key temperature measurement technologies for the enhancement of product and equipment integrity in the light controlled factory. *Procedia CIRP* 2014;25:114–21. doi:10.1016/j.procir.2014.10.019.
- [19] Ross-pinnock D, Mullineux G. Compensating for thermal and gravitational effects in structures and assemblies. 2016.
- [20] Puttock M. Large Scale metrology. 1978.
- [21] Wendt K, Franke M, Härtig F. Mobile Multilateration Measuring System for High Accurate and Traceable 3D Measurements of Large Objects. *Proceedings of the 10th ISMQC, the 10th International Symposium on Measurement and Quality Control Tokyo: JSPE Techn. Committee for Intelligent Nanomeasure (Paper No. 25): E3-025-1–E3-025-4, 2010*.

-
- [22] ISO. JCGM 100:2008 (GUM 1995 with minor corrections). Evaluation of measurement data — Guide to the expression of uncertainty in measurement. 2008.
- [23] ISO. ISO/TS 15530-3: 2004. Geometrical Product Specifications (GPS) — Coordinate measuring machines (CMM): Technique for determining the uncertainty of measurement — Part 3: Use of calibrated workpieces or standards. 2004.
- [24] Physikalisch-Technische Bundesanstalt (PTB). Traceable in-process dimensional measurements (TIM) EMRP project IND 62 n.d. <https://www.ptb.de/emrp/ind62-home.html>.
- [25] Acko B, Milfelener M. Temperature-invariant material Standard for monitoring performance of machine tools. Proc. 18th International Research/Expert Conference "Trends in the Development of Machinery and Associated Technology", 2014, p. 297–300.
- [26] Acko B, Klobucar R, Acko M. Traceability of in-process measurement of workpiece geometry. *Procedia Engineering* 2015;100:376–83. doi:10.1016/j.proeng.2015.01.381.
- [27] Viprey F, Nouira H, Lavernhe S, Tournier C. Novel multi-feature bar design for machine tools geometric errors identification. *Precision Engineering* 2016;46:323–38. doi:10.1016/j.precisioneng.2016.06.002.
- [28] Widmaier T, Kuosmanen P, Hemming B, Esala V, Brabandt D. New material standards for traceability of roundness measurements of large-scale rotors. 58th IWK, Ilmenau Scientific Colloquium Technische Universität, 2014.
- [29] Woodward S, Brown S, Dury M, McCarthy M. Producing dimensional transfer material standards for the assessment of workshop machine tool performance. Euspen's 16th International Conference & Exhibition, 2016.
- [30] Zeleny J, Linkeova I. Design and calibration of free-form standard. *Laser Metrology and Machine Performance XI*, 2015, p. 147–8.
- [31] Zeleny J, Linkeova I, Skalnik P. Calibrated CAD model of freeform standard. Proc. XXI IMEKO World Congress, 2015.
- [32] ISO. ISO/TS 15530-4:2008. Geometrical Product Specifications (GPS) — Coordinate measuring machines (CMM): Technique for determining the uncertainty of measurement — Part 4: Evaluating task-specific measurement uncertainty using simulation. 2008.
- [33] Trapet E, Wäldele F. Trapet, Waldele - 1991 - A reference object based method to determine the parametric error components of coordinate measuring machines and machine tools.pdf. *Measurement* 1991;9:17–22. doi:http://dx.doi.org/10.1016/0263-2241(91)90022-l.
- [34] Trapet E. Traceability of Coordinate Measurements According to the Method of the Virtual Measuring Machine: Part 2 of the Final Report Project MAT1-CT94-0076. vol. Volumen 35. 1999.
- [35] Härtig F, Kniel K, Schulze K. Messunsicherheitsermittlung: Ermittlung einer aufgabenspezifischen Messunsicherheit von 3D-Verzahnungsmessungen. 2008.
- [36] Maropoulos PG, Guo Y, Jamshidi J, Cai B. Large volume metrology process models: A framework for integrating measurement with assembly planning. *CIRP Annals - Manufacturing Technology* 2008;57:477–80. doi:10.1016/j.cirp.2008.03.017.
- [37] Verein Deutscher Ingenieure (VDI). VDI/VDE 2617-11-Accuracy of Coordinate Measuring Machines - Characteristics and Their Checking - Determination of the Uncertainty of Measurement for Coordinate Measuring Machines Using Uncertainty Budgets. 2011.
- [38] García M. In-Process Inspection of Large High Value Components on a Machine Tool Platform. 2016.
- [39] ISO. ISO 10360-1, Geometrical Product Specifications (GPS) -- Acceptance and reverification tests for coordinate measuring machines (CMM) -- Part 1: Vocabulary. 2000.
- [40] Flack D. Measurement Good Practice Guide No. 42: CMM verification. 2001.
- [41] Slocum A. Precision machine-design - Macromachine Design Philosophy and its applicability to the design of Micromachines. IEEEMEMS '92, proceedings. An Investigation of Micro Structures, Sensors, Actuators, Machines and Robot. IEEE, 1992. doi:10.1109/MEMSYS.1992.187687.
- [42] Slocum A. Fundamentals of Design: Error budgets. 2012.
- [43] Weekers WG, Schellekens PHJ. Compensation for dynamic errors of coordinate measuring machines.

- Precision Engineering 1997;20:197–209.
- [44] Soons JA. Accuracy Analysis of Multi-Axis Machines 1993. doi:10.6100/IR400139.
- [45] Hocken RJ. Technology of machine tools. Volume 5. Machine tool accuracy 1980.
- [46] Knapp W, Matthias E. Test of the Three-Dimensional Uncertainty of Machine Tools and Measuring Machines and its Relation to the Machine Errors. CIRP Annals - Manufacturing Technology 1983;32:459–64. doi:10.1016/S0007-8506(07)63440-4.
- [47] Dassanayake KMM, Tsutsumi M, Saito A. A strategy for identifying static deviations in universal spindle head type multi-axis machining centers. International Journal of Machine Tools and Manufacture 2006;46:1097–106. doi:10.1016/j.ijmachtools.2005.08.010.
- [48] Donmez MA, Blomquist DS, Hocken RJ, Liu CR, Barash MM. A general methodology for machine tool accuracy enhancement by error compensation. Precision Engineering 1986;8:187–96. doi:10.1016/0141-6359(86)90059-0.
- [49] Hocken RJ. Three dimensional Metrology. Annals of the CIRP, 1977, p. 403–8.
- [50] Huang T, Whitehouse D. A simple yet effective approach for error compensation of a tripod-based parallel kinematic machine. CIRP Annals-Manufacturing Technology 2000;49:285–8.
- [51] Soons JA, Theuws FC, Schellekens PH. Modeling the errors of multi-axis machines: a general methodology. Precision Engineering 1992;14:5–19. doi:10.1016/0141-6359(92)90137-L.
- [52] Zhang G, Veale R, Charlton T, Borchardt B, Hocken R. Error Compensation of Coordinate Measuring Machines. CIRP Annals - Manufacturing Technology 1985;34:445–8. doi:10.1016/S0007-8506(07)61808-3.
- [53] Schellekens P, Rosielle N, Vermeulen H, Vermeulen M, Wetzels S, Pril W. Design for Precision: Current Status and Trends. CIRP Annals - Manufacturing Technology 1998;47:557–86. doi:10.1016/S0007-8506(07)63243-0.
- [54] ISO (Technical committee ISO/TC 39/SC 2). ISO 230-1:2012, Test code for machine tools -- Part 1: Geometric accuracy of machines operating under no-load or quasi-static conditions. 2012.
- [55] Uriarte L, Zatarain M, Axinte D, Yague-Fabra J, Ihlenfeldt S, Eguia J, et al. Machine tools for large parts. CIRP Annals - Manufacturing Technology 2013;62:731–50. doi:10.1016/j.cirp.2013.05.009.
- [56] ISO. ISO 230-7: 2015, Test code for machine tools -- Part 7: Geometric accuracy of axes of rotation. 2015.
- [57] Cauchick-Miguel P, King T, Davis J. CMM verification: A survey. Measurement: Journal of the International Measurement Confederation 1996;17:1–16. doi:10.1016/0263-2241(96)00001-2.
- [58] Knapp W, Tschudi U, Bucher A. Vergleich von Prüfkörpern zur Abnahme von Koordinatenmessgeräten. 1990.
- [59] Weckenmann A. Comparison of CMM length measurement tests conducted with different 1D, 2D and 3D standards. proceedings of the 11th National, 2nd International Scientific Conference Metrology in Production Engineering, At Lublin, Poland, 2005.
- [60] Kunzmann H, Trapet E, Wäldele F. A Uniform Concept for Calibration, Acceptance Test, and Periodic Inspection of Coordinate Measuring Machines Using Reference Objects. CIRP Annals - Manufacturing Technology 1990;39:561–4. doi:10.1016/S0007-8506(07)61119-6.
- [61] Pahk HJAE, Kimt YSAM, Moon JHEE. A New Technique for Volumetric Error Assessment of CNC MTs Incorporating Ball Bar Measurement and 3D Volumetric Error Model. International Journal of Machine Tools & Manufacture 1997;37:1583–96.
- [62] Zargarbashi SHH, Mayer JRR. Assessment of machine tool trunnion axis motion error, using magnetic double ball bar. International Journal of Machine Tools and Manufacture 2006;46:1823–34. doi:10.1016/j.ijmachtools.2005.11.010.
- [63] Knapp W. Machine Tool Testing Methods: Overview over ISO Standards and other Special Tests for Machine Tool Performance Evaluation and Interim Checking. Proceedings of METROMEET 2005, Bilbao, Spain, 2005.
- [64] Belforte G, Bona B, Canuto E, Donati F, Ferraris F, Gorini I, et al. Coordinate Measuring Machines and Machine Tools Selfcalibration and Error Correction. CIRP Annals - Manufacturing Technology 1987;36:359–64. doi:10.1016/S0007-8506(07)62622-5.

- [65] Knapp W. Comparison of National and International Standards for Evaluation of Positioning Accuracy and Repeatability of NC Axes. 1992.
- [66] Renishaw. The benefits of remote interferometry for linear, angular and straightness measurements. Technical white paper: TE335. n.d.
- [67] Hickman PA. Optical tilting viewed in a new light. *Laser Focus* 1968;4:22.
- [68] Salisbury JG, Hocken RJ. Taut Wire Straightedge Reversal Artifact. *Initiatives of Precision Engineering at the Beginning of a Millennium*, 2002, p. 644–8.
- [69] Quesnel J, Durand HM, Touzé T. Stretched Wire Offset Measurements: 40 Years of Practice of This Technique At Cern. *International Workshop on Accelerator Alignment 2008*:1–6.
- [70] Schwenke H. The latest trends and future possibilities of volumetric error compensation for machine tools. The 15th International Machine Tool Engineers' Conference, IMEC, Tokyo, Japan, 2-3 November, 2012, p. 57–71.
- [71] CIRP Unification document. Axes of Rotation. *Annals of the CIRP*, 1976, p. 545–64.
- [72] Chapman MAV, Fergusson-Kelly R, Holloway A, Lock D, Lee W. Interferometric angle measurement and the hardware options available from Renishaw-Technical white paper: TE326. n.d.
- [73] Estler WT. Uncertainty Analysis for Angle Calibrations Using Circle Closure. *J Res Natl Inst Stand Technol* 1998;103:11. doi:10.6028/jres.103.008.
- [74] Automated Precision Inc. (API). XD laser measuring solution. [Http://www.apisensor.com/products/mth/xd-Laser/](http://www.apisensor.com/products/mth/xd-Laser/) n.d.
- [75] SIOS. Calibration Interferometer: SP 15000 C Series. [Http://www.sios-De.com/products/calibration-Interferometer/](http://www.sios-De.com/products/calibration-Interferometer/) 2015.
- [76] Renishaw. XM-60 multi-axis calibrator. 2016.
- [77] Ibaraki S, Knapp W. Indirect Measurement of Volumetric Accuracy for Three-Axis and Five-Axis Machine Tools : A Review. *International Journal of Automation Technology* 2012;6:110–24.
- [78] ISO (Technical committee ISO/TC 39/SC 2). ISO 230-4:2005, Test Code for MTs. Part 4. Circular Tests for Numerically Controlled machine tools. 2005.
- [79] ISO. ISO 230-6:2002, Test Code for Machine tools. Part 6. Determination of Positioning Accuracy on Body and Face Diagonals (Diagonal Displacement Tests). 2002.
- [80] Kruth JP, Zhou L, Van den Bergh C, Vanherck P. A Method for Squareness Error Verification on a Coordinate Measuring Machine. *International Journal of Advanced Manufacturing Technology* 2003;21:874–8. doi:10.1007/s00170-002-1408-x.
- [81] Bringmann B, Küng A, Knapp W. A Measuring Artefact for true 3D Machine Testing and Calibration. *CIRP Annals - Manufacturing Technology* 2005;54:471–4. doi:10.1016/S0007-8506(07)60147-4.
- [82] Peggs GN, Maropoulos PG, Hughes EB, Forbes AB, Robson S, Ziebart M, et al. Recent developments in large-scale dimensional metrology. *Proceedings of the Institute of Mechanical Engineers, Part B: Journal of Engineering Manufacture* 2009;223:571–95. doi:10.1243/09544054JEM1284.
- [83] Kenta U, Ryosyu F, Sonko O, Toshiyuki T, Tomizo K. Geometric calibration of a coordinate measuring machine using a laser tracking system. *Measurement Science and Technology* 2005;16:2466. doi:10.1088/0957-0233/16/12/010.
- [84] Schwenke H, Franke M, Hannaford J, Kunzmann H. Error mapping of CMMs and machine tools by a single tracking interferometer. *CIRP Annals - Manufacturing Technology* 2005;54:475–8. doi:10.1016/S0007-8506(07)60148-6.
- [85] ISO. ISO 10791-1:2015: Test conditions for machining centres -- Part 1: Geometric tests for machines with horizontal spindle (horizontal Z-axis). 2015.
- [86] ISO. ISO 10791-6:2014: Test conditions for machining centres -- Part 6: Accuracy of speeds and interpolations. 2014.
- [87] Florussen GHJ, Spaan HAM. Dynamic R-test for rotary tables on 5-axes machine tools 2012;1:536–9.
- [88] Florussen GHJ, Spaan HAM. Static R-Test: Allocating the Centreline of Rotary Axes of Machine Tools. *Laser Metrology and Machine Performance VIII*, Lamdamap, Euspen, Bedford, 2007.

- [89] Florussen GHJ, Spaan HAM. Determining the machine tool contouring performance with dynamic R-test measurements 3D probe head Masterball C-axis. Proceedings of the 12th euspen International Conference, Stockholm., 2012, p. 1–5.
- [90] Siemens. Kinematics measuring cycle CYCLE996 n.d. https://www.industry.siemens.com/topics/global/en/cnc4you/tips_and_tricks/pages/kinematics-measuring-cycle996.aspx.
- [91] Standard NA. Uniform cutting test – NAS series. Metal cutting equip- ments. 1969.
- [92] Hughes EB, Wilson A, Peggs GN. Design of a High-Accuracy CMM Based on Multilateration Techniques. *CIRP Annals - Manufacturing Technology* 2000;49:391–4. doi:10.1016/S0007-8506(07)62972-2.
- [93] Weckenmann A, Jiang X, Sommer KD, Neuschaefer-Rube U, Seewig J, Shaw L, et al. Multisensor data fusion in dimensional metrology. *CIRP Annals - Manufacturing Technology* 2009;58:701–21. doi:10.1016/j.cirp.2009.09.008.
- [94] Aguado S, Santolaria J, Samper D, Aguilar JJ. Influence of measurement noise and laser arrangement on measurement uncertainty of laser tracker multilateration in machine tool volumetric verification. *Precision Engineering* 2013;37:929–43. doi:10.1016/j.precisioneng.2013.03.006.
- [95] Brecher C, Flore J, Haag S, Wenzel C. High precision, fast and flexible calibration of robots and large multi-axis machine tools. *MM Science Journal* 2012.
- [96] Schmitt R, Peterek M, Quinders S. Concept of a Virtual Metrology Frame Based on Absolute Interferometry for Multi Robotic Assembly 2014;m:79–86.
- [97] Olarra A, Zubeldia M, Gomez-acedo E, Kortaberria G. Measuring positioning accuracy of large machine tools. 2012.
- [98] Schwenke H. Accuracy Improvement of Machine Tool via New Laser Measurement Methods. 2015.
- [99] Schwenke H, Schmitt R, Jatzkowski P, Warmann C. On-the-fly calibration of linear and rotary axes of machine tools and CMMs using a tracking interferometer. *CIRP Annals - Manufacturing Technology* 2009;58:477–80. doi:10.1016/j.cirp.2009.03.007.
- [100] Etalon AG. Laser tracer MT. <http://www.etalon-ag.com/en/products/lasertracer-MT/> 2016. <http://www.etalon-ag.com/en/products/lasertracer-mt/>.
- [101] Leica. Leica absolute tracker AT402 brochure 2018. <https://www.hexagonmi.com/products/laser-tracker-systems/leica-absolute-tracker-at403>.
- [102] Metrology H. Leica absolute tracker AT930. <http://www.hexagonmi.com/products/laser-Tracker-Systems/leica-Absolute-Tracker-at930> n.d. <http://www.hexagonmi.com/products/laser-tracker-systems/leica-absolute-tracker-at930>.
- [103] ISO. ISO 10360-2:2009. Geometrical product specifications (GPS) -- Acceptance and reverification tests for coordinate measuring machines (CMM) -- Part 2: CMMs used for measuring linear dimensions. 2009.
- [104] Trapet E, Aguilar Martín JJ, Yagüe JA, Spaan H, Zelený V. Self-centering probes with parallel kinematics to verify machine-tools. *Precision Engineering* 2006;30:165–79. doi:10.1016/j.precisioneng.2005.07.002.
- [105] Etalon AG. Linecal-automatic volumetric calibration. 2017.
- [106] Verein Deutscher Ingenieure (VDI). VDI/DGQ 3441 Statistical Testing of the Operational and Positional Accuracy of Machine Tools; Basis. 1982.
- [107] ISO. ISO 230-2: Test code for machine tools — Part 2: Determination of accuracy and repeatability of positioning of numerically controlled axes. 2014.
- [108] Longstaff AP, Fletcher S, Myers A. Volumetric error compensation through a Siemens controller. *European Society for Precision Engineering and Nanotechnology*, 2005.
- [109] Duffie NA, Yang SM, Bollinger JG. Generation of Parametric Kinematic Error-Correction Functions from Volumetric Error Measurements. *CIRP Annals - Manufacturing Technology* 1985;34:435–8. doi:10.1016/S0007-8506(07)61806-X.
- [110] Ispas C, Anania D, Mohora C. Contribution concerning machine tool accuracy using software methods for geometrical errors compensation 2006:26–7.
- [111] Liu H, Xue X, Tan G. Backlash Error Measurement and Compensation on the Vertical Machining Center

- 2010;2010:403–7. doi:10.4236/eng.2010.26053.
- [112] Weikert S. When five axes have to be synchronized. Proceedings of the 7th Lamdamap Conference, 2005, p. 87–96.
- [113] Weekers W. Compensation for Dynamic Errors of Coordinate Measuring Machines. Eindhoven University of Technology, 1996.
- [114] Rehsteiner F, Weikert S, Rak Z. Accuracy Optimization of Machine Tools under Acceleration Loads for The Demands of High-Speed-Machining. Proceedings of the annual meeting - American Society for Precision Engineering, 1998, p. 602–5.
- [115] van den Bergh C. Reducing thermal errors of CMM located on the shop- floor. Katholieke Umniversiteit Leuven, Belgium, 2001.
- [116] Delbressine FLM, Florussen GHJ, Schijvenaars LA, Schellekens PHJ. Modelling thermomechanical behaviour of multi-axis machine tools. Precision Engineering 2006;30:47–53. doi:10.1016/j.precisioneng.2005.05.005.
- [117] Gruber R, Knapp W. Temperatureinflüsse auf die Werkzeugmaschi- nengenaugigkeit. 1998.
- [118] Weckenmann A, Estler T, Peggs G, McMurtry D. Probing systems in dimensional metrology. CIRP Annals - Manufacturing Technology 2004;53:657–684.
- [119] National physical laboratory (NPL). LUMINAR EMRP project n.d. <http://projects.npl.co.uk/luminar/>.
- [120] Muelaner JE, Maropoulos PG. Large volume metrology technologies for the light controlled factory. Procedia CIRP 2014;25:169–76. doi:10.1016/j.procir.2014.10.026.
- [121] Leica. Leica absolute interferometer, a new approach to laser tracker absolute distance meter n.d. <https://www.hexagonmi.com/solutions/technical-resources/technical-articles/the-leica-absolute-interferometer>.
- [122] Warden MS. Absolute distance metrology using frequency swept lasers. University of Oxford, 2011.
- [123] Etalon AG. Absolute multiline technology 2017. <http://www.etalon-ag.com/produkte/absolute-multiline-technologie/>.
- [124] Hughes B, Warden MS. Novel Coordinate Measurement System Based on Frequency Scanning Interferometry. Proceedings of CSMC, 2013, p. 19–24.
- [125] Gomez-Acedo E, Olarra A, Zubieta M, Kortaberria G, Ariznabarreta E, de Lacalle LN. Method for measuring thermal distortion in large machine tools by means of laser multilateration. The International Journal of Advanced Manufacturing Technology 2015;80:523–34. doi:10.1007/s00170-015-7000-y.
- [126] Martin O. Baseline: Benchmarking a new machine tool verification system. MetMap, 2019, p. 16.
- [127] Ibaraki S, Blaser P, Shimoike M, Takayama N, Nakaminami M, Ido Y. Measurement of thermal influence on a two-dimensional motion trajectory using a tracking interferometer. CIRP Annals - Manufacturing Technology 2016;65:483–6. doi:10.1016/j.cirp.2016.04.067.
- [128] Berger D, Brabandt D, Lanza G. Conception of a mobile climate simulation chamber for the investigation of the influences of harsh shop floor conditions on in-process measurement systems in machine tools. Measurement: Journal of the International Measurement Confederation 2015;74:233–7. doi:10.1016/j.measurement.2015.07.010.
- [129] Renishaw. OMP400 optical machine probe systems. Technical paper: H-5069-8504-05-A. 2008.
- [130] Weckenmann A. Comparability of tactile and optical form measuring techniques with resolution in the nanometre range. Proceedings of X. International Colloquium on Surfaces, 2000, p. 50–62.
- [131] Yang Q, Butler C. A 3-D noncontact trigger probe for coordinate measuring machines. Measurement: Journal of the International Measurement Confederation 1996;17:39–44. doi:10.1016/0263-2241(96)00004-8.
- [132] Lukacs G, Lockhart J, Facello M. Non-contact whole-part inspection. 2013.
- [133] Marsh B. An Investigation of Diameter Measurement Repeatability Using A Coordinate Measuring Machine And A Multi-Baseline Repeatability Assessment Methodology. 2nd Annual Quality & Metrology Symposium Proceedings, Center for Quality, Measurement, and Automation, Bowling Green State University, 1996.

- [134] Dove J. Probe qualification and precision coordinate metrology. 2000.
- [135] Renishaw. Measurement on CMMs. White paper H-1000-3218-01. n.d.
- [136] Imkamp D, Schepperle K. The Application Determines the Sensor: VAST Scanning Probe Systems. 2006.
- [137] Ali SHR. Probing System Characteristics in Coordinate Metrology. *Measurement Science Review* 2010;10:120–9. doi:10.2478/v10048-010-0023-5.
- [138] Berisso K, Ollison T. Coordinate Measuring Machine Variations for Selected Probe Head Configurations. *Journal of Industrial Technology* 2010;26.
- [139] Renishaw. Probing systems for CNC machine tools. n.d.
- [140] Renishaw. SPRINT high-speed scanning system. H-5465-8399-03 white paper. n.d.
- [141] Novotest B. Digilog touch probes n.d. <http://www.blum-novotest.com/en/products/measuring-components/digilog-touch-probes/tc63-tc64-digilog.html>.
- [142] Weckenmann A, Kampa H. Koordinaten messgeraete, VDI-Z. 1983.
- [143] Weckenmann A, Kampa H, Georgi B, Goch G, Hesper H. Koordinatenmessgeraete. 1984.
- [144] Aston R, Davis J, Stout K. A probing question: A customer's investigation into the directional variability of a coordinate measuring machine touch trigger probe 1998;38:15–27. doi:10.1016/S0890-6955(97)00011-4.
- [145] Chan FMM, Davis EJ, King TG, Stout KJ. Some performance characteristics of a multi-axis touch trigger probe. *Measurement Science and Technology* 1997;8:837. doi:10.1088/0957-0233/8/8/002.
- [146] Dobosz M, Woźniak A. Metrological feasibilities of CMM touch trigger probes. *Measurement* 2003;34:287–99. doi:10.1016/j.measurement.2003.05.002.
- [147] Shen Y-L, Zhang X. Pretravel compensation for vertically oriented touch-trigger probes with straight styli. *International Journal of Machine Tools and Manufacture* 1997;37:249–62. doi:10.1016/S0890-6955(96)00060-0.
- [148] Kishinami T, Nakamura H, Saito K. Three Dimensional Curved Surfaces measurement using Newly Developed Three Dimensional Tactile Sensing Probe. *Proceedings of the International Symposium on Metrology for Quality Control in Production Tokyo, 1984*, p. 288–93.
- [149] Moons S, Shen Y-L. Errors in probe offset Vectors of multiple orientations in CMM measurements. *ASPE proceedings*, 1998, p. 512–5.
- [150] Ogura I, Okazaki Y. A Study for Development of Small-CMM Probe detecting Contact Angle. *Proceedings ASPE Summer Topical Meeting on Coordinate Measuring Machines, 2003*, p. 74–7.
- [151] Li YF, Liu ZG. Method for determining the probing points for efficient measurement and reconstruction of freeform surfaces. *Measurement Science and Technology* 2003;14:1280–8. doi:10.1088/0957-0233/14/8/313.
- [152] Uhlmann E, Oberschmidt D, Kunath-fandrei G. 3D-Analysis of Microstructures with Confocal Laser Scanning Microscopy. *ASPE Winter Topical Meeting 1, 2003*, p. 93–7.
- [153] Lonardo PM, Lucca D a., De Chiffre L. Emerging Trends in Surface Metrology. *CIRP Annals - Manufacturing Technology* 2002;51:701–23. doi:10.1016/S0007-8506(07)61708-9.
- [154] Puttock MJ, Thwaite EG. Elastic Compression of Spheres and Cylinders at Point and Line Contact. *National Standards Laboratory Technical Paper* 1969;25:64.
- [155] Zahwi S, Mekawi AM. Some effects of stylus force on scratching surfaces. *International Journal of Machine Tools and Manufacture* 2001;41:2011–5. doi:10.1016/S0890-6955(01)00065-7.
- [156] Edgeworth R, R.G. W. Uncertainty Management for CMM Probe Sampling of Complex Surfaces. *ASME Manufacturing Science and Engineerin*, 1996, p. 511–8.
- [157] Aoyama H, Kawai M, Kishinami T. A New Method for Detecting the Contact Point between a Touch Probe and a Surface 1989;38:7–10.
- [158] ISO. ISO 230-10:2016. Test code for machine tools -- Part 10: Determination of the measuring performance of probing systems of numerically controlled machine tools. 2011.
- [159] Marshall S, Gilby J. New Opportunities in Non-Contact 3D Measurement. 2002.
- [160] Keferstein C, Züst R. Minimizing technical and financial risk when integrating and applying optical sensors

- for in- process measurement. n.d.
- [161] Karadayi R. Blue Light Laser Sensor Integration and Point Cloud Metrology. CMSC conference, 2016.
- [162] Paulo de Moraes J, Peterek M. Integration of a laser scanner into a machine tool for an in-process 3D measurement. 2012.
- [163] Streppel AH, Lutters D, Brinke E ten, Pijlman H, Kals HJ. Selective measuring of freeform surfaces for quality control and selective maintenance of bending tools. *Journal of Materials Processing Technology* 2001;115:147–52. doi:10.1016/S0924-0136(01)00755-5.
- [164] Savio E, De Chiffre L. Inspection of free form functional surfaces on fan blades. *Proceedings of PRIME 2001 Int. Conf.*, Sestri Levante, Italy, 20-22 June, 2001.
- [165] Savio E, Chiffre L De, Schmitt R. *Metrology of freeform shaped parts* 2007;56:810–35. doi:10.1016/j.cirp.2007.10.008.
- [166] Brinksmeier E, Preuss W. Diamond machining of the 3 m reflector of the KOSMA submillimeter telescope by a single-point fly-cutting process. *Proceedings of the annual meeting - American Society for Precision Engineering*, 1996, p. 56–61.
- [167] Brinksmeier E, Riemer E, Glabe O. *Process Chains for the Replication of Complex Optical Elements*. 2004.
- [168] Mian NS, Fletcher S, Longstaff AP, Myers A. Efficient estimation by FEA of machine tool distortion due to environmental temperature perturbations. *Precision Engineering* 2013;37:372–9. doi:10.1016/j.precisioneng.2012.10.006.
- [169] Maier T, Zaeh MF. Modeling of the thermomechanical process effects on machine tool structures. *Procedia CIRP* 2012;4:73–8. doi:10.1016/j.procir.2012.10.014.
- [170] Klocke F, Lung D, Puls H. FEM-Modelling of the thermal workpiece deformation in dry turning. *Procedia CIRP* 2013;8:240–5. doi:10.1016/j.procir.2013.06.096.
- [171] Makino. Vertical machining center - ps-series-vmc n.d. [https://www.makino.com/vertical-machining-centers/ps-series-vmc/ps-brochure-\(electronic\).pdf](https://www.makino.com/vertical-machining-centers/ps-series-vmc/ps-brochure-(electronic).pdf).
- [172] Keller F. Traceability of on-machine measurements under a wide range of working conditions, Traceable in-process dimensional measurement Final Workshop 2016.
- [173] Zayer. KAIROS machine tool n.d. <http://www.zayer.com/en/product/movingcolumn/kairos/25>.
- [174] Kortaberria G. Characterization of large machine tool volumetric behaviour in workshop conditions - (TIM) EMRP project IND 62. 2015.
- [175] Wennemer M. A case study on a very large machine tool: systematic deviations and thermo-elastic deformations - Etalon Forum. 2016.
- [176] Mutilba U, Sandá A, Vega I, Gomez-acedo E, Bengoetxea I, Yagüe JA. Traceability of on-machine tool measurement : Uncertainty budget assessment on shop floor conditions. *Measurement* 2019;135:180–8. doi:10.1016/j.measurement.2018.11.042.
- [177] ISO 10791-7:2014. Test conditions for machining centres -- Part 7: Accuracy of finished test pieces. 2014.
- [178] Mutilba U, Gomez-Acedo E, Sandá A, Vega I, Yagüe-Fabra JA. Uncertainty assessment for on-machine tool measurement: an alternative approach to the ISO 15530-3 technical specification. *Precision Engineering* 2019;57:45–53. doi:10.1016/j.precisioneng.2019.03.005.
- [179] Mutilba U, Yagüe-Fabra JA, Gomez-Acedo E, Kortaberria G, Olarra A. Integrated multilateration for machine tool automatic verification. *CIRP Annals* 2018;67:555–8. doi:10.1016/j.cirp.2018.04.008.
- [180] (JCGM) JC for G in M. JCGM 101:2008 – Evaluation of measurement data - Supplement 1 to the “Guide to the expression of uncertainty in measurement” – Propagation of distributions using a Monte Carlo method. 2008.
- [181] Calkins JM. Quantifying coordinate uncertainty fields in coupled spatial measurement systems. 2002.
- [182] Mutilba U, Egaña F, Kortaberria G, Gomez-Acedo E, Olarra A, Yagüe-Fabra JA. Integrated volumetric error mapping for large machine tools : An opportunity for more accurate and geometry connected machines. *Procedia Manufacturing* 2019:1–8.
- [183] LSST. Large Synoptic survey Telescope (LSST) website n.d. <https://www.lsst.org/>.
- [184] Mutilba U, Kortaberria G, Egaña F, Yagüe-Fabra JA. 3D Measurement Simulation and Relative Pointing Error

- Verification of the Telescope Mount Assembly Subsystem for the Large Synoptic Survey Telescope †. *Sensors* 2018;18:20–2. doi:10.3390/s18093023.
- [185] Callahan S, Gressler W, Thomas SJ, Gessner C, Warner M, Lotz PJ, et al. Large Synoptic Survey Telescope mount final design n.d.;9906:1–20. doi:10.1117/12.2232996.
- [186] Mutilba U, Kortaberria G, Egaña F, Yagüe-Fabra JA. Relative pointing error verification of the Telescope Mount Assembly subsystem for the Large Synoptic Survey Telescope. 5th IEEE International Workshop on Metrology for AeroSpace (MetroAeroSpace), Rome, Italy: 2018. doi:10.1109/MetroAeroSpace.2018.8453570.
- [187] D. Neill, Sebag J, Gressler W, Warner M, Wiecha O. LTS-103 Telescope Mount Assembly (TMA) Specifications. Tucson: 2016.
- [188] Bindel D, Goodman J. Principles of Scientific Computing Monte Carlo methods. 2009.
- [189] Rakich A. Using a laser tracker for active alignment on the Large Binocular Telescope. *Proceedings of SPIE* 7733, vol. 8444, 2012, p. 844454. doi:10.1117/12.928706.
- [190] Mutilba U, Kortaberria G, Egaña F, Yagüe-Fabra JA. Telescope mount assembly pointing accuracy assessment for the Large Synoptic Survey Telescope : A large-scale metrology challenge. *EUSPEN 19th International Conference & Exhibition 2019*;1:9–12.
- [191] Schmitt R, Jatzkowski P, Peterek M. Traceable Measurements using Machine Tools. *Laser metrology and machine performance X : 10th International Conference and Exhibition on Laser Metrology, Machine Tool, CMM and Robotic Performance, Lamdamap*, 2013.
- [192] Sebag J, Gressler W, Neill D, Barr J, Claver C, Andrew J. LSST telescope integration and tests. *Proceedings of SPIE* 2014;9145:91454A. doi:10.1117/12.2055241.

Esta tesis doctoral persigue la mejora de las funcionalidades de las máquinas herramienta para la fabricación de componentes de alto valor añadido. En concreto, la tesis se centra en mejorar la precisión de las máquinas-herramienta en todo su volumen de trabajo y en desarrollar el conocimiento para realizar la medición por coordenadas trazable con este medio productivo. En realidad, la tecnología para realizar mediciones en máquina herramienta ya está disponible, como son los palpadores de contacto y los softwares de medición, sin embargo, hay varios factores que afectan a la trazabilidad de la medición realizada en condiciones de taller, que no permiten emplear las estas medidas para controlar el proceso de fabricación o validar la pieza en la propia máquina-herramienta, asegurando un proceso de fabricación de cero-defectos. Aquí, se propone el empleo del documento técnico ISO 15530-3 para piezas de tamaño medio. Para las piezas de gran tamaño se presenta una nueva metodología basada en la guía VDI 2617-11, que no está limitada por el empleo de una pieza patrón para caracterizar el error sistemático de la medición por coordenadas en la máquina-herramienta. De esta forma, se propone una calibración previa de la máquina-herramienta mediante una solución de multilateración integrada en máquina, que se traduce en la automatización del proceso de verificación y permite reducir el tiempo y la incertidumbre de medida. En paralelo, con el conocimiento generado en la integración de esta solución en la máquina-herramienta, se propone un nuevo procedimiento para la caracterización de la precisión de apunte del telescopio LSST en todo su rango de trabajo. Este nuevo procedimiento presenta una solución automática e integrada con tecnología láser tracker para aplicaciones de gran tamaño donde la precisión del sistema es un requerimiento clave para su buen funcionamiento.

